1-1-1970

Analysis of gridwork in skew bridges.

Pijush Kanti Chowdhury

University of Windsor

ANALYSIS OF

GRIDWORK IN SKEW BRIDGES

A THESIS
submitted to the Faculty of Graduate Studies
in Partial Fulfilment of the Requirement
for the Degree of Master of Applied
Science in Civil Engineering from
the University of Windsor.

by

Pijush Kanti Chowdhury, B.Sc. Engg.
(Dacca, E. Pakistan, 1963)

Windsor, Ontario, Canada

1970

APPROVED BY:

G. Abdel-Sayed

ABSTRACT

An elastic analysis of gridwork in skew bridges by the method of finite differences has been presented through this investigation. The analysis is based on the theory of equivalent orthotropic plate which is considered to be a substitute of gridwork and slab system of skew bridges.

By using appropriate boundary conditions finite difference equations have been derived for different typical network points covering the entire bridge which is simply supported on the two opposite sides and free at the other two. Simple formulae have been presented for computing bending moments in longitudinal and transverse girders of the grillage skew bridge. Several factors such as number of girders and diaphragms, their spacing and stiffness ratio, aspect ratio of the bridge and skew angle have been studied. A study of the influence of Poisson's ratio on the stress distribution has also been made.

An experimental study was performed on a model skew bridge under three different types of loadings. The results obtained from the tests are found to be in satisfactory agreement with the theoretical solutions.

TABLE OF CONTENTS

LIST OF PHOTOPLATES

LIST OF FIGURES

COMPARISON OF EXPERIMENTAL AND
THEORETICAL RESULTS

PAGE

LIST OF FIGURES

THEORETICAL RESULTS

FIGURE: PAGE

ACKNOWLEDGEMENT

I wish to express my sincere gratitude to Dr. J.B. Kennedy for his guidance and encouragement during the course of making this investigation.

Thanks are expressed to the Computer Centre staff and to the staff of the Laboratory of Civil Engg. Department for their active help and to Mr. Roy F. Allen for typing of the thesis.

The financial assistance for this work by the National Research Council of Canada is also thankfully acknowledged.

NOMENCLATURE

Bx, By	Orthotropic flexural rigidities per unit width in x and y directions
Bxy, Byx, γ_T, γ_P	Orthotropic torsional rigidities per unit width in x and y directions
bo, lo	Spacing of longitudinal girders and cross beams
C	Torsional rigidity constant
C_1	Shape factor involved in the torsion constant of rectangular section
E	Modulus of elasticity
F_T, F_P	Torsion constants of plane areas in longitudinal and transverse directions
G	Shear modulus of rigidity
H	Apparent torsional rigidity of the equivalent orthotropic plate
I_T, I_P	Moment of inertia of plane areas with respect to longitudinal and transverse directions
Lx, Ly	Span length and width of the bridge
Mx, My	Bending moments per unit width, acting on sections, normal to x and y axes, respectively
Mxy, Myx	Twisting moments per unit length acting on sections normal to x and y axes, respectively
Po	Concentrated load
p_o	Uniformly distributed load
q(x,y)	Load intensity at point (x,y)
q_o	Line load per unit length in x direction
$\bar{q}_o$	Equivalent combined load acting at node point

Q_x, Q_y	Shear force per unit length perpendicular to x and y axes
V_x, V_y	Support reactions per unit length on edges perpendicular to x and y axes
w	Displacement component in z direction w is called 'deflection'
x,y	Horizontal rectangular co-ordinates
u,v	Oblique co-ordinate axes as shown in Fig. 5
Ω	Torsional parameter
τ_x, τ_y	Distances between node points in x and y directions
τ_u, τ_v	Distances between node points in u and v directions
μ_x, μ_y	Poisson's ratio associated with x and y directions
σ_x, σ_y	Unit normal stresses in x and y directions
τ_{xy}, τ_{yx}	Unit shearing stresses on planes perpendicular to z axis but parallel to y and x axes
$\nabla^2 = \frac{\partial^2}{\partial x^2} + \frac{\partial^2}{\partial y^2}$	Laplace's operator in two variables
$U = \nabla^2 w$	
ϕ	Angle of skew

INTRODUCTION

A grillage or gridwork is a structure composed of two systems of intersecting flexural members, the members in each system being parallel to one another and continuous through the point of intersections.

In the field of reinforced concrete the study of gridwork in skew bridges is of considerable interest and practical importance when a highway bridge is to cross streams, railways or other highways below at an oblique angle. Because of the present practice of transporting heavy loads, an accurate method of analyzing the behaviour of main girder and cross beam is essential. Owing to the high degree of statical indeterminancy, the actual stress distribution imposed on such a grid system by an external load is a problem in itself. The number of redundant components is generally considerable which complicates the numerical calculations so that analytical investigations become highly involved.

To reduce the size of the problem, Hendry and Jaeger [1]* assumed that the transverse members of a skew grid may be replaced by a continuous torsion-free spread medium of equivalent elastic rigidity. Further, the whole grid is taken as a simply supported

---

* Numbers in brackets refer to the number of reference in the Bibliography of this thesis.

beam carrying all the applied loads. The solution is then obtained in the form of first harmonic distribution coefficients, in terms of two dimensionless parameters. The method is restricted to a limited number of longitudinal girders and the engineer is to be satisfied with determining only the approximate critical moments because the complete solution of even a simple grid including the evaluation of all the stress resultants and deformations at every point of the structure is very impractical. Furthermore any change in loading data entail a separate series of calculations.

Langendonck [2] presented a method to analyse gridworks of skew bridges consisting of only two simply supported equal longitudinal girders connected by equal and equidistant transverse cross beams. With the assumption that the loads are applied at the intersections of the cross beams with the girders it was possible to yield an exact solution to the problem in terms of trigonometric polynomials, by satisfying conditions of static equilibrium and geometric compatibility. But the extension of this method to the case of bridges with a greater number of longitudinal girders involves cumbersome arithmetical computations.

Recently a remarkable change has taken place in the manner of the approach applied in structural analysis to the solution of gridwork problem. This is the new concept of 'Equivalent orthotropy' [14, 3, 11, 13]. For the purpose of estimating overall deflections and stresses, the skew bridge stiffened with longitudinal and cross beams may be conceived to be replaced by a substitute 'Equivalent orthotropic plate' of a uniform spread longitudinal stiffness and a uniform spread transverse stiffness.

R. Bares and C. Massonet [3] have presented tables and diagrams for the distribution coefficients based on the theory of 'equivalent orthotropic plates' which are very effective in the analysis and design calculations of right girder bridges. Extending the theory of equivalent orthotropic plate to the analysis of skew grillage, Naruoka and Ohmura [4] derived skew network finite difference equations using Marcus' finite difference approach to calculate the influence coefficients for deflections and bending moments for simply supported orthotropic parallelogrammic plate. They employed a network proposed by Favre, dividing the plate into a 6x6 skew mesh.

Based on this analysis, Fujio, Ohmura and Naruoka [5] proposed formulae to calculate the longitudinal bending moment at mid.span of interior girder in grillage skew girder bridges. In formulating the finite difference equations they neglected the Poisson's ratio effect on deflections and moments of the equivalent orthotropic skew slab. But Kennedy and Tamberg [6] in their broad and critical discussions against the background of available analytical and experimental method of solution of skew bridges have given special considerations on the influence of Poisson's ratio on the stress distribution of a skew slab.

Based on the same network as suggested by Favre, Basar and Yuksul [7] have also developed the finite difference equations for an orthotropic skew slab. No numerical results were given. But some difficulty was experienced by Basar and Yuksul (and presumably Naruoka and Ohmura) in satisfying the condition U=0 (Eq. 4.2) along the simply supported boundary of the orthotropic plates and a constraint is imposed near these edges, since they used six equations to eliminate five unknowns.

A similar problem occurs if Jensen's [17] network is used.

Fawcett [8] has suggested that the external points to the simply supported edges be left initially in the finite difference equations to be eliminated later on when the final set of simultaneous equations is being formed. Situations arising from the suggestions of Fawcett have been examined in this investigation.

Coull [18] has published an approximate method for the analysis of simply supported uniformly loaded orthotropic skew bridge slabs with two opposite edges free. He used the principle of least work in conjunction with the assumption that the load and stress components may be represented by a power series in the chordwise co-ordinates, the coefficients of this series being functions of spanwise position only. He found, on comparison with model tests on isotropic slabs, that agreement between theoretical and experimental results deteriorated with increasing skew.

Cheung, King and Zienkiewicz [19] applied the finite element method for the solution of isotropic skew plate problems. Recently Powell and Ogden [20] have published a paper on finite element method of analysis of orthotropic steel plate bridge decks in orthogonal configuration. This work can be extended to include the effects of skew for the analysis of gridwork in skew bridges. But the choice of a proper displacement function, satisfying not only the curvature criterion along the interface of the elements but also slope compatibility, appears to be a problem for an idealized orthotropic equivalent skew slab [19] .

When the two systems of intersecting beams forming the gridwork of a skew bridge are not orthogonal, skew anisotropic plate theory as proposed by Lie [24] can be applied to the solution of gridwork in skew bridges. Since the governing differential equation of an anisotropic plate in skew configuration is very involved, a transformation of the flexural and torsional rigidities from a skew anisotropic plate to an equivalent orthotropic parallelogrammic plate may be made and the analysis of grillage skew bridge can be based on the theory of equivalent orthotropic skew plate. However, the additional work taking the anisotropic form of the system into account as well as an experimental test on a plate with orthogonal beams will be carried out in near future and will be reported in the literature.

The present investigation stems from the need to study by means of an elastic theory several factors that enter into the analysis and design of gridwork in skew bridges. Such factors include number of girders and diaphragms, their spacing and stiffness ratios in flexure and torsion, aspect ratios of the bridge and skew angle.

Based on the theory of equivalent orthotropic parallelogrammic plate which is assumed to be a substitute of gridwork and slab system of a skew bridge, finite difference equations have been developed and compared with those of available solutions [4,7] . A comparison of present analysis with a numerical solution of a skew grillage based on the theory of anisotropic plate [24,25] has also been made. Favre's skew network has been used for deriving the finite difference equations for deflections, bending and twisting moments.

Theoretical solutions have also been verified with experimental results.

I

THE THEORY OF ORTHOTROPIC PLATE AS APPLIED TO THE ANALYSIS OF A GRIDWORK AND SLAB SYSTEM IN ORTHOGONAL CONFIGURATION.

The study of the composite action of grid and slab system may be arranged to form a sequence of structural forms, the sequence beginning with an ideal orthotropic plate, a simple gridwork and ultimately ending with a slab and grid pattern.

1.1 Orthotropic plate

The analytical approach to the problem of an ideal orthotropic plate, which is composed of materials exhibiting elastic symmetry with respect to three mutually perpendicular planes (i.e. materials which are orthogonally anisotropic), is based on the classical Poisson-Kirchoff's simplifying assumptions [3] relating to the form of the material of the plate and to the state of strains induced by external loading. These are the same usual assumptions as used in the small deflection theory of isotropic plate.

The differential equation giving the relationship between the deflection and the loading of an ideal orthotropic plate, often referred to as Huber's equation [10] is :

$$B_{x_1} \frac{\partial^4 w}{\partial x^4} + 2H_1 \frac{\partial^4 w}{\partial x^2 \partial y^2} + B_{y_1} \frac{\partial^4 w}{\partial y^4} = q(x,y) \qquad (1.1)$$

where w is the deflection of the middle surface of the plate at any point (x,y) and q(x,y) is the loading intensity.

The rigidities are defined as:

$$\left.\begin{aligned} B_{x_1} &= \frac{E_x h^3}{12(1-\mu_x\mu_y)}, \quad B_{y_1} = \frac{E_y h^3}{12(1-\mu_x\mu_y)} \\ 2H_1 &= 2(2\gamma' + B_{xy_1}) \\ &= 2\left[2\frac{Gh^3}{12} + \mu_x B_{y_1}\right] \\ B_{xy_1} &= \mu_x B_{y_1} = \mu_y B_{x_1} \\ \gamma' &= Gh^3/12 . \end{aligned}\right\} \quad (1.2)$$

Following Huber we define the shear modulus as:

$$G = \frac{E}{2(1+\sqrt{\mu_x\mu_y})} \qquad \text{where } E_x = E_y = E \qquad (1.3)$$

1.2 Simple Gridwork

Mathematical similarity which exists between the behaviour of plates and grillage seems to have been realised first by Timoshenko [14] . This basic concept has been used by Guyon and Massonet [3] who used Huber's solution of orthotropic plates and applied it to the analysis of right girder grillage.

Fig. 1 shows a system consisting of n simply supported longitudinal beams of span Lx running in the x-direction and m cross beams of length Ly running in the y-direction and free at the ends $y = \pm \frac{L_y}{2}$.

For the purpose of analysis, the concept of 'Equivalent orthotropic plate' as a substitute of original gridwork is utilized where the elastic stiffness in both flexure and torsion of discrete beams are assumed to be continuously distributed to have a uniform spread longitudinal and transverse stiffness. The system is now submitted to a virtual deformation defined by the elastic surface w = w(x,y) which yields the governing equation for the equivalent substitute of a simple gridwork in the form:

$$\left.\begin{aligned} & B_x' \frac{\partial^4 w}{\partial x^4} + 2H' \frac{\partial^4 w}{\partial x^2 \partial y^2} + B_y' \frac{\partial^4 w}{\partial y^4} = q(x,y) \\ & \text{where} \quad B_x' = \frac{B_T}{b_o}, \quad B_y' = \frac{B_P}{L_o} \\ & 2H' = \gamma_T' + \gamma_P' \\ & \gamma_T' = \frac{C_T}{b_o}, \quad \gamma_P' = \frac{C_P}{l_o} \end{aligned}\right\} \quad (1.4)$$

$B_T = E_x I_T$ and $B_P = E_y \cdot I_P$ are the flexural rigidities of the longitudinal and cross beams, respectively.

C_T and C_P are the torsional rigidities of the longitudinal and cross beams, respectively.

1.3 Slab with grillage in two mutually perpendicular direction.

The slab stiffened by longitudinal and cross beams may also be replaced by an 'Equivalent orthotropic plate' provided the ratio of gridwork spacing to slab boundary dimensions are small enough ($\frac{L_o}{L_x}, \frac{b_o}{L_y} \ll 1$) to ensure approximate homogeneity of stiffness [11]. The elastic parameters relating to the substitute system are assumed to be continuously distributed in the two mutually perpendicular directions.

The theory of the 'Equivalent orthotropic plate' presupposes that both the longitudinal and transverse beams of a composite system are symmetrically placed with respect to the middle surface of the equivalent slab so that the true system possesses a horizontal plane of symmetry. But in a bridge deck system, both longitudinal and transverse beams are placed asymmetrically with respect to the slab portion of the cross section. An eighth order partial differential equation [3] is obtained as a more rigorous solution based on the consideration of displacement components u, v, and w in all the three x, y and z directions. Bares [3] has shown, from the analysis of the three dimensional problem mentioned, the important fact that the shear distribution is considerably dependent on support condition and loading intensity.

For the plane stress analysis, in order to minimise the error due to eccentric position of the beams with respect to the middle surface of the plate and hence the problems entailed with the torsional rigidity have been investigated by many authors [3, 11, 13, 23]. Huber's fourth order differential equation for the equivalent orthotropic plate which must satisfy both equation (1.1) governing the problem of orthotropic slab, and equation (1.4) corresponding to the problem of simple grid of beams was finally obtained in the form:

$$B_x \frac{\partial^4 w}{\partial x^4} + 2H \frac{\partial^4 w}{\partial x^2 \partial y^2} + B_y \frac{\partial^4 w}{\partial y^4} = q(x,y) \qquad (1.5)$$

where

$$\left.\begin{aligned} B_x &= \frac{E_x \cdot h^3}{12(1-\mu_x \mu_y)} + \frac{E_x \cdot I_{sx}}{b_o} + \frac{E_x \cdot Z_1^2 h}{1-\mu_x \mu_y} & \text{(a)} \\ B_y &= \frac{E_y \cdot h^3}{12(1-\mu_x \mu_y)} + \frac{E_y \cdot I_{sy}}{l_o} + \frac{E_y \cdot Z_2^2 h}{1-\mu_x \mu_y} & \text{(b)} \\ 2H &= B_x \mu_y + B_y \mu_x + 4C & \text{(c)} \end{aligned}\right\} (1.6)$$

and h = thickness of the slab

b_o = spacing of the main girder

l_o = spacing of the cross beam

Z_1 and Z_2 are the distances of the neutral surface of the repeating section from the middle plane of the slab in longitudinal and transverse directions, respectively.

I_{sx} = Moment of inertia of the longitudinal beam about the neutral surface i.e. Z_1 below the middle plane of the slab.

I_{sy} = Moment of inertia of the cross beam about the neutral surface i.e. Z_2 below the middle plane of the slab.

I_{sx} and I_{sy} are calculated for the beam-sections without regard to the slab.

$4C = \bar{\gamma}_T + \bar{\gamma}_P$

The values of $\bar{\gamma}_T$ and $\bar{\gamma}_P$ are the torsional rigidities determined by means of torsion constants F_T and F_P of the sectional areas corresponding to the different elements constituting a section.

In case of an open slab and beam section (T-beam) as in Fig. 2, the torsion constant of the entire repeating cross-sectional area is given by the formula [3]

$$\left.\begin{array}{l} F_T = \frac{1}{2} b_o h^3 C_1 + b_1^3 (h_1 - h) C_1 ; \begin{pmatrix} h < b_o \\ b_1 < (h_1 - h) \end{pmatrix}, \\ F_P = \frac{1}{2} l_o h^3 C_1 + b_2^3 (h_2 - h) C_1 ; \begin{pmatrix} h < l_o \\ b_2 < (h_2 - h) \end{pmatrix} \end{array}\right\} \quad (1.7)$$

where the first term of the right hand side refer to the slab portion and the second term to the beam portion of the section. The value of the factor C_1 depends on the shape (side ratio) and is called the shape factor involved in the torsion constant of a rectangular section.

The value of C_1 is given in the following table.

$\frac{h_1}{b_1}$	1	1.5	1.75	2	2.5	3	4	6	8	∞
C_1	0.141	0.196	0.214	0.229	0.249	0.263	0.281	0.299	0.307	0.333

Now Equation (1.6C) of the apparent torsional rigidity of the equivalent system:

$$2H = B_x \mu_y + B_y \mu_x + 4C \quad \text{is defined such that}$$

$$4C = \bar{\gamma}_T + \bar{\gamma}_P = G_X \frac{F_T}{b_o} + G_Y \cdot \frac{F_P}{l_o} \quad (1.8)$$

Gx and Gy are the shear modulus in x and y direction, respectively and are defined as:

$$G_x = \frac{E_x}{2(1+\sqrt{\mu_x \mu_y})} \text{ and } G_y = \frac{E_y}{2(1+\sqrt{\mu_x \mu_y})}$$

The stress couples, shear resultants and the vertical reactions are expressed as:

$$\left.\begin{aligned}
Mx &= -B_x\left(\frac{\partial^2 w}{\partial x^2} + \mu_y \frac{\partial^2 w}{\partial y^2}\right) && \text{(a)}\\
My &= -B_y\left(\frac{\partial^2 w}{\partial y^2} + \mu_x \frac{\partial^2 w}{\partial x^2}\right) && \text{(b)}\\
Mxy &= -2C \frac{\partial^2 w}{\partial x \partial y} && \text{(c)}\\
Qx &= -B_x \frac{\partial^3 w}{\partial x^3} - \left(B_x \mu_y + 2C\right)\frac{\partial^3 w}{\partial x \partial y^2} && \text{(d)}\\
Qy &= -B_y \frac{\partial^3 w}{\partial y^3} - \left(B_y \mu_x + 2C\right)\frac{\partial^3 w}{\partial x^2 \partial y} && \text{(e)}\\
Vx &= -B_x\left[\frac{\partial^3 w}{\partial x^3} + \left(\frac{4C}{B_x} + \mu_y\right)\frac{\partial^3 w}{\partial x \partial y^2}\right] && \text{(f)}\\
Vy &= -B_y\left[\frac{\partial^3 w}{\partial y^3} + \left(\frac{4C}{B_y} + \mu_x\right)\frac{\partial^3 w}{\partial x^2 \partial y}\right] && \text{(g)}
\end{aligned}\right\} \quad (1.9)$$

Positive directions of stresses, stress couples and the shear resultants of an orthotropic plate elements are shown in Fig. 3 and Fig. 4, respectively.

1.4 Dimensionless parameter:

A dimensionless parameter Ω is introduced which is characteristic for the resistance in torsion of the structural pattern and limited by the values 0 and 1. This interval covers all the structural systems. For the simple grid of beams of weak torsional resistance $\Omega = 0$, while $\Omega = 1$ relates to the true slab. Ω is expressed in the form:

$$\Omega = \frac{\mu_y B_x + \mu_x B_y + \bar{\gamma}_T + \bar{\gamma}_P}{2\sqrt{B_x B_y}} \qquad (1.10)$$

and is evaluated by employing the theorem of Betti which proves that:

$$B_x \mu_y = B_y \mu_x$$

$$\text{or} \quad \mu_y = \frac{B_y}{B_x} \mu_x \qquad (1.11)$$

1.5 Orthotropy of form:

In the analysis of gridwork, it is recognised at this state that the factors μ_x and μ_y although represent the relationship between the stress σ and the transverse strain ϵ, are not material constants as 'Poisson's ratio' proper but are elastic constants corresponding to the form of the system. Hence the name 'orthotropy of form' as distinct from the 'orthotropy of material.'

The value of μ_y may be evaluated from the relations of Eq. (1.6) and (1.11). In the present analysis of gridwork in skew bridge, the influence of Poisson's ratio on the stress distribution will be studied for different values of μ_x and its relative importance will be discussed in details.

For the case where Ex = Ey = E and

$$G_x = \frac{E}{2(1+\sqrt{\mu_x \mu_y})} = G_y$$

Eq. (1.10) reduces to:

$$\Omega = \frac{\mu_x B_y + \frac{E}{4(1+\sqrt{\mu_x \mu_y})}\left[\frac{F_T}{b_o} + \frac{F_P}{l_o}\right]}{B_y \sqrt{\frac{\mu_x}{\mu_y}}} \qquad (1.12)$$

Ref. [3] has given several values of μ_x corresponding to the different types of gridwork with regard to the different material of construction. For simple beam grids without slab the value of $\mu_x = 0$ is acceptable. For reinforced and prestressed concrete box section $\mu_x = 0.10$ and for open section comprising a single slab (e.g. T-beam section) $\mu_x = 0.15$ are sufficiently accurate. In case of orthotropic steel deck bridges the value of μ_x may be taken as 0.3.

The flexural and torsional rigidities as defined in Eq. (1.6) for orthogonal equivalent gridwork will be assumed to be valid for an equivalent orthotropic skew plate. The differential equation governing the problem of the equivalent orthotropic skew plate which is a substitute of grillage in skew bridges will be derived in the next chapter.

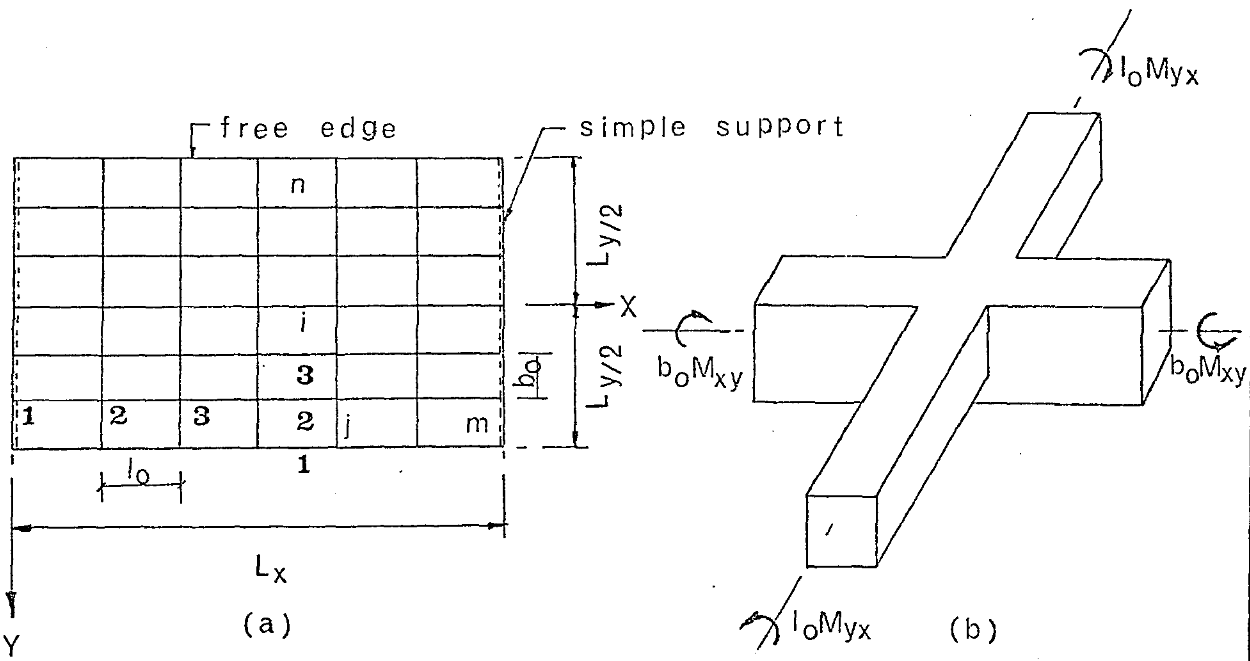

FIG.1 SIMPLE GRIDWORK

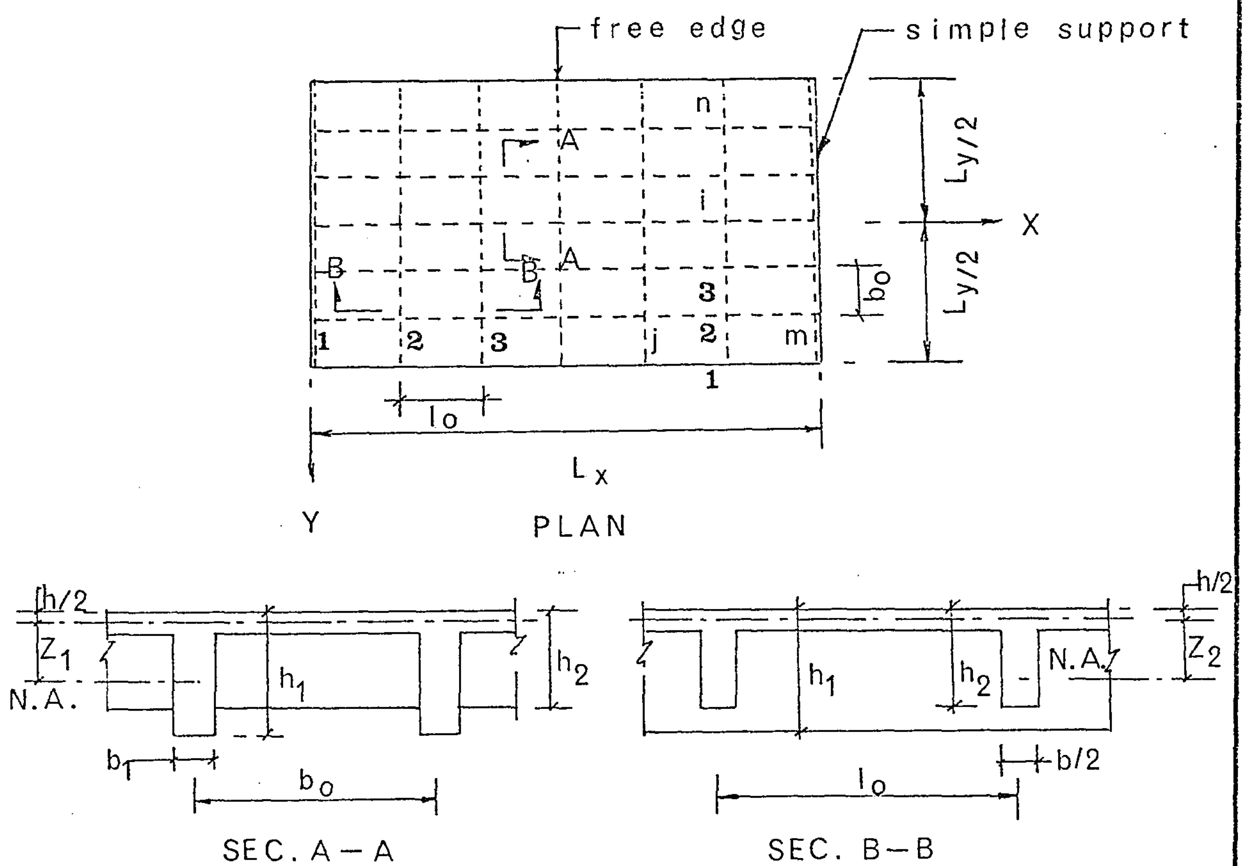

FIG.2 GRIDWORK WITH SLAB

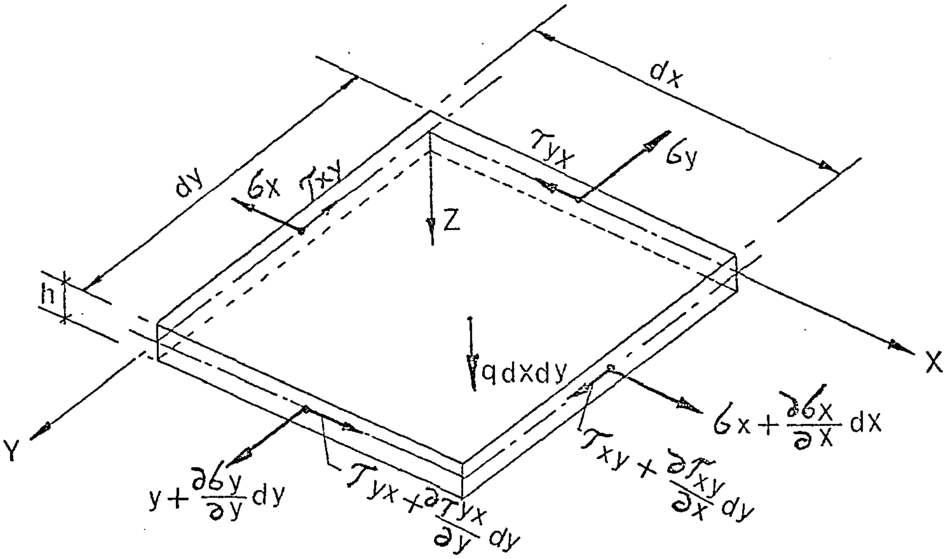

FIG. 3 POSITIVE DIRECTIONS OF STRESSES

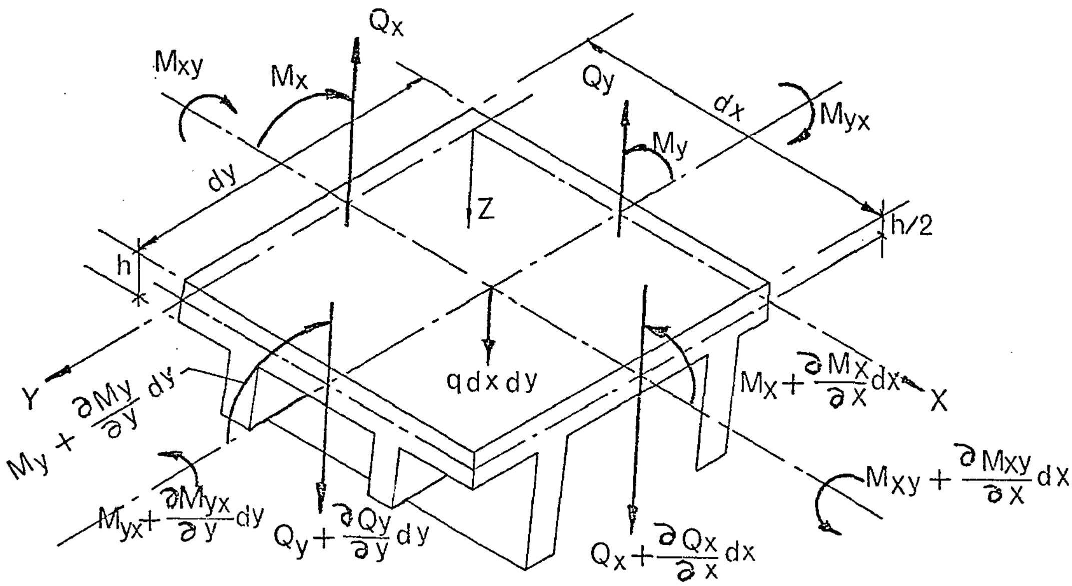

FIG. 4 ORTHOTROPIC PLATE ELEMET SHOWING
POSITIVE DIRECTIONS OF STRESS
COUPLES AND SHEAR RESULTANTS

II

APPLICATION OF ORTHOTROPIC PLATE THEORY IN THE ANALYSIS OF GRIDWORK IN SKEW BRIDGES

Theoretical Background:

The plane stress solution obtained for orthogonal grid systems by orthotropic plate theory proved to be well in accordance with numerous experimental data and comparative analytical investigations gave further justification to this new method of solution.

Naruka and Ohmura [4] were the first to assume that the theory of orthotropic parallelogrammic plates will be effective to the same degree in the analysis of skew girder bridges as the orthotropic rectangular plate in the analysis of right girder bridges. Applying this basic concept the governing differential equation (1.5) of equivalent orthotropic plate may be transformed to skew co-ordinates parallel to the edges (u, v) for a skew gridwork system as follows:

If (x, y) are the rectangular co-ordinates of a point (Fig. 5) in the middle surface of the plate, with (u, v) the corresponding oblique co-ordinates and ϕ the skew angle

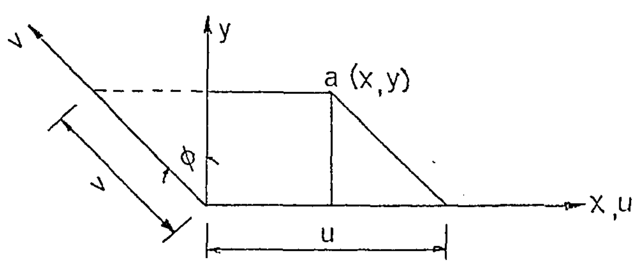

Fig. 5

then

$$\left.\begin{aligned} u &= x + y\tan\phi \\ v &= y\sec\phi \end{aligned}\right\} \quad (2.1)$$

Differentiating Eq. (2.1) with respect to x and y one obtains:

$$\left.\begin{aligned} \frac{\partial u}{\partial x} &= 1 \quad , \quad \frac{\partial u}{\partial y} = \tan\phi \\ \frac{\partial v}{\partial x} &= 0 \quad , \quad \frac{\partial v}{\partial y} = \sec\phi \end{aligned}\right\} \quad (2.2)$$

Since w is a function of both u and v

$$\left.\begin{aligned} \frac{\partial w}{\partial x} &= \frac{\partial w}{\partial u}\cdot\frac{\partial u}{\partial x} + \frac{\partial w}{\partial v}\cdot\frac{\partial v}{\partial x} = \frac{\partial w}{\partial u} \\ \frac{\partial w}{\partial y} &= \frac{\partial w}{\partial u}\cdot\frac{\partial u}{\partial y} + \frac{\partial w}{\partial v}\cdot\frac{\partial v}{\partial y} \\ &= \frac{\partial w}{\partial u}\cdot\tan\phi + \frac{\partial w}{\partial v}\cdot\sec\phi \end{aligned}\right\} \quad (2.3)$$

After successive partial differentiation of Eq. (2.3) the following relations are obtained:

$$\left.\begin{aligned} \frac{\partial^2 w}{\partial x^2} &= \frac{\partial^2 w}{\partial u^2} && \text{(a)} \\ \frac{\partial^2 w}{\partial x\,\partial y} &= \frac{\partial^2 w}{\partial u^2}\tan\phi + \frac{\partial^2 w}{\partial u\,\partial v}\sec\phi && \text{(b)} \\ \frac{\partial^2 w}{\partial y^2} &= \frac{\partial^2 w}{\partial u^2}\tan^2\phi + 2\frac{\partial^2 w}{\partial u\,\partial v}\tan\phi\sec\phi && \text{(c)} \\ &\quad + \frac{\partial^2 w}{\partial v^2}\sec^2\phi \end{aligned}\right\} \quad (2.4)$$

$$\left.\begin{aligned} \frac{\partial^3 w}{\partial x^3} &= \frac{\partial^3 w}{\partial u^3} && \text{(a)} \\ \frac{\partial^3 w}{\partial x^2\,\partial y} &= \frac{\partial^3 w}{\partial u^3}\tan\phi + \frac{\partial^3 w}{\partial u^2\,\partial v}\sec\phi && \text{(b)} \\ \frac{\partial^3 w}{\partial x\,\partial y^2} &= \frac{\partial^3 w}{\partial u^3}\tan^2\phi + 2\frac{\partial^3 w}{\partial u^2\,\partial v}\tan\phi\sec\phi && \text{(c)} \\ &\quad + \frac{\partial^3 w}{\partial u\,\partial v^2}\sec^2\phi \\ \frac{\partial^3 w}{\partial y^3} &= \frac{\partial^3 w}{\partial u^3}\tan^3\phi + 3\frac{\partial^3 w}{\partial u^2\,\partial v}\tan^2\phi\sec\phi && \text{(d)} \\ &\quad + 3\frac{\partial^3 w}{\partial u\,\partial v^2}\tan\phi\sec^2\phi + \frac{\partial^3 w}{\partial v^3}\sec^3\phi \end{aligned}\right\} \quad (2.5)$$

$$\left.\begin{aligned}
\frac{\partial^4 w}{\partial x^4} &= \frac{\partial^4 w}{\partial u^4} && \text{(a)}\\
\frac{\partial^4 w}{\partial x^2 \partial y^2} &= \frac{\partial^4 w}{\partial u^4}\tan^2\phi + 2\frac{\partial^4 w}{\partial u^3 \partial v}\tan\phi\sec\phi && \text{(b)}\\
&\quad + \frac{\partial^4 w}{\partial u^2 \partial v^2}\sec^2\phi &&\\
\frac{\partial^4 w}{\partial y^4} &= \frac{\partial^4 w}{\partial u^4}\tan^4\phi + 4\frac{\partial^4 w}{\partial u^3 \partial v}\tan^3\phi\sec\phi &&\\
&\quad + 6\frac{\partial^4 w}{\partial u^2 \partial v^2}\tan^2\phi\sec^2\phi && \text{(c)}\\
&\quad + 4\frac{\partial^4 w}{\partial u \partial v^3}\tan\phi\sec^3\phi + \frac{\partial^4 w}{\partial v^4}\sec^4\phi &&
\end{aligned}\right\} \quad (2.6)$$

Putting the values of $\frac{\partial^4 w}{\partial x^4}$, $\frac{\partial^4 w}{\partial x^2 \partial y^2}$, $\frac{\partial^4 w}{\partial y^4}$ into Equation (1.5), one obtains the fourth order partial differential equation of the equivalent orthotropic skew plate which is a substitute of gridwork in skew bridge in the following form:

$$\begin{aligned}
&\frac{\partial^4 w}{\partial u^4}\left(B_x + 2H\tan^2\phi + B_y\tan^4\phi\right)\\
&\quad + \frac{\partial^4 w}{\partial u^3 \partial v}\left(4H\tan\phi\sec\phi + 4B_y\tan^3\phi\sec\phi\right)\\
&\quad + \frac{\partial^4 w}{\partial u^2 \partial v^2}\left(2H\sec^2\phi + 6B_y\tan^2\phi\sec^2\phi\right)\\
&\quad + \frac{\partial^4 w}{\partial u\, d v^3}\left(4B_y\tan\phi\sec^3\phi\right) + \frac{\partial^4 w}{\partial v^4}\left(B_y\sec^4\phi\right) = q(x,y) \qquad (2.7)
\end{aligned}$$

The stress couples, shear resultants and vertical reactions of Eq. (1.9) may be expressed in skew co-ordinates as:

$$\left.\begin{aligned}
M_x &= -B_x\left[\frac{\partial^2 w}{\partial u^2} + \mu_y\left\{\frac{\partial^2 w}{\partial u^2}\tan^2\phi + 2\frac{\partial^2 w}{\partial u \partial v}\tan\phi\sec\phi + \frac{\partial^2 w}{\partial v^2}\sec^2\phi\right\}\right] && \text{(a)}\\
M_y &= -B_y\left[\frac{\partial^2 w}{\partial u^2}\tan^2\phi + 2\frac{\partial^2 w}{\partial u \partial v}\tan\phi\sec\phi + \frac{\partial^2 w}{\partial v^2}\sec^2\phi + \mu_x\frac{\partial^2 w}{\partial u^2}\right] && \text{(b)}\\
M_{xy} &= -2C\left[\frac{\partial^2 w}{\partial u^2}\tan\phi + \frac{\partial^2 w}{\partial u \partial v}\sec\phi\right] && \text{(c)}\\
Q_x &= -B_x\frac{\partial^3 w}{\partial u^3} - (B_x\mu_y + 2C)\left[\frac{\partial^3 w}{\partial u^3}\tan^2\phi + 2\frac{\partial^3 w}{\partial u^2 \partial v}\tan\phi\sec\phi\right. && \text{(d)}\\
&\quad \left. + \frac{\partial^3 w}{\partial u \partial v^2}\sec^2\phi\right] &&
\end{aligned}\right\} \quad (2.8)$$

$$Qy = -By\left[\frac{\partial^3 w}{\partial u^3}\tan^3\phi + 3\frac{\partial^3 w}{\partial u^2 \partial v}\tan^2\phi\sec\phi + 3\frac{\partial^3 w}{\partial u \partial v^2}\tan\phi\sec^2\phi + \frac{\partial^3 w}{\partial v^3}\sec^3\phi\right] - (By\mu x + 2c)\left(\frac{\partial^3 w}{\partial u^3}\tan\phi + \frac{\partial^3 w}{\partial u^2 \partial v}\sec\phi\right) \quad (e)$$

$$Vx = -Bx\left[\frac{\partial^3 w}{\partial u^3} + \left(\frac{4c}{Bx} + \mu y\right)\left\{\frac{\partial^3 w}{\partial u^3}\tan^2\phi + 2\frac{\partial^3 w}{\partial u^2 \partial v}\tan\phi\sec\phi + \frac{\partial^3 w}{\partial u \partial v^2}\sec^2\phi\right\}\right] \quad (f)$$

$$Vy = -By\left[\frac{\partial^3 w}{\partial u^3}\tan^3\phi + 3\frac{\partial^3 w}{\partial u^2 \partial v}\tan^2\phi\sec\phi + 3\frac{\partial^3 w}{\partial u \partial v^2}\tan\phi\sec^2\phi + \frac{\partial^3 w}{\partial v^3}\sec^3\phi + \left(\frac{4c}{By} + \mu x\right)\left\{\frac{\partial^3 w}{\partial u^3}\tan\phi + \frac{\partial^3 w}{\partial u^2 \partial v}\sec\phi\right\}\right] \quad (g)$$

Recently Patterson and Cusens [21] have presented a solution of orthotropic skew plate under uniform load. The solution is an extension of an early work by Kennedy and Huggins [22] who developed a method using a single infinite series representation of the deflection of an isotropic plate with edge stiffening beam. Results for the case of a slab simply supported on the two opposite sides and free at the other two were found unreliable due to the use of Kirchoff's two boundary equations instead of three. Moreover the method presented by Patterson and Cusen [21] does not consider the application of the concentrated loadings on the skew orthotropic slab.

Because of the complicated boundary conditions, an exact solution of the fourth order differential equation governing the behaviour of simply supported orthotropic skew slab with two opposite edges free has so far proved impossible. Since in a bridge structure a loaded vehicle would act more as a point load distributed only over a small portion of the deck slab, finite difference method seems to be the best analytical method [8] available in dealing with such point loads. In the present investigation, the same approach which Basar and Yuksul [7] have utilized in their formulation of finite difference equations for a simply supported orthotropic skew slab has been followed in a somewhat different manner that leads to a fairly simple solution incorporating all the essential parameters of a gridwork in skew bridge which is simply supported on the two opposite edges and free at the other two.

III

THE METHOD AND SOLUTION

Due to rapid development of the computing machines and the good convergence properties of the method of finite difference which replaces functions and their derivatives by algebraic expressions involving only the values of the functions at a finite number of points in or near the region or interval of interest, the complicated boundary value problems involved in this present investigation will be solved by this method. Replacement of functions reduces the problem to a set of simultaneous algebraic equations.

The method permits the immediate writing of the force-displacement relations in the form [15, 16]

$$\left[A\right]\left\{w\right\}=\left\{q\right\} \qquad (3.1)$$

where $\{q\}$ is a column of static loads acting at a predetermined set of points (called node points of a certain network) and $\{w\}$ is the column corresponding to vertical displacements. $[A]$ is the conventional stiffness matrix obtained by a few algebraic operations.

The method of central finite differences will be applied in the solution of the problem.

3.1 Computation of Equivalent Plate Moments:

Solution of Eq. (3.1) yields numerical values of deflections at the nodal points of the equivalent plate. By substitution of these values in appropriate moment equations (Eq. 2.8), numerical values of moments are found. Combining the sets of influence coefficients for Mx, My and Mxy, influence coefficients for the equivalent principal moments with their directions at all the network points may be computed according to the equations below:

$$\left.\begin{aligned} M_{\substack{max\\min}} &= \frac{M_x + M_y}{2} \pm \sqrt{\left(\frac{M_x - M_y}{2}\right)^2 + M_{xy}^2} \\ \theta &= \frac{1}{2}\tan^{-1}\frac{2M_{xy}}{M_x - M_y} \end{aligned}\right\} \quad (3.2)$$

3.2 Computation of Beam Moments:

The moments acting on the equivalent orthotropic plate may now be integrated over the whole flange width of the beam to compute the bending moments which are of greatest importance for design purposes. For example, the moment in longitudinal beam B in Fig. 6A in x-direction is given by:

$$M_{B(x)} = \int_{0.5 b_0}^{1.5 b_0} M_x \, dy \qquad (3.5)$$

Similarly moment in transverse beam C in the y-direction is given by:

$$M_{C(y)} = \int_{0.5 l_0}^{1.5 l_0} M_y \, dx \qquad (3.6a)$$

If the cross beams are in a direction at an angle Ø with the y-axis, the bending and twisting moment of the transverse beam in the oblique direction v, for example at point A, in Fig. 6A are given by [12]

$$M_v = Mx'\sin^2\phi + My'\cos^2\phi - 2Mxy'\sin\phi\cos\phi \quad (3.6b)$$

$$M_{v\eta} = (Mx' - My')\sin\phi\cos\phi + Mxy'(\sin^2\phi - \cos^2\phi) \quad (3.6c)$$

where Mx', My' and Mxy' are the integrated moments over the spacing of the gridwork at the section under considerations.

Equation (3.6b) and (3.6c) can be derived from the equilibrium of an element of the plate as shown in Fig. 6.

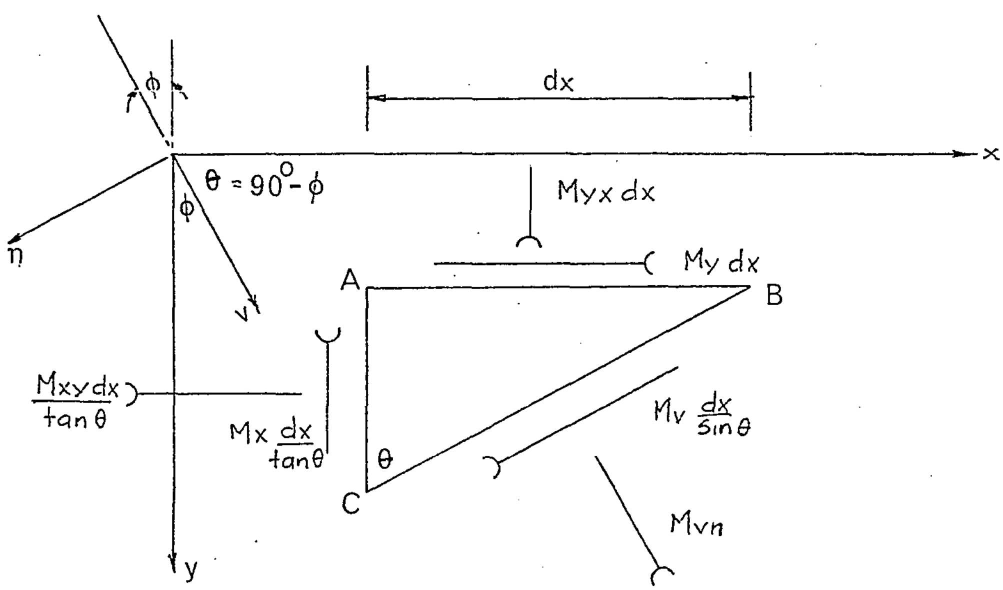

Fig. 6. Moments acting on different planes

The integration of the equivalent plate moment for the beam may be carried out by Simpson's Rule [9]. Thus for a mesh size of n division, the integral of a function $f(y)$ may be evaluated by:

$$\int_0^{y_n} f(y)\,dy = \frac{y_n - y_0}{3n}\Big[f(y_0) + 4f(y_1) + 2f(y_2) + \cdots 4f(n-1) + f(y_n)\Big] \tag{3.7}$$

where $(y_n - y_0)$ represents the spacing of the gridwork in either x or y direction and $f(y_0)$, $f(y_1)$, $f(y_2)$ .... etc., corresponds to the magnitude of functions of moments within the region y_n and y_0. If the spacing of the longitudinal and cross beam is small and coincides with the mesh point layout, equivalent plate moment can be considered to be the average value within the flange-width of the gridwork.

3.3 Limitation and Accuracy of the Method of Finite Differences

The approximations by the finite difference method can be limited to a minor interference which breaks the deflection curve at discrete points and join them in straight lines. Hence the finite difference equations representing the original differential equations are valid as long as the finite number of points which have been reduced from an infinite number of points on the deflection surface and arranged to form a certain network are close enough for straight line approximations. Of course finite difference equations do not exactly represent the original governing equations and hence it is not an exact mathematical method. However, when properly applied, using finite number of network points it is a sufficiently accurate tool for analysis of complicated structural systems.

3.4 Selection of Mesh Sizes:

In the present investigations since seven number of longitudinal and cross beams at different spacings have been provided for the model skew bridge, numerical solutions were obtained by dividing the equivalent bridge system into 6x6 skew panels so that nodal points of skew meshes coincided with the point of intersections of grid-work in both longitudinal and transverse directions to facilitate direct comparison between experimental and theoretical results at these points. However, the effect of different network spacings on the accuracy of the results has been examined by dividing the plate into 4x4, 6x6 and 8x8 meshes which resulted into 8, 18 and 32 simultaneous equations, respectively. It was observed that finer mesh sizes produced about 3% and 6% more accurate deflection and girder moment Mx, respectively, at the point of maximum stress intensity than the coarser mesh size. This is expected because of the inherent limitations of finite difference approximations.

Though the number of simultaneous equations increases considerably with the choice of finer mesh sizes, it does not impose a problem to the solution of the structural system when an electronic computer can be conveniently used for this purpose.

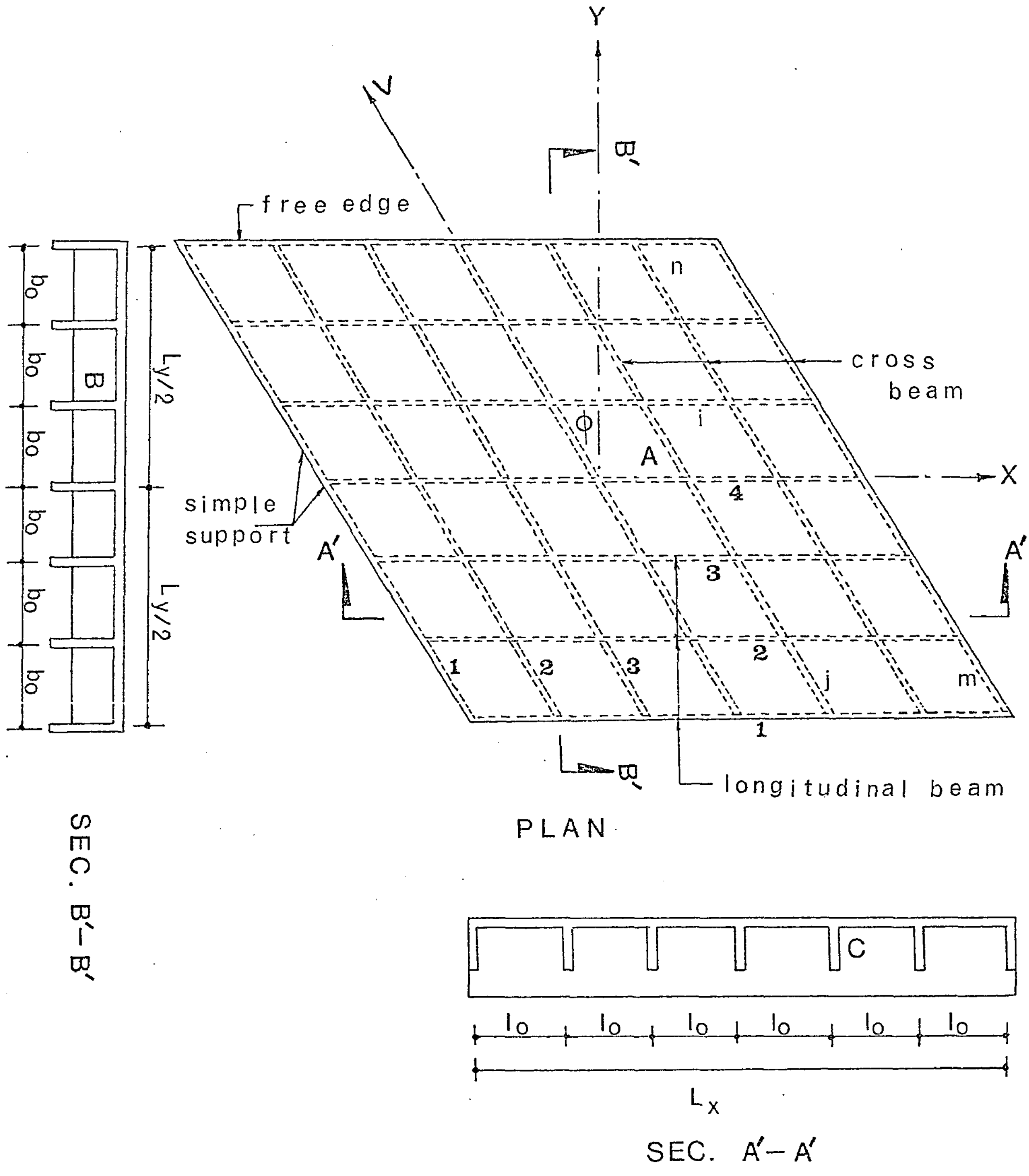

FIG. 6A GRIDWORK WITH DECK SLAB IN SKEW BRIDGE

IV

OUTLINE OF THE METHOD OF FINITE DIFFERENCES AS APPLIED TO THE SOLUTION OF SKEW GRIDWORK

4.1 General Approach

Adopting Marcus' method, the fourth order differential equations of equivalent orthotropic plate can be split up into two equations of second order as given in reference [7] in the following form:

$$\left.\begin{aligned} B_x \frac{\partial^4 w}{\partial x^4} + 2H \frac{\partial^4 w}{\partial x^2 \partial y^2} + B_y \frac{\partial^4 w}{\partial y^4} &= q(x,y) \\ &= \left(\frac{\partial}{\partial x^2} + \frac{\partial}{\partial y^2}\right)\left(B_x \frac{\partial^2 w}{\partial x^2} + B_y \frac{\partial^2 w}{\partial y^2}\right) \\ &\quad + (2H - B_x - B_y) \frac{\partial^2}{\partial y^2}\left(\frac{\partial^2 w}{\partial x^2}\right) \\ &= \left(\frac{\partial}{\partial x^2} + \frac{\partial}{\partial y^2}\right)\left(B_x \frac{\partial^2 w}{\partial x^2} + B_y \frac{\partial^2 w}{\partial y^2}\right) \\ &\quad + (2H - B_x - B_y) \frac{\partial^2}{\partial x^2}\left(\frac{\partial^2 w}{\partial y^2}\right) \end{aligned}\right\} \quad (4.1)$$

Writing

$$B_x \frac{\partial^2 w}{\partial x^2} + B_y \frac{\partial^2 w}{\partial y^2} = U \quad (4.2)$$

$$\left.\begin{aligned} \frac{\partial^2 w}{\partial x^2} = X \quad &, \quad \frac{\partial^2 w}{\partial y^2} = Y \\ \text{and} \quad 2H - B_x - B_y &= D \end{aligned}\right\} \quad (4.3)$$

Eq. (4.1) reduces to

$$\frac{\partial^2 U}{\partial x^2} + \frac{\partial^2 U}{\partial y^2} + D \frac{\partial^2 X}{\partial y^2} = q \quad (4.4a)$$

and

$$\frac{\partial^2 U}{\partial x^2} + \frac{\partial^2 U}{\partial y^2} + D \frac{\partial^2 Y}{\partial x^2} = q \quad (4.4b)$$

Eq. (4.4a) can now be easily put into finite difference form using Favres' skew network for the gridwork in skew bridges.

Naruoka and Ohmura split up the fourth order differential equation in the form:

$$\frac{\partial^2 w}{\partial y^2} + n\frac{\partial^2 w}{\partial x^2} = U$$

$$\frac{\partial^2 U}{\partial y^2} + m\frac{\partial^2 U}{\partial x^2} = \frac{q}{B_y}$$

where $m = \frac{1}{B_y}\left[H + i\sqrt{B_x B_y - H^2}\right]$

$n = \frac{1}{B_y}\left[H - i\sqrt{B_x B_y - H^2}\right]$

which are further abbreviations for the complicated terms that occur in the derivations of the equations.

Since the approach followed by Basar and Yuksul is relatively simple compared to that of Naruoka and Ohmura, derivation of finite difference equations in the present investigation is primarily based on Ref. [7].

The final expressions of the equations derived here, have been compared with those of Naruoka and Ohmura [4] which appear to agree when μ_x and μ_y in the present solution are put equal to zero. Comparison of the present solution with those of Basar and Yuksul [7] revealed minor discrepancies between the two solutions which may be attributed to the arithmetical computations for (1) interior point near the acute corner, (2) interior point near the obtuse corner, (3) general edge point and edge points near the acute and obtuse corners, respectively.

A comparison of the present solution by equivalent orthotropic plate theory for gridwork in skew bridges with the solution based on the theory of skew anisotropic slab formulated by Lie [24] and used by Naruoka [25] for analysis of grillage
by Lie [24] and used by Naruoka [25]
skew bridge system revealed very close agreement between the two solutions near the central portion. But a discrepency in the value of deflection and moment at the free edge was observed which may be attributed to the unsatisfied boundary conditions as discussed in Section (b) of Chapter VIII of this thesis.

The simply supported edge boundary conditions and the boundary conditions of the free edge have been discussed and mathematically formulated when deriving the finite difference equations at different typical network points. Since six equations are to be used to eliminate five unknowns at the bridge boundaries, a constraint $(w_4 + w_4' - 2w_0 = 0)$ Eq. (5.4e & 5.4f) is imposed near the simple support. However, it is felt reasonable to assume that this constraint imposed near the simply supported edges is valid, since the deflections at these points of questions are sufficiently small so that the value of $(w_4 + w_4' - 2w_0)$ tends to zero in the limit. The suggestion by Faucett [8] of leaving the external points to be eliminated later when final set of equations is being formed, has been examined. Since it does not solve the boundary value problem, the external points for the typical network points near the boundary have been expressed in terms of deflections of internal points while formulating the finite difference operators.

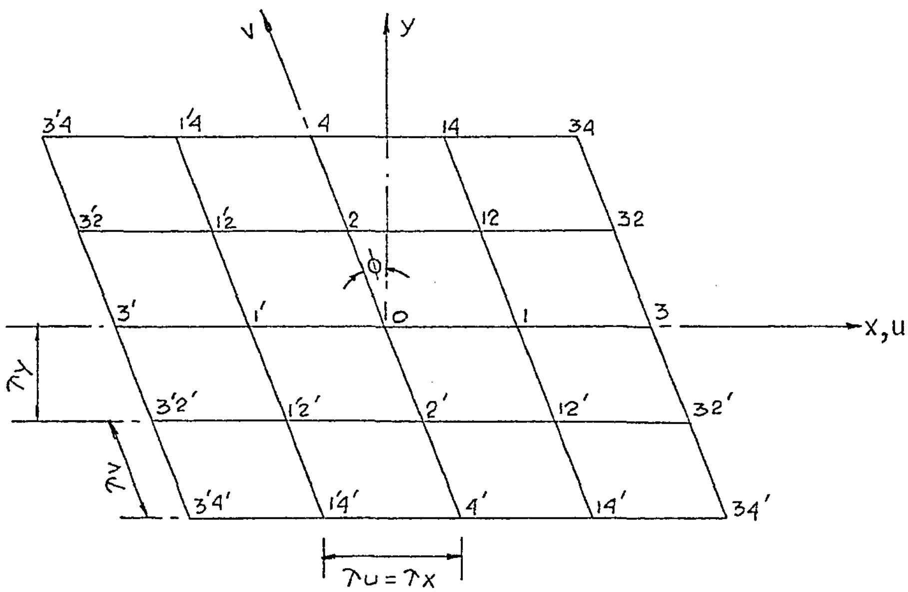

Fig. 7. Favre's Finite Difference Network

4.2 Finite Difference Approximations:

The deformation of the equivalent skew slab defined by the elastic surface $w = w(x,y)$ is also a function of $w = w(u,v)$.

Recalling the finite difference approximations for the partial derivatives at a point (x,y) or (u,v) ranging over the domain of definition of the function, derivatives can be approximated in terms of deflections of nodal points of Favre's skew network as follows:

$$\left.\begin{aligned} \left(\frac{\partial^2 w}{\partial u^2}\right)_0 &= \frac{1}{\lambda_u^2}\left(w_{1'} - 2w_0 + w_1\right) \\ \left(\frac{\partial^2 w}{\partial u\,\partial v}\right)_0 &= \frac{1}{4\lambda_u\lambda_v}\left(w_{12} - w_{1'2} + w_{1'2'} - w_{12'}\right) \\ \left(\frac{\partial^2 w}{\partial v^2}\right)_0 &= \frac{1}{\lambda_v^2}\left(w_{2'} - 2w_0 + w_2\right) \end{aligned}\right\} \quad (4.5)$$

Eq. (2.4) can now be written in finite difference approximations as:

$$\left(\frac{\partial^2 w}{\partial x^2}\right)_o = \frac{1}{\lambda_u^2}\left(w_1' - 2w_o + w_1\right)$$

$$= \frac{\chi^2}{\lambda_y^2}\left(w_1' - 2w_o + w_1\right) \qquad (4.6a)$$

where $\chi = \frac{\lambda_y}{\lambda_x}$ and $\lambda_x = \lambda_u$

$$\left(\frac{\partial^2 w}{\partial y^2}\right)_o = \tan^2\phi\left\{\frac{\chi^2}{\lambda_y^2}\left(w_1' - 2w_o + w_1\right)\right\} + \frac{1}{2\lambda_u \lambda_v}\left(w_{12} - w_{1'2} + w_{1'2'} - w_{12'}\right)\tan\phi \sec\phi$$
$$+ \frac{1}{\lambda_v^2}\left(w_2' - 2w_o + w_2\right)\sec^2\phi$$

but $\lambda_v = \lambda_y \sec\phi$ and putting $\beta = \chi \tan\phi$

one can write

$$\left(\frac{\partial^2 w}{\partial y^2}\right)_o = \frac{1}{\lambda_y^2}\Big[\beta^2\left(w_1' + w_1\right) - \left(2 + 2\beta^2\right)w_o + \frac{\beta}{2}\left(-w_{1'2} + w_{12} + w_{1'2'} - w_{12'}\right)$$
$$+ w_2' + w_2\Big] \qquad (4.6b)$$

Hence
$$\left(\frac{\partial^2 w}{\partial x^2} + \frac{\partial^2 w}{\partial y^2}\right)_o = \frac{1}{\lambda_y^2}\Big[\left(\chi^2 + \beta^2\right)\left(w_1' + w_1\right) - \left(2 + 2\beta^2 + 2\chi^2\right)w_o$$
$$+ \frac{\beta}{2}\left(-w_{1'2} + w_{12} + w_{1'2'} - w_{12'}\right) + w_2' + w_2\Big]$$
$$= \frac{1}{\lambda_y^2}\Big[\alpha\left(w_1' + w_1\right) - \left(2 + 2\alpha\right)w_o$$
$$+ \frac{\beta}{2}\left(-w_{1'2} + w_{12} + w_{1'2'} - w_{12'}\right) + w_2' + w_2\Big] \qquad (4.6c)$$

where $\alpha = \beta^2 + \chi^2$

$$U_o = B_x\left(\frac{\partial^2 w}{\partial x^2}\right)_o + B_y\left(\frac{\partial^2 w}{\partial y^2}\right)_o$$
$$= \frac{1}{\lambda_y^2}\Big[\left(B_x\chi^2 + B_y\beta^2\right)\left(w_1' + w_1\right) - \left(2B_x\chi^2 + 2B_y + 2\beta^2 B_y\right)w_o$$
$$+ \frac{\beta}{2}B_y\left(-w_{1'2} + w_{12} + w_{1'2'} - w_{12'}\right) + B_y\left(w_2' + w_2\right)\Big]$$
$$= \frac{1}{\lambda_y^2}\Big[A\left(w_1' + w_1\right) - \left(2A + 2B_y\right)w_o$$
$$+ \frac{\beta}{2}B_y\left(-w_{1'2} + w_{12} + w_{1'2'} - w_{12'}\right) + B_y\left(w_2' + w_2\right)\Big] \qquad (4.7)$$

where $A = B_x\chi^2 + B_y\beta^2$

Following equations (4.6b) and (4.6c) the governing equation of the equivalent orthotropic skew plate Eq. (4.4a) for general interior point (Point 0) can be written as:

$$\nabla\nabla W = \frac{1}{\lambda_y^2}\Big[\alpha\,(U_1' + U_1) - (2+2\alpha)\,U_0 + \frac{\beta}{2}\,(-U_{1'2} + U_{12} + U_{1'2'} - U_{12'})$$

$$+ U_2' + U_2\Big] + \frac{D}{\lambda_y^2}\Big[\beta^2\,(X_1' + X_1) - (2+2\beta^2)\,X_0$$

$$+ \frac{\beta}{2}\,(-X_{1'2} + X_{12} + X_{1'2'} - X_{12'})$$

$$+ X_2' + X_2\Big] = \bar{q}_0 \qquad (4.8)$$

where, from Equation (4.7) and (4.3) it follows:

$$U_1' = \frac{1}{\lambda_y^2}\Big[A\,(W_3' + W_0) - (2A + 2B_y)\,W_1'$$

$$+ \beta\cdot\frac{B_y}{2}\,(-W_{3'2} + W_2 + W_{3'2'} - W_2') + B_y\,(W_{1'2'} + W_{1'2})\Big] \qquad (4.9\text{a})$$

$$U_1 = \frac{1}{\lambda_y^2}\Big[A\,(W_3 + W_0) - (2A + 2B_y)\,W_1$$

$$+ \beta\cdot\frac{B_y}{2}\,(-W_2 + W_{32} + W_2' - W_{32'}) + B_y\,(W_{12'} + W_{12})\Big] \qquad (4.9\text{b})$$

$$U_{1'2} = \frac{1}{\lambda_y^2}\Big[A\,(W_{3'2} + W_2) - (2A + 2B_y)\,W_{1'2}$$

$$+ \beta\cdot\frac{B_y}{2}\,(-W_{3'4} + W_4 + W_3' - W_0) + B_y\,(W_1' + W_{1'4})\Big] \qquad (4.9\text{c})$$

$$U_{12} = \frac{1}{\lambda_y^2}\Big[A\,(W_2 + W_{32}) - (2A + 2B_y)\,W_{12}$$

$$+ \beta\cdot\frac{B_y}{2}\,(-W_4 + W_{34} + W_0 - W_3) + B_y\,(W_1 + W_{14})\Big] \qquad (4.9\text{d})$$

$$U_{1'2'} = \frac{1}{\lambda_y^2}\Big[A\,(W_{3'2'} + W_2') - (2A + 2B_y)\,W_{1'2'}$$

$$+ \beta\cdot\frac{B_y}{2}\,(-W_3' + W_0 + W_{3'4'} - W_4') + B_y\,(W_1' + W_{1'4'})\Big] \qquad (4.9\text{e})$$

$$U_{12'} = \frac{1}{\lambda_y^2}\Big[A\,(W_2' + W_{32'}) - (2A + 2B_y)\,W_{12'}$$

$$+ \beta\cdot\frac{B_y}{2}\,(-W_0 + W_3 + W_4' - W_{34'}) + B_y\,(W_{14'} + W_1)\Big] \qquad (4.9\text{f})$$

$$U_2' = \frac{1}{\lambda_y^2}\Big[A\,(W_{1'2'} + W_{12'}) - (2A + 2B_y)\,W_2'$$

$$+ \beta\cdot\frac{B_y}{2}\,(-W_1' + W_1 + W_{1'4'} - W_{14'}) + B_y\,(W_4' + W_0)\Big] \qquad (4.9\text{g})$$

$$U_2 = \frac{1}{\lambda y^2}\Big[A\,(w_{1'2} + w_{12}) - (2A + 2B_y)\,w_2$$

$$+ \beta \cdot \frac{B_y}{2}\,(-w_{1'4} + w_{14} + w_{1'} - w_1) + B_y\,(w_0 + w_4)\Big] \quad (4.9h)$$

and

$$\left.\begin{aligned}
X_{1'} &= \left(\frac{\partial^2 w}{\partial x^2}\right)_{1'} = \frac{\chi^2}{\lambda y^2}\,(w_{3'} - 2w_{1'} + w_0) && \text{(a)}\\
X_1 &= \frac{\chi^2}{\lambda y^2}\,(w_0 - 2w_1 + w_3) && \text{(b)}\\
X_0 &= \frac{\chi^2}{\lambda y^2}\,(w_{1'} - 2w_0 + w_1) && \text{(c)}\\
X_{1'2} &= \frac{\chi^2}{\lambda y^2}\,(w_{3'2} - 2w_{1'2} + w_2) && \text{(d)}\\
X_{12} &= \frac{\chi^2}{\lambda y^2}\,(w_2 - 2w_{12} + w_{32}) && \text{(e)}\\
X_{1'2'} &= \frac{\chi^2}{\lambda y^2}\,(w_{3'2'} - 2w_{1'2'} + w_{2'}) && \text{(f)}\\
X_{12'} &= \frac{\chi^2}{\lambda y^2}\,(w_{2'} - 2w_{12'} + w_{32'}) && \text{(g)}\\
X_{2'} &= \frac{\chi^2}{\lambda y^2}\,(w_{1'2'} - 2w_{2'} + w_{12'}) && \text{(h)}\\
X_2 &= \frac{\chi^2}{\lambda y^2}\,(w_{1'2} - 2w_2 + w_{12}) && \text{(i)}
\end{aligned}\right\} \quad (4.10)$$

These finite difference approximations which have been used successfully in complicated boundary value problems can be utilized to formulate difference operators to be applied to different types of skew girder bridges, e.g. single span simply supported bridge, continuous bridge over several spans etc., by incorporating suitable boundary conditions. In what follows, the solution for a simply supported bridge grillage, pertaining to this investigation, will be obtained in terms of finite difference equations.

V

DERIVATIONS OF FINITE DIFFERENCE EQUATIONS

In this Chapter finite difference equations for a simply supported skew grillage bridge with two opposite edges free at $y = \pm \frac{L_y}{2}$ will be derived. To cover the entire equivalent plate it is necessary to formulate difference equations for nine typical network points. These are: 1) General Interior Point, 2) Interior Point near the left simple support, 3) Interior Point near the right simple support, 4) Interior Point near the edge girder, 5) Interior Point near the acute corner, 6) Interior Point near the obtuse corner, 7) General edge Point, 8) Edge Point near the acute corner, 9) Edge Point near the obtuse corner, respectively.

5.1 General Interior Point:

Putting the values of U and X in terms of displacements from Eq. (4.7), (4.9) and (4.10) into equation (4.8) one can deduce the governing equation for general interior point as:

$$\nabla\nabla w = \Big[\alpha A(w_{3'} + 2w_o + w_3) - \alpha(2A + 2B_y)(w_{1'} + w_1)$$

$$+ \alpha\beta \frac{B_y}{2}(-w_{3'2} + w_{3'2'} + w_{32} - w_{32'}) + \alpha B_y(w_{1'2'} + w_{1'2} + w_{12'} + w_{12})$$

$$- (2 + 2\alpha)\Big\{A(w_{1'} + w_1) - (2A + 2B_y)w_o + \beta \cdot \frac{B_y}{2}(-w_{1'2} + w_{12} + w_{1'2'} - w_{12'})$$

$$+ B_y(w_{2'} + w_2)\Big\}$$

$$+\frac{\beta}{2}\Big\{A\left(-w_{3'2}+w_{32}+w_{3'2'}-w_{32'}\right)-(2A+2B_Y)\left(-w_{1'2}+w_{12}+w_{1'2'}-w_{12'}\right)$$

$$+\beta\cdot\frac{B_Y}{2}\left(4w_0-2w_3-2w_{3'}-2w_4-2w_{4'}+w_{34}+w_{3'4}+w_{3'4'}+w_{34'}\right)$$

$$+B_Y\left(w_{14}-w_{1'4}+w_{1'4'}-w_{14'}\right)\Big\}$$

$$+A\left(w_{1'2'}+w_{12'}+w_{1'2}+w_{12}\right)-(2A+2B_Y)\left(w_2+w_{2'}\right)$$

$$+\beta\cdot\frac{B_Y}{2}\left(w_{14}-w_{1'4}+w_{1'4'}-w_{14'}\right)+B_Y\left(w_{4'}+2w_0+w_4\right)\Big]$$

$$+D\chi^2\Big[\beta^2\left(w_{3'}-2w_{1'}+2w_0-2w_1+w_3\right)-(2+2\beta^2)\left(w_{1'}-2w_0+w_1\right)$$

$$+\frac{\beta}{2}\left(-w_{3'2}+2w_{1'2}-2w_{12}+w_{32}+w_{3'2'}-2w_{1'2'}+2w_{12'}-w_{32'}\right)$$

$$+\left(w_{1'2'}-2w_{2'}+w_{12'}+w_{1'2}-2w_2+w_{12}\right)\Big]=\frac{\bar{q}}{B_0}\lambda_Y^4 \quad (5.1)$$

From equation (5.1), coefficients associated with deflection of different nodal points can be separated as shown below:

Coefft. of w_0 : $2A(3\alpha+2)+B_Y(\beta^2+4\alpha+6)+D\chi^2(6\beta^2+4)$

" " w_1 : $-2\alpha(2A+B_Y)-2D\chi^2(2\beta^2+1)-2A$

" " $w_{1'}$: $-2\alpha(2A+B_Y)-2D\chi^2(2\beta^2+1)-2A$

" " w_2 : $-2B_Y(\alpha+2)-2(A+D\chi^2)$

" " $w_{2'}$: $-2B_Y(\alpha+2)-2(A+D\chi^2)$

" " w_3 : $\alpha A+\beta^2\left(D\chi^2-\frac{B_Y}{2}\right)$

" " $w_{3'}$: $\alpha A+\beta^2\left(D\chi^2-\frac{B_Y}{2}\right)$

" " w_4 : $B_Y\left(1-\frac{\beta^2}{2}\right)$

Coefft. of $w_{4'}$: $By(1-\frac{\beta^2}{2})$

" " w_{12} : $(1-\beta)(\alpha By + A + Dx^2) - 2\beta \cdot By$

" " $w_{12'}$: $(1+\beta)(\alpha By + A + Dx^2) + 2\beta . By$

" " $w_{1'2}$: $(1+\beta)(\alpha By + A + Dx^2) + 2\beta . By$

" " $w_{1'2'}$: $(1-\beta)(\alpha By + A + Dx^2) - 2\beta . By$

" " w_{14} : $\beta . By$

" " $w_{14'}$: $-\beta . By$

" " $w_{1'4}$: $-\beta . By$

" " $w_{1'4'}$: $\beta . By$

" " w_{34} : $\beta^2 \cdot \frac{By}{4}$

" " $w_{3'4}$: $\beta^2 \cdot \frac{By}{4}$

" " $w_{3'4'}$: $\beta^2 \cdot \frac{By}{4}$

" " $w_{34'}$: $\beta^2 \cdot \frac{By}{4}$

" " w_{32} : $\frac{\beta}{2}(\alpha By + A + Dx^2)$

" " $w_{3'2'}$: $\frac{\beta}{2}(\alpha By + A + Dx^2)$

" " $w_{3'2}$: $-\frac{\beta}{2}(\alpha By + A + Dx^2)$

" " $w_{32'}$: $-\frac{\beta}{2}(\alpha By + A + Dx^2)$

Using Favre's skew network, Equation (5.1) can now be conveniently presented as in Fig. 8(b).

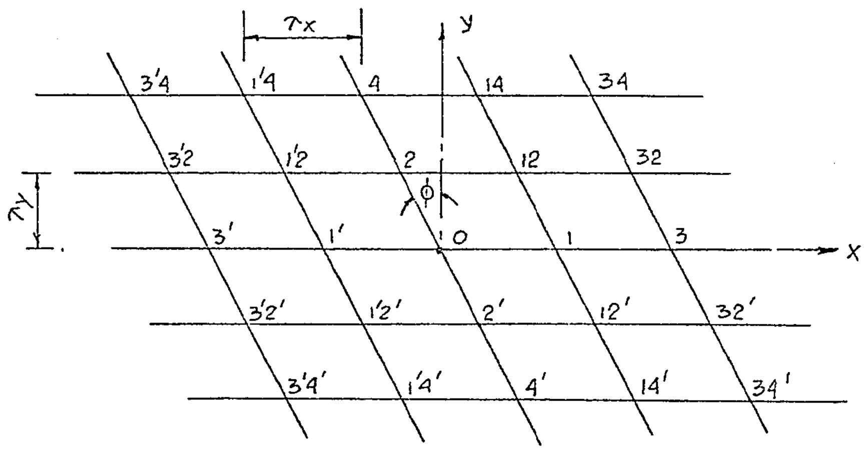

Fig. 8(a)

General Interior Point

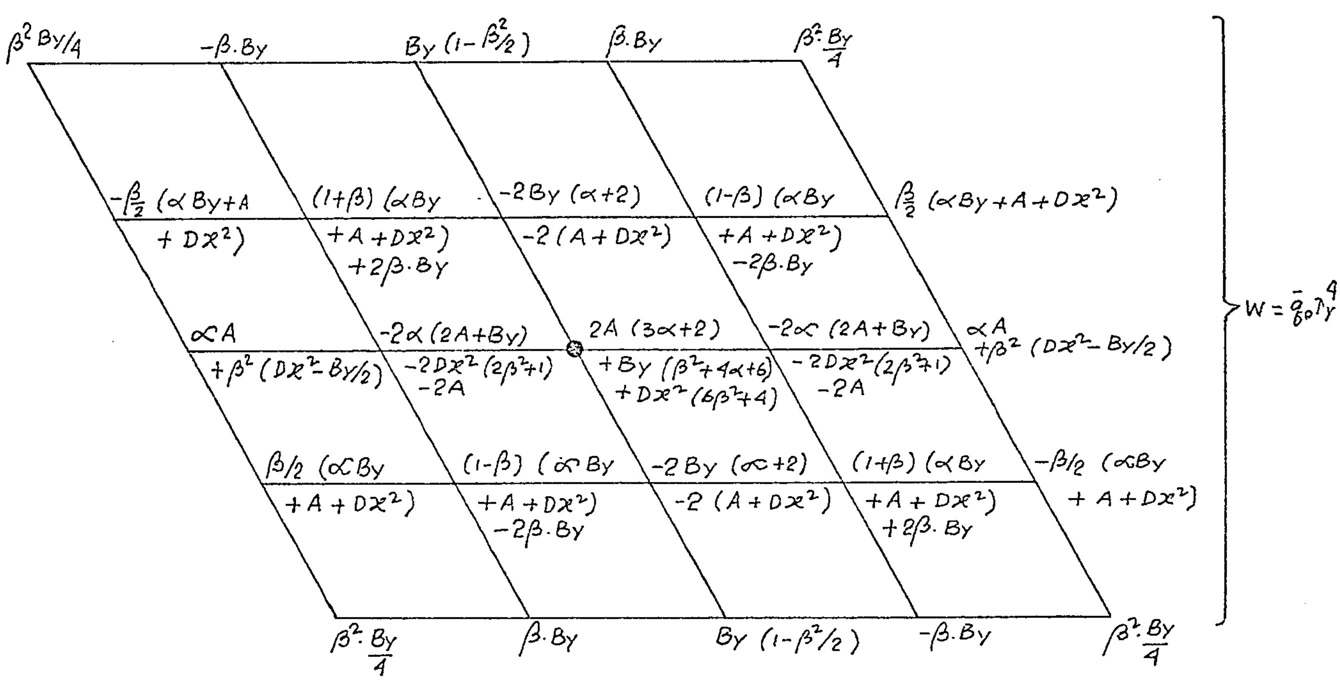

Fig. 8(b). Finite difference equation for general Interior Point

$$
\left.
\begin{aligned}
\text{where} \quad \varkappa &= \frac{\lambda_y}{\lambda_x} \\
\beta &= \varkappa \tan\phi \\
\alpha &= \beta^2 + \varkappa^2 \\
A &= B_x \varkappa^2 + B_y \beta^2 \\
D &= 2H - B_x - B_y
\end{aligned}
\right\} \quad (5.2)
$$

5.2 Interior Point near the left simple support

Boundary Conditions:

The conditions on the simple support are as follows:

(I) Deflections along the edge are zero. i.e. $w = 0$

Hence $w_{1'4} = w_{1'2} = w_{1'} = w_{1'2'} + w_{1'4'} = 0$

(II) Since the condition of zero slope along the edge gives $\frac{\partial^2 w}{\partial v^2} = 0$ and moment perpendicular to the edge are zero ($M_n = 0$), these lead to the boundary condition that sum of the curvatures in two mutually perpendicular direction is zero along the edge.

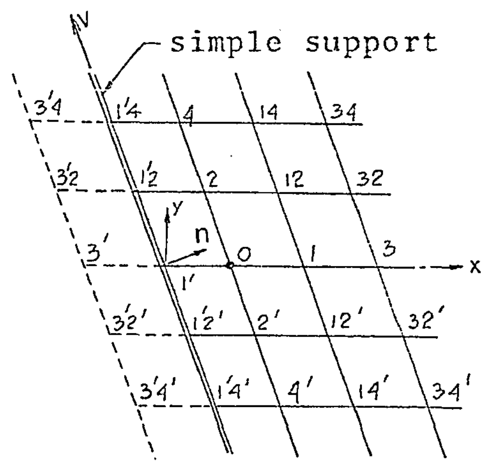

Fig. 9(a) Interior Point near the simple support.

Hence in terms of moments one can write:

$$(M_n + M_v)_{support} = (M_x + M_y)_{support} = 0$$

From Eq. (1.9) it follows:

$$-B_x\left(\frac{\partial^2 w}{\partial x^2}+\mu_y\frac{\partial^2 w}{\partial y^2}\right)-B_y\left(\frac{\partial^2 w}{\partial y^2}+\mu_x\frac{\partial^2 w}{\partial x^2}\right)=0$$

or $$\frac{\partial^2 w}{\partial x^2}\left(B_x+B_y\mu_x\right)+\frac{\partial^2 w}{\partial y^2}\left(B_y+B_x\mu_y\right)=0 \qquad (5.3a)$$

Following Eq. (4.6a) and (4.6b)

$$\left(\frac{\partial^2 w}{\partial x^2}\right)_{1'}=\frac{\varkappa^2}{\lambda_y^2}\left(w_{3'}-2w_{1'}+w_0\right) \qquad (5.3b)$$

and $$\left(\frac{\partial^2 w}{\partial y^2}\right)_{1'}=\frac{1}{\lambda_y^2}\Big[\beta^2\left(w_{3'}+w_0\right)-\left(2+2\beta^2\right)w_{1'}+\frac{\beta}{2}\left(-w_{3'2}+w_2+w_{3'2'}-w_{2'}\right)$$

$$+w_{1'2'}+w_{1'2}\Big] \qquad (5.3c)$$

Let $B_x+B_y\mu_x=K_x$

and $B_y+B_x\mu_y=K_y$

Combining condition (I) into Eq. (5.3a) with the values of curvature from Eq. (5.3b) and (5.3c) one can write:

$$\left(K_x\varkappa^2+K_y\beta^2\right)\left(w_{3'}+w_0\right)+\frac{K_y\beta}{2}\left(-w_{3'2}+w_2+w_{3'2'}-w_{2'}\right)=0 \qquad (5.4a)$$

From the condition of zero slope along the edge and by the method of interpolation one can deduce:

$$\left(\frac{\partial w}{\partial v}\right)_{1'}=\frac{1}{2}\left[\left(\frac{\partial w}{\partial v}\right)_{3'}+\left(\frac{\partial w}{\partial v}\right)_0\right]=0$$

or $$\frac{1}{2}\left[\frac{w_{3'2}-w_{3'2'}}{2\lambda_v}+\frac{w_2-w_{2'}}{2\lambda_v}\right]=0$$

or $$w_{3'2}-w_{3'2'}=w_{2'}-w_2 \qquad (5.4b)$$

Let $K_x \varkappa^2 + K_y \beta^2 = \delta$

From Eq. (5.4a) and (5.4b) it follows:

$$w_{3'} = \frac{\beta . K_y}{\delta} (w_{2'} - w_2) - w_o \quad (5.4c)$$

Following the same procedure one can obtain:

$$w_{3'2} = \frac{\beta . K_y}{\delta} (w_o - w_4) - w_2 \quad (5.4d)$$

$$w_{3'2'} = \frac{\beta . K_y}{\delta} (w_{4'} - w_o) - w_{2'} \quad (5.4e)$$

From Eq. (5.4b) it follows:

$$w_{3'2'} = \frac{\beta . K_y}{\delta} (w_o - w_4) - w_{2'} \quad (5.4f)$$

Since $w_{3'4} - w_{3'} = w_o - w_4$ (5.4g)

and $w_{3'} - w_{3'4'} = w_{4'} - w_o$ (5.4h)

Hence $w_{3'4} = \beta \frac{K_y}{\delta} (w_{2'} - w_2) - w_4$ (5.5a)

and $w_{3'4'} = \beta . \frac{K_y}{\delta} (w_{2'} - w_2) - w_{4'}$ (5.5b)

The set of two equations (5.4e) and (5.4f) which have different values for the same external point, imposes a constraint $w_4 + w_{4'} - 2 w_o = 0$, near the simple support. It is, however, assumed in the present investigation that this constraint is valid near the simple support.

Now, putting the values of exterior mesh points outside the boundary of the plate in terms of deflections of interior mesh points into Eq. (1.5) and maintaining the condition of zero deflections along the edge, the finite difference equation for interior point near the left simple support is obtained as follows:

$$
\begin{aligned}
\nabla\nabla w = \Big[& \alpha A\left\{\beta \frac{k_Y}{\delta}(w_2' - w_2) - w_0 + 2w_0 + w_3\right\} - \alpha(2A + 2B_Y)\, w_1 \\
& + \alpha\beta \cdot \frac{B_Y}{2}\left\{-\beta\cdot\frac{k_Y}{\delta}(w_0 - w_4) + w_2 + \beta\cdot\frac{k_Y}{\delta}(w_0 - w_4) - w_2' + w_{32} - w_{32}'\right\} \\
& + \alpha B_Y (w_{12}' + w_{12}) - (2 + 2\alpha)\Big\{A w_1 - (2A + 2B_Y) w_0 \\
& \qquad + \beta\cdot\frac{B_Y}{2}(w_{12} - w_{12}') + B_Y (w_2' + w_2)\Big\} \\
& + \frac{\beta}{2}\Big\{A\left(-\beta\cdot\frac{k_Y}{\delta}(w_0 - w_4) + w_2 + w_{32} + \beta\cdot\frac{k_Y}{\delta}(w_4' - w_0) - w_2' - w_{32}'\right) \\
& - (2A + 2B_Y)(w_{12} - w_{12}') \\
& + \beta\cdot\frac{B_Y}{2}\Big(4w_0 - 2w_3 - 2\beta\frac{k_Y}{\delta}(w_2' - w_2) + 2w_0 - 2w_4 - 2w_4' + w_{34} \\
& \qquad + \beta\cdot\frac{k_Y}{\delta}(w_2' - w_2) - w_4 + \beta\cdot\frac{k_Y}{\delta}(w_2' - w_2) - w_4' + w_{34}'\Big) \\
& + B_Y (w_{14} - w_{14}')\Big\} + A(w_{12}' + w_{12}) - (2A + 2B_Y)(w_2 + w_2') \\
& + \beta\cdot\frac{B_Y}{2}(w_{14} - w_{14}') + B_Y (w_4' + 2w_0 + w_4)\Big] \\
& + D\chi^2\Big[\beta^2\left(\beta\cdot\frac{k_Y}{\delta}(w_2' - w_2) - w_0 + 2w_0 - 2w_1 + w_3\right) - (2 + 2\beta^2)(-2w_0 + w_1) \\
& + \frac{\beta}{2}\Big(-\beta\cdot\frac{k_Y}{\delta}(w_0 - w_4) + w_2 - 2w_{12} + w_{32} + \beta\cdot\frac{k_Y}{\delta}(w_0 - w_4) - w_2' \\
& + 2w_{12}' - w_{32}'\Big) + \left(-2w_2' + w_{12}' - 2w_2 + w_{12}\right)\Big] = \bar{q}_0 \lambda_Y^4 \qquad (5.6)
\end{aligned}
$$

Separating the coefficients associated with the different nodal point deflections, in the same way as in Section 5.1, Eq. (5.6) can be conveniently presented as in Fig. 10(b).

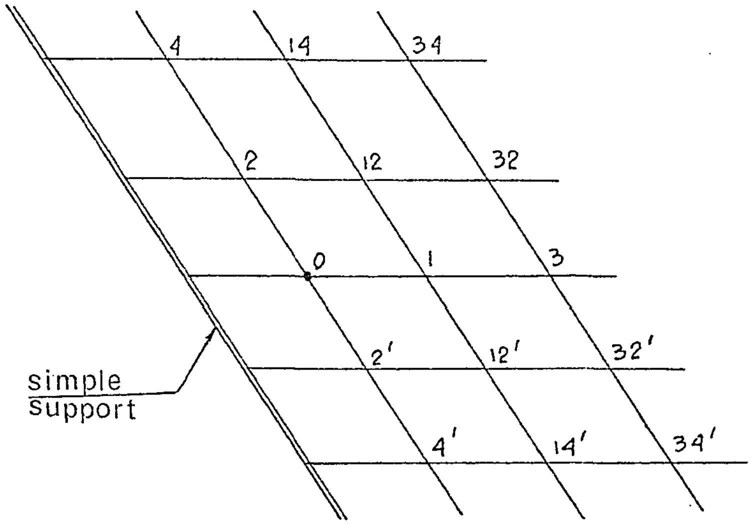

Fig. 10(a)

Interior Point near the left simple support.

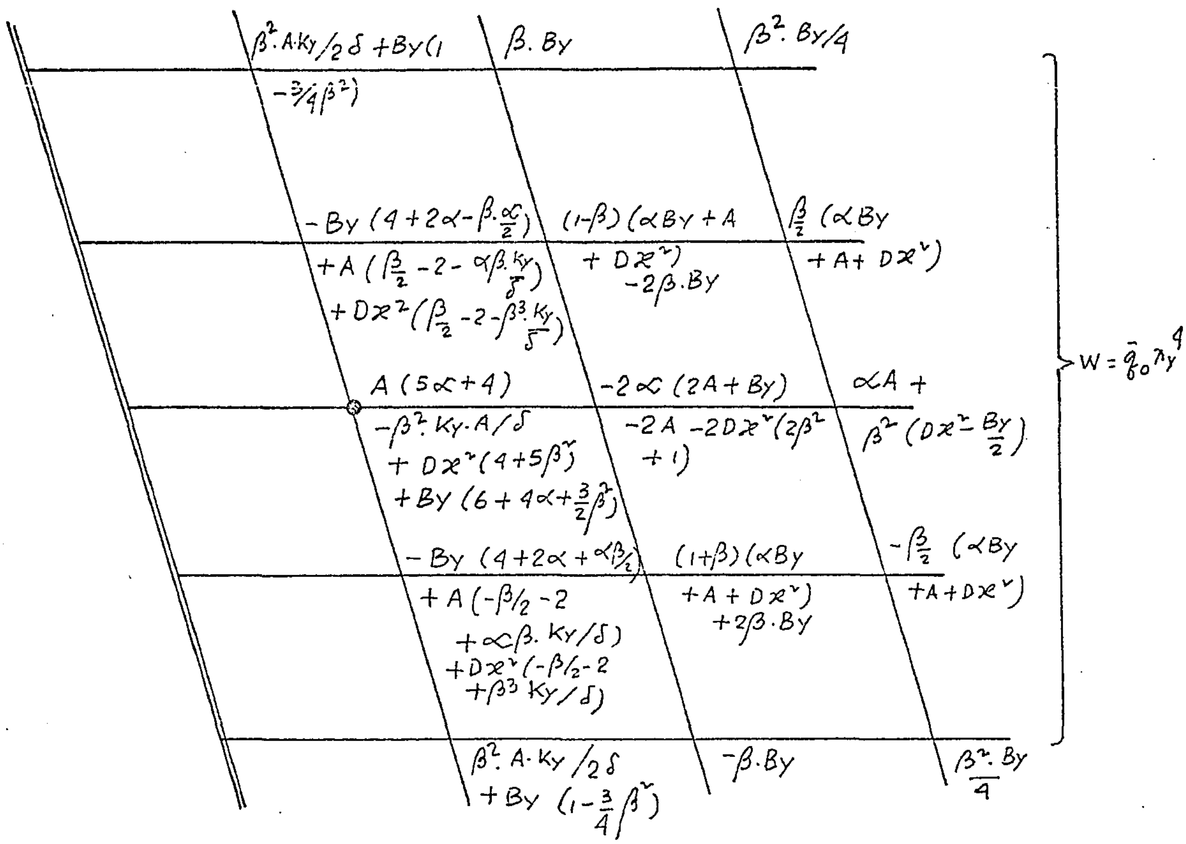

Fig. 10(b) Finite difference equation for Interior Point near the left simple support.

5.3 Interior Point near the Right Simple Support:

From the same boundary condition as in Sec. 5.2, external mesh points outside the boundary can be expressed as:

$$w_3 = \frac{K_y\beta}{\delta}(w_2 - w_{2'}) - w_0 \qquad (5.7a)$$

$$w_{32} = \frac{K_y\beta}{\delta}(w_4 - w_0) - w_2 \qquad (5.7b)$$

$$\left.\begin{aligned} w_{32'} &= \frac{K_y\beta}{\delta}(w_0 - w_{4'}) - w_{2'} \\ w_{32'} &= \frac{K_y\beta}{\delta}(w_4 - w_0) - w_{2'} \end{aligned}\right\} \qquad (5.7c)$$

$$w_{34} = \frac{K_y\beta}{\delta}(w_2 - w_{2'}) - w_4 \qquad (5.7d)$$

$$w_{34'} = \frac{K_y\beta}{\delta}(w_2 - w_{2'}) - w_{4'} \qquad (5.7e)$$

and condition of zero deflection along the edge yields:

$$w_{14} = w_{12} = w_1 = w_{12'} = w_{14'} = 0$$

Putting these values in Equation (5.1) one can deduce the finite difference Equation near right simple support as:

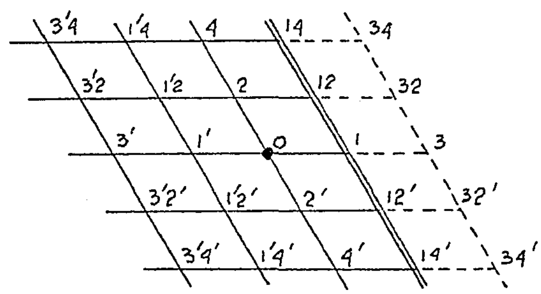

Fig. 11(a)

$$\nabla\nabla w = \Big[\alpha A\Big(w_{3'} + 2w_0 + \frac{K_y\beta}{\delta}(w_2 - w_{2'}) - w_0\Big) - \alpha(2A + 2B_y)(w_{1'})$$

$$+ \alpha\beta\frac{B_y}{2}\Big\{-w_{3'2} + w_{3'2'} + \frac{K_y\beta}{\delta}(w_4 - w_0) - w_2 - \frac{K_y\beta}{\delta}(w_4 - w_0) + w_{2'}\Big\}$$

$$+ \alpha . B_y(w_{1'2'} + w_{1'2}) - (2 + 2\alpha)\Big\{A(w_{1'}) - (2A + 2B_y)w_0$$

$$+ \beta . \frac{B_y}{2}(-w_{1'2} + w_{1'2'}) + B_y(w_{2'} + w_2)\Big\} + \frac{\beta}{2}\Big\{A\Big(-w_{3'2} + \frac{K_y\beta}{\delta}(w_4 - w_0)$$

$$-w_2 + w_{3'2'} - \frac{K_y\beta}{\delta}(w_0 - w_{4'}) + w_{2'}\Big)$$

$$- (2A + 2B_Y)(-w_{1'2} + w_{1'2'}) + \beta \cdot \frac{B_Y}{2}\Big(4w_0 - 2\frac{K_Y\beta}{\delta}(w_2 - w_{2'}) + 2w_0 - 2w_{3'}$$

$$- 2w_4 - 2w_{4'} + \frac{K_Y\beta}{\delta}(w_2 - w_{2'}) - w_4 + w_{3'4} + w_{3'4'} + \frac{K_Y}{\delta}\beta(w_2 - w_{2'}) - w_{4'}\Big)$$

$$+ B_Y(-w_{1'4} + w_{1'4'})\Big\} + A(w_{1'2'} + w_{1'2}) - (2A + 2B_Y)(w_2 + w_{2'})$$

$$+ \beta \cdot \frac{B_Y}{2}(-w_{1'4} + w_{1'4'}) + B_Y(w_{4'} + 2w_0 + w_4)\Big]$$

$$+ D\varkappa^2\Big[\beta^2\Big(w_{3'} - 2w_{1'} + 2w_0 + \frac{K_Y\beta}{\delta}(w_2 - w_{2'}) - w_0\Big) - (2 + 2\beta^2)(w_{1'} - 2w_0)$$

$$+ \frac{\beta}{2}\Big(-w_{3'2} + 2w_{1'2} + \frac{K_Y\beta}{\delta}(w_4 - w_0) - w_2 + w_{3'2'} - 2w_{1'2'} - \frac{K_Y\beta}{\delta}(w_4 - w_0)$$

$$+ w_{2'}\Big) + (w_{1'2'} - 2w_{2'} + w_{1'2} - 2w_2)\Big] = \bar{q}_0\lambda_Y^4 \qquad (5.8)$$

Separating the coefficients associated with the different nodal deflections in the same way as in Section 5.1, Equation (5.8) can be presented as in Fig. 11(b).

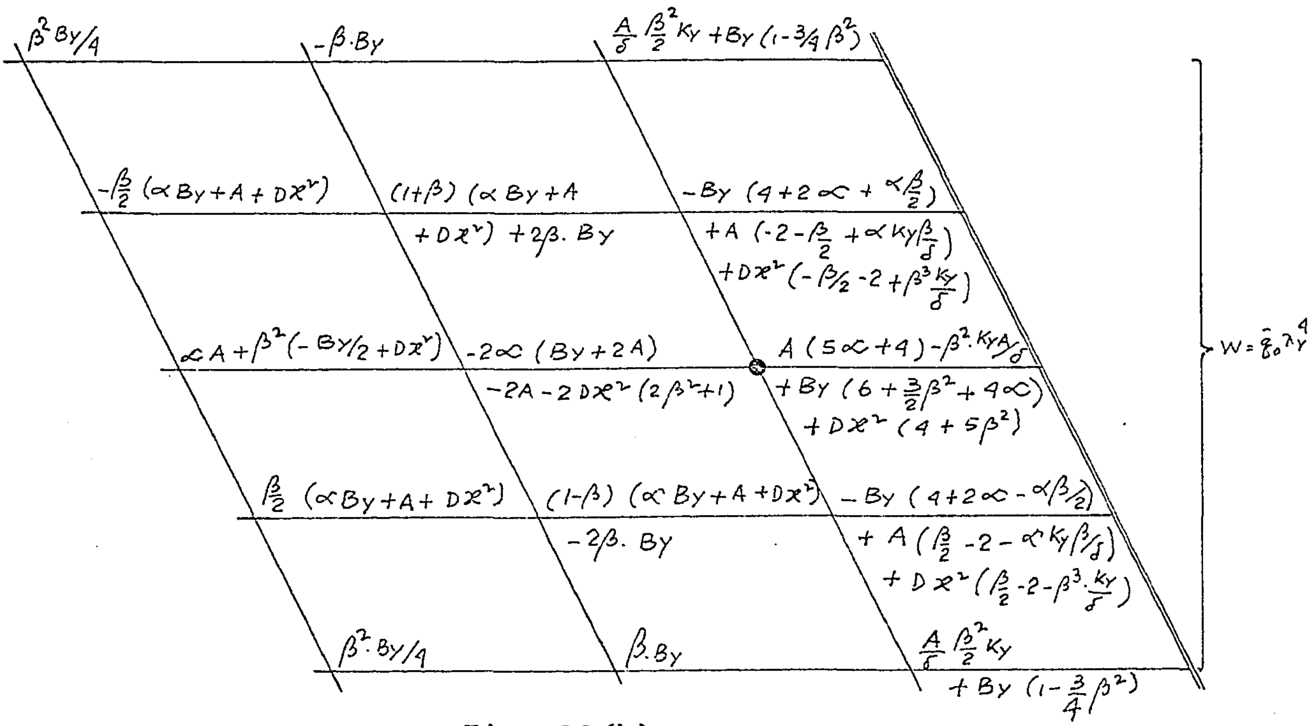

Fig. 11(b)

Finite difference equation for Interior Point near the right simple support.

5.4 Interior Point near the free edge:

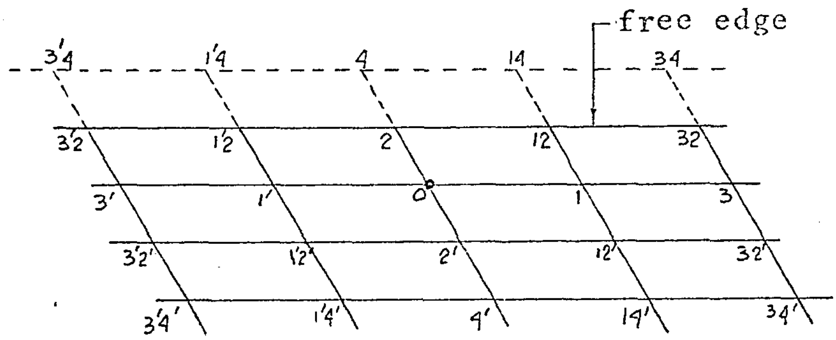

Fig. 12(a)

On the free edge at nodal points 3'2 , 1'2 , 2, 12 and 32, My = 0

$$(M_y)_{edge} = -B_y \left(\frac{\partial^2 w}{\partial y^2} + \mu_x \frac{\partial^2 w}{\partial x^2} \right) = 0$$

$$B_y \left(\frac{\partial^2 w}{\partial y^2} + \mu_x \frac{\partial^2 w}{\partial x^2} \right) = 0$$

Adding and subtracting $B_x \frac{\partial^2 w}{\partial x^2}$ to the above expression:

$$B_x \frac{\partial^2 w}{\partial x^2} + B_y \frac{\partial^2 w}{\partial y^2} - B_x \frac{\partial^2 w}{\partial x^2} + B_y \mu_x \frac{\partial^2 w}{\partial x^2} = 0$$

but $U = B_x \frac{\partial^2 w}{\partial x^2} + B_y \frac{\partial^2 w}{\partial y^2}$

Hence $U_{edge} = (B_x - B_y \mu_x) \left(\frac{\partial^2 w}{\partial x^2} \right)_{edge}$ (5.9)

For points 1'2, 2, and 12, from Eq. (5.9) one obtains

$$U_{1'2} = (B_x - B_y \mu_x) \frac{\mathcal{X}^2}{\lambda_y^2} (w_{3'2} - 2 w_{1'2} + w_2)$$

$$= \frac{\gamma}{\lambda_y^2} (w_{3'2} - 2 w_{1'2} + w_2) \qquad \text{(a)}$$

Similarly $U_2 = \frac{\gamma}{\lambda_y^2} (w_{1'2} - 2 w_2 + w_{12})$ (b) (5.10)

$$U_{12} = \frac{\gamma}{\lambda_y^2} (w_2 - 2 w_{12} + w_{32}) \qquad \text{(c)}$$

where $\gamma = (B_x - B_y/\mu_x)\,\chi^2$

Comparing Equation (4.9c), (4.9d), (4.9h) with Eq. (5.10) one obtains the following relations:

$$\frac{\beta}{2} B_y(-w_{3'4} + w_4) + B_y w_{1'4} = -B_y w_{1'} - \frac{\beta}{2} B_y (w_{3'} - w_0)$$

$$+ (2B_y + 2A - 2\gamma) w_{1'2} + (\gamma - A)(w_{3'2} + w_2) \qquad (5.11a)$$

$$\frac{\beta}{2} B_y(-w_{1'4} + w_{14}) + B_y w_4 = -B_y w_0 - \frac{\beta}{2} B_y (w_{1'} - w_1)$$

$$+ (2B_y + 2A - 2\gamma) w_2 + (\gamma - A)(w_{1'2} + w_{12}) \qquad (5.11b)$$

$$\frac{\beta}{2} B_y(-w_4 + w_{34}) + B_y w_{14} = -B_y w_1 - \frac{\beta}{2} B_y (w_0 - w_3)$$

$$+ (2B_y + 2A - 2\gamma) w_{12} + (\gamma - A)(w_2 + w_{32}) \qquad (5.11c)$$

From Eq. (5.11) one can deduce:

$$\beta^2 \frac{B_y}{4}(w_{3'4} + w_{34} - 2w_4) + \beta B_y(-w_{1'4} + w_{14}) + B_y w_4$$

$$= -B_y w_0 + (\gamma - A)(w_{1'2} + w_{12}) + (2B_y + 2A - 2\gamma) w_2$$

$$+ \beta^2 \frac{B_y}{4}(w_{3'} - 2w_0 + w_3) + \frac{\beta}{2}(2B_y + 2A - 2\gamma)(w_{12} - w_{1'2})$$

$$+ \frac{\beta}{2}(\gamma - A)(w_{32} - w_{3'2}) \qquad (5.12)$$

With these values of nodal deflections outside the boundary Eq. (5.1) reduces to:

$$\nabla\nabla w = \Big[\alpha A (w_{3'} + 2w_0 + w_3) - \alpha(2A + 2B_y)(w_{1'} + w_1)$$

$$+ \beta \frac{\alpha}{2} B_y (-w_{3'2} + w_{3'2'} + w_{32} - w_{32'}) + \alpha B_y (w_{1'2'} + w_{1'2} + w_{12'} + w_{12})$$

$$- (2 + 2\alpha)\Big\{ A(w_{1'} + w_1) - (2A + 2B_y) w_0 + \frac{\beta}{2} B_y (-w_{1'2} + w_{12} + w_{1'2'} - w_{12'})$$

$$+ B_y\,(w_2' + w_2)\Big\} + \frac{\beta}{2} A \left(-w_3'{}_2 + w_{32} + w_3'{}_2' - w_{32}'\right)$$

$$- \frac{\beta}{2}(2B_y + 2A)\left(-w_1'{}_2 + w_{12} + w_1'{}_2' - w_{12}'\right) + \beta^2 \cdot \frac{B_y}{4}\left(-2w_3' + 4w_0 + w_3'{}_4' + w_{34}' - 2w_3\right.$$

$$\left. - 2w_4'\right) + \frac{\beta}{2} B_y \left(w_1'{}_4' - w_{14}'\right) + A\left(w_1'{}_2' + w_{12}' + w_1'{}_2 + w_{12}\right) - (2B_y + 2A)(w_2'$$

$$+ w_2) + \frac{\beta}{2} B_y \left(w_1'{}_4' - w_{14}'\right) + B_y\left(w_4' + 2w_0\right) - B_y(w_0)$$

$$+ (\gamma - A)\left(w_1'{}_2 + w_{12}\right) + (2B_y + 2A - 2\gamma)\, w_2 + \beta^2 \cdot \frac{B_y}{4}\left(w_3' - 2w_0 + w_3\right)$$

$$+ \frac{\beta}{2}(2B_y + 2A - 2\gamma)\left(w_{12} - w_1'{}_2\right) + \frac{\beta}{2}(\gamma - A)\left(w_{32} - w_3'{}_2\right)\Big]$$

$$+ D\chi^2\Big[\beta^2\left(w_3' - 2w_1' + 2w_0 - 2w_1 + w_3\right) - (2 + 2\beta^2)\left(w_1' - 2w_0 + w_1\right)$$

$$+ \frac{\beta}{2}\left(-w_3'{}_2 + 2w_1'{}_2 - 2w_{12} + w_{32} + w_3'{}_2' - 2w_1'{}_2' - w_{32}' + 2w_{12}'\right)$$

$$+ w_1'{}_2' - 2w_2' + w_{12}' + w_1'{}_2 - 2w_2 + w_{12}\Big] = \bar{q}_0 \lambda_y^4 \qquad (5.13)$$

Separating the coefficients of deflections; Eq. (5.13) can be presented as in Fig. 12(b).

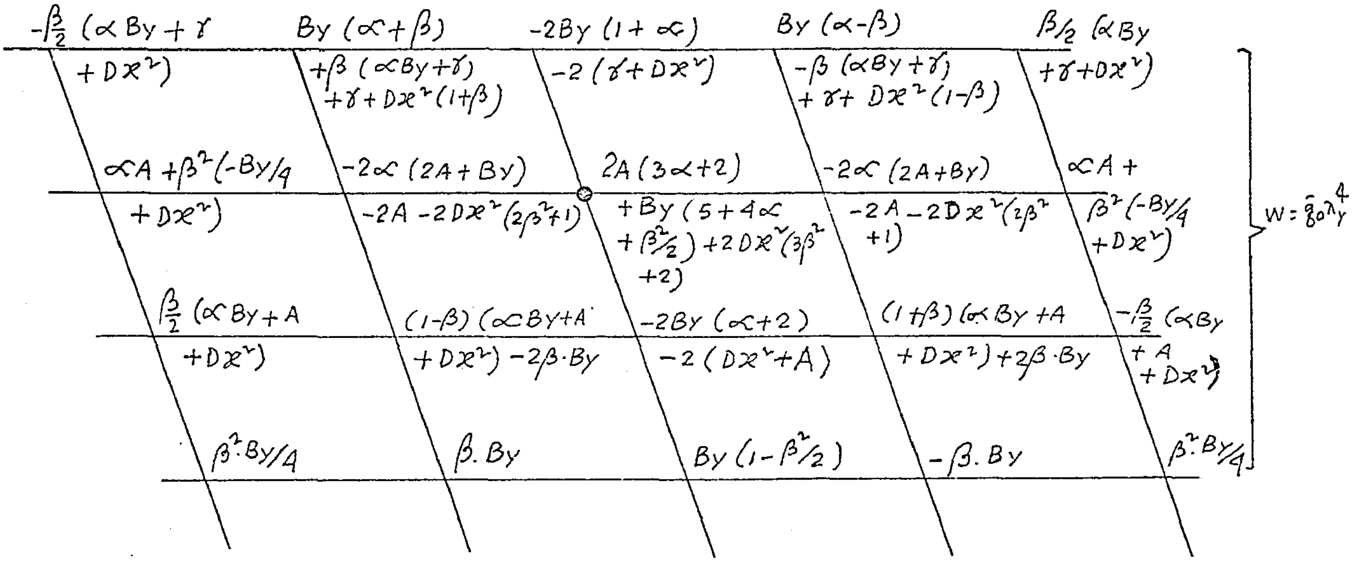

Fig. 12(b) Finite difference equation for Interior Point near the free edge.

5.5 Interior Point near the Acute Corner:

From the boundary conditions of Section 5.2 and 5.4, it follows that when the exterior points (Eq. 5.4 (b, c, d, g, h)) outside the boundary

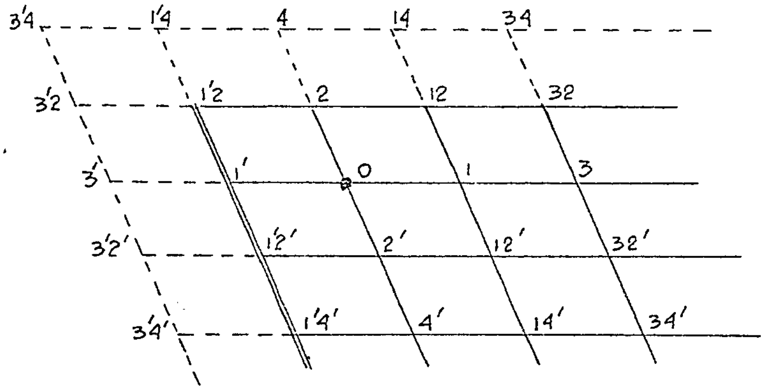

Fig. 13(a)

Interior Point on Acute Corner

and (Eq. 5.11(a, b, c), (5.12)) are put into Eq. (5.1), finite difference equation for interior point near the acute corner is obtained as shown below:

$$\nabla\nabla w = \Big[\alpha A\Big\{\beta\cdot\frac{K_y}{\delta}(w_{2'}-w_2)+w_0+w_3\Big\} - \alpha\,(2A+2B_y)\,w_1$$

$$+\beta\cdot\frac{\alpha}{2}B_y\Big(-\beta\cdot\frac{K_y}{\delta}(w_{4'}-w_0)+w_2+\beta\cdot\frac{K_y}{\delta}(w_{4'}-w_0)-w_{2'}+w_{32}-w_{32'}\Big)$$

$$+\alpha B_y\,(w_{12'}+w_{12}) - (2+2\alpha)\Big\{A w_1 - (2A+2B_y)w_0 + \beta\cdot\frac{B_y}{2}(w_{12}-w_{12'})$$

$$+B_y\,(w_{2'}+w_2)\Big\} + \frac{\beta}{2}\Big\{A\Big(-\beta\cdot\frac{K_y}{\delta}(w_{4'}-w_0)+w_2+w_{32}+\beta\cdot\frac{K_y}{\delta}(w_{4'}-w_0)$$

$$-w_{2'}-w_{32'}\Big) - (2B_y+2A)(w_{12}-w_{12'}) + \beta\cdot\frac{B_y}{2}\Big(4w_0-2w_3-2\beta\cdot\frac{K_y}{\delta}(w_{2'}-w_2)$$

$$+2w_0+\beta\cdot\frac{K_y}{\delta}(w_{2'}-w_2)-w_{4'}+w_{34'}-2w_{4'}\Big) - B_y\,w_{14'}\Big\}\Big]$$

$$+A(w_{12'}+w_{12}) - (2B_y+2A)(w_{2'}+w_2) - \frac{\beta}{2}B_y\,w_{14'} + B_y\,(w_{4'}+2w_0)$$

$$-B_y w_0 + (\gamma-A)\,w_{12} + (2B_y+2A-2\gamma)\,w_2 + \beta^2\cdot\frac{B_y}{4}\Big\{\beta\cdot\frac{K_y}{\delta}(w_{2'}-w_2)-w_0-2w_0+w_3\Big\}$$

$$+ \frac{\beta}{2}(2B_y + 2A - 2\gamma)\, w_{12} + \frac{\beta}{2}(\gamma - A)\left(w_{32} - \beta \cdot \frac{K_y}{\delta}(w_4' - w_0) + w_2 \right) \Bigg]$$

$$+ D\chi^2 \Bigg[\beta^2 \left\{ \beta \cdot \frac{K_y}{\delta}(w_2' - w_2) - w_0 + 2w_0 - 2w_1 + w_3 \right\} - (2 + 2\beta^2)(-2w_0 + w_1)$$

$$+ \frac{\beta}{2} \Big\{ -\beta \cdot \frac{K_y}{\delta}(w_4' - w_0) + w_2 - 2w_{12} + w_{32} + \beta \cdot \frac{K_y}{\delta}(w_4' - w_0) - w_2'$$

$$- w_{32}' + 2w_{12}' \Big\} - 2w_2' + w_{12}' - 2w_2 + w_{12} \Bigg] = \bar{q}_0 \lambda_y^4 \qquad (5.14)$$

Separating the coefficients of deflections, Eq. 5.14 can be conveniently presented as in Fig. 13(b).

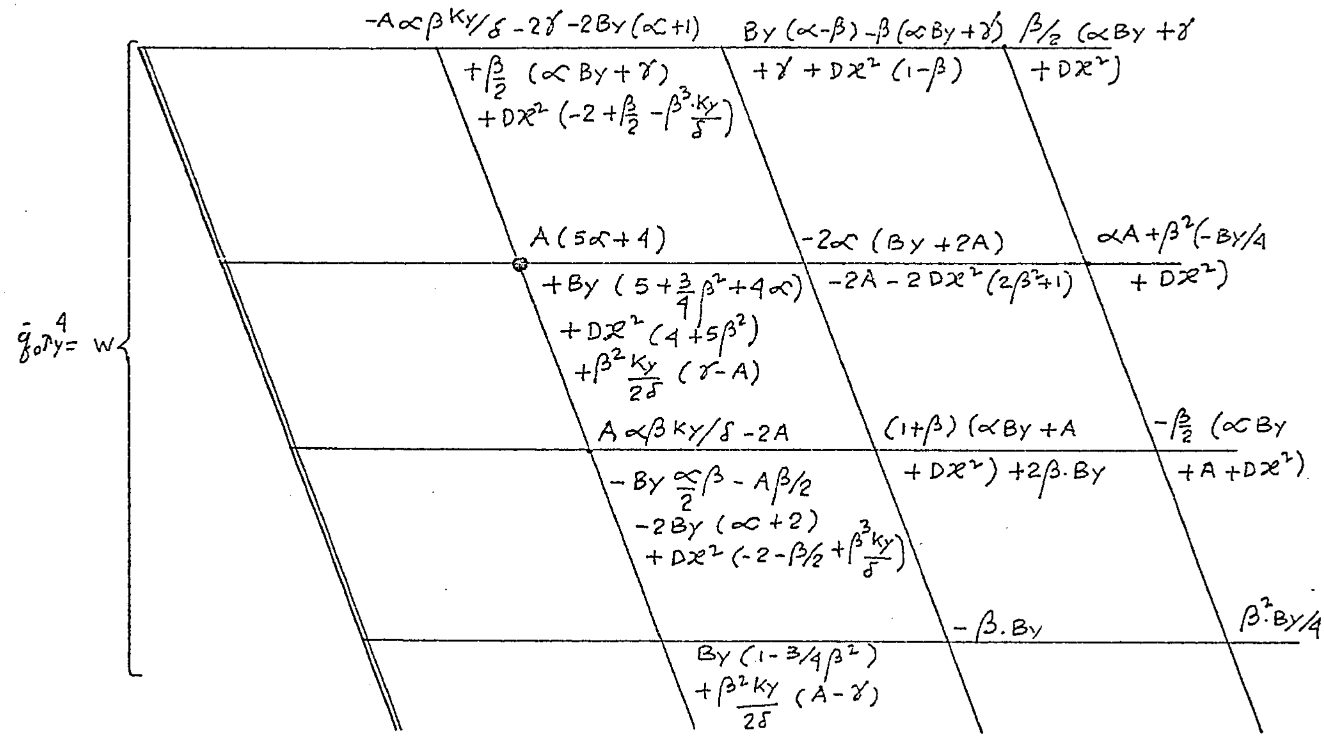

Fig. 13(b)

Finite difference equation for Interior Point near the Acute Corner.

5.6 Interior Point near the Obtuse Corner:

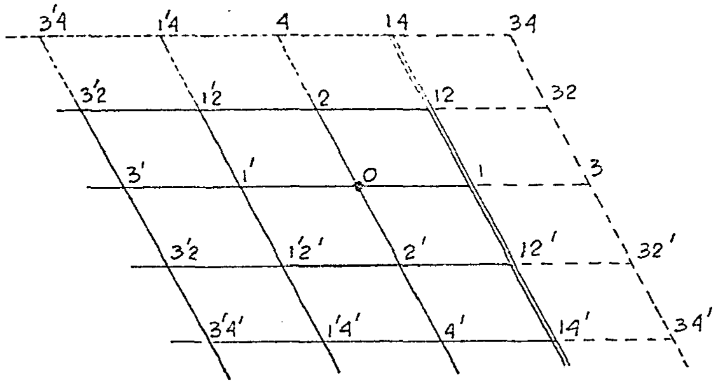

Fig. 14(a)

Interior Point near the Obtuse Corner

Putting the values of nodal points outside the boundary (Eq. 5.7(a, b, c, d, e), Eq. 5.11 (a, b, c) and Eq. (5.12)) in Eq. (5.1) one can deduce the finite difference equation for Interior Point near the obtuse corner as:

$$
\begin{aligned}
\nabla\nabla w = \Big[& \alpha A \left(w_{3'} + 2w_0 + \frac{K_y\beta}{\delta}(w_2 - w_{2'}) - w_0 \right) - \alpha (2B_y + 2A) w_{1'} \\
& + \beta \frac{\alpha}{2} B_y \left(-w_{3'2} + w_{3'2'} + \frac{K_y\beta}{\delta}(w_0 - w_{4'}) - w_2 - \frac{K_y\beta}{\delta}(w_0 - w_{4'}) + w_{2'} \right) \\
& + \alpha B_y (w_{1'2'} + w_{1'2}) - (2 + 2\alpha)\Big\{ A w_{1'} - (2B_y + 2A) w_0 + \frac{\beta}{2} B_y (-w_{1'2} + w_{1'2'}) \\
& + B_y (w_{2'} + w_2) + \frac{\beta}{2}\Big\{ A \left(-w_{3'2} + \frac{K_y\beta}{\delta}(w_0 - w_{4'}) - w_2 + w_{3'2'} - \frac{K_y\beta}{\delta}(w_0 - w_{4'}) + w_{2'} \right) \\
& - (2B_y + 2A)(-w_{1'2} + w_{1'2'}) \Big\} + \frac{\beta^2 B_y}{4}\Big\{ -2w_{3'} + 4w_0 + w_{3'4'} + \frac{K_y\beta}{\delta}(w_2 - w_{2'}) - w_{4'} \\
& - 2\frac{K_y\beta}{\delta}(w_2 - w_{2'}) + 2w_0 - 2w_{4'} \Big\} + \frac{\beta}{2} B_y w_{1'4'} + A(w_{1'2'} + w_{1'2}) \\
& - (2B_y + 2A)(w_{2'} + w_2) + \frac{\beta}{2} B_y w_{1'4'} + B_y (w_{4'} + 2w_0) \\
& - B_y w_0 + (\gamma - A) w_{1'2} + (2A + 2B_y - 2\gamma) w_2 + \frac{\beta^2 B_y}{4}\left(w_{3'} - 2w_0 + \frac{K_y\beta}{\delta}(w_2 - w_{2'}) - w_0 \right) \\
& + \frac{\beta}{2}(\gamma - A)\left(\frac{K_y\beta}{\delta}(w_0 - w_{4'}) - w_2 - w_{3'2} \right) + \frac{\beta}{2}(2A + 2B_y - 2\gamma)(-w_{1'2})
\end{aligned}
$$

$$+ D\chi^2\Big[\beta^2\Big(w_3' - 2w_1' + 2w_0 + \frac{K_y}{\delta}\beta(w_2 - w_2') - w_0\Big) - (2 + 2\beta^2)(w_1' - 2w_0)$$

$$+ \frac{\beta}{2}\Big(-w_{3'2} + 2w_{1'2} + \frac{K_y\beta}{\delta}(w_0 - w_4') - w_2 + w_{3'2'} - 2w_{1'2'} - \frac{K_y\beta}{\delta}(w_0 - w_4') + w_2'\Big)$$

$$+ w_{1'2'} - 2w_2' + w_{1'2} - 2w_2\Big] = \bar{q}_0 \lambda_y^4 \qquad (5.15)$$

Separating the coefficients of deflections associated with different nodal points Eq. (5.15) can be conveniently presented as in Fig. 14(b).

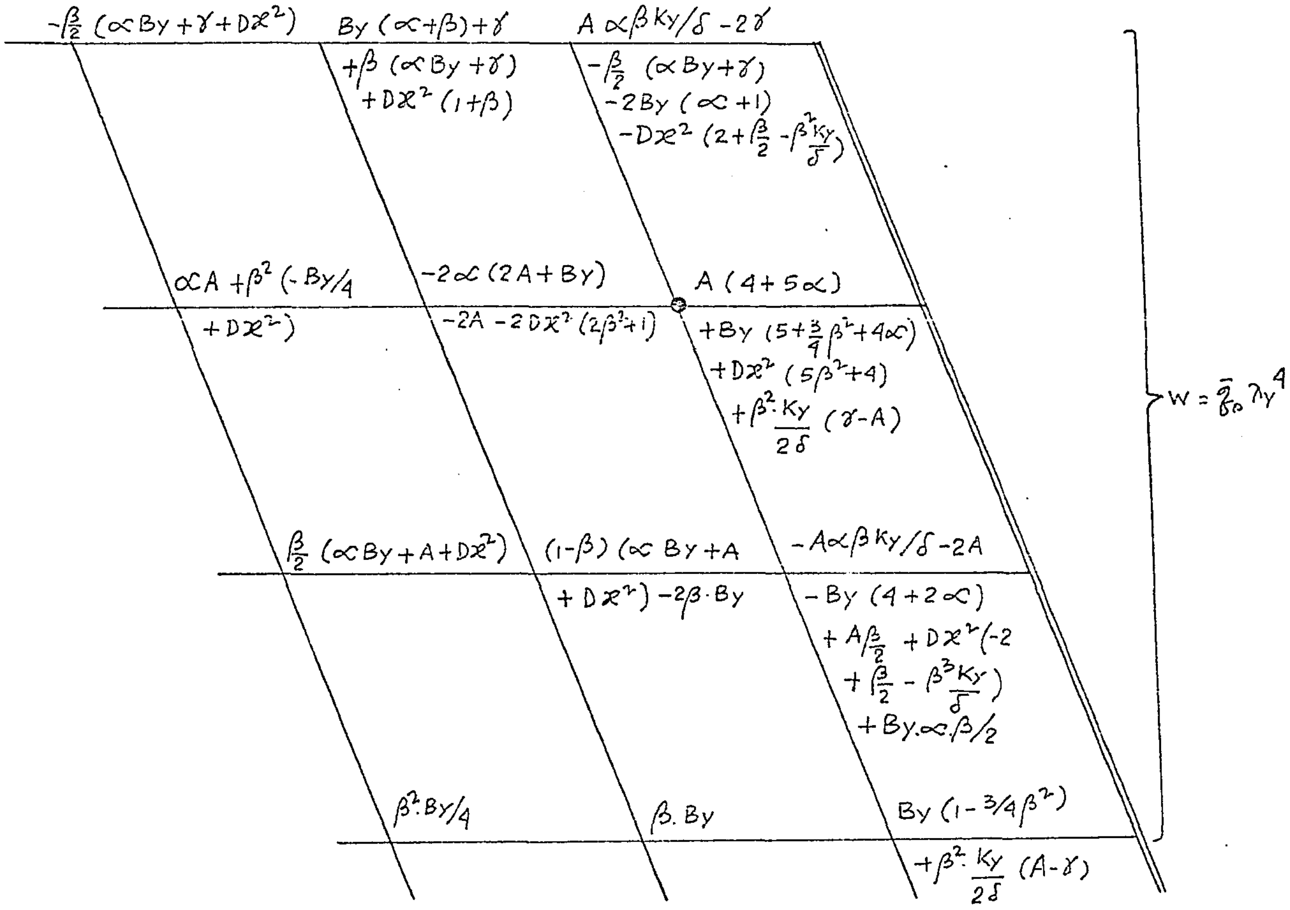

Fig. 14(b)

Finite difference Equation for Interior Point near the Obtuse Corner

5.7 General Free Edge Point:

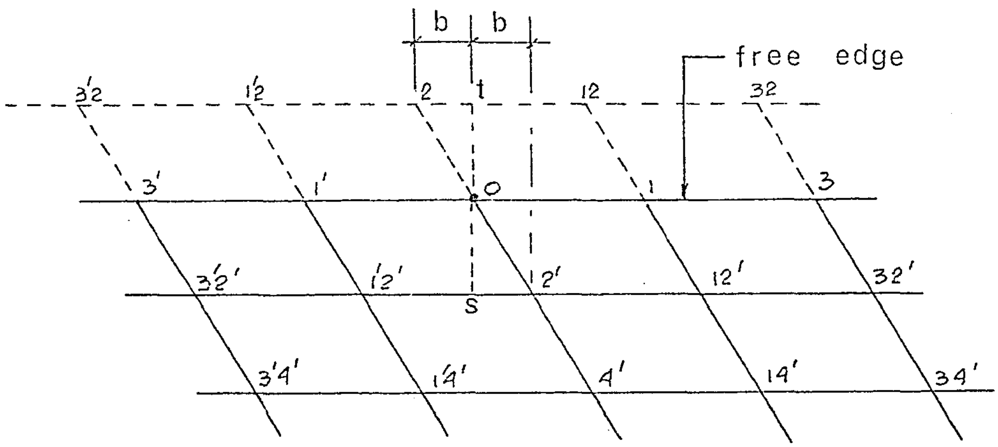

Fig. 15(a) General free edge point

For the General Point on the free edge the second order differential equation (4.4b) is taken as the governing equation, i.e.

$$\nabla\nabla w = \frac{\partial^2 U}{\partial x^2} + \frac{\partial^2 U}{\partial y^2} + D\frac{\partial^2 Y}{\partial x^2} = q(x,y)$$

Following Eq. (4.6a) and (4.6c) one can deduce:

$$\frac{1}{\lambda_y^2}\Big[\alpha\,(U_{1'} + U_1) - (2+2\alpha)\,U_o + \frac{\beta}{2}\,(-U_{1'2} + U_{12} + U_{1'2'} - U_{12'})$$

$$+ U_{2'} + U_2\Big] + \frac{D\chi^2}{\lambda_y^2}\Big[Y_{1'} - 2Y_o + Y_1\Big] = \bar{q}_o \qquad (5.16)$$

From Eq. (5.9) for Points $1', o, 1$ one obtains the following relations:

$$\left.\begin{aligned} U_{1'} &= \frac{\gamma}{\lambda_y^2}\,(w_{3'} - 2w_{1'} + w_o) && \text{(a)}\\ U_o &= \frac{\gamma}{\lambda_y^2}\,(w_{1'} - 2w_o + w_1) && \text{(b)}\\ U_1 &= \frac{\gamma}{\lambda_y^2}\,(w_o - 2w_1 + w_3) && \text{(c)} \end{aligned}\right\} \qquad (5.17)$$

Since $M_y = 0$ on the edge

$$-B_y \left(\frac{\partial^2 w}{\partial y^2} + \mu_x \frac{\partial^2 w}{\partial x^2} \right) = 0$$

or $$\left(\frac{\partial^2 w}{\partial y^2} \right)_{edge} = -\mu_x \left(\frac{\partial^2 w}{\partial x^2} \right)_{edge}$$

Following equation (4.3) one can now deduce:

$$Y_1' = -\mu_x X_1'$$

$$= -\mu_x \frac{\varkappa^2}{\lambda_y^2} \left(w_3' - 2w_1' + w_0 \right)$$

$$Y_0 = -\mu_x \frac{\varkappa^2}{\lambda_y^2} \left(w_1' - 2w_0 + w_1 \right) \qquad (5.18)$$

$$Y_1 = -\mu_x \frac{\varkappa^2}{\lambda_y^2} \left(w_0 - 2w_1 + w_3 \right)$$

Again, from the boundary condition of free edge, i.e. vertical reaction

$(V_y)_{edge} = 0$ Eq. (1.9g) and Eq. (1.8) lead to:

$$-B_y \left[\frac{\partial^3 w}{\partial y^3} + \left(\frac{4C}{B_y} + \mu_x \right) \frac{\partial^3 w}{\partial x^2 \partial y} \right] = 0$$

or $$B_y \frac{\partial^3 w}{\partial y^3} + \left(2H - B_x \mu_y \right) \frac{\partial^3 w}{\partial x^2 \partial y} = 0 \qquad (5.19)$$

Since $$U = B_x \frac{\partial^2 w}{\partial x^2} + B_y \frac{\partial^2 w}{\partial y^2}$$

$$\frac{\partial U}{\partial y} = B_x \frac{\partial^3 w}{\partial x^2 \partial y} + B_y \frac{\partial^3 w}{\partial y^3}$$

Eq. (5.19) can now be written as:

$$\frac{\partial U}{\partial y} + \left(2H - B_x \mu_y - B_x \right) \frac{\partial^3 w}{\partial x^2 \partial y} = 0 \qquad (5.20)$$

Let $F(x,y)$ be a function of x and y. From general edge point 0, (Fig. 15(a)) a perpendicular is drawn parallel to y axis touching the network line at t and s respectively. Ref. [7].

Hence $b = \lambda y \tan\phi$

At Point 0, $\left(\frac{\partial F}{\partial y}\right)_0 = \frac{F_t - F_s}{2\lambda y}$

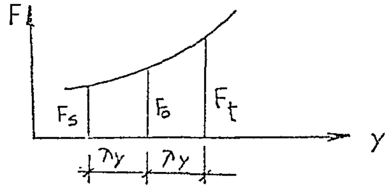

Fig. 15(b)

By interpolation:

$$F_t = F_2 + \frac{F_{12} - F_{1'2}}{2\lambda x} b$$

$$= F_2 + \frac{1}{2}\beta \, (F_{12} - F_{1'2})$$

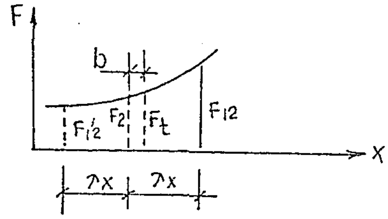

Fig. (15c)

Similarly

$$F_s = F_2' - \frac{1}{2}\beta \, (F_{12}' - F_{1'2}')$$

Hence $\left(\frac{\partial F}{\partial y}\right)_0 = \frac{1}{2\lambda y}\left[\left\{F_2 + \frac{1}{2}\beta \, (F_{12} - F_{1'2}\right\} - \left\{F_2' - \frac{1}{2}\beta \, (F_{12}' - F_{1'2}')\right\}\right]$ (5.21)

Proceeding in the same way, for the function U , one can deduce:

$$\left(\frac{\partial U}{\partial y}\right)_0 = \frac{1}{2\lambda y}\left[\left\{U_2 + \frac{1}{2}\beta \, (U_{12} - U_{1'2})\right\} - \left\{U_2' - \frac{1}{2}\beta \, (U_{12}' - U_{1'2}')\right\}\right] \quad (5.22)$$

Similar to Eq. (5.22)

$$\left\{\frac{\partial^3 w}{\partial x^2 \partial y}\right\}_0 = \left\{\frac{\partial}{\partial y}\left(\frac{\partial^2 w}{\partial x^2}\right)\right\}_0$$

$$= \frac{\partial}{\partial y}\left\{\frac{\varkappa^2}{\lambda y^2} \, (w_1' - 2w_0 + w_1)\right\}$$

$$= \frac{\varkappa^2}{2\lambda y^3}\left[\left\{w_{1'2} + \frac{1}{2}\beta \, (w_2 - w_{3'2})\right\} - \left\{w_{1'2}' - \frac{1}{2}\beta \, (w_2' - w_{3'2}')\right\}\right.$$

$$- 2\left\{w_2 + \frac{1}{2}\beta \, (w_{12} - w_{1'2})\right\} + 2\left\{w_2' - \frac{1}{2}\beta \, (w_{12}' - w_{1'2}')\right\}$$

$$+ \left\{w_{12} + \frac{1}{2}\beta \, (w_{32} - w_2)\right\}$$

$$\left. - \left\{w_{12}' - \frac{1}{2}\beta \, (w_{32}' - w_2')\right\}\right] \quad (5.23)$$

Putting the values of Eq. (5.22) and (5.23) into Eq. (5.20) one obtains:

$$U_2 + \frac{1}{2}\beta\,(U_{12} - U_1'2) - U_2' + \frac{1}{2}\beta\,(U_{12}' - U_1'2)$$

$$= -\frac{\psi}{\lambda y^2}\Big[\{W_1'2 + \frac{1}{2}\beta\,(W_2 - W_3'2)\} - \{W_1'2' - \frac{1}{2}\beta\,(W_2' - W_3'2')\}$$

$$- 2\{W_2 + \frac{1}{2}\beta\,(W_{12} - W_1'2)\} + 2\{W_2' - \frac{1}{2}\beta\,(W_{12}' - W_1'2')\}$$

$$+ \{W_{12} + \frac{1}{2}\beta\,(W_{32} - W_2)\}$$

$$- \{W_1'2 - \frac{1}{2}\beta\,(W_{32}' - W_2')\}\Big] \qquad (5.24)$$

where $\psi = (2H - B_x\mu_y - B_x)\chi^2$.

Putting the value of U_2 from Eq. (5.24) into Eq. (5.16), the governing equation for general edge point is obtained as follows:

$$\nabla\nabla w = \frac{1}{2}\lambda y^2\Big[2U_2' - \beta\,(U_{12}' - U_1'2')\Big] + \lambda y^2 \frac{\alpha}{2}\,(U_1' + U_1) - \lambda y^2 (1+\alpha) U_0$$

$$- \frac{\psi}{2}\Big[W_1'2 + \frac{1}{2}\beta\,(W_2 - W_3'2) - \{W_1'2' - \frac{1}{2}\beta\,(W_2' - W_3'2')\}$$

$$- 2\{W_2 + \frac{1}{2}\beta\,(W_{12} - W_1'2)\} + 2\{W_2' - \frac{1}{2}\beta\,(W_{12}' - W_1'2')\}$$

$$+ \{W_{12} + \frac{1}{2}\beta\,(W_{32} - W_2)\} - \{W_{12}' - \frac{1}{2}\beta\,(W_{32}' - W_2')\}\Big]$$

$$+ D\chi^2 \frac{\lambda y^2}{2}\,(Y_1' - 2Y_0 + Y_1) = \frac{\bar{q}_0 \lambda y^4}{2} \qquad (5.25)$$

Comparing Eq. (5.17) with (4.9a), (4.7) and (4.9b) one can deduce the following relations:

$$\frac{\beta}{2} B_y\,(-W_3'2 + W_2) + B_y W_1'2 = -B_y W_1'2' - \frac{\beta}{2} B_y\,(W_3'2' - W_2') + (2A + 2B_y - 2\gamma) W_1'$$

$$+ (\gamma - A)\,(W_3' + W_0) \qquad \text{(a)}$$

$$\frac{\beta}{2} B\gamma (-w_1'2 + w_{12}) + B\gamma w_2 = -B\gamma w_2' - \frac{\beta}{2} B\gamma (w_1'2' - w_{12}') + (2A + 2B\gamma - 2\gamma) w_0$$
$$+ (\gamma - A)(w_1' + w_1) \qquad \text{(b)}$$

$$\frac{\beta}{2} B\gamma (-w_2 + w_{32}) + B\gamma w_{12} = -B\gamma w_{12}' - \frac{\beta}{2} B\gamma (w_2' - w_{32}') + (2A + 2B\gamma - 2\gamma) w_1$$
$$+ (\gamma - A)(w_0 + w_3) \qquad \text{(c)} \quad (5.26)$$

and $-\psi\left[w_1'2 + \frac{1}{2}\beta (w_2 - w_3'2) - 2w_2 - \beta (w_{12} - w_1'2) + w_{12} + \frac{1}{2}\beta (w_{32} - w_2)\right]$

$$= \frac{\psi}{B\gamma}\Big[-B\gamma w_1'2' - \frac{\beta}{2} B\gamma (w_3'2' - w_2') + (2A + 2B\gamma - 2\gamma) w_1'$$
$$+ (\gamma - A)(w_3' + w_0) - 2\Big\{-B\gamma w_2' - \frac{\beta}{2} B\gamma (w_1'2' - w_{12}')$$
$$+ (2A + 2B\gamma - 2\gamma) w_0 + (\gamma - A)(w_1' + w_1)\Big\}$$
$$- B\gamma w_{12}' - \frac{\beta}{2} B\gamma (w_2' - w_{32}') + (2A + 2B\gamma - 2\gamma) w_1$$
$$+ (\gamma - A)(w_0 + w_3)\Big] \qquad \text{(d)}$$

From the relations of Eq. (5.17), (5.18), (5.26) and (4.9) finite difference equations (5.25) for general edge point reduces to:

$$\nabla\nabla w = A(w_1'2' + w_{12}') - (2A + 2B\gamma) w_2' + \frac{\beta}{2} B\gamma (-w_1' + w_1 + w_1'4' - w_{14}')$$
$$+ B\gamma (w_0 + w_4') - \frac{\beta}{2}\Big\{A(w_2' + w_{32}') - (2A + 2B\gamma) w_{12}'$$
$$+ \frac{\beta}{2} B\gamma (-w_0 + w_3 + w_4' - w_{34}') + B\gamma (w_1 + w_{14}') - A(w_3'2' + w_2')$$
$$+ (2A + 2B\gamma) w_1'2' - \frac{\beta}{2} B\gamma (-w_3' + w_0 + w_3'4' - w_4') - B\gamma (w_1' + w_1'4')\Big\}$$
$$+ \frac{\alpha\gamma}{2}(w_3' - 2w_1' + w_0) + \frac{\alpha\gamma}{2}(w_0 - 2w_1 + w_3) - \gamma(1 + \alpha)(w_1' - 2w_0 + w_1)$$
$$+ \frac{\psi}{2}\Big\{w_1'2' - \frac{1}{2}\beta (w_2' - w_3'2')\Big\} - \psi\Big\{w_2' - \frac{1}{2}\beta (w_{12}' - w_1'2')\Big\}$$
$$+ \frac{\psi}{2}\Big\{w_{12}' - \frac{1}{2}\beta (w_{32}' - w_2')\Big\}$$
$$- \frac{\psi}{2B\gamma}\Big[-B\gamma w_1'2' - \frac{\beta}{2} B\gamma (w_3'2' - w_2') + (2A + 2B\gamma - 2\gamma) w_1'$$

$$+ (\gamma - A)(w_{3'} + w_0) - 2\Big\{ -B_y w_{2'} - \frac{\beta}{2} B_y (w_{1'2'} - w_{12'})$$

$$+ (2A + 2B_y - 2\gamma) w_0 + (\gamma - A)(w_{1'} + w_1)\Big\} - B_y w_{12'} - \frac{\beta}{2} B_y (w_{2'} - w_{32'})$$

$$+ (2A + 2B_y - 2\gamma) w_1 + (\gamma - A)(w_0 + w_3)\Big]$$

$$-D\chi^4 \frac{\mu_x}{2} (w_{3'} - 4w_{1'} + 6w_0 - 4w_1 + w_3) = \frac{\bar{q}_0 \lambda_y^4}{2} \qquad (5.27)$$

Separating the coefficient of deflections associated with different nodal points Eq. (5.27) can be presented as in Fig. 15(d).

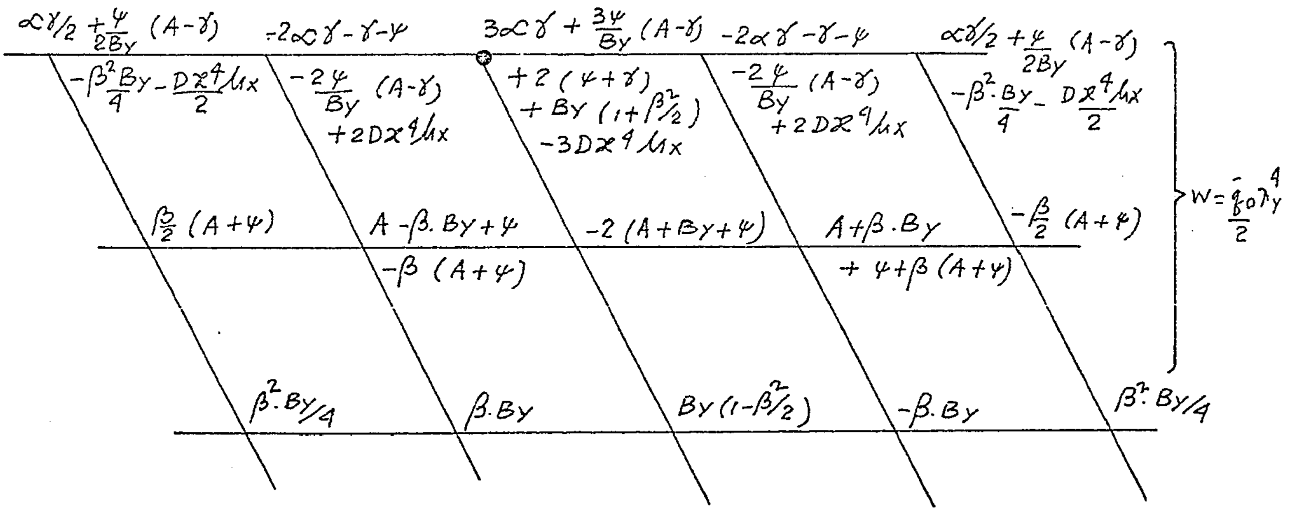

Fig. 15(d)

Finite difference Equation for general free edge point.

5.8 Edge point near the Acute Corner:

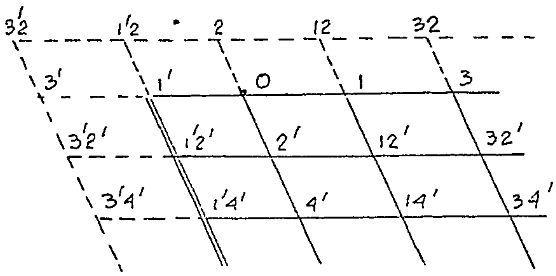

Fig. 16(a)

From the boundary conditions of Sec. 5.2 and 5.7 it follows:

$$W_{1'} = W_{1'2'} = W_{1'4'} = 0$$

$$W_{3'} = \frac{K_Y\beta}{\delta}(W_{2'} - W_2) - \frac{K_Y}{\delta}W_{1'2} - W_0 \qquad \text{(a)}$$

$$W_{3'4'} = \frac{K_Y\beta}{\delta}(W_{2'} - W_2) - \frac{K_Y}{\delta}W_{1'2} - W_{4'} \qquad \text{(b)}$$

$$W_{3'2'} = \frac{K_Y\beta}{\delta}(W_{4'} - W_0) - W_{2'} \qquad \text{(c)}$$

$$W_{3'2} = \frac{K_Y\beta}{\delta}(W_{4'} - W_0) - W_2 \qquad \text{(d)}$$

(5.28)

and from Eq. (5.17a) and the relation $W_{3'2} = -W_2 + W_{3'2'} + W_{2'}$ one can deduce:

$$\beta W_2 + W_{1'2} - \frac{(\gamma - A)}{B_Y} W_{3'} = \beta W_{2'} + \frac{\gamma - A}{B_Y} W_0 \qquad (5.29)$$

Comparing (5.28a) and (5.29) it can be shown that

$$W_{3'} = -W_0$$

Putting these values into Equation (5.27) for general edge Point, equation for edge Point near the Acute Corner is obtained as follows:

$$\begin{aligned}
\nabla\nabla W &= A(W_{12'}) - (2A + 2B_Y)W_{2'} + \frac{\beta}{2}B_Y(W_1 - W_{14'}) + B_Y(W_0 + W_{4'}) \\
&- \frac{\beta}{2}\Big[A(W_{2'} + W_{32'}) - (2A + 2B_Y)W_{12'} + \beta\cdot\frac{B_Y}{2}(-W_0 + W_3 + W_{4'} - W_{34'}) \\
&+ B_Y(W_1 + W_{14'}) - A\Big\{\frac{K_Y\beta}{\delta}(W_{4'} - W_0)\Big\} - \frac{\beta}{2}B_Y(2W_0 - 2W_{4'})\Big] \\
&+ \frac{\alpha\gamma}{2}(W_0 - 2W_1 + W_3) - \gamma(1 + \alpha)(-2W_0 + W_1) \\
&+ \left(\frac{\psi}{2}\right)\left(-\frac{\beta}{2}\right)\Big\{W_{2'} - \frac{K_Y\beta}{\delta}(W_{4'} - W_0) + W_{2'}\Big\} - \psi\left(W_{2'} - \frac{1}{2}\beta W_{12'}\right) \\
&+ \frac{\psi}{2}\Big\{W_{12'} - \frac{1}{2}\beta(W_{32'} - W_{2'})\Big\} - \frac{\psi}{2B_Y}\Big[-\frac{\beta}{2}B_Y\Big\{\frac{K_Y\beta}{\delta}(W_{4'} - W_0) - 2W_{2'}\Big\}
\end{aligned}$$

$$-2\left\{-B_Y w_2' - \frac{\beta}{2} B_Y (-w_{12}') + (2A+2B_Y-2\gamma)w_0 + (\gamma-A)w_1\right\}$$

$$- B_Y w_{12}' - \frac{\beta}{2} B_Y (w_2' - w_{32}') + (2A+2B_Y-2\gamma)w_1 + (\gamma-A)(w_0+w_3)\Big]$$

$$- \frac{D\chi^4/\mu_x}{2}\left\{-w_0 + 6w_0 - 4w_1 + w_3\right\} = \frac{\bar{q}_0 \lambda_Y^4}{2} \qquad (5.30)$$

Separating the coefficients associated with different nodal points Eq. (5.30) can be presented as in Fig. 16(b)

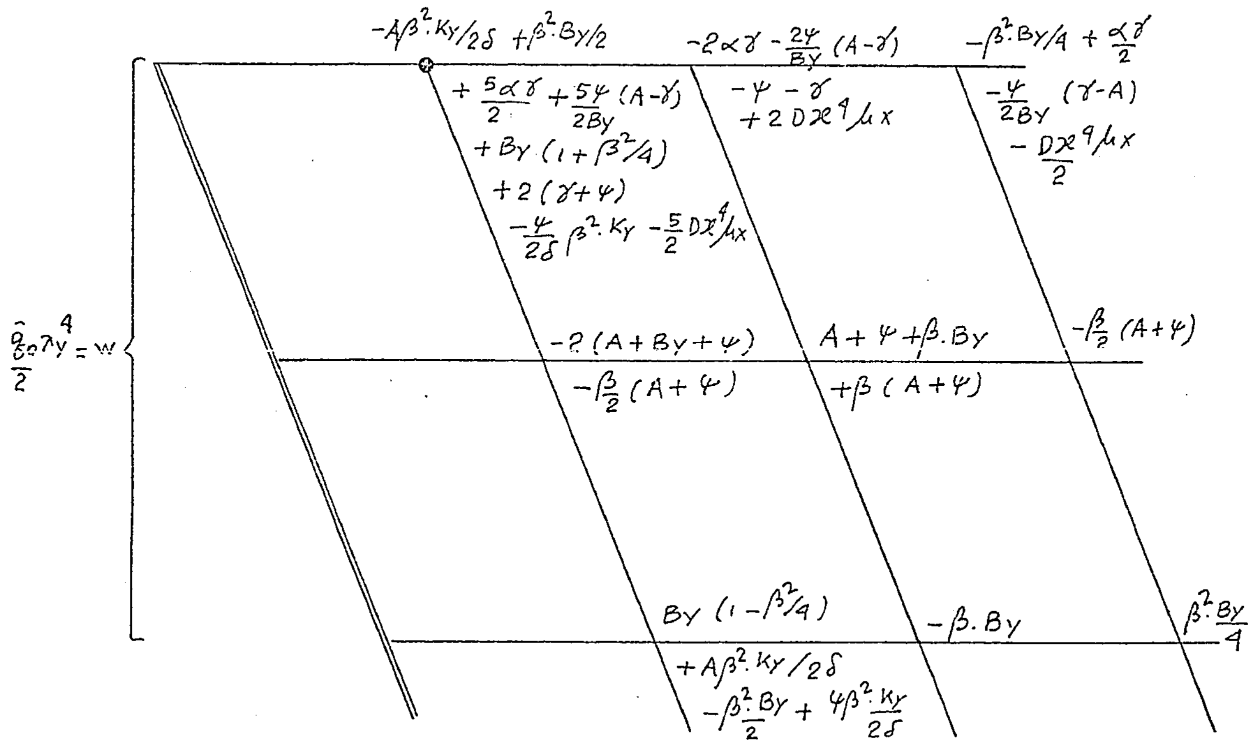

Fig. 16(b)

Finite difference equation

for edge Point near the Acute Corner

5.9 Edge Point near the Obtuse Corner:

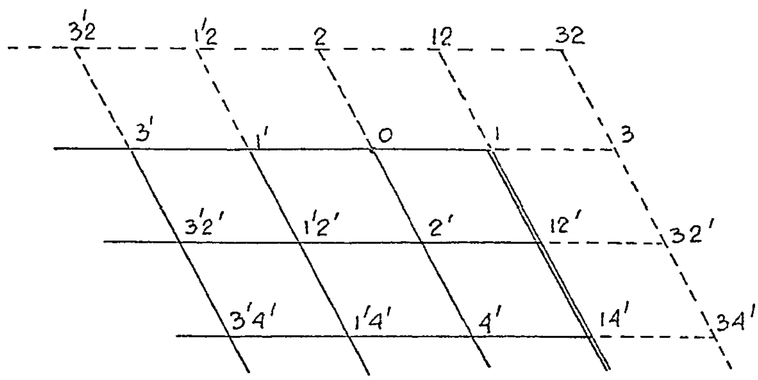

Fig. 17(a)

Edge Point on Obtuse Corner

From the boundary conditions of Sec. 5.2 and 5.7 it follows:

$$w_1 = w_{12'} = w_{14'} = 0$$

$$w_3 = \frac{K_y\beta}{\delta}(w_2 - w_{2'}) - \frac{K_y}{\delta} w_{12} - w_0 \qquad \text{(a)}$$

$$w_{34'} = \frac{K_y\beta}{\delta}(w_2 - w_{2'}) - \frac{K_y}{\delta} w_{12} - w_{4'} \qquad \text{(b)}$$

$$w_{32'} = \frac{K_y\beta}{\delta}(w_0 - w_{4'}) - w_{2'} \qquad \text{(c)}$$

$$w_{32} = \frac{K_y\beta}{\delta}(w_0 - w_{4'}) - w_2 \qquad \text{(d)}$$

(5.31)

and from the Eq. (5.17c) and the relation $w_{32} = -w_2 + w_{32'} + w_{2'}$ one can deduce:

$$-\beta \cdot w_2 + w_{12} - \frac{(\gamma - A)}{B_y} w_3 = -\beta \cdot w_{2'} + \frac{(\gamma - A)}{B_y} w_0 \qquad (5.32)$$

Comparing (5.31a) and (5.32) it can be shown that

$$w_3 = -w_0$$

Putting these values into Eq. (5.27) for general edge point equation for edge point near the obtuse corner is obtained as follows:

$$
\begin{aligned}
\nabla\nabla w = {} & A(w_{1'2'}) - (2A+2B_y)w_{2'} + \frac{\beta}{2}B_y(-w_{1'} + w_{1'4'}) + B_y(w_0 + w_{4'}) \\
& - \frac{\beta}{2}\Big[A\Big\{w_{2'} + \beta\frac{K_y}{\delta}(w_0 - w_{4'}) - w_{2'}\Big\} + \frac{\beta}{2}(-2w_0 + 2w_{4'}) - A(w_{3'2'} + w_{2'}) \\
& + (2A+2B_y)w_{1'2'} - \frac{\beta}{2}B_y(-w_{3'} + w_0 + w_{3'4'} - w_{4'}) - B_y(w_{1'} + w_{1'4'})\Big] \\
& + \frac{\alpha\gamma}{2}(w_{3'} - 2w_{1'} + w_0) - \gamma(1+\alpha)(w_{1'} - 2w_0) \\
& + \frac{\psi}{2}\Big\{w_{1'2'} - \frac{\beta}{2}(w_{2'} - w_{3'2'})\Big\} - \psi\Big\{w_{2'} - \frac{1}{2}\beta(-w_{1'2'})\Big\} \\
& + \frac{\psi}{2}\chi - \frac{1}{2}\beta\Big\{\beta\frac{K_y}{\delta}(w_0 - w_{4'}) - 2w_{2'}\Big\} \\
& - \frac{\psi}{2B_y}\Big[-B_y w_{1'2'} - \frac{\beta}{2}B_y(w_{3'2'} - w_{2'}) + (2A+2B_y-2\gamma)w_{1'} + (\gamma - A)(w_{3'} + w_0) \\
& \quad - 2\Big\{-B_y(w_{2'}) - \beta\frac{B_y}{2}(w_{1'2'}) + (2A+2B_y-2\gamma)w_0 + (\gamma - A)w_{1'}\Big\} \\
& \quad - \frac{\beta}{2}B_y\Big\{w_{2'} - \beta\frac{K_y}{\delta}(w_0 - w_{4'}) + w_{2'}\Big\}\Big] \\
& - \frac{D\chi^4}{2}/\mu_x\,(w_{3'} - 4w_{1'} + 6w_0 - w_0) = \frac{\bar{q}_0}{2}\lambda_y^4 \qquad (5.31)
\end{aligned}
$$

Separating the coefficients associated with different nodal points Eq. (5.31) can be presented as in Fig. 17(b)

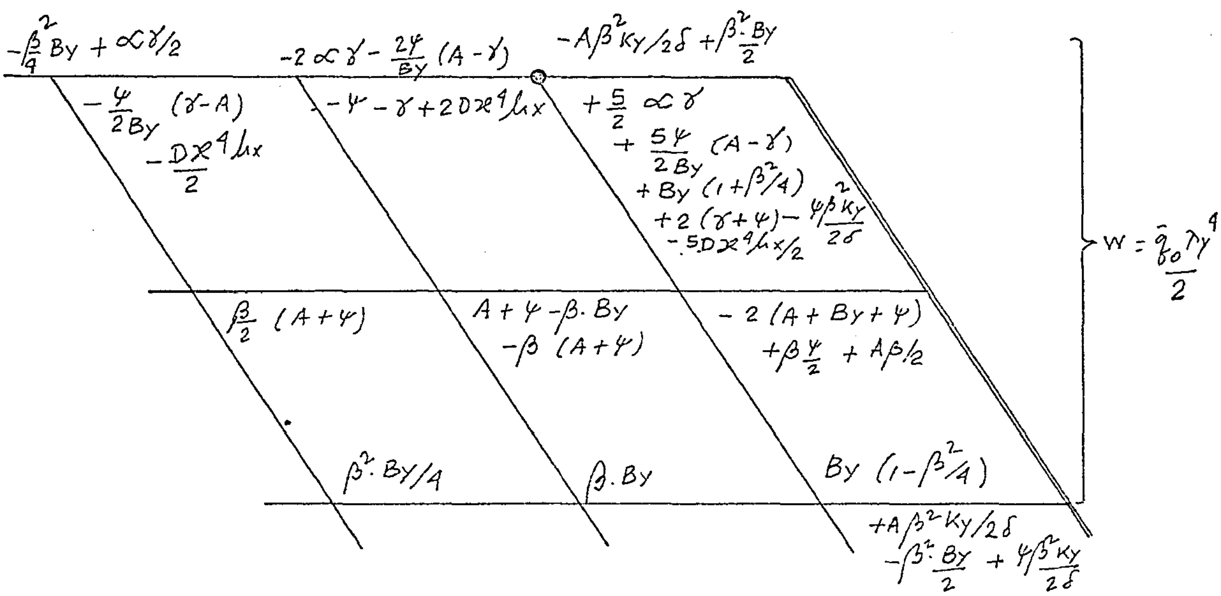

Fig. 17(b)
Finite difference equation for edge point near the obtuse corners.

In these equations the quantity $\bar{q}_o$ is the equivalent combined effects in terms of load per unit area for all the loads which act upon at point 0.

If a uniformly distributed load of p_o per unit area, a line load of q_o per unit of the length in x direction and a concentrated load P_o act at point 0, $\bar{q}_o$ is given by:

$$\bar{q}_o = p_o + \frac{q_o}{\lambda y} + \frac{P_o}{\lambda x \lambda y}$$

If point 0 lies on an exterior edge of the plate, $\bar{q}_o$ is given by

$$\bar{q}_o = p_o + \frac{q_o}{.5\lambda y} + \frac{P_o}{.5\lambda x \lambda y}$$

5.10 Finite Difference Equations for Moments:

Finite difference equations for moments Mx, My and Mxy can be derived by substituting the finite difference approximations Eq. (4.6a), (4.6b) into appropriate moment equations (1.9). Their final expressions are the same as in Ref. [7] except for equation (5.38). However, complete derivations of moment equations are presented in this Section.

(a) General Interior Point:

$$M_x = -B_x\left[\left(\frac{\partial^2 w}{\partial x^2}\right)_0 + \mu_y\left(\frac{\partial^2 w}{\partial y^2}\right)_0\right]$$

$$= -\frac{B_x}{\lambda y^2}\left[\chi^2(w_{1'} - 2w_o + w_1) + \mu_y\left\{\beta^2(w_{1'} + w_1) - (2 + 2\beta^2)w_o + \frac{\beta}{2}\left(-w_{1'2} + w_{12} + w_{1'2'} - w_{12'}\right) + w_{2'} + w_2\right\}\right] \quad (5.32)$$

Similarly:

$$M_y = -\frac{B_y}{\lambda_y^2}\Big[\Big\{\beta^2(w_1'+w_1) - (2+2\beta^2)w_0 + \frac{\beta}{2}(-w_{1'2}+w_{12}+w_{1'2'}-w_{12'})$$
$$+ w_2'+w_2\Big\} + \mu_x \varkappa^2 (w_1'-2w_0+w_1)\Big] \qquad (5.33)$$

and
$$M_{xy} = -2C\left[\frac{\partial^2 w}{\partial u^2}\tan\phi + \frac{\partial^2 w}{\partial u \partial v}\sec\phi\right]$$
$$= -\frac{2C\varkappa}{\lambda_y^2}\Big[\beta(w_1'-2w_0+w_1) + \frac{1}{4}(w_{12}-w_{1'2}+w_{1'2'} - w_{12'})\Big] \qquad (5.34)$$

These moment equations can be presented as in Fig. 18(a), 18(b) and (18c), respectively.

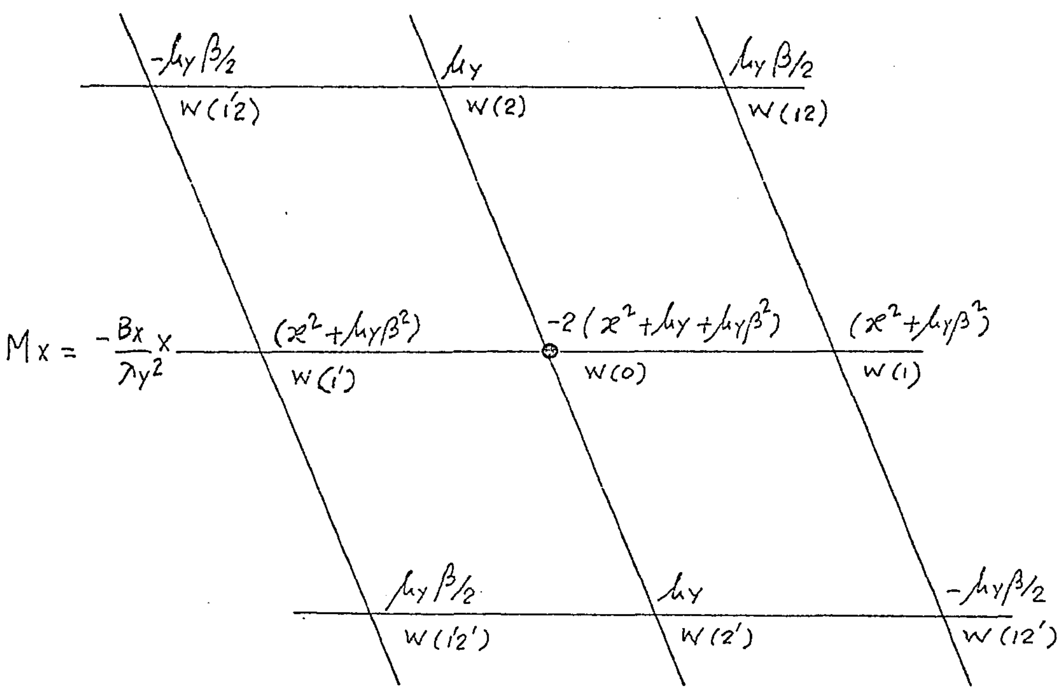

Fig. 18(a)

Finite difference equation

for Mx at general interior Point

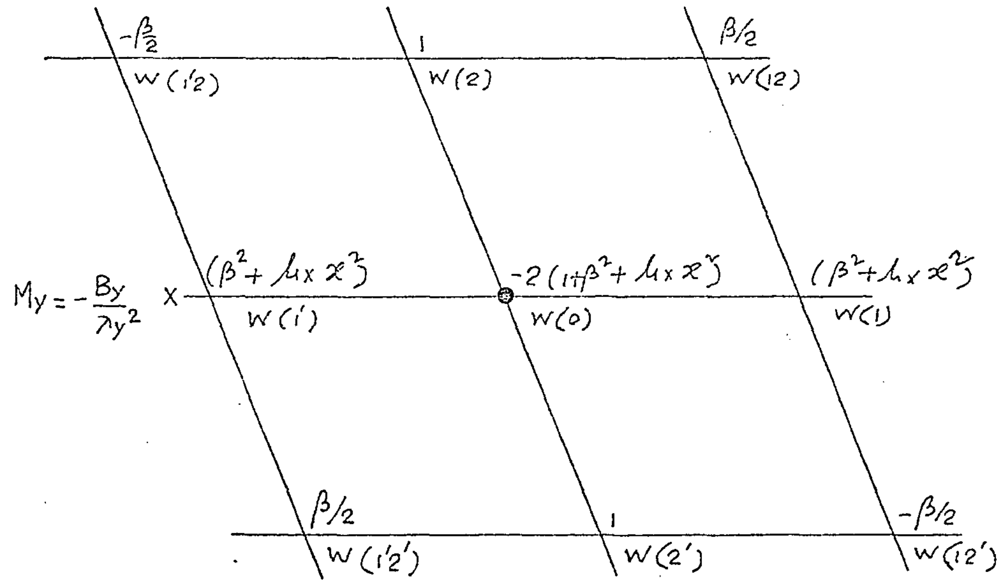

Fig. 18(b)

Finite difference equation

for My at general interior Point

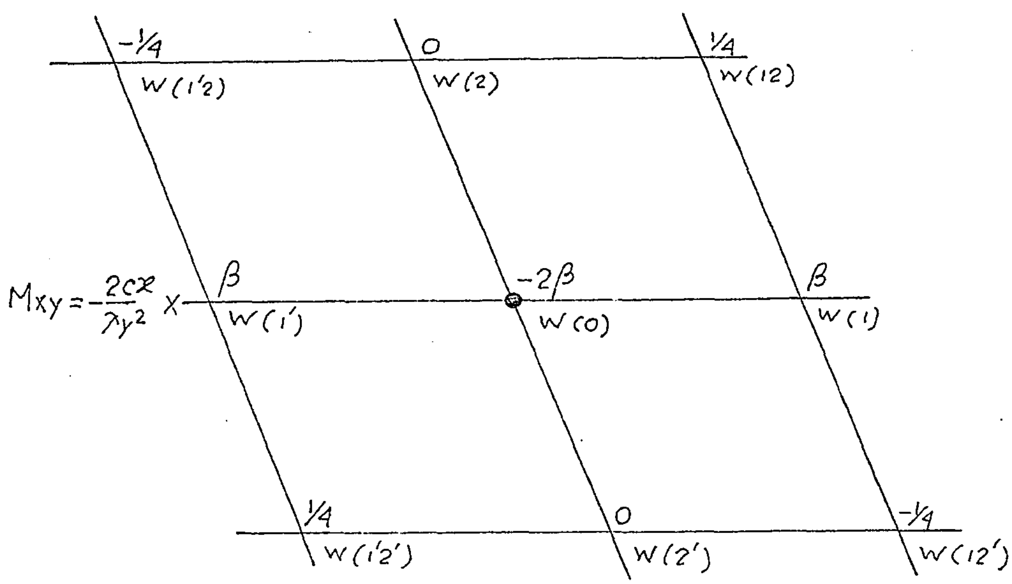

Fig. 18(c)

Finite defference equation

for Mxy at general interior Point

(b) Points on the left simple support:

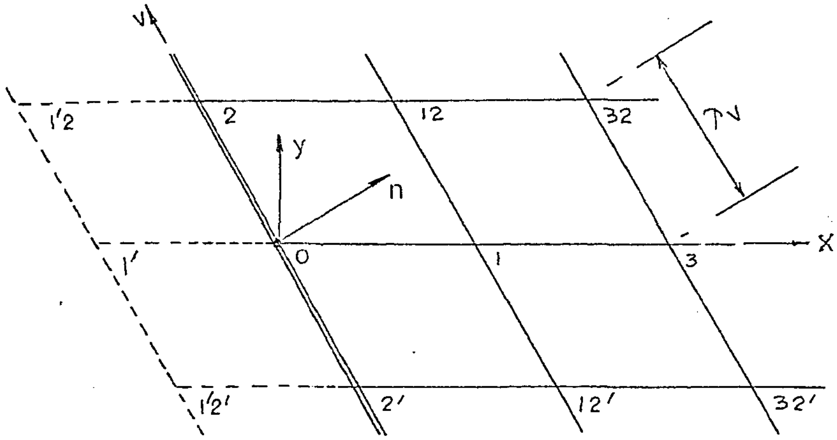

Fig. 19(a)

Interior Point on support

From the boundary conditions as derived in Sec. 5.2 it follows that:

$$w_2 = w_0 = w_{2'} = 0$$

(5.35a)

$$M_n + M_v = M_x + M_y = 0$$

and $$\left(\frac{\partial w}{\partial v}\right)_0 = \frac{1}{2}\left[\left(\frac{\partial w}{\partial v}\right)_{1'} + \left(\frac{\partial w}{\partial v}\right)_1\right] = 0$$

or $$\frac{1}{2}\left[\frac{w_{1'2} - w_{1'2'}}{2\lambda v} + \frac{w_{12} - w_{12'}}{2\lambda v}\right] = 0$$

or $$w_{1'2} - w_{1'2'} = w_{12'} - w_{12} \qquad (5.35b)$$

From the relation:

$$K_x\left(\frac{\partial^2 w}{\partial x^2}\right)_0 + K_y\left(\frac{\partial^2 w}{\partial y^2}\right)_0 = 0$$

it follows: $$w_{1'} = -\beta \cdot \frac{K_y}{\delta}(w_{12} - w_{12'}) - w_1 \qquad (5.35c)$$

Substituting these values of exterior nodal points into moment equations (5.32) and (5.34) one obtains:

$$M_x = -\frac{B_x}{\lambda_y^2}\left[\left\{\beta K_y - \beta\cdot\frac{K_y}{\delta}\left(\chi^2+\mu_y\beta^2\right)\right\} W_{12} - \left\{\beta\mu_y - \beta\cdot\frac{K_y}{\delta}\left(\chi^2+\mu_y\beta^2\right)\right\} W_{12'}\right] \tag{5.36}$$

$$M_y = -M_x \tag{5.37}$$

$$M_{xy} = -\frac{2(\chi}{\lambda_y^2}\left[\left(-\beta^2\frac{K_y}{\delta}+\frac{1}{2}\right)W_{12} + \left(\beta^2\cdot\frac{K_y}{\delta}-\frac{1}{2}\right)W_{12'}\right] \tag{5.38}$$

Equations (5.36), (5.37) and (5.38) may be presented as in Fig. 19(b), (c) and (d), respectively.

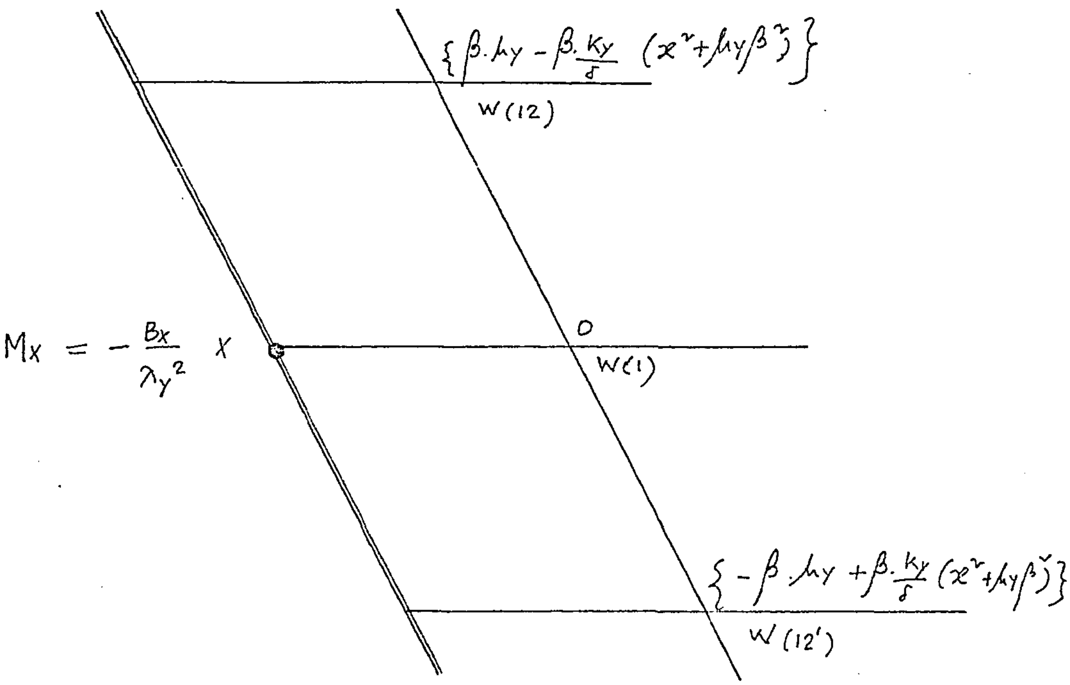

Fig. 19(b)

Finite difference equation for Mx on simple support

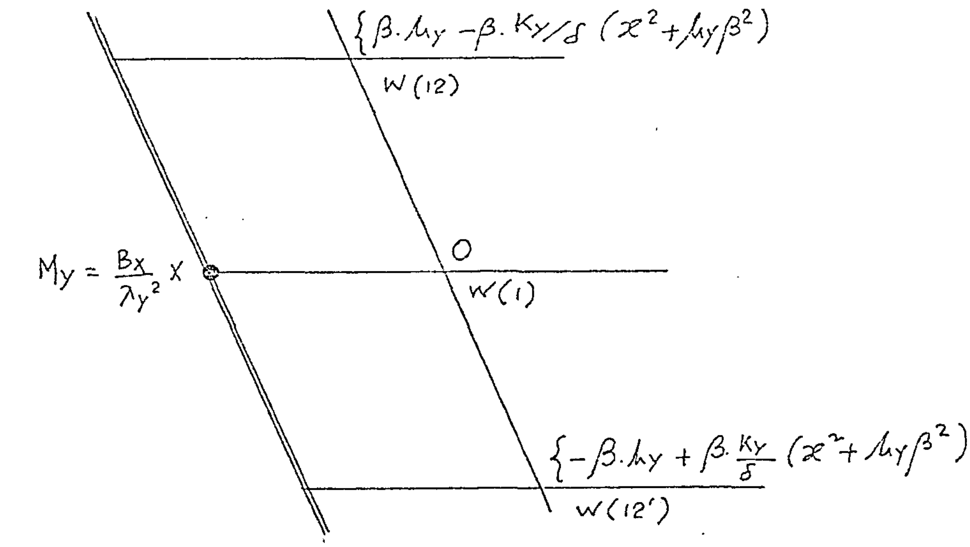

Fig. 19(c)

Finite difference equation

for My on simple support

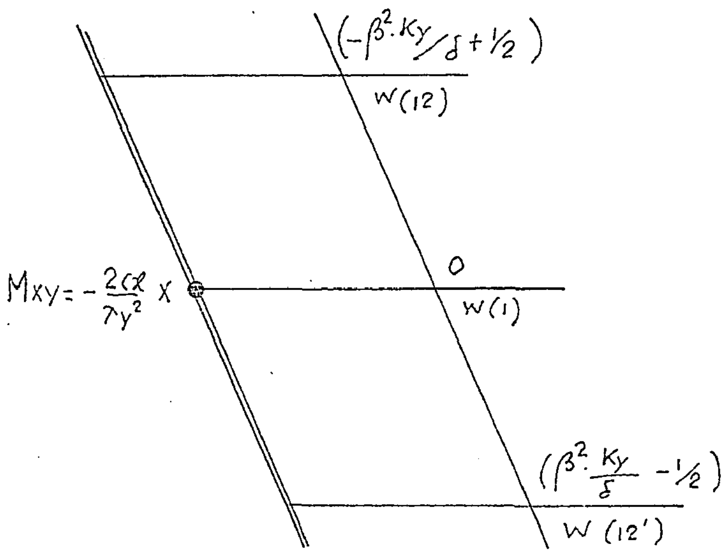

Fig. 19(d)

Finite difference equation

for Mxy on simple support

(c) Points on the right simple support:

In a similar manner equations for moments on Point of right simple support may be derived from the relations:

$$\left.\begin{aligned} & w_4 = w_4' = w_2 = w_0 = w_2' = 0 \\ & w_{12} - w_{12}' = w_{1'2'} - w_{1'2} \\ & w_1 = -\frac{K_Y \beta}{\delta}\left(w_{1'2'} - w_{1'2}\right) - w_{1'} \end{aligned}\right\} \quad (5.39)$$

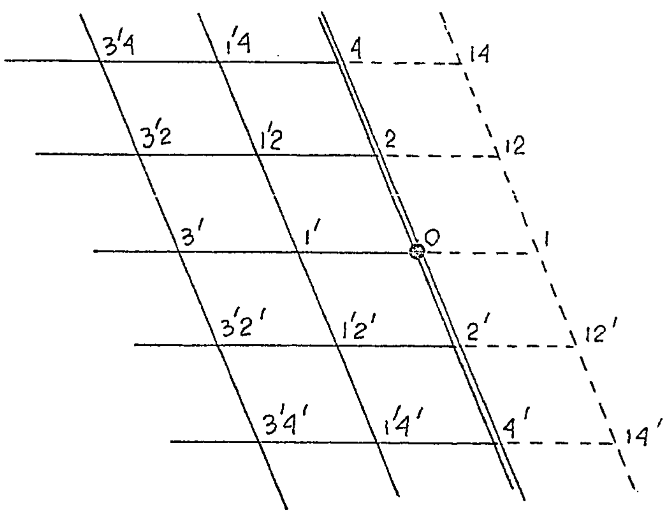

Fig. 20(a)

Point on Right Simple Support

These moment equations can be presented as in Fig. 20(b), and Fig. 20(c), respectively:

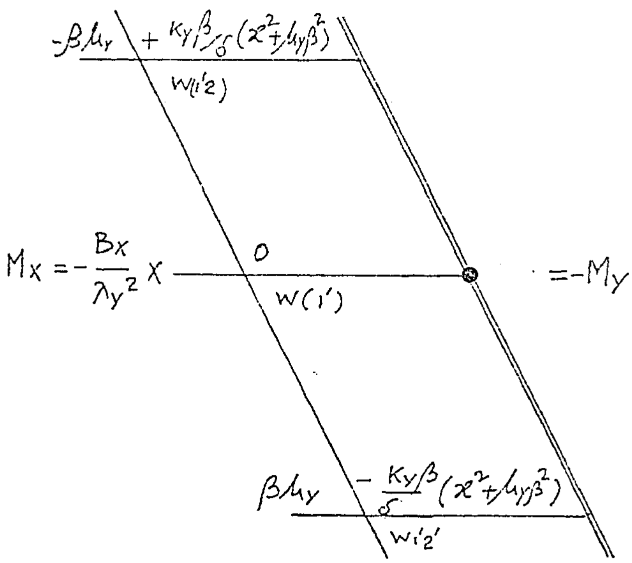

Fig. 20(b)

Finite difference equation

for Mx and My on right simple support

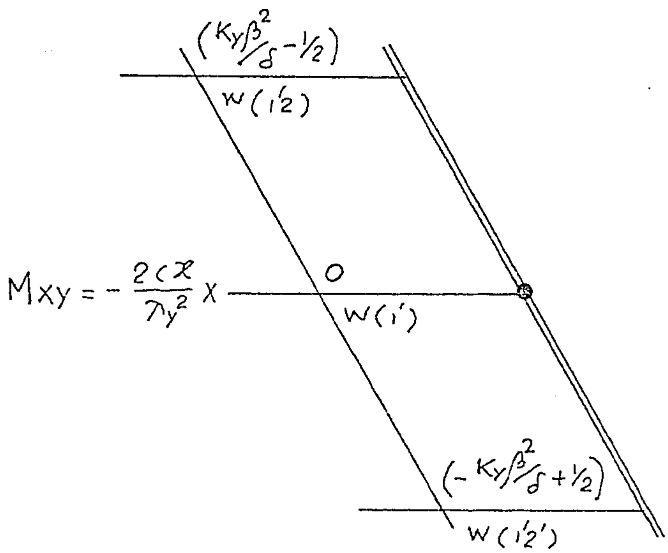

Fig. 20(c)

Finite difference equation

for Mxy on right simple support

(d) Points on the free edge:

on the free edge $My = 0$

Hence $-By\left(\frac{\partial^2 w}{\partial y^2} + \mu x \frac{\partial^2 w}{\partial x^2}\right) = 0$

or $\frac{\partial^2 w}{\partial y^2} = -\mu x \frac{\partial^2 w}{\partial x^2}$

but $Mx = -Bx\left(\frac{\partial^2 w}{\partial x^2} + \mu y \frac{\partial^2 w}{\partial y^2}\right)$

$= -Bx\,(1 - \mu x \mu y)\,\frac{\partial^2 w}{\partial x^2}$

Hence $(Mx)_0 = -Bx\,(1 - \mu x \mu y)\,\frac{\varkappa^2}{\lambda y^2}\,(w_{1'} - 2w_0 + w_1)$ (5.40)

Eq. (5.40) can be presented as in Fig. 21(a)

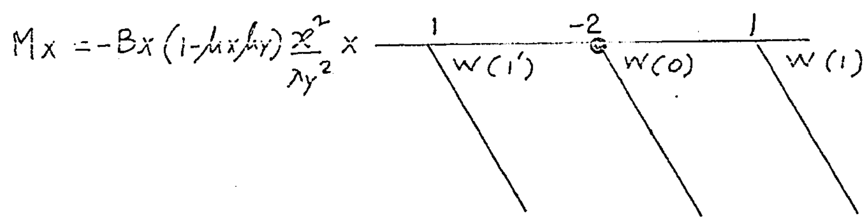

Fig. 21(a)

Finite difference equation
for Mx on free edge.

For deriving the equation for Mxy on free edge the nodal points outside the boundary can be expressed in terms of interior points as follows:

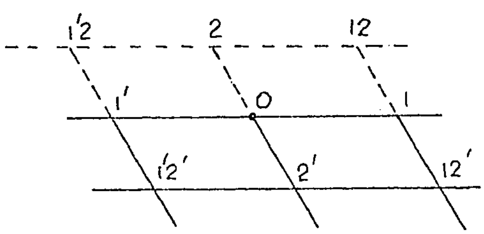

Fig. 21(b)

Point on free edge.

Since $\left(\frac{\partial w}{\partial x}\right)_0 = \frac{1}{2}\left[\left(\frac{\partial w}{\partial x}\right)_2 + \left(\frac{\partial w}{\partial x}\right)_{2'}\right]$

hence $\frac{w_1 - w_1'}{2\lambda x} = \frac{1}{2}\left[\frac{w_{12} - w_1'_2}{2\lambda x} + \frac{w_{12}' - w_1'_2{}'}{2\lambda x}\right]$

or $\frac{1}{2}(w_{12} - w_{1'2}) = w_1 - w_1' - \frac{1}{2}(w_{12}' - w_{1'2}')$ (5.41)

Putting the value of w_{12} and $w_{1'2}$ into equation (5.34) one can deduce:

$$Mxy = -\frac{2\alpha}{\lambda_y^2}\left[(\beta+\tfrac{1}{2})w_1 + (\beta-\tfrac{1}{2})w_1' - 2\beta w_0 + \tfrac{1}{2}(w_{1'2}' - w_{12}')\right] \quad (5.42)$$

Eq. (5.42) can be presented as in Fig. 21(c)

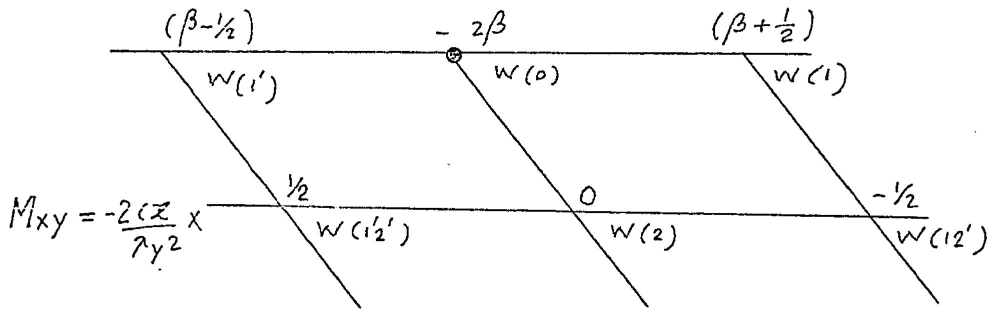

Fig. 21(c)

Finite difference equation for Mxy on free edge.

5.11 Application of the method of finite difference:

By superposing the skew network on the equivalent orthotropic skew plate and applying the typical finite difference equations for each network points yield a set of simultaneous equations, the solution of which yields the numerical values of deflections at all network points. By substituting the values of deflection in proper moment equations as derived in Sec. 5.10 of this chapter, numerical values of moments acting on the equivalent orthotropic skew plate can be obtained.

Bending moments acting at different sections of longitudinal girder and transverse beams can be computed by integrating the equivalent plate moment over the flange width, according to the formula presented in Chapter Three.

VI

GENERAL SOLUTION AND STUDY OF THE FACTORS THAT ENTER INTO THE ANALYSIS AND DESIGN OF GRIDWORK IN SKEW BRIDGES

General Solution:

Finite difference equations as derived in Chapter V can be applied for each of network points (Fig. 22) to yield the force displacement relations in the form:

$$[A]\{W\} = \{\bar{q}_0\}\lambda_y^4$$

where $\{\bar{q}_0\}$ is the column of static load acting at the predetermined set of points and $\{W\}$ is the column corresponding to the vertical displacement. $[A]$ is the conventional stiffness matrix and is obtained by a few algebric operations in the following form:

$$\begin{bmatrix} A_{1,1} & A_{1,2} & A_{1,3} & A_{1,4} & - & - & - & - & A_{1,18} \\ A_{2,1} & A_{2,2} & A_{2,3} & A_{2,4} & - & - & - & - & A_{2,18} \\ A_{3,1} & A_{3,2} & A_{3,3} & A_{3,4} & - & - & - & - & A_{3,18} \\ A_{4,1} & A_{4,2} & A_{4,3} & A_{4,4} & - & - & - & - & A_{4,18} \\ | & & & & & & & & \\ | & & & & & & & & \\ | & & & & & & & & \\ A_{18,1} & A_{18,2} & A_{18,3} & A_{18,4} & - & - & - & - & A_{18,18} \end{bmatrix}$$

To clarify the application, some of the equations for two typical network points are shown in the appendix.

By inverting the stiffness matrix $[A]$ and carrying out the multiplication with the load vector $\{\bar{q}_o\}$, deflections at different network points can be obtained. By substituting these values in proper moment equation as described in Sec. 5.11, numerical values of moments acting on the equivalent plate can be easily computed.

Computation of longitudinal and cross beam moments can be performed as outlined in Chapter III.

The finite difference solution for the gridwork with slab representing the modal skew bridge has been obtained. The deck slab is assumed to be an isotropic plate having dimension 36" x 30" x $\frac{3}{16}$" (Fig. 22) and stiffened by longitudinal and cross beams of different stiffnesses in both flexure and torsion. The material of the plate was hot rolled structural steel having Young's modulus of elasticity $E = 30 \times 10^6$ psi and Poisson's ratio $\mu_x = 0.3$.

The following are the loading conditions for which the solution has been obtained.

(a) A single concentrated load P, located at centre.

(b) Two equal concentrated loads each of magnitude P/2, located symmetrically along the longitudinal axis $(-\frac{L_x}{6}, 0)$ and $(\frac{L_x}{6}, 0)$.

(c) Two equal concentrated load each of magnitude P/2 located symmetrically along the transverse axis $(0, Ly/6)$ and $(0, -Ly/6)$

Since the loading conditions and plate geometry are symmetrical about the central axis, only one half of the plate has been considered.

Factors that enter into the analysis and design of gridwork in skew bridges are: (a) Number of girders and diaphragms, their spacing and stiffness ratio in both flexure and torsion; (b) Aspect ratio $(\frac{Lx}{Ly})$ of the bridge where Lx is the skew span between the supports parallel to the roadway and Ly is the width of the bridge and (c) skew angle.

Theoretical solutions for the different factors influencing the analysis and design of gridwork in skew bridges have been presented graphically (Figs. 3.1 to 3.29). In varying the number of longitudinal and cross beams the total cross-sectional area in the two directions has been kept constant so that the cost per linear distance of the span length does not change appreciably, (Figs. 3.1 to 3.4).

Aspect ratio which is treated as one of the variables was varied from 1, 1.25, 1.5, 1.75 to 2.0 and its effects on deflections and intensity of moments are presented in Figs. 3.5 to 3.15.

The change of skew angle from 0, 15, 30, 45 to 60 degrees is treated as another variable and their effects on deflections and moments are presented in Figs. 3.16 to 3.23.

A disputable question in the value of Poisson's ratio which is not a material constant as Poisson's ratio proper but an elastic constant depending on the orthotropic form of the system has been treated as another variable. The value of μ_x was varied from 0, 0.10, 0.15, 0.20, 0.25, 0.30 and 0.33 and their effects are shown in Figs. 3.24 to 3.29.

Graphical representation showing the influence of these different factors upon deflections and moment intensity Mx, My, Mxy and equivalent principal moments, have been presented for some typical node points, e.g. central point of the bridge, interior point near the obtuse corner, interior point near the acute corner, and central point on the free edge. In all cases the solutions have been obtained in the form of influence coefficients of deflections and moments for a unit central point loading. Influence coefficients have also been obtained for uniformly distributed loading, two point loadings and for aspect ratio at a different skew angle. The plate geometry is the same as for the model skew bridge. (Fig. 22).

VII

EXPERIMENTAL VERIFICATION OF THE THEORY

7.1 Description of the Model Bridge:

The gridwork and the deck plate of the model skew bridge were fabricated from a 36" (skew length) x 30" x 3/16" thick plate, 7 nos. of longitudinal beams (3/16" x 2") and 7 nos. of cross beams (3/16" x 1½") - all made of hot rolled structural steel. The two sets of intersecting flexural members forming the gridwork were welded intermittently to one side of the deck plate to form a skew mesh as shown in Fig. 22. Inspite of cooling the model with cold water during the welding process, a considerable local warping resulted from the intense heat of welding. In order to have a flattened surface and to reduce the locked-in stresses the bridge model was annealed. Four flat bars of the same material were also subjected to the same heat treatment. They were tested in the universal testing machine to evaluate the modulus of elasticity E and Poisson's ratio μ_x under uniaxial tensile test, the average value of which were found to be 30×10^6 psi and 0.3, respectively. In order to have a simple line support along the two edges, the gap between the longitudinal beam and cross beam was filled up with pieces of ½" x ½" x 6½" long square bars by spot welding with the cross beams (Fig. 1.1).

7.2 Abutment Frame:

The model bridge was simply supported on the two specially machined 1" diameter steel rods resting on the two opposite edges of the abutment frame. The frame was fabricated from two ½" x 3½" x 15" deep channels which were rigidly connected to each other by two ¼" x 3" x 8" deep I-beams welded to the frame -6" below the bridge deck level. The frame was in turn supported on six-standard steel blocks resting on a flat steel base (Fig. 1.2).

7.3 Loading Device:

The model skew grillage bridge was tested within the elastic range under the following types of loadings:

1. Concentrated load at the center:

The load was simulated concentrically on the central point of the bridge deck plate through a Thawing-Albert load cell which was attached to a hydraulic ram mounted under the beam of the testing structure. The load cell was calibrated by recording increments of strains corresponding to the direct load increments with a Budd portable type strain indicator (Model P-350) and a PCA - 300,000 lb. testing machine. (Calibration curve Fig. 2.24). A skew steel block (3½" x 3½" - 1" thick) with a groove underneath to accomodate the strain gage was placed below the load cell for transferring the load to the deck plate. (Fig. 1.4).

2. Two equal concentrated loads applied on the longitudinal axis $(-L_x/6, 0)$ and $(L_x/6, 0)$.

For this type of loading a Strainsert 100,000 lb. flat load cell was used which was calibrated with the same Budd portable type strain indicator and the PCA - 300,000 lb. testing machine. (Calibration curve Fig. 2.25). The load was simulated by using the same hydraulic ram as in Case 1 on a 4" x 4" - 2' ft. long solid bar resting symmetrically on two skew steel blocks dividing the central load into two equal concentrated loads. (Fig. 1.5).

3. Two equal concentrated loads applied on the transverse axis $(0, L_y/6)$ and $(0, -L_y/6)$.

For this type of loading the same loading device as in Case 2 was used except that the two skew steel blocks were placed symmetrically on the transverse axis of the bridge model along the V-direction. (Fig. 1.6).

7.4 Testing Procedure and Recording of Data:

The PCA - 300,000 lbs. testing machine was used to simulate the load through the hydraulic ram in all the three cases.

Deflections at different points of intersections of gridwork were recorded by dial gauges (Mercer Dial gauges, accuracy 10^{-3} in.). To measure the strains, electrical resistance strain gauges were used. Strain rosettes (Type EA-06-125 RA - 120) were mounted on the top face of the deck plate and linear gauges (Type EA - 06-062 AK - 120) were mounted on the bottom face of the longitudinal beams. Fig. 23 shows the location of the strain gages on both loaded and unloaded side of the model bridge. A Datron Digital strain indicator together with a switch and balance unit, a Datron polarity transposer and printer control unit was used to record the strains. (Fig. 1.7).

The results of the experimental tests under different types of loading conditions are presented in the form of figures, comparing the experimental and theoretical values at various points of gridwork of the skew model bridge. (Figs. 2.1 to 2.23).

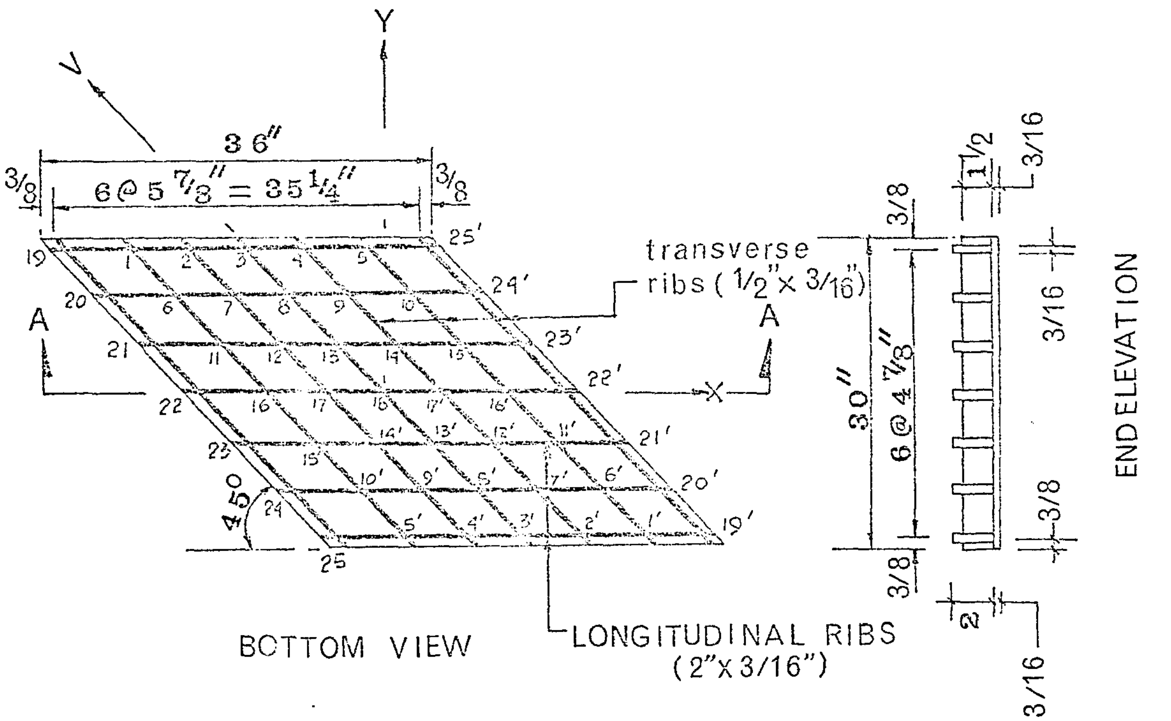

LAYOUT OF NET WORK POINTS

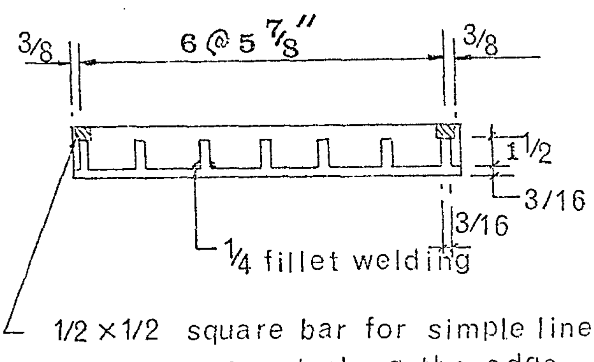

SEC. A – A

FIG. 22 GRIDWORK IN MODEL SKEW BRIDGE

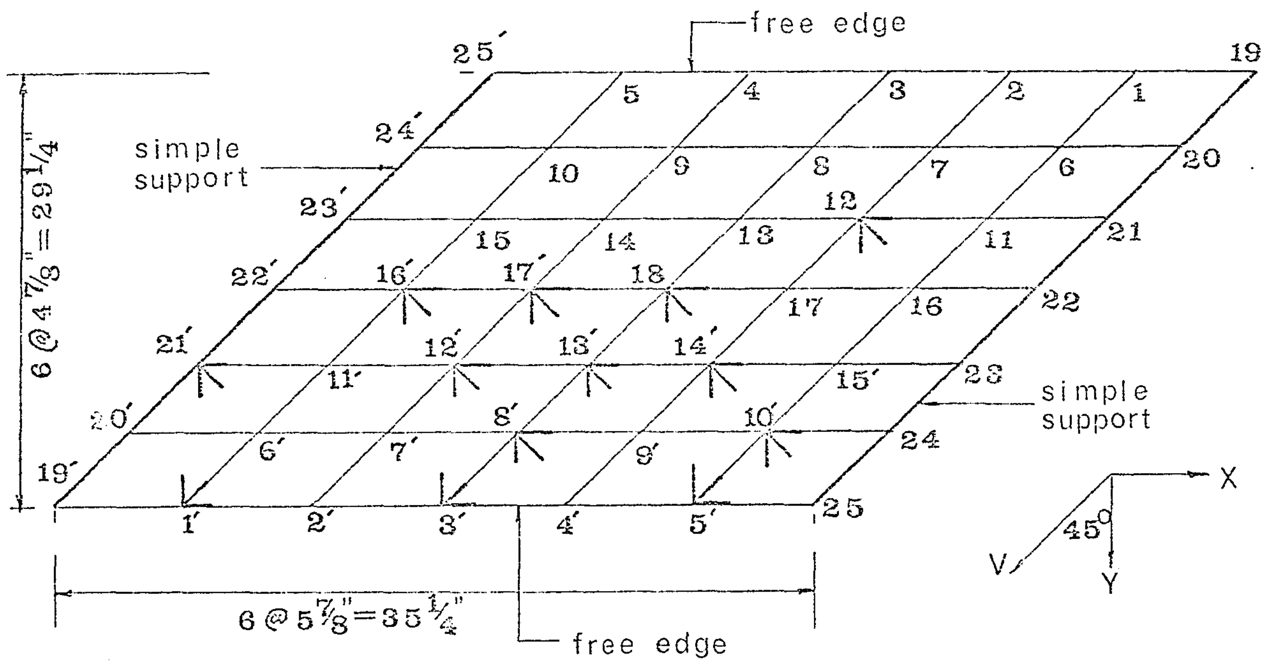

LAYOUT OF STRAIN ROSETTES ON LOADED SIDE

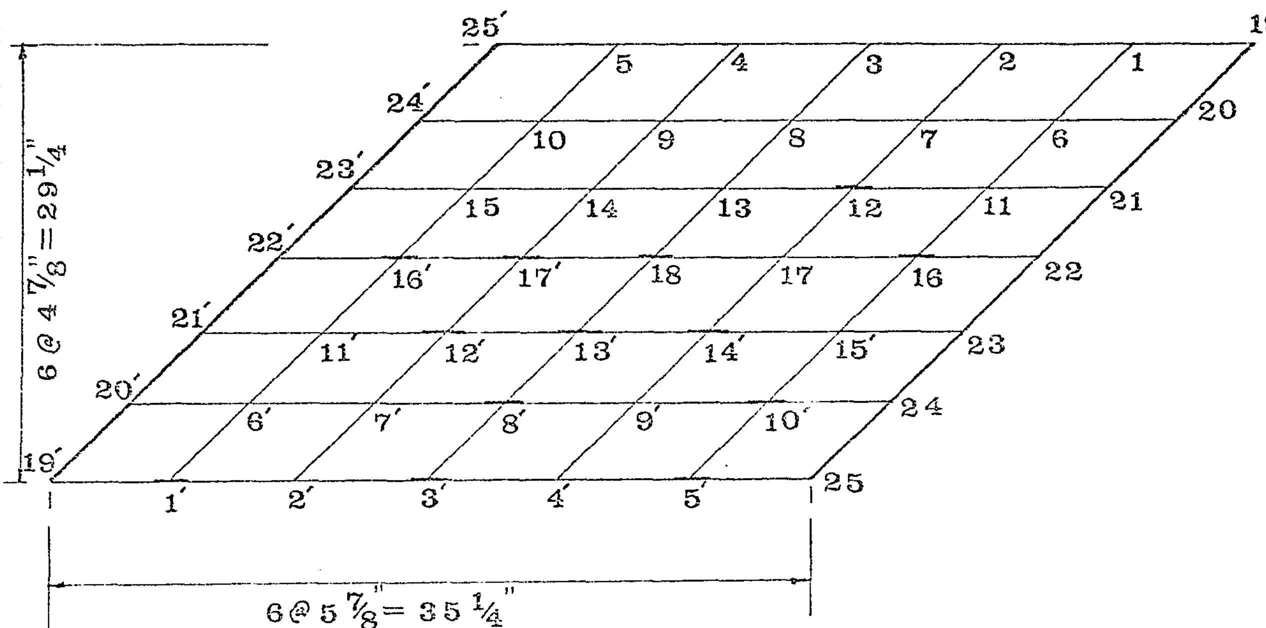

FIG. 23 LAYOUT OF LINEAR STRAIN GAGES ON THE UNLOADED SIDE

VIII

DISCUSSIONS, CONCLUSIONS AND SUGGESTIONS FOR FURTHER RESEARCH

8.1 Discussions of Experimental and Theoretical Results:

For a single point loading on the midspan of central longitudinal girder, comparison of Figs. 2.1 to 2.4 shows that experimental values of deflections are higher (14% maximum) than the theoretical values. For the same type of loading comparison of girder bending moments calculated from the measured strain gauge readings (Figs. 2.5 to 2.11) shows that the moments are at some point 12% higher (Fig. 2.5) than the theoretical values and at some points 11% (Fig. 2.10) lower than the theoretical ones.

For two point loadings on the longitudinal and transverse axes, the experimental values of deflections are observed to be 13% (maximum) and 14% (maximum) higher than the theoretical ones (Figs. 2.12 and 2.19). For the same type of loadings experimental values of girder moments were within ±12% (maximum) of the theoretical values (Fig. 2.21).

A comparison of the normal stress distribution along the depth of the longitudinal beam (Fig. 2.23) shows that experimental values are 13% (maximum) higher than the theoretical ones.

Both experimental and theoretical values of deflections and moments are observed to have higher magnitude towards the obtuse corner than those at the acute corner (Figs. 2.2 and 2.6). On the average, experimental values are observed to be higher than the theoretical solutions.

The deviation of the theoretical solutions from the experimental results may be attributed to the following:

(a) Effect of discontinuity on deflections and stresses:

Since the spacing of gridworks, the rigidity of which is assumed to be continuously distributed for the substitute orthotropic plate, is larger than the dimension of the applied load [23], which is usually the case in bridge deck design using concentrated wheel load, the discontinuity of steel plate deck system is of consequence in determinations of deflections of the system and bending moments and stresses of the individual members. The effect of the actual discontinuity could be considered by taking an effective width in computing rigidities of the equivalent system. Hence, it may be inferred that higher values of rigidities in the stiffness matrix, equation (3.1), result in lower theoretical deflections and consequently lower values of moment than the experimental results.

In order to examine the effect of effective width on the theoretical solutions of the problem, 90% of the rib spacing in the longitudinal direction of the bridge was considered instead of the full flange width of the original programme [23]. The results for deflections and moments were found to be only 2% higher than the original solutions. This, however, justifies the introduction of the concept of an effective width in the solution of gridwork problems, the value of which depends on the span of ribs and load distribution on the deck floor. Ref. [23] gives an excellent treatment of the effective width of deck plate in orthotropic steel deck bridges. The same values of effective width as applied in the orthogonal bridge structures may be assumed to be valid for the skewed configuration of this structural system.

(b) Effect of unsatisfied boundary conditions at the free edge and imposition of constraints near the simple support:

The boundary conditions at a free edge were first expressed by Poisson as:

$$M_y = 0, \quad M_{yx} = 0, \quad Q_y = 0$$

But due to the nature of the fourth order differential equation governing the behaviour of the plate system, which is based on the small deflection theory, only two boundary conditions are possible at the free edge, and later on Kirchoff proved that the last two conditions concerning the twisting moment and shear force could be combined into one single condition in the form of an edge force expression as in equation (1.9g). These two boundary conditions, $M_y = 0$ and $V_y = 0$, which have been utilized in the formulation of finite difference equations for typical network points on the free edge, give rise to a value of M_{xy} at the free edge (Eq. 5.42). Similar expressions for M_{xy} at the free edge have been presented in

Ref. [4, 7, 17]. This violates the Poisson's original boundary conditions at the free edge and will have some effect in the deviation of experimental values from the theoretical solutions. Similarly, the constraints imposed near the simple support as discussed in Section 5.2 may be of some consequence in the determination of deflections and bending moments of the structural system.

(c) Effect of experimental and constructional inaccuracies of the model bridge:

Instead of cooling the model bridge with cold water, the substantial warping resulting from the intense heat of welding, could not be totally balanced by subsequent annealing of the system. The model had an uneven initial curvature in its neutral plane in both longitudinal and transverse directions. During the welding process and fitting of the ribs with deck plates, a great deal of residual stresses might have also been induced in the structure. The strain gage readings on which bending moments and stresses have been computed could give lower values than the theoretical ones because of these unbalanced locked-in stresses at some points (Figs. 2.5, 2.16, 2.21).

Due to the warping and non uniformity of the simple support condition along the edge because of shimming, the slightly unsymmetrical deflections of the model bridge under the symmetrical loading is one of the major causes of deviation between the experimental and theoretical results.

8.2 Discussions of Factors that influence the Analysis and Design of the Gridwork in Skew Bridges:

(a) Number of girders and diaphragms with different spacing and stiffness ratio:

Figs. 3.1 to 3.4 show the effects of variation of the number of longitudinal and transverse beams on deflections and moments of the gridwork system under a unit concentrated load at centre. As would be expected, larger errors can occur for decks with smaller number of girders (Fig. 3.1), since the assumption of the uniform spread medium will not be satisfied in that case. A system with seven number of girders seems to approach an optimum design as far as deflections and bending moments are concerned (Figs. 3.2, 3.3, and 3.4). Negative moment Mx (Fig. 3.2) at the simple support indicates the effect of skew and the restraint imposed by the cross diaphragms on the free deflection surface of the central longitudinal girder.

In actual practice the road width, the skew span of the bridge and the type of highway loadings to which the bridge is anticipated to be subjected should determine the spacing of the girders and diaphragms to obtain an economical design. For this purpose several trial programmes can be.run on a computer with different number of girders and diaphragms having different spacings and stiffness ratios in both flexure and torsion.

(b) Aspect ratio of the bridge:

The effects of aspect ratio on deflections and moments of the gridwork in skew bridges are shown in Figs. 3.5 to 3.15. Figs. 3.5 to 3.9 show the variation of deflections and moments with aspect ratio for a skew angle of 45°, under a central concentrated load. Deflections of network points sharply decrease with decrease in aspect ratio (Fig. 3.5). While at this angle of skew, longitudinal girder moment Mx decreases slowly with decrease of aspect ratio, transverse moment My at a point near the acute corner tends to increase sharply with decrease of aspect ratio (Fig. 3.7). The twisting moment Mxy and the principal moment of the equivalent system decrease at all points with decrease of aspect ratio (Fig. 3.8 and 3.9).

Examination of Figs. 3.10 and 3.11 shows that with a large skew angle of 60°, the variation of deflections and moments Mx with aspect ratio are more rapid than the case with a 45° angle of skew under the same central concentrated load. Variations of deflections and moment Mx for two point loading on the transverse axis and uniformly distributed load over the whole bridge deck are shown in Figs. 3.12 to 3.15. The variation appears to be similar in the two cases for the same angle of skew.

An aspect ratio in between 1 to 1.5 appears to be desirable, although in practice, the anticipated traffic density will determine the width of the skew bridge and hence the aspect ratio.

(c) Skew Angle:

Figures 3.16 to 3.23 show the effect of variations of skew angle on deflections and moments of the skew grillage system. With increase of skew angle, under a concentrated load at the centre, deflections of central nodal point decrease sharply after the skew angle has exceeded 30°. Up to 30 degrees, variations of deflections with the angle of skew is not very appreciable. Similar is the variation of longitudinal moment Mx with the angle of skew (Fig. 3.17). A slight increase in the value of deflections and moment (Figs. 3.16 and 3.17) is observed at the mid point of free edge girder with an increase of skew angle up to 30°.

Fig. 3.18 shows that after the skew angle has exceeded 30°, the transverse moment My at central interior point increases slowly up to a skew angle of 45° and tends to decrease slowly beyond this value. While My at the interior acute corner decreases appreciably, it increases sharply at the interior obtuse corner with further increase of skew angle. This points to stress concentration near the obtuse corner with increase of skew angle.

The influence of increasing angle of skew for two point loadings and uniformly distributed load on the deflections and moment Mx are shown in Figs. 3.20 to 3.23.

From this study it can be justified that up to a skew angle of 22°, the grillage in skew bridges can be analyzed in the same way as the right girder bridge by the method of lateral distribution and distribution coefficients [3].

(d) Poisson's Ratio:

The value of μ_x was varied from 0.0 to 0.33 to show its influence on deflections and moments of the structural system (Figs. 3.24 to 3.29). Under a concentrated load acting at the centre, a change in the value of μ_x from 0.0 to 0.33 resulted in a decrease of deflection up to 15% at central point, 3% at the mid point of free edge, 11% at the interior point near the obtuse corner and 8% at the interior point near the acute corner, respectively (Fig. 3.24). The influence of Poisson's ratio on moment Mx (Fig. 3.25) for a concentrated load at centre appears to be appreciable. An increase of 8% and a decrease of 7% in the value of Mx were observed for central interior point and mid point on the free edge for an increase in the value of μ_x from 0.0 to 0.33 (Fig. 3.25). While a change of Poisson's ratio does not have an appreciable effect on moment My at interior central point (Fig. 3.26), a sharp decrease of My was observed at the interior point near the acute corner.

Figures 3.28 and 3.29 show the influence of Poisson's ratio on deflections and moments Mx at different points on the bridge under uniformly distributed load. At the mid point of the free edge deflections increased by 4% for an increase of Poisson's ratio from 0 to 0.33 whereas deflections at the central point decreased by 10%. For the same variation of μ_x, the interior acute corner deflection increased by 4% and the interior obtuse corner deflections decreased by 3%. Under the same uniform loading, though the moment Mx does not change appreciably at the central point and interior point near the acute corner, an increase of 5% in the value of Mx at the mid point of edge girder was observed for the same variation of μ_x (Fig. 3.29).

From this study it is clear that a proper value of μ_x which is not a material constant as Poisson's ratio proper but an elastic constant corresponding to the form of the system (since the value of μ_y is determined from the relation $\mu_y = \frac{B_y}{B_x}\mu_x$) should be incorporated in the analysis of gridwork with deck slab to yield a more accurate solution.

8.3 Conclusions:

From the investigation of this problem it has been shown that the theory of orthotropic plate can be effectively used in the analysis of gridwork in skew bridges.

The difficulties encountered in satisfying the boundary conditions along the simply supported edge and free edge of the structural system (the imposition of constraint $w_{4'} + w_4 - 2w_o = 0$ near the simple support may not always be true depending on the loading condition) are not of a serious nature, since in actual practice extra reinforcement would be provided along the simply supported edge to take the support reactions and the free edge would normally have some form of footpath which would prevent heavy loads to be applied at the free edge of the skew bridge.

By simply changing the data cards in the general computer programme, all the variable parameters such as number of girders and diaphragms, their spacing and stiffness ratios and aspect ratio for a particular alignment of a skew bridge can be examined to obtain an optimum design.

Due to simplicity in application and quite a good degree of accuracy in results, orthotropic plate analysis of gridwork in skew bridges by the method of finite differences, may be used as a powerful design tool.

8.4 Suggestions for further Research:

Though the elastic analysis dominates the field of bridge engineering, it is now generally acceptable that the understanding of any structure is incomplete unless its behaviour beyond the elastic range is fully investigated. Hence the elasto-plastic and plastic behaviour of gridwork in skew bridges may be of considerable interest and practical value for economical design purposes.

Since the ultimate strength design presupposes that the governing forces acting in the structure due to dead load and live load are calculated by elastic theory [6], it is recognized at this point that further research beyond the elastic range should be carried out to have a clear insight of the structural behaviour of gridworks in skew bridges.

BIBLIOGRAPHY

1. Hendry, A.W. and Jaeger, L.G., 'The Analysis of Grid Framework and Related Structures', Chatto and Windus, London, 1958.

2. Langendonck, T.V., 'Gridworks of Skew Bridges', Publ. of the Intn. Assoc. for Bridge and Struct. Eng., Vol. 26, 1966.

3. Bares, R. and Massonet, C., 'Analysis of Beam Grids and Orthotropic Plates by the Guyon-Massonet-Bares Method', Frederick Unger Publishing Co., New York, 1968.

4. Naruoka, M. and Ohmura, H., 'On the Analysis of a Skew Girder Bridge by the theory of Orthotropic Parallelogram Plate', Publ. of the Intn. Assoc. for the Bridge and Struct. Eng., Vol. 19, 1959.

5. Fujio, T., Ohmura, H. and Naruoka, M., 'On the Rapid and Rational Calculation of Bending Moment Of Skew Girder Bridges', Publ. of the Intn. Assoc. for Bridge and Struct. Eng., Vol. 25, 1965.

6. Kennedy, J.B. and Tamberg, K.G., 'Problems of Skew in Concrete Bridge Design', Department of Highways, Ontario, Canada, March, 1969.

7. Basar, Y. and Yuksel, F., 'Zur Berechnung schiefwinkliger orthotroper und isotroper platten', Beton und Stahlbetonbau, Nov. and Dec. 1961.

8. Fawcett, F.B., 'The Elastic Analysis of Skew Slab Bridges', Dept. of Sc. and Ind. Res., Rd. Res. Lab. Note No. LN/697/FBF, Nov. 1964.

9. Vitols, V., Rodney, J. and Tung, Au., 'Analysis of Composite Beam Bridges by orthotropic plate theory', ASCE, Proc. Vol. 89 (J. Structural Division), nST4. Aug. 1963.

10. Huber, M.T., 'Die Theorie der Kreuzweise bewehrten Eisenbeton platten', Der Bauingenieur, Vol. 4, pp. 354-360. Germany, 1923.

11. Huffington Jr., N.J., 'Theoretical Determination of Rigidity Properties of orthogonally stiffened plates', Doctoral Dissertation, The Johns Hopkins University, 1954.

12. Kärrholm, G., 'Parallelogram Plates Analysed by Strip Method', Doctorsavhanlingar Vid chalmers Tekniska hogskola, NR 11 Goteborg, 1956.

13. Cornelius, W., 'Die Berechnung der ebenen Flachen-trawgwerke mit Hilfe der Theorie der orthogonal-anisotropen platte', Stahlbau, Vol. 21, pp. 21-24; 43-48; 60-63, Germany, 1952.

14. Timoshenko, S.P. and Krieger, S.W., 'Theory of Plates and Shells', McGraw-Hill Book Company, 1940.

15. Foye, R.L., 'Difference Equations and Elastic Plates', Doctoral Dissertation, Department of Engineering Mechanics, Ohio State University, Ohio, 1963.

16. Shaw, F.S., 'An Introduction to Relaxation Methods', Dover Publications, New York, 1965.

17. Jensen, V.P., 'Analysis of Skew Slabs', Univ. of Illinois, Eng. Expt. Sta., Bul. 332, Sept. 1941.

18. Coull, A., 'The Stress Analysis of orthotropic skew Bridge Decks', Structural Engineer, Vol. 42, No. 7, July, 1964. pp. 235-241.

19. Cheung, Y., King, I., and Zienkiewicz, O., 'Slab Bridges with arbitrary shape and support conditions', Journal of the Institution of Civil Engineers, Vol. 40, May, 1968, pp. 9-36.

20. Powell, G.H. and Ogden, D.W., 'Analysis of orthotropic Steel Plate Bridge Decks', ASCE, Proc. Vol. 95 (J. Structural Division), N. ST5, May, 1969.

21. Paterson, D.K.W. and Cusens, A.R., 'Skew Orthotropic Plate under uniform loading', Department of Civil Engineering, University of Dundee, Sept. 1969.

22. Kennedy, J.B. and Huggins, M.W., 'Series Solution of Skewed Stiffened Plates', Journal of the Engineering Mechanics Division, ASCE, Vol. 90, No. EM1, Proc. Paper NO. 3795, Feb. 1964, pp. 1-22.

23. 'Orthotropic Steel Deck Bridges', Design Manual of American Institute of Steel Constructions Inc., Nov. 1962.

24. Lie, K., 'Theorie der Schiefwinklig-anisotropen platte und ihre Anwendungauf schiefe Bruken', Acta Mechanica Sinica, 2.1, 1958, pp. 78-89.

25. Naruoka, M., 'Uber die Berechnung schiefer anisotroper Platten', Vol. 37, No. 11, Nov. 1962, pp. 422-426.

PHOTO PLATES

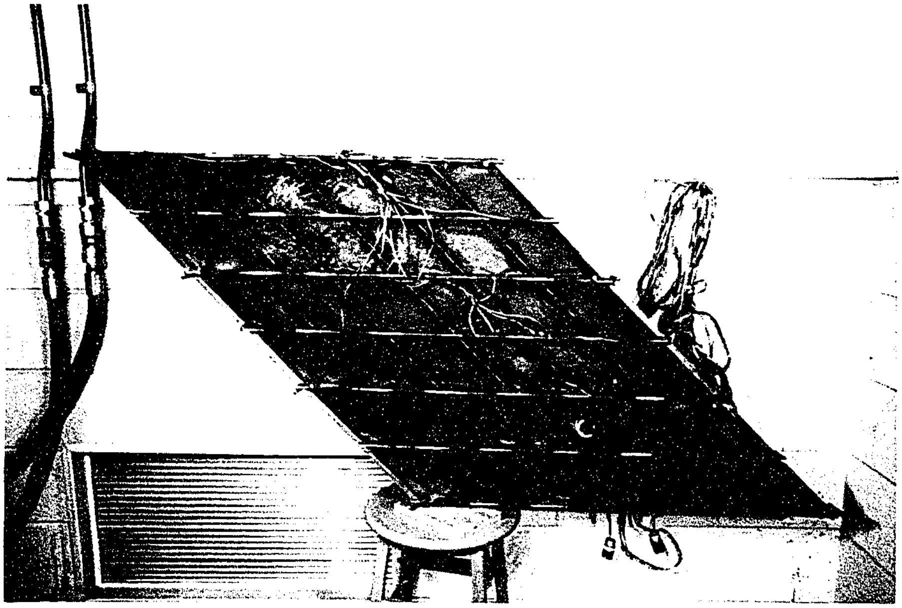

FIG. 1.1 MODEL BRIDGE

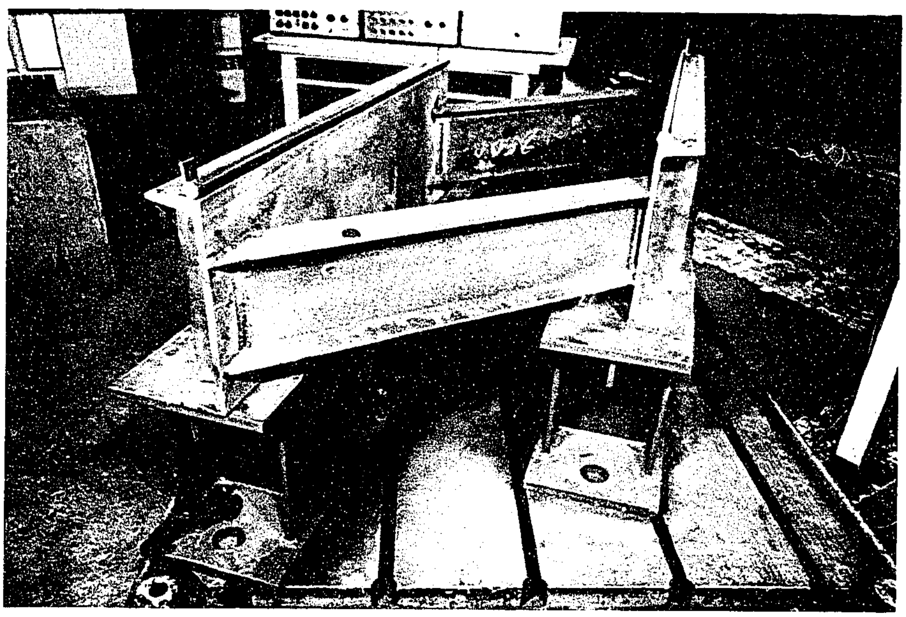

FIG. 1.2 ABUTMENT FRAME

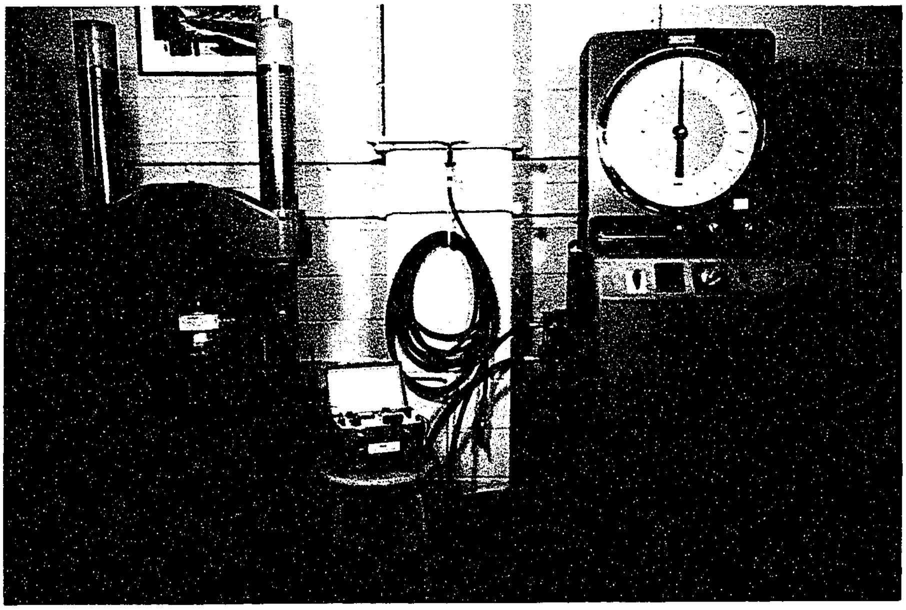

Fig. 1.3 Calibration of Load Cell

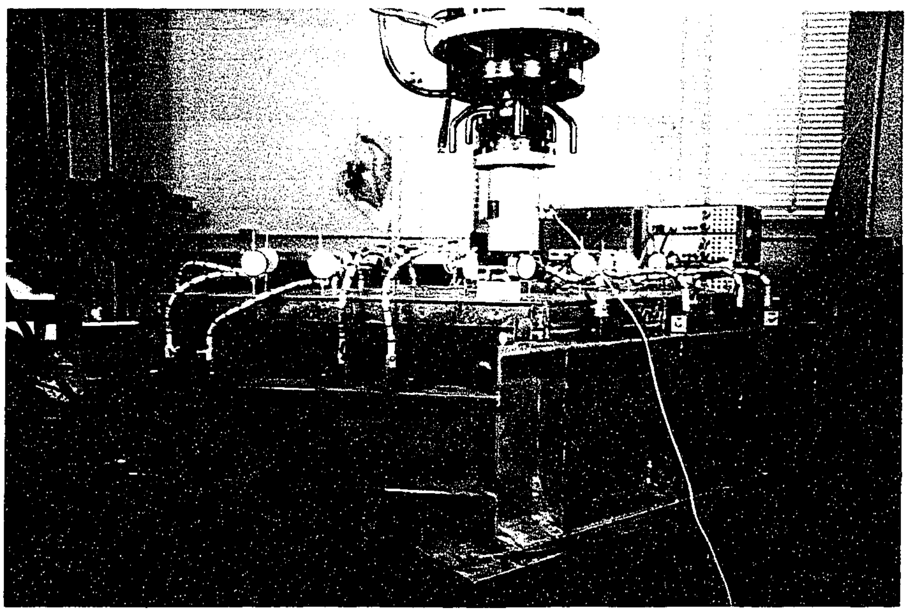

Fig. 1.4 Loading Device for a Concentrated Load at Centre.

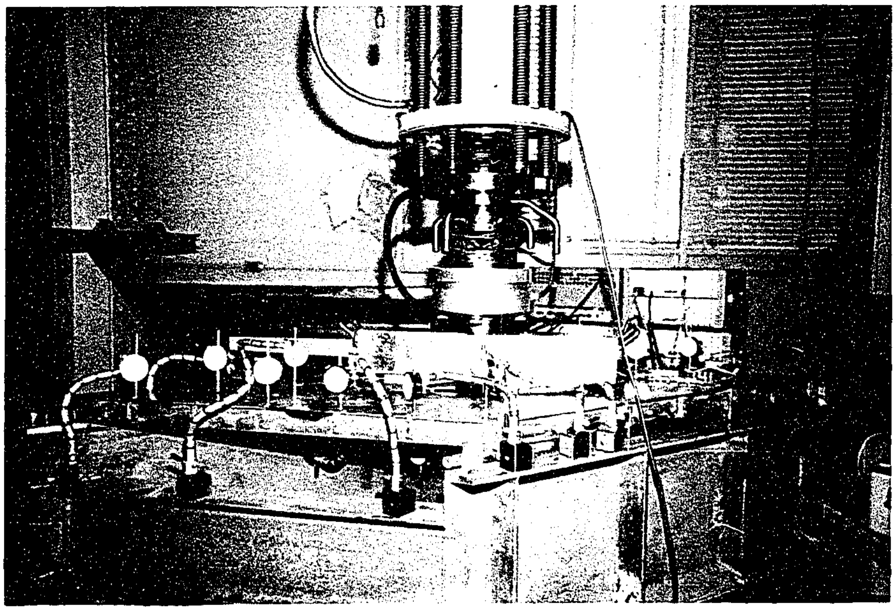

Fig. 1.5 Loading Device for Two Point Loading on the Longitudinal Axis

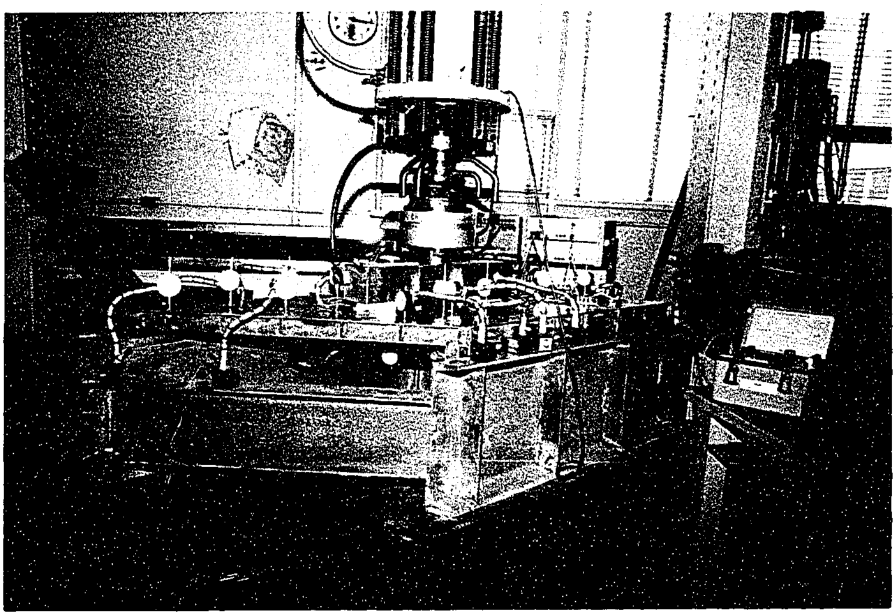

Fig. 1.6 Loading Device for Two Point Loading on the Transverse Axis

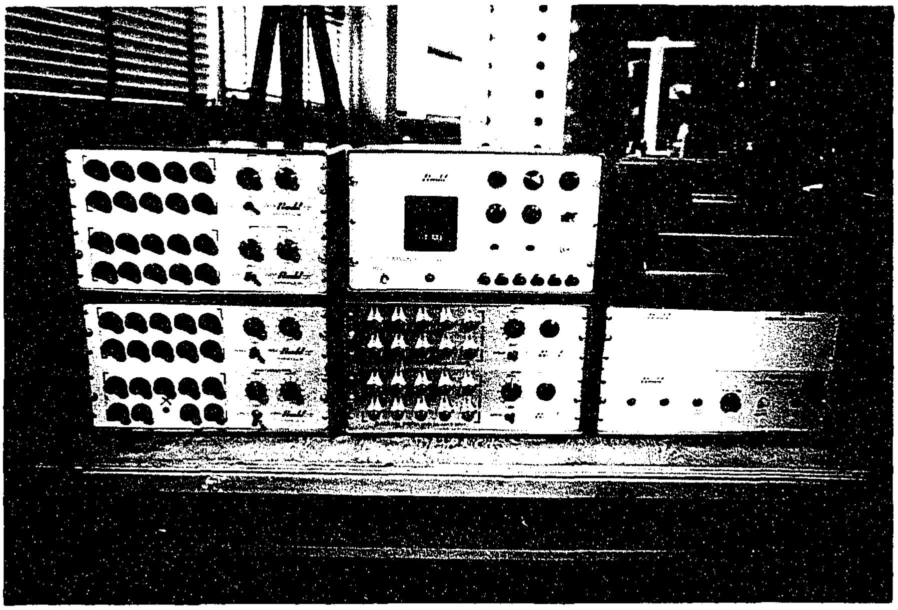

Fig. 1.7 Digital Strain Indicator

FIGURES

COMPARISON OF EXPERIMENTAL

AND THEORETICAL RESULTS

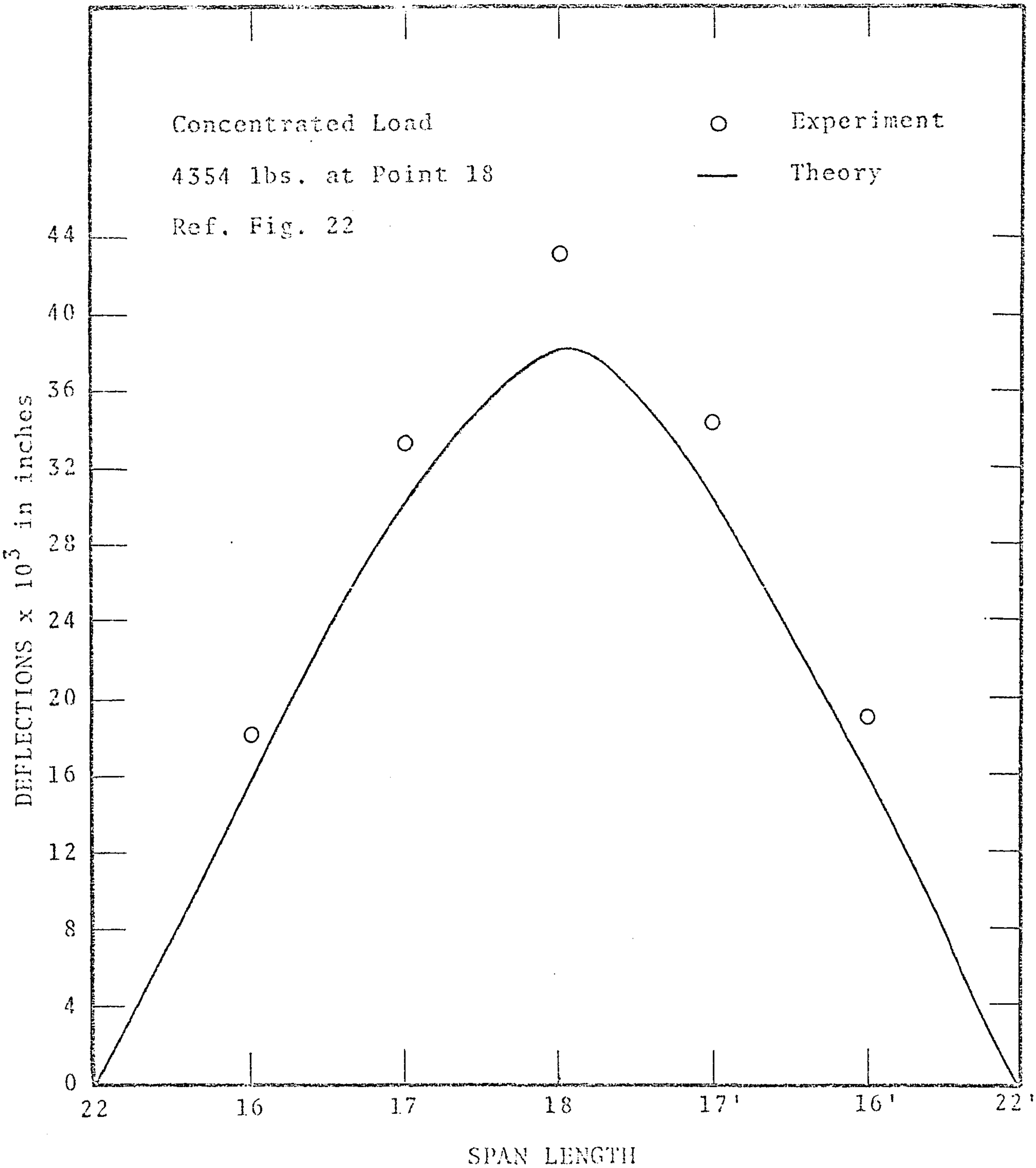

FIG. 2.1

Variations of Longitudinal Central
Girder Deflections with Span Length.

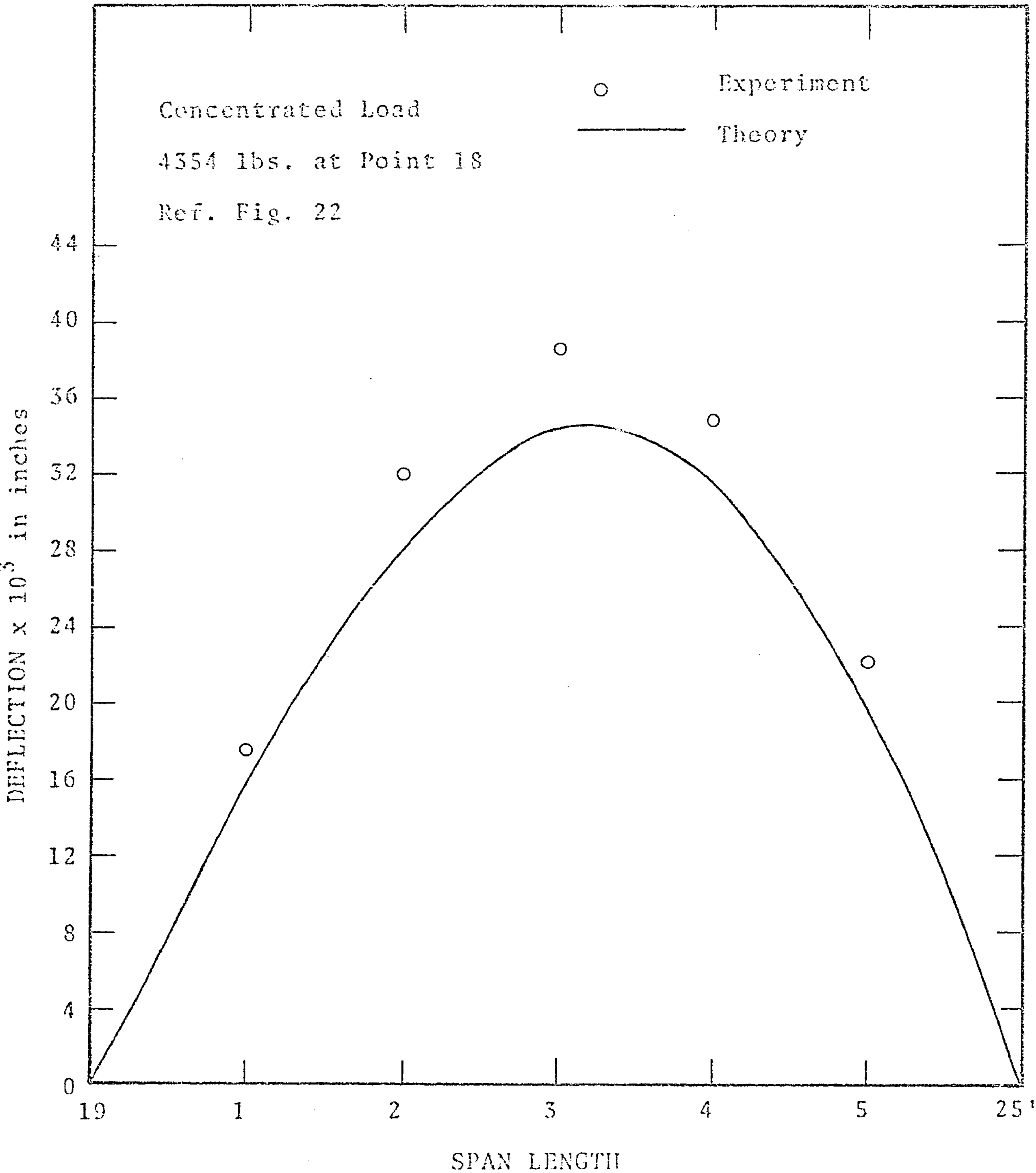

FIG. 2.2

Variations of Longitudinal Edge Girder Deflections with Span Length.

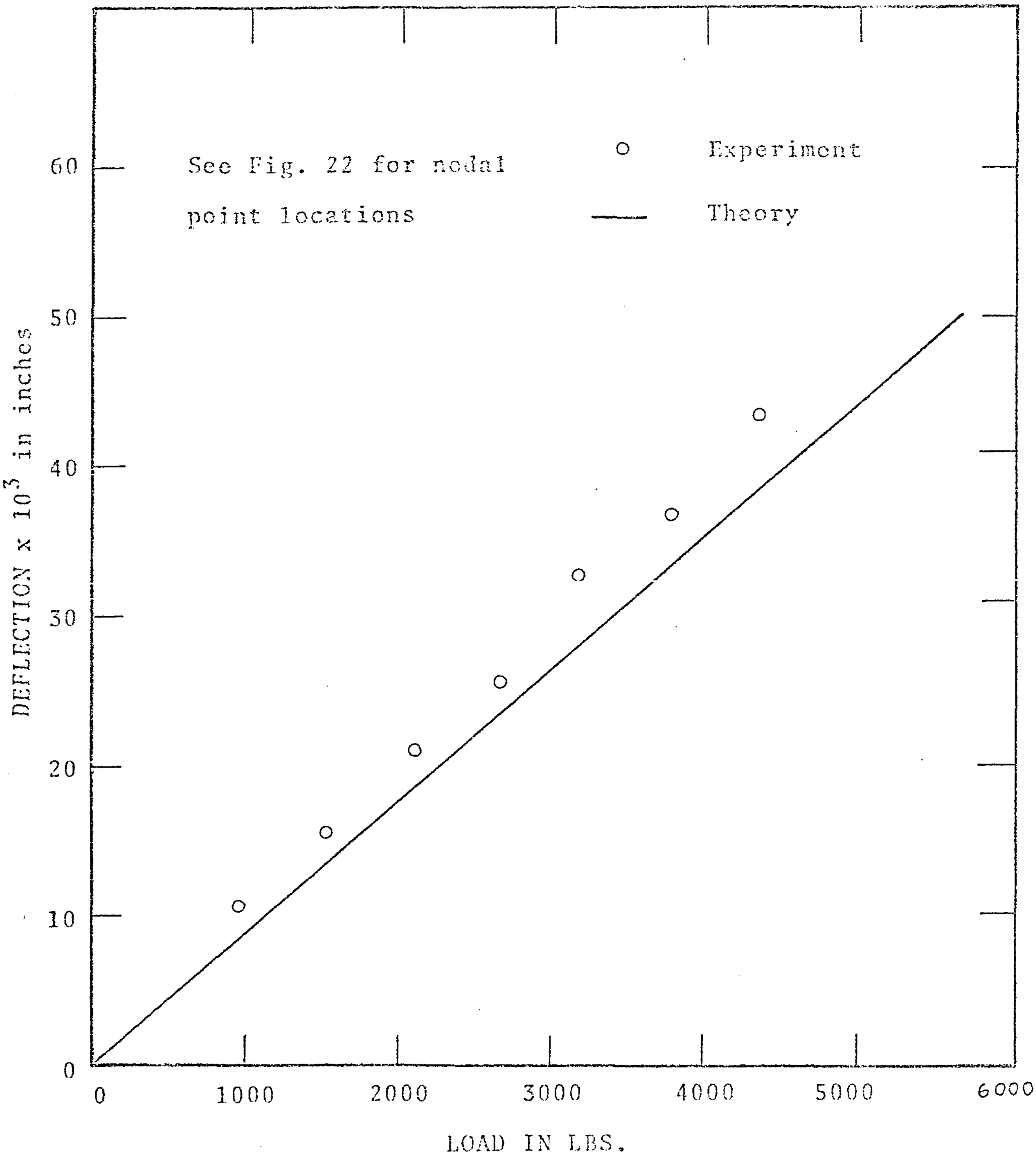

FIG. 2.3

DEFLECTION AT POINT 18
FOR CONCENTRATED LOAD AT CENTRE

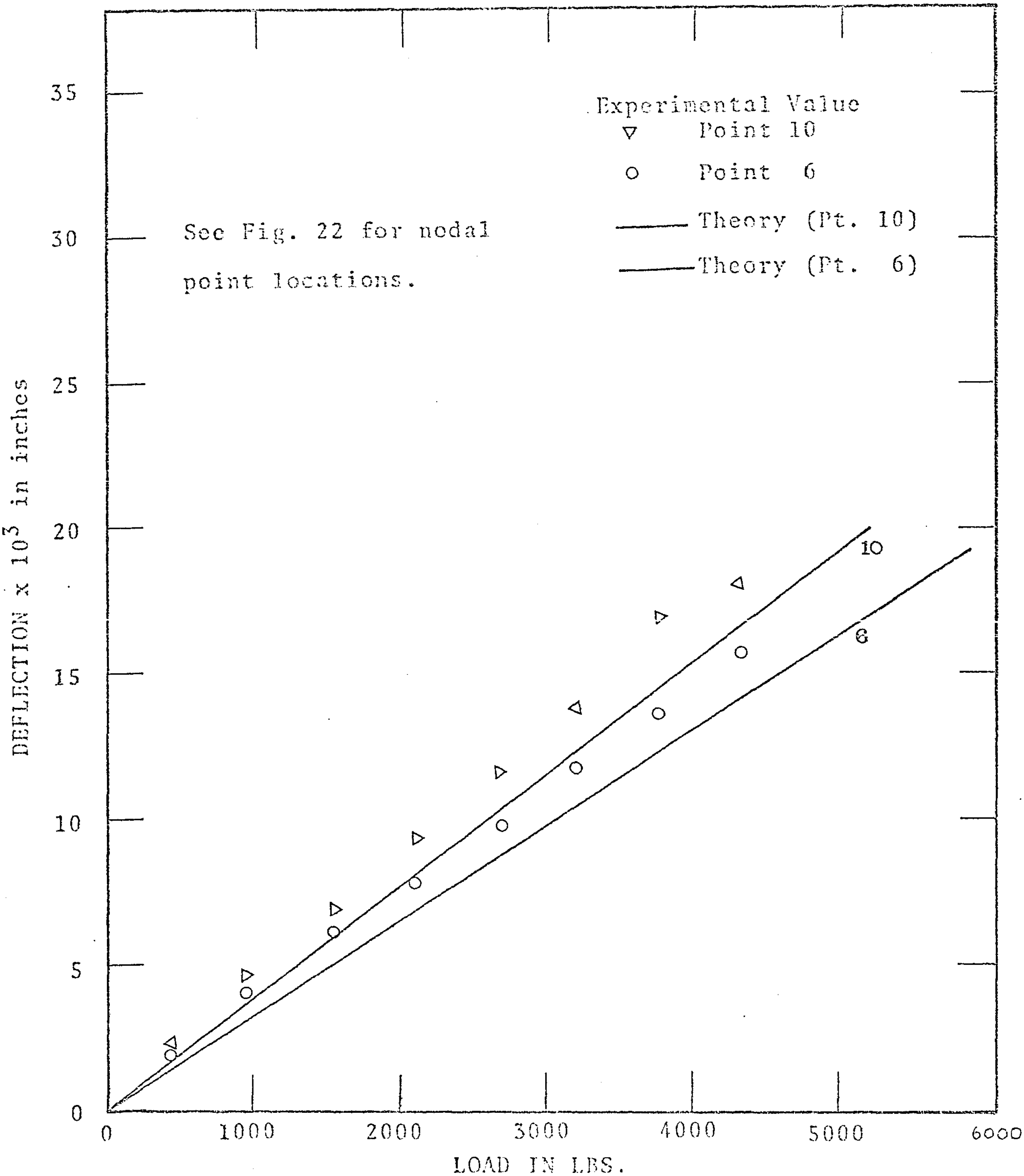

FIG. 2.4

DEFLECTIONS OF INTERIOR OBTUSE AND ACUTE CORNERS FOR CONCENTRATED LOAD AT CENTRE.

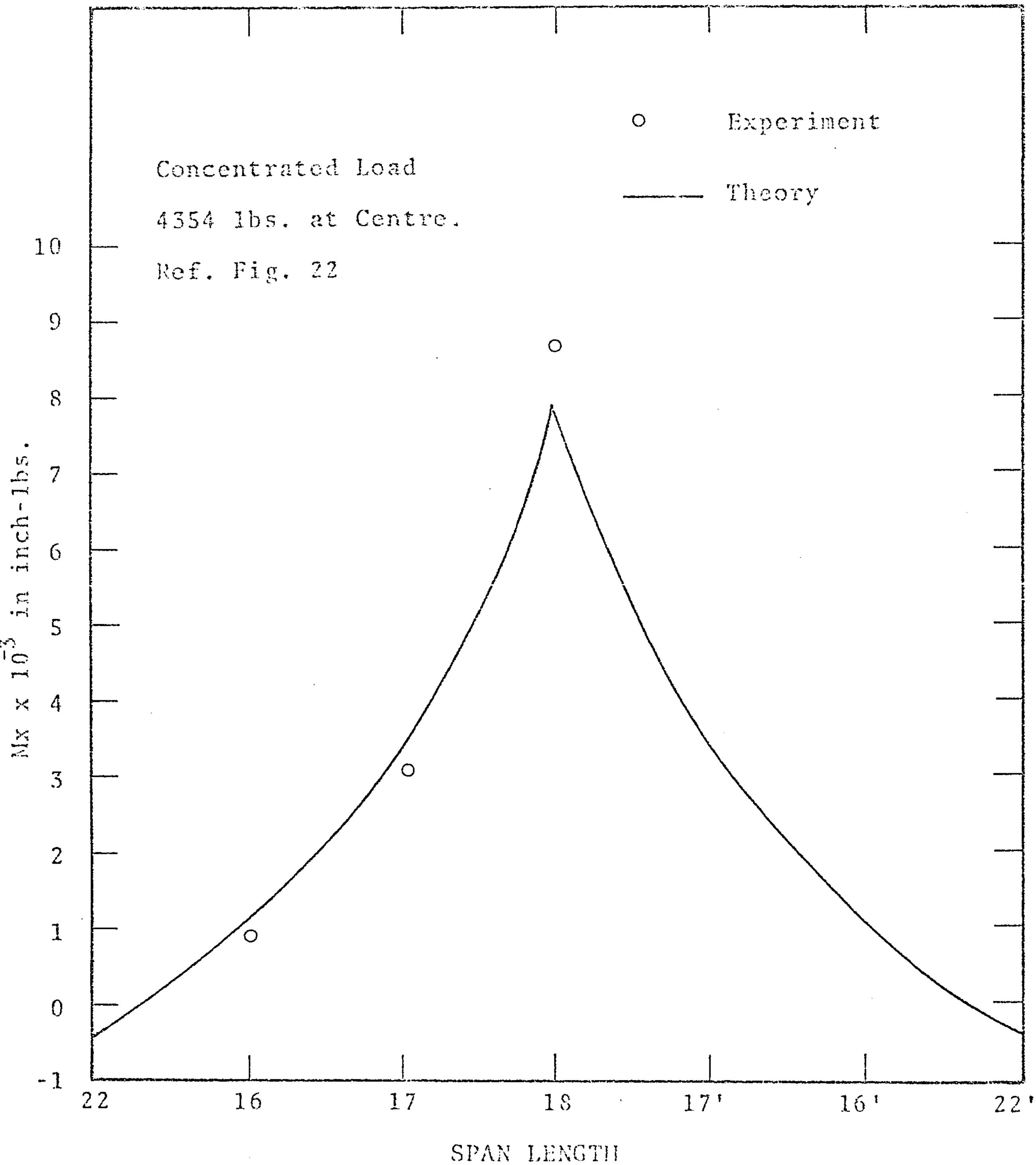

FIG. 2.5

VARIATIONS OF LONGITUDINAL CENTRAL GIRDER MOMENT Mx WITH SPAN LENGTH.

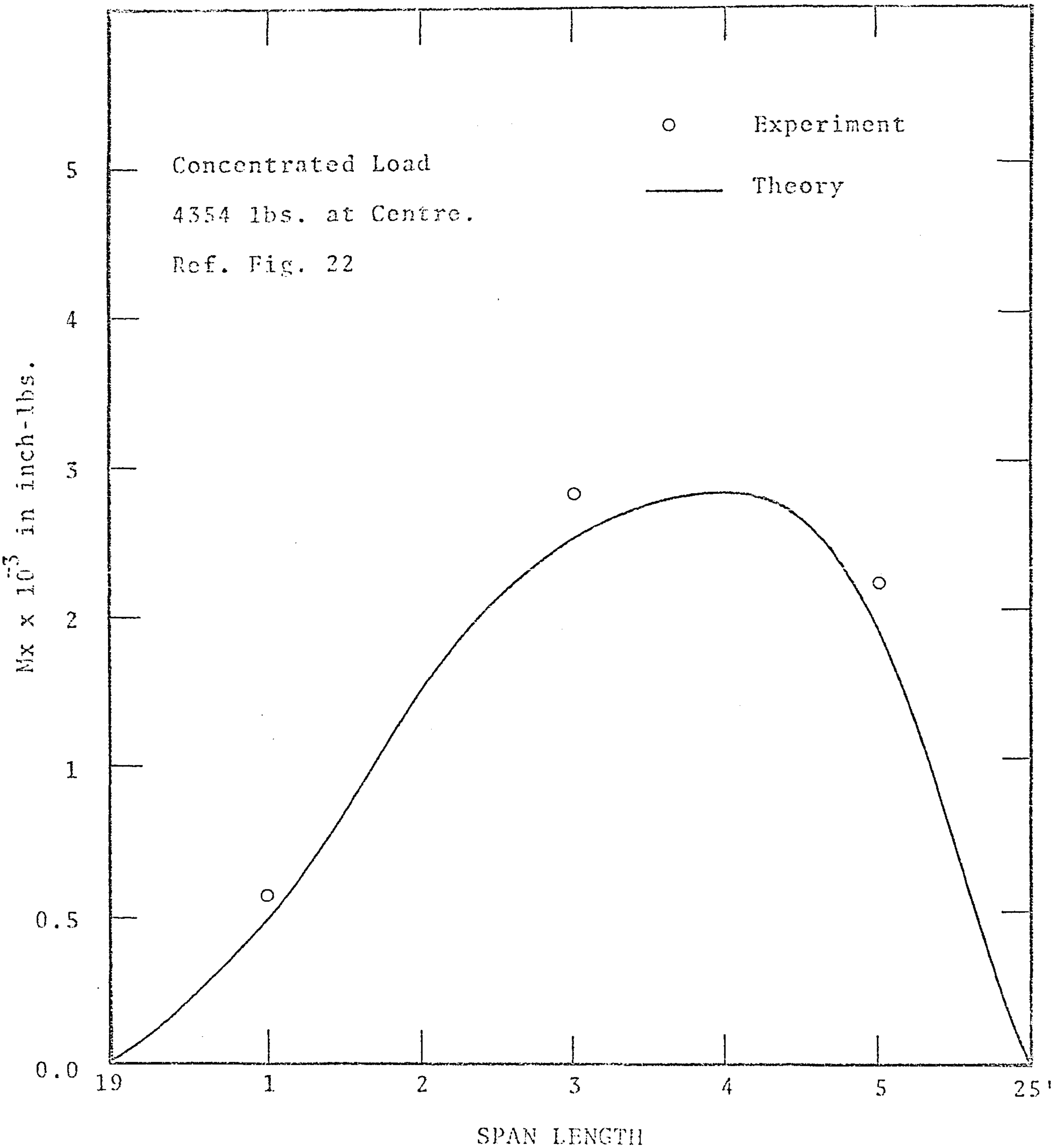

FIG. 2.6

VARIATIONS OF LONGITUDINAL EDGE
GIRDER MOMENT Mx WITH SPAN LENGTH.

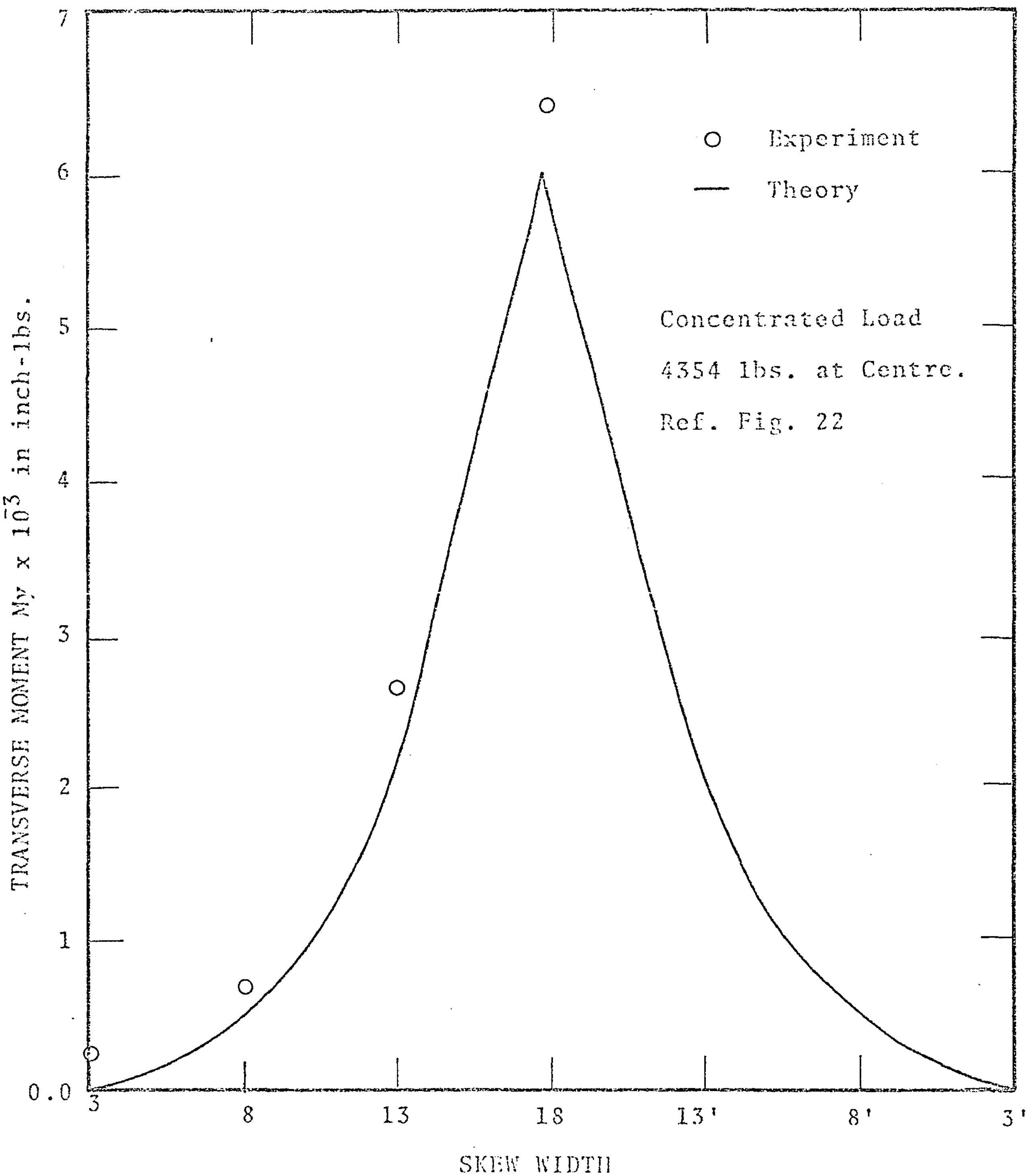

FIG. 2.7

VARIATION OF TRANSVERSE CROSS BEAM
MOMENT My WITH SKEW WIDTH.

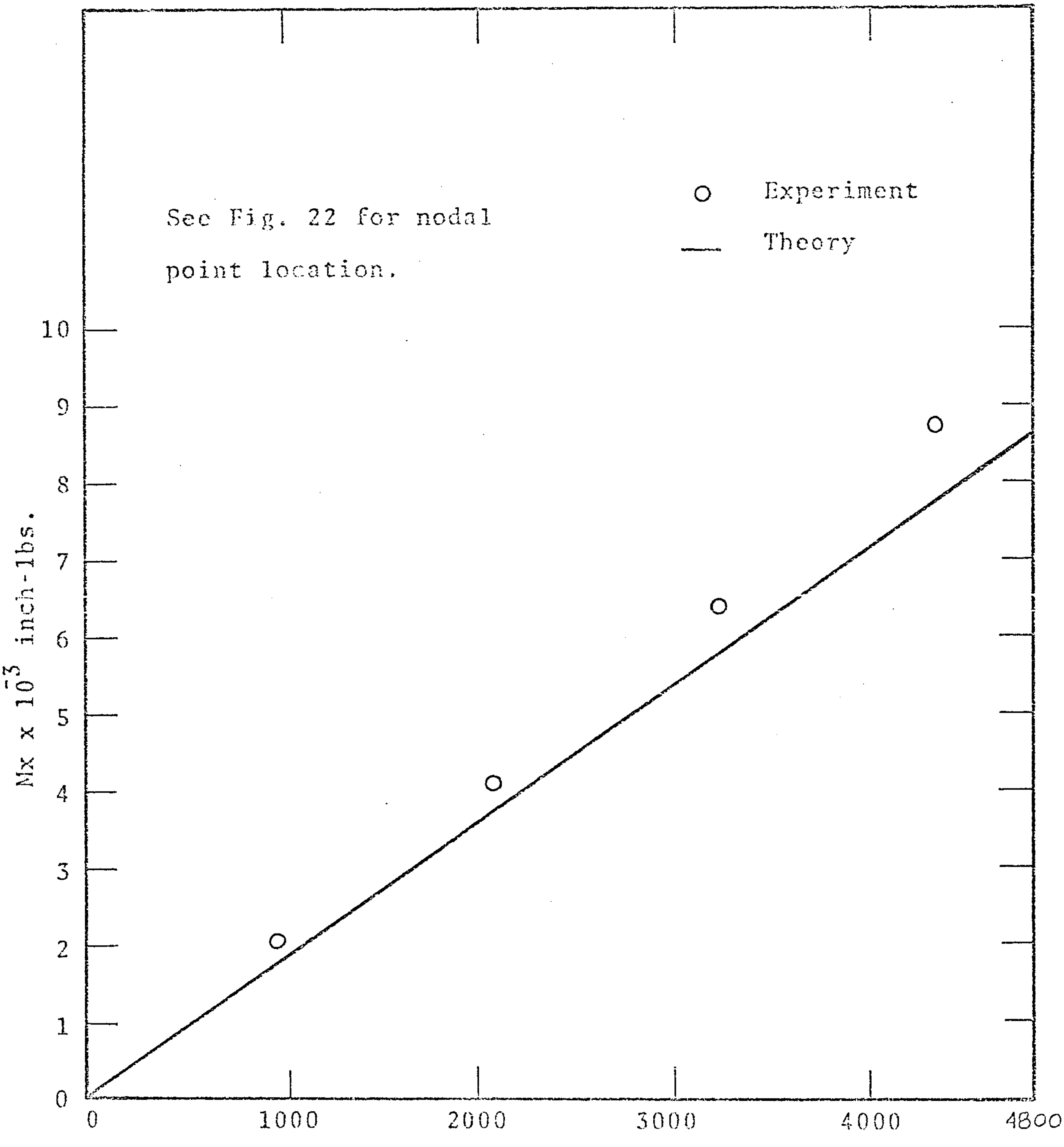

FIG. 2.8

Mx AT POINT 18 FOR
CONCENTRATED LOAD AT CENTRE.

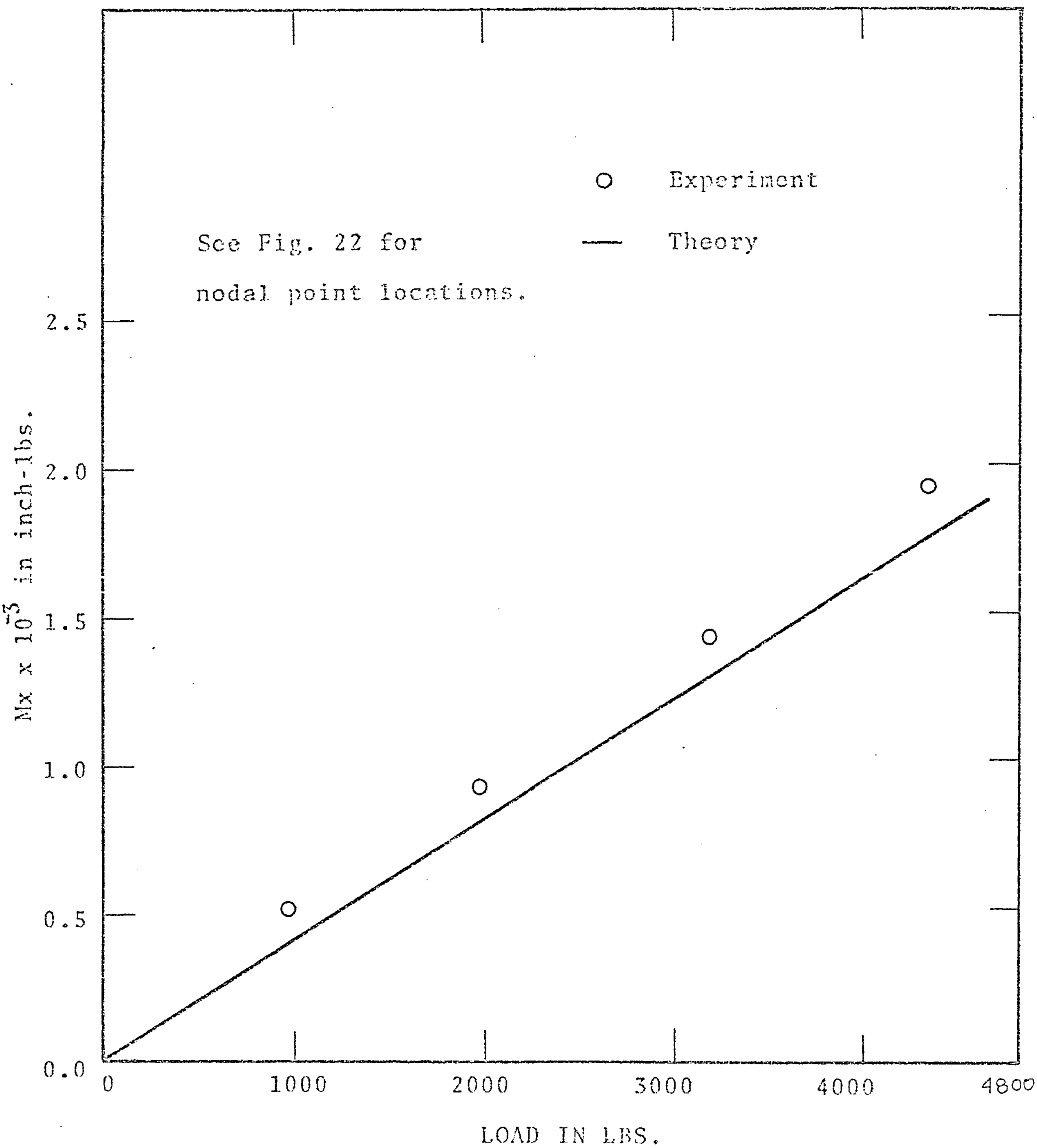

FIG. 2.9

Mx AT POINT 3 FOR CONCENTRATED
LOAD AT CENTRE.

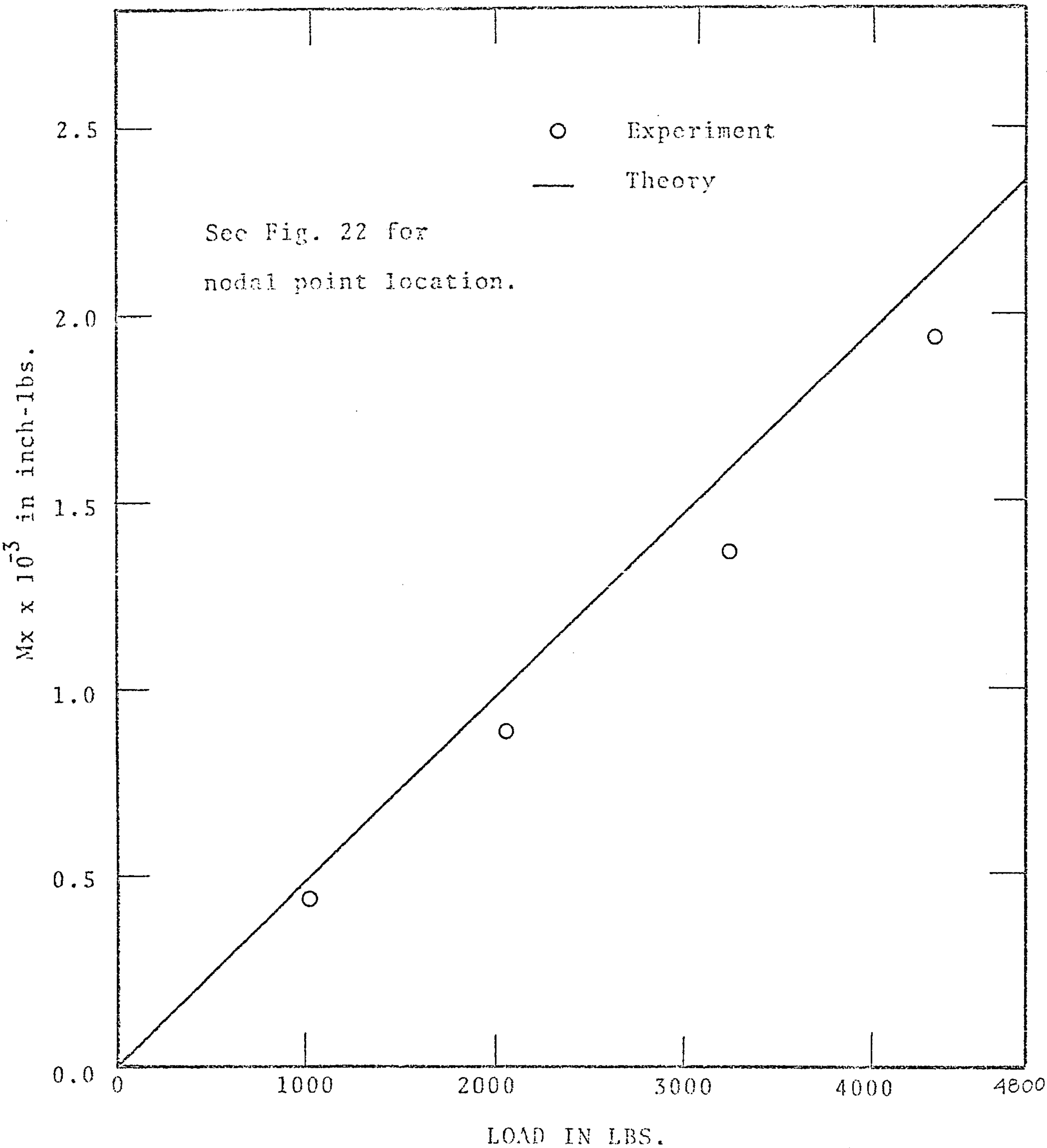

FIG. 2.10

Mx AT POINT 10 FOR CONCENTRATED LOAD AT CENTRE.

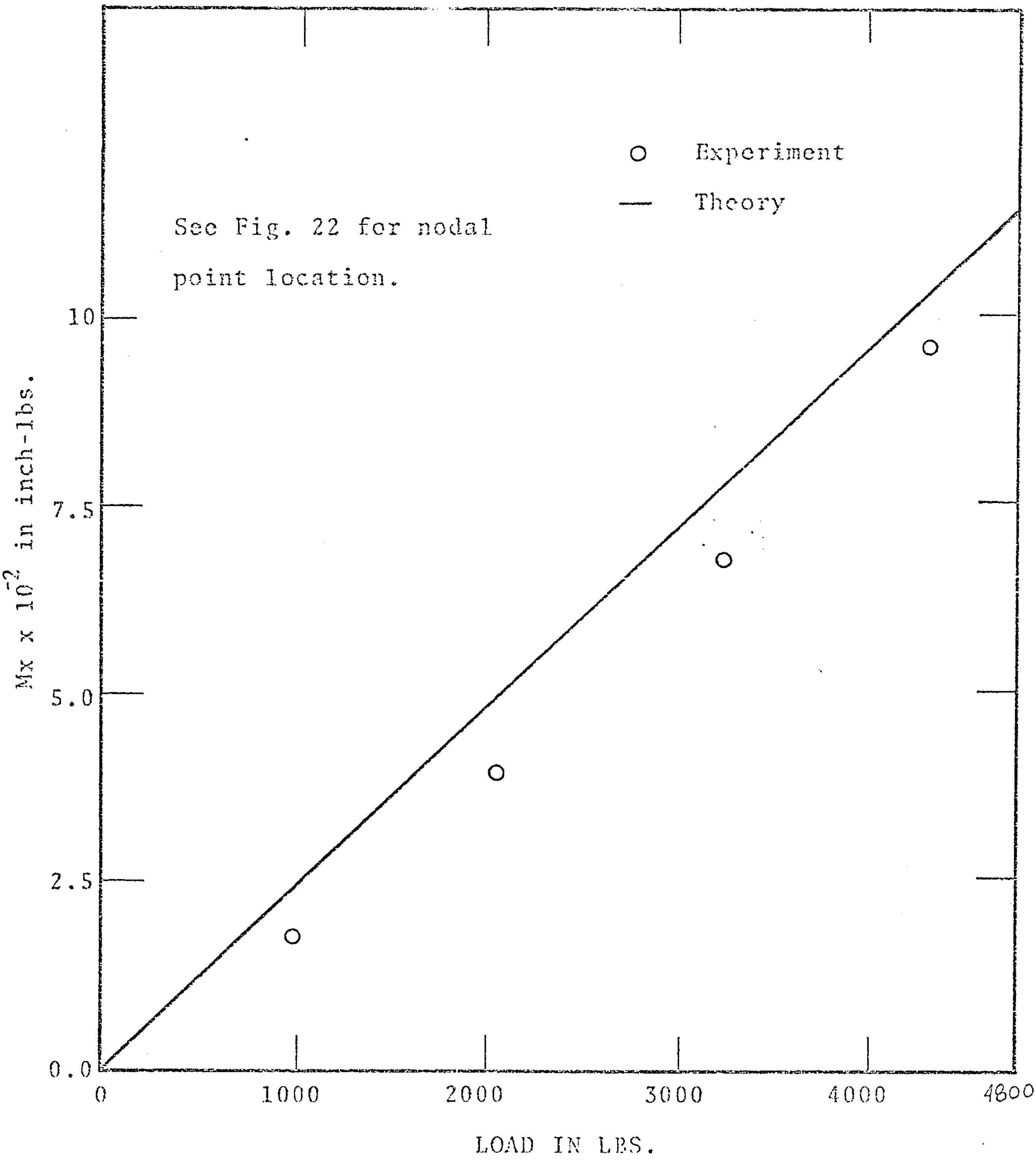

FIG. 2.11

Mx AT POINT 16 FOR CONCENTRATED
LOAD AT CENTRE.

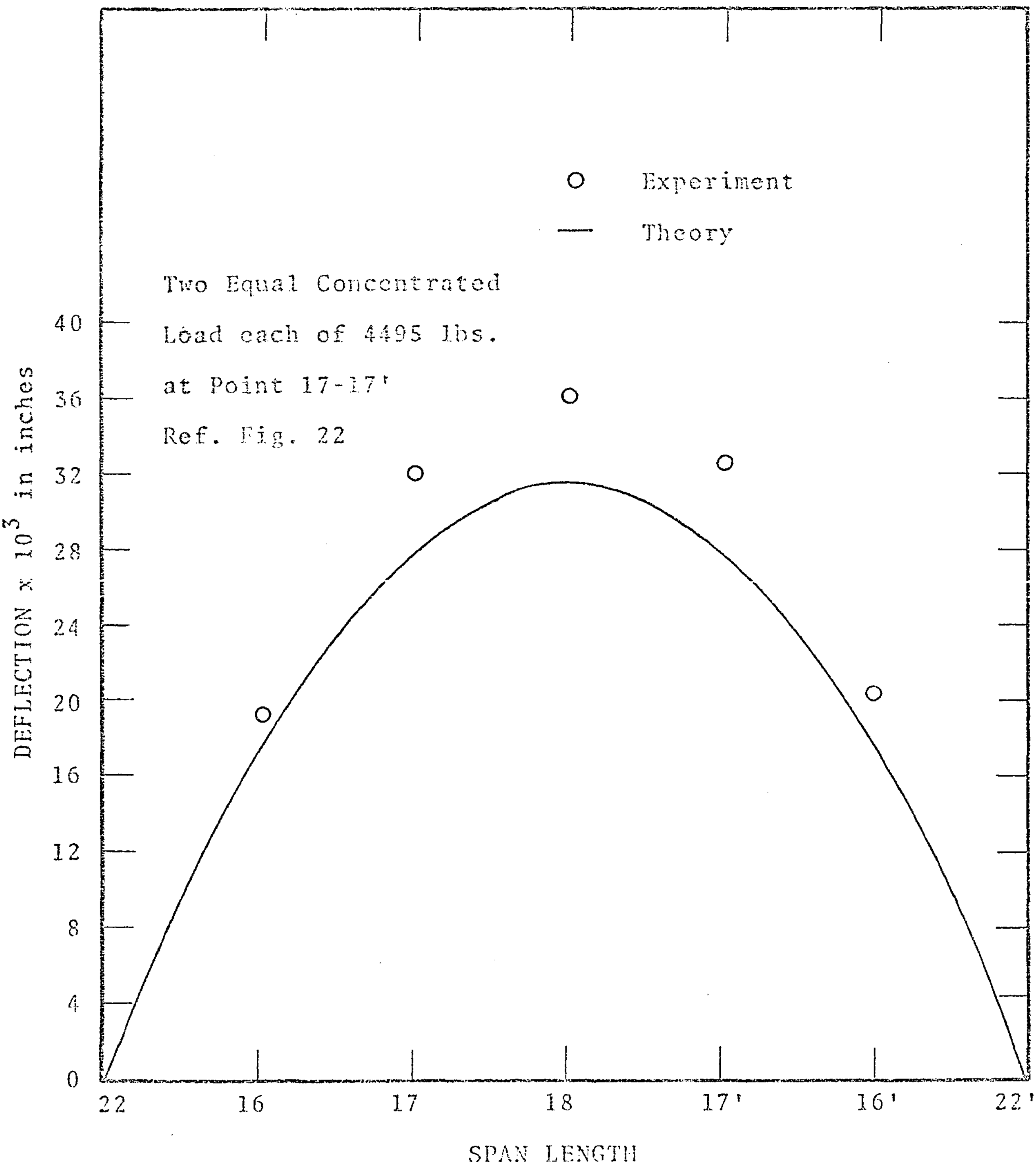

FIG. 2.12

VARIATIONS OF LONGITUDINAL CENTRAL
GIRDER DEFLECTIONS WITH SPAN LENGTH.

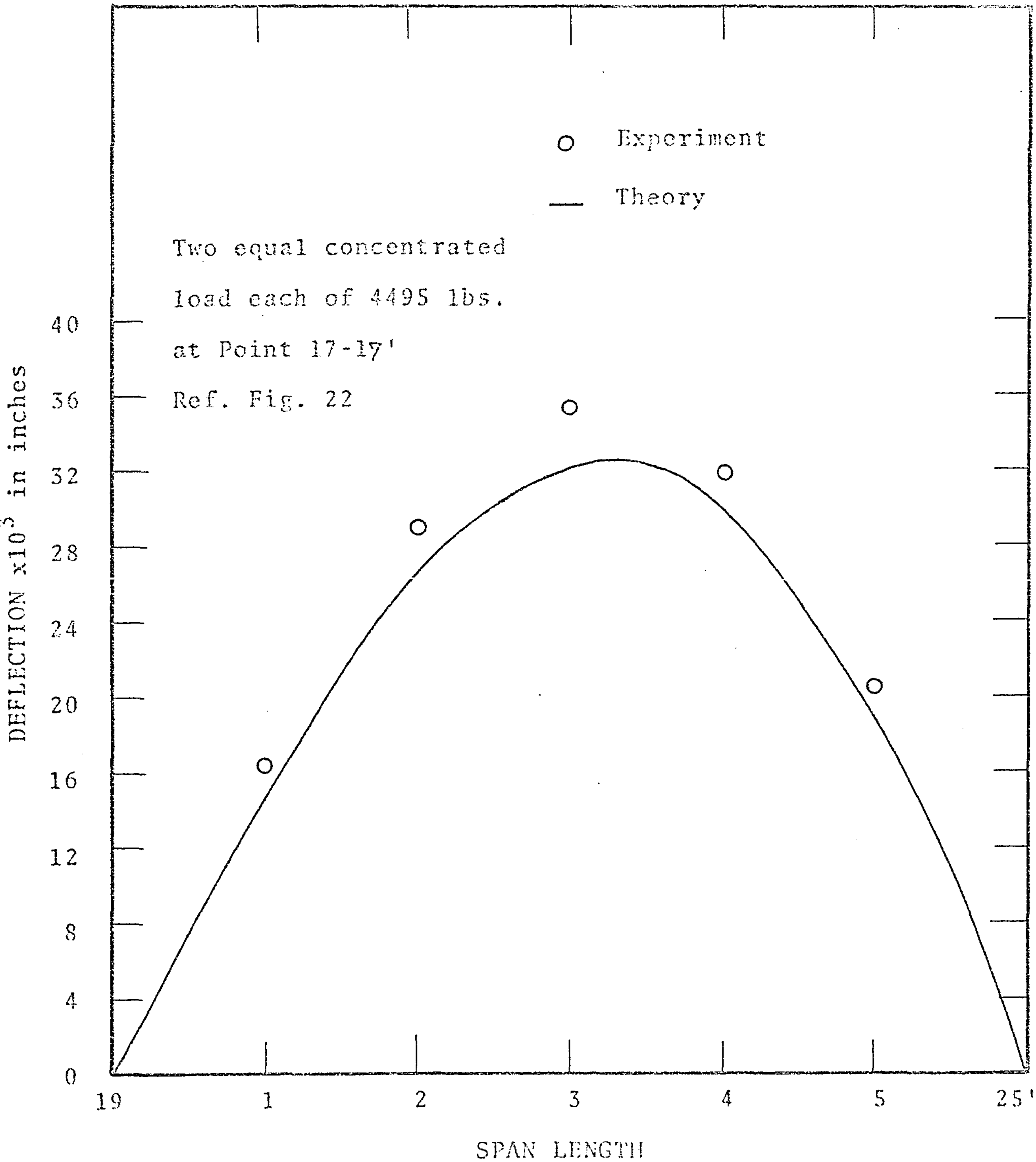

FIG. 2.13

VARIATIONS OF LONGITUDINAL EDGE
GIRDER DEFLECTIONS WITH SPAN LENGTH.

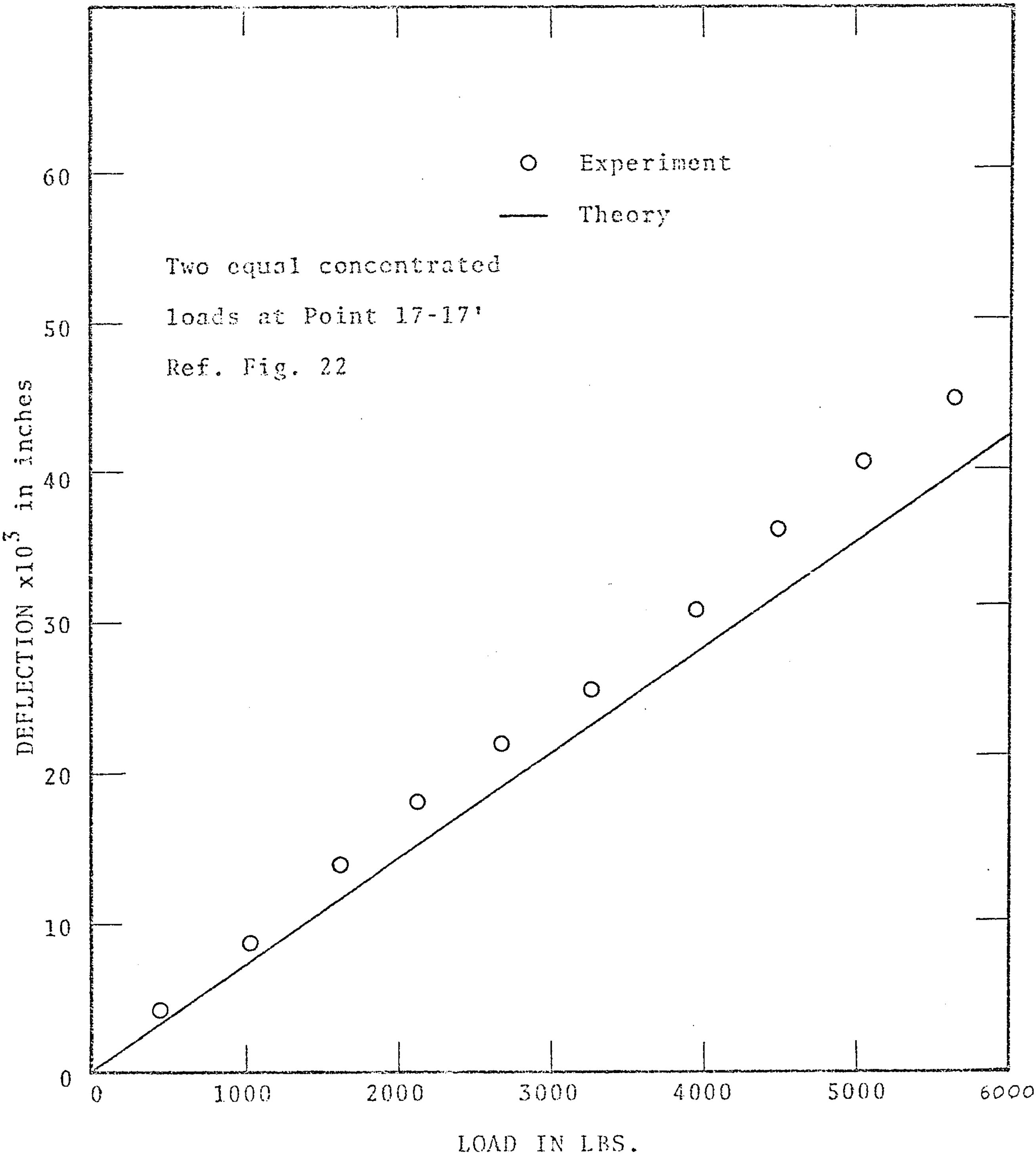

FIG. 2.14

DEFLECTIONS AT POINT 18 FOR TWO EQUAL CONCENTRATED LOADS ON LONGITUDINAL AXIS.

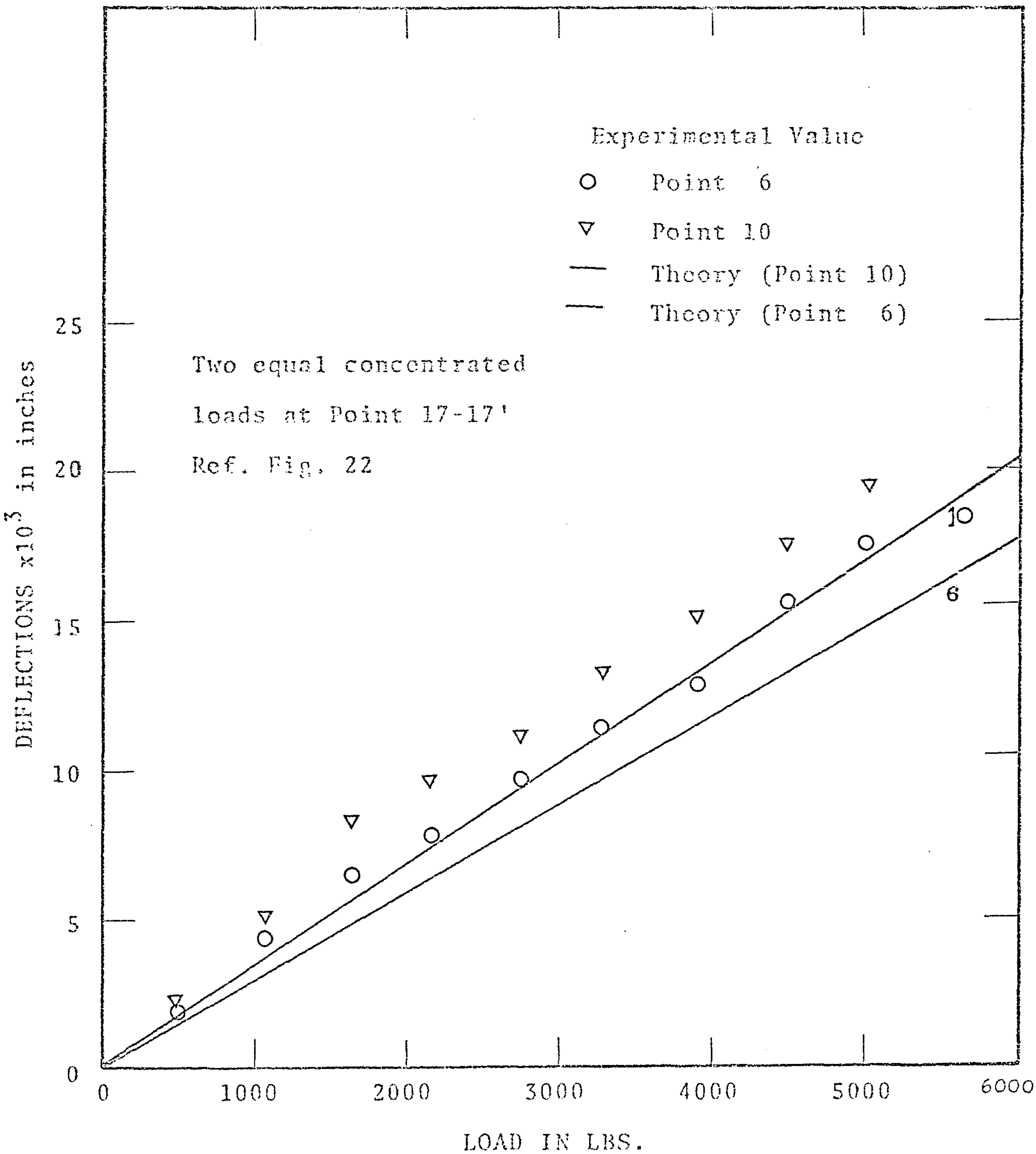

FIG. 2.15

DEFLECTIONS OF INTERIOR OBTUSE AND ACUTE CORNER POINTS.

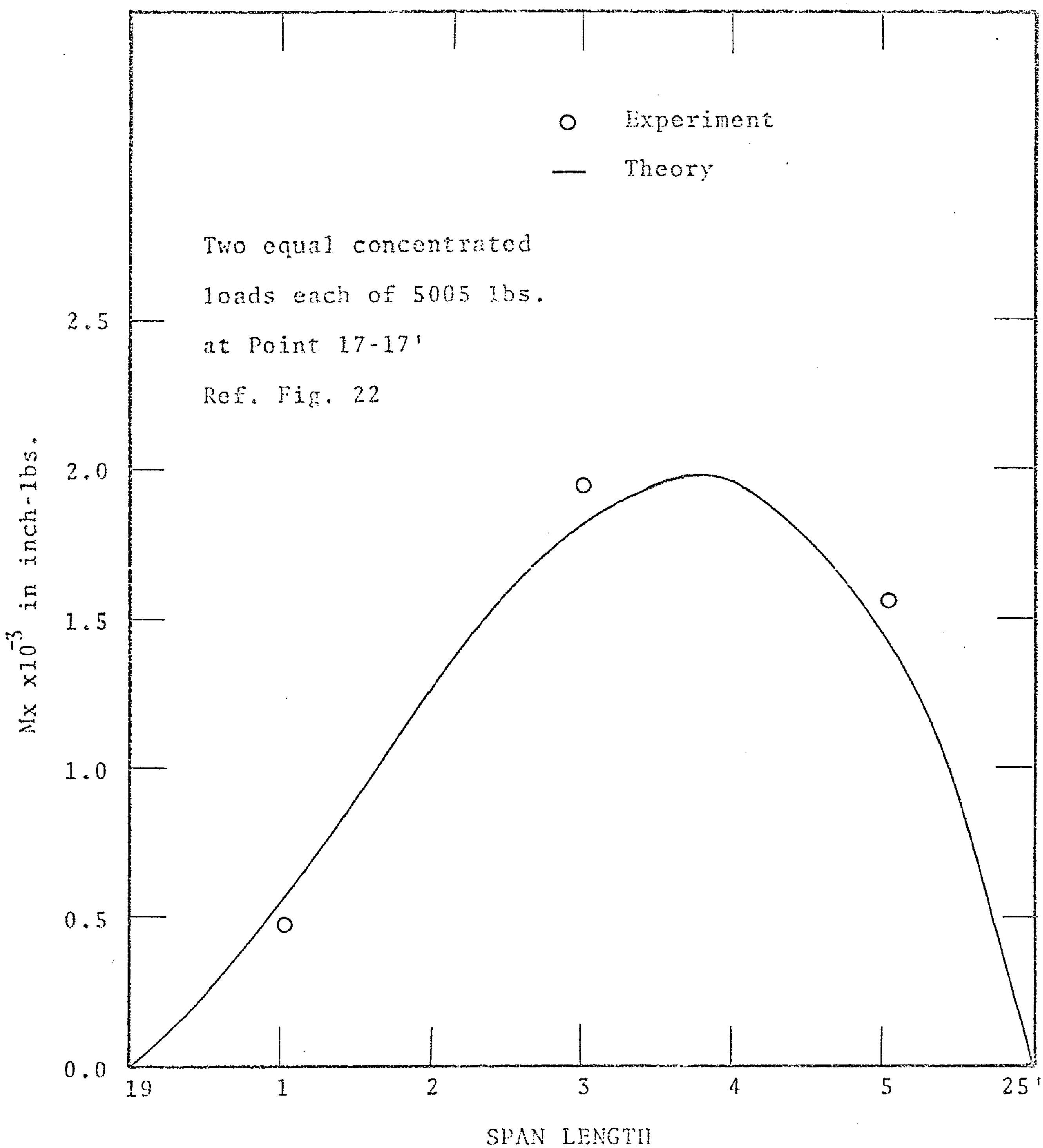

FIG. 2.16

VARIATIONS OF LONGITUDINAL EDGE GIRDER MOMENT WITH SPAN LENGTH.

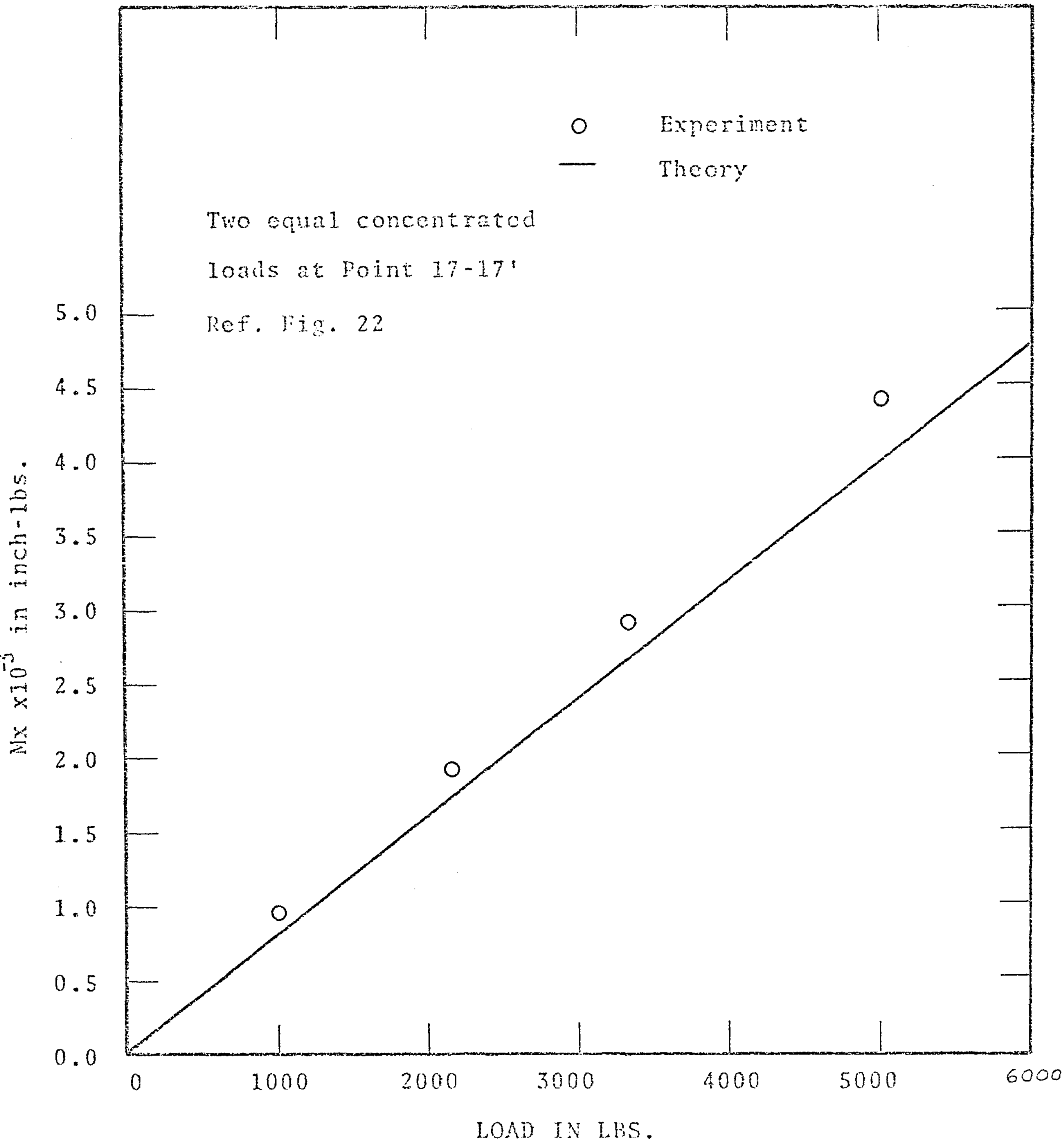

FIG. 2.17

Mx AT POINT 18 FOR TWO POINT
LOADING ON LONGITUDINAL AXIS

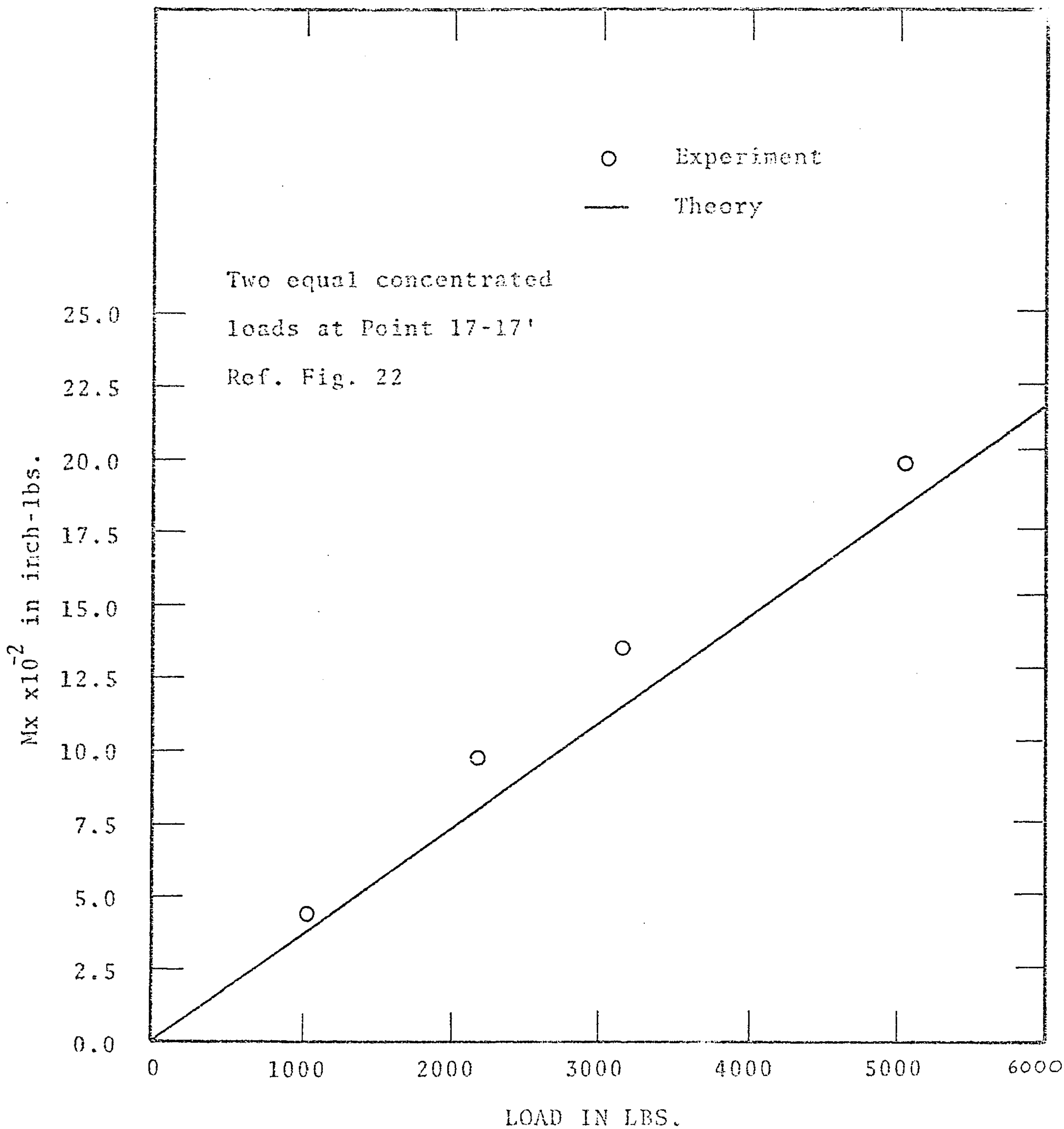

FIG. 2.18

Mx AT POINT 3 FOR TWO POINT
LOADING ON LONGITUDINAL AXIS

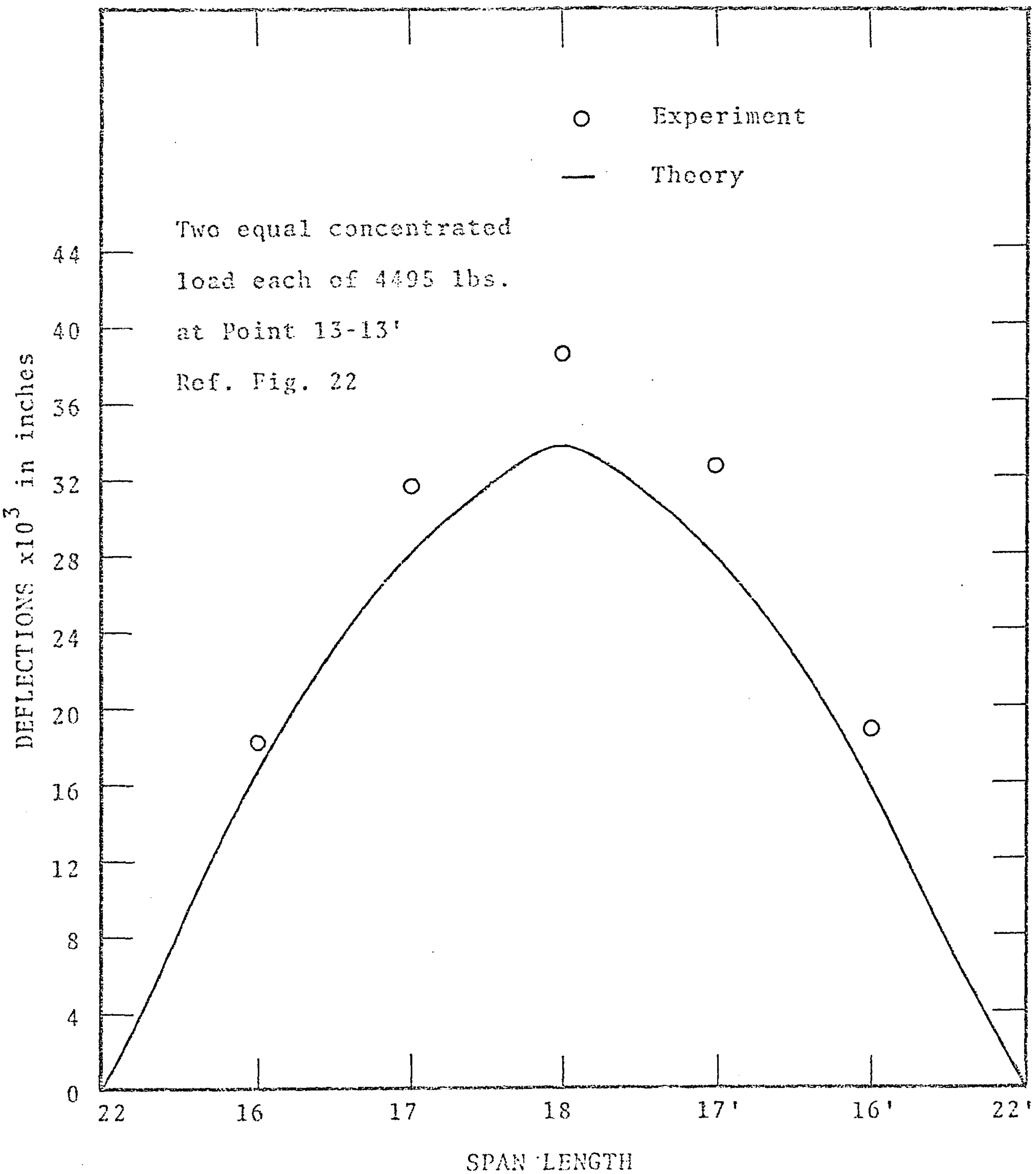

FIG. 2.19

VARIATIONS OF LONGITUDINAL CENTRAL GIRDER DEFLECTIONS WITH SPAN LENGTH.

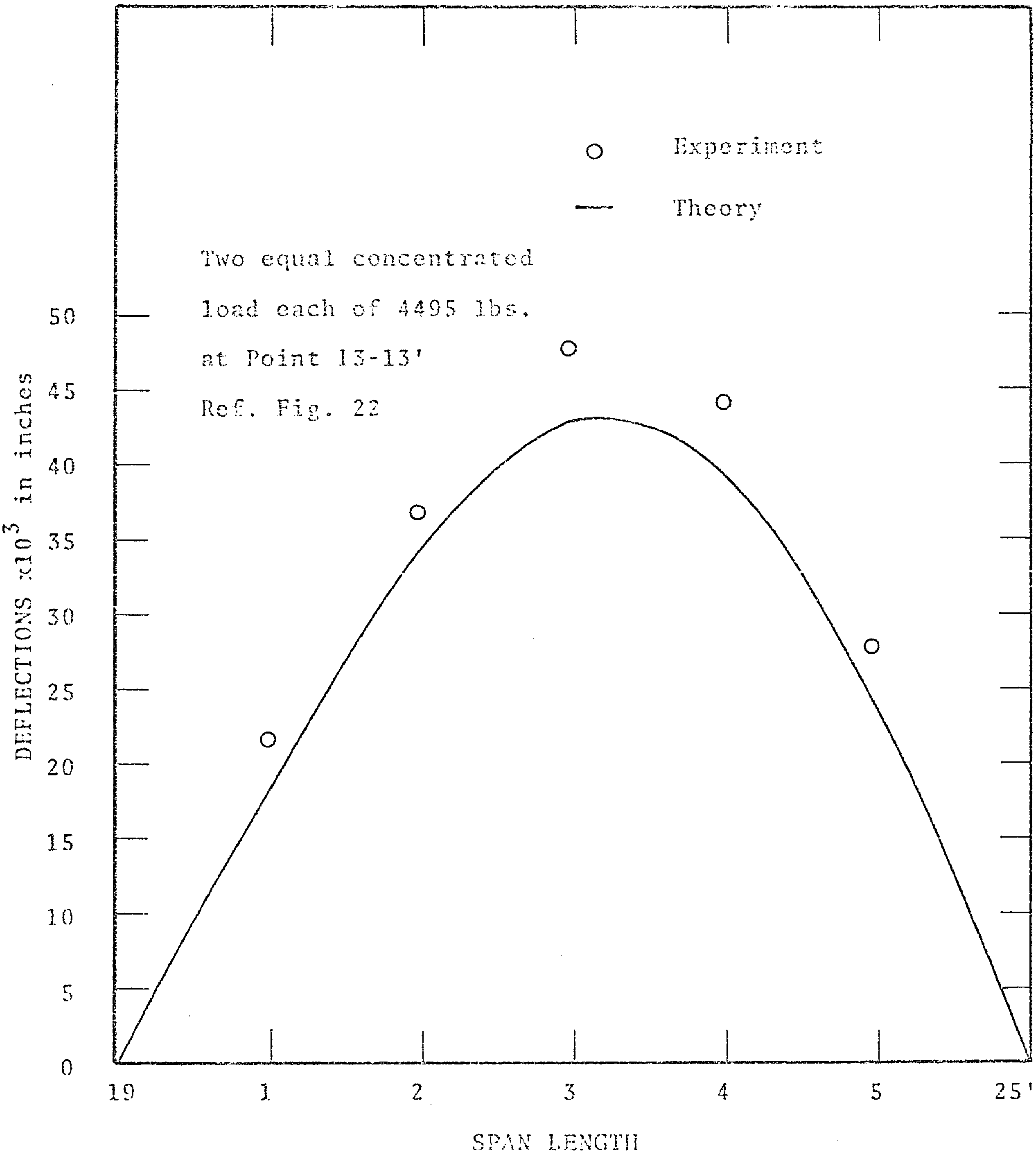

FIG. 2.20

VARIATION OF EDGE GIRDER
DEFLECTIONS WITH SPAN LENGTH

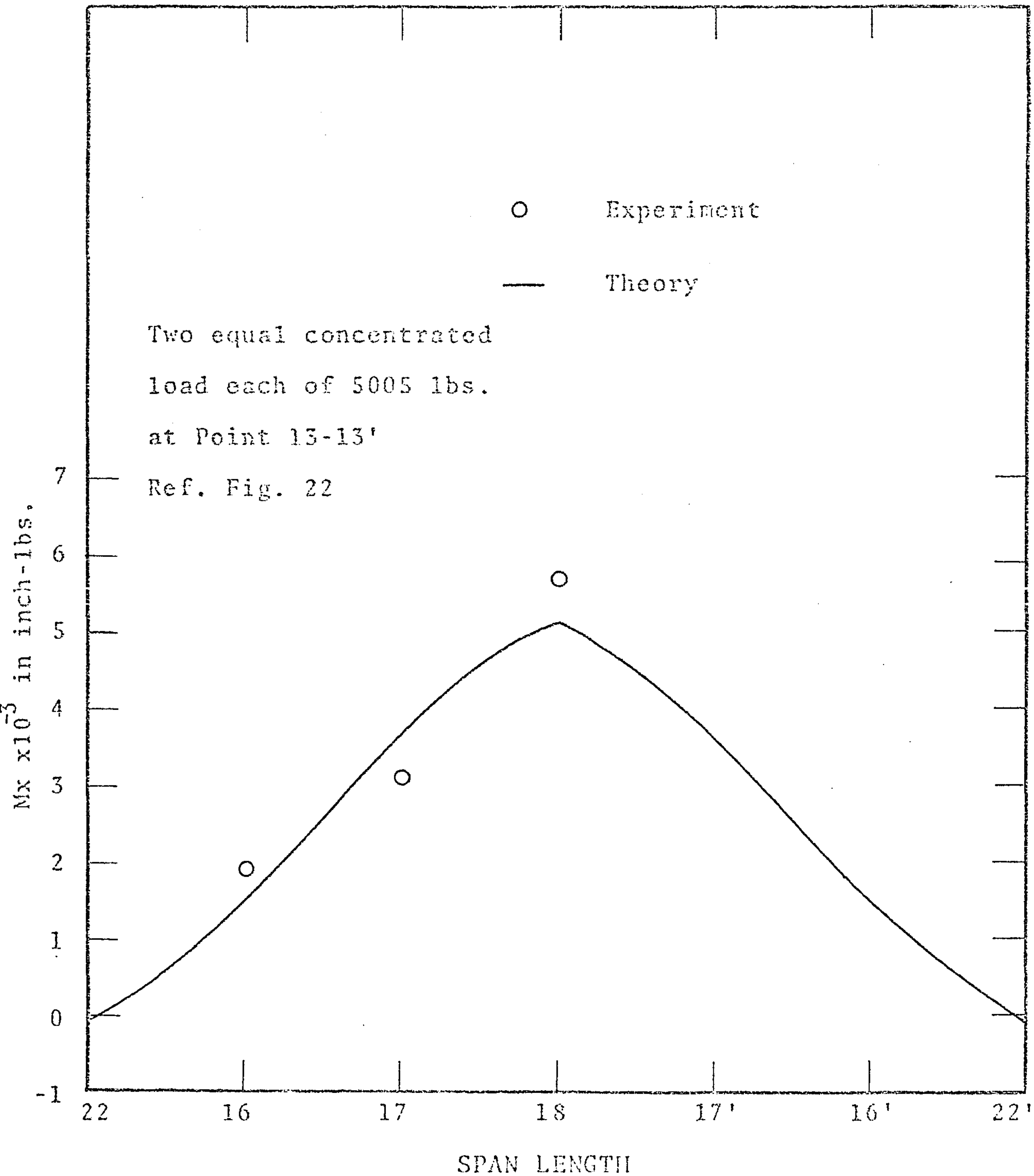

FIG. 2.21

VARIATION OF LONGITUDINAL CENTRAL GIRDER MOMENT Mx WITH SPAN LENGTH

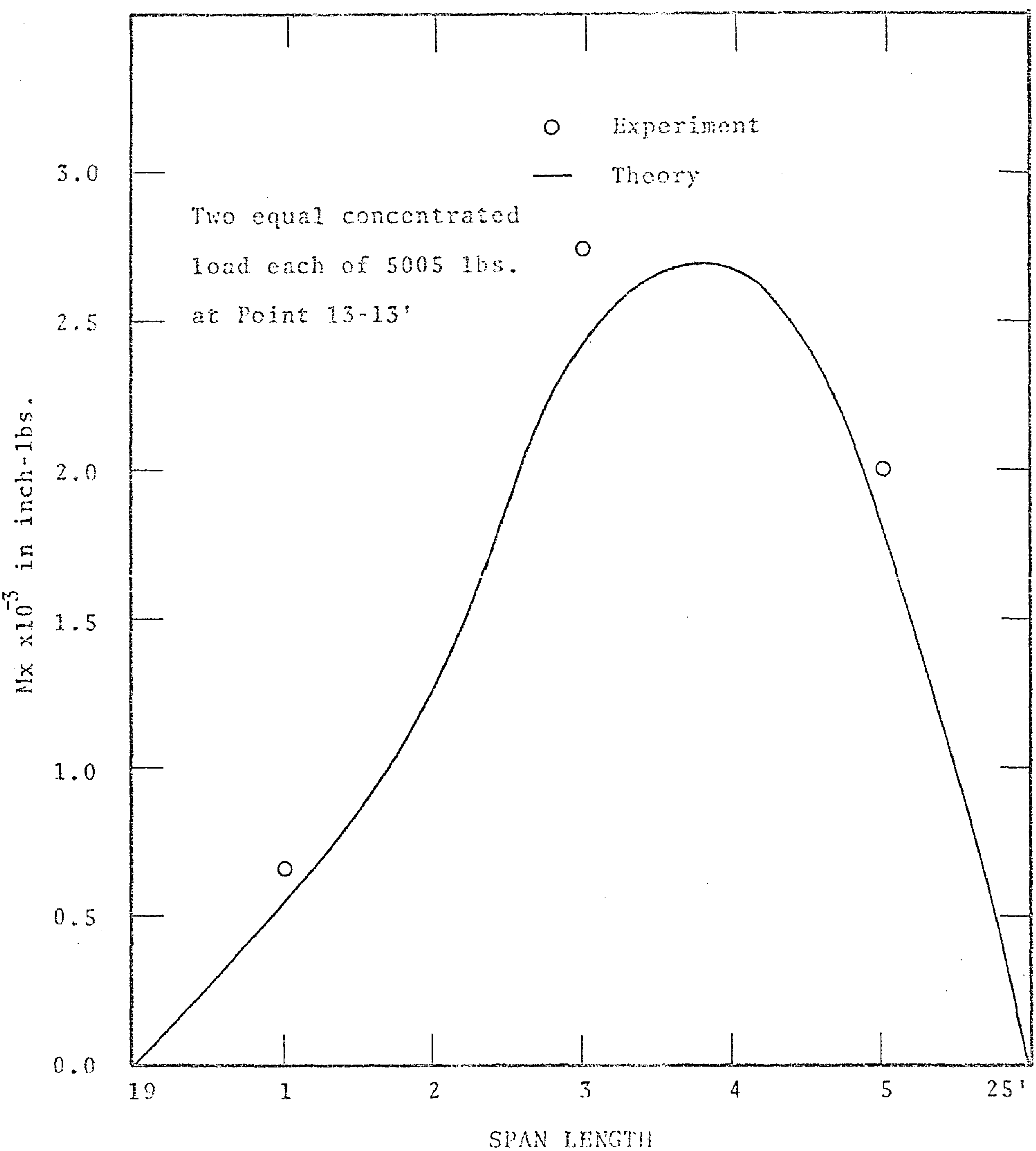

FIG. 2.22

VARIATION OF LONGITUDINAL EDGE
GIRDER MOMENT Mx WITH SPAN LENGTH.

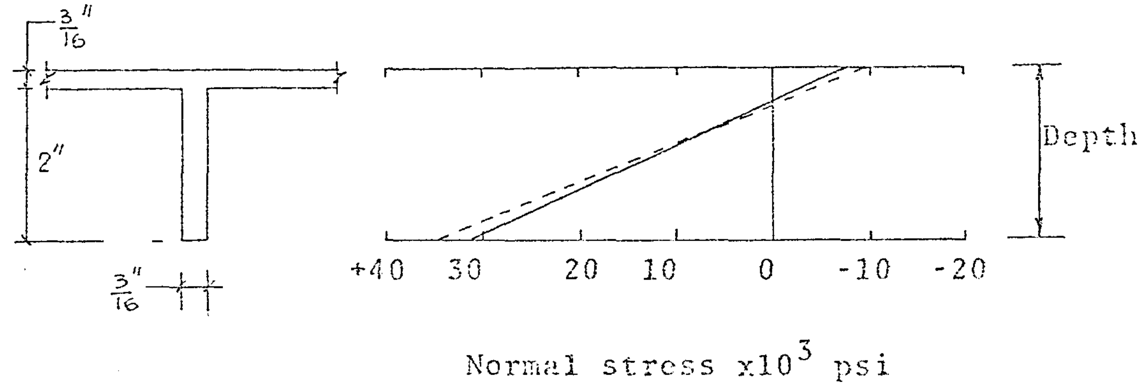

Concentrated load 4354 lbs. at Centre

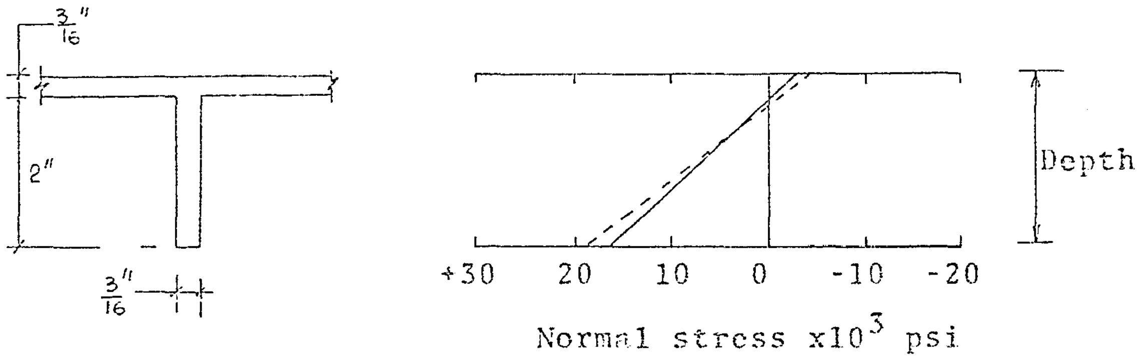

Two equal concentrated load each of 5005 lbs. at Point 17-17'

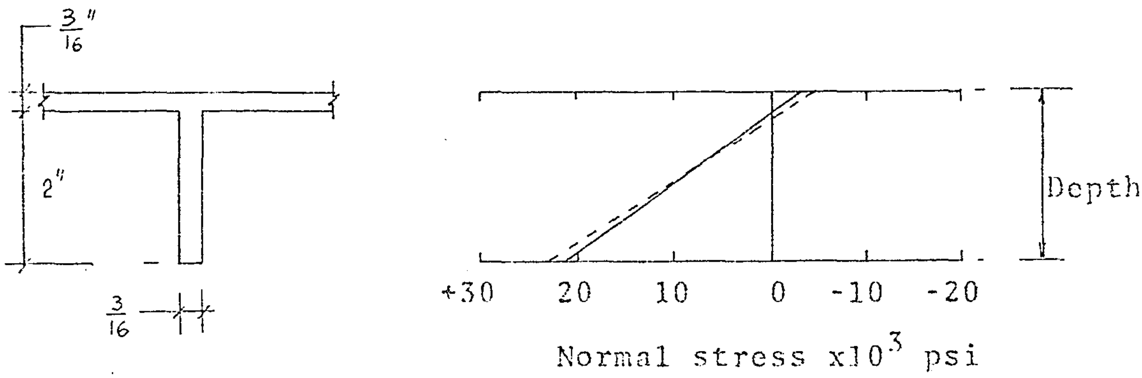

Two equal concentrated load of 5005 lbs. at Point 13-13'

FIG. 2.23

NORMAL STRESS DISTRIBUTION ALONG DEPTH AT POINT 18

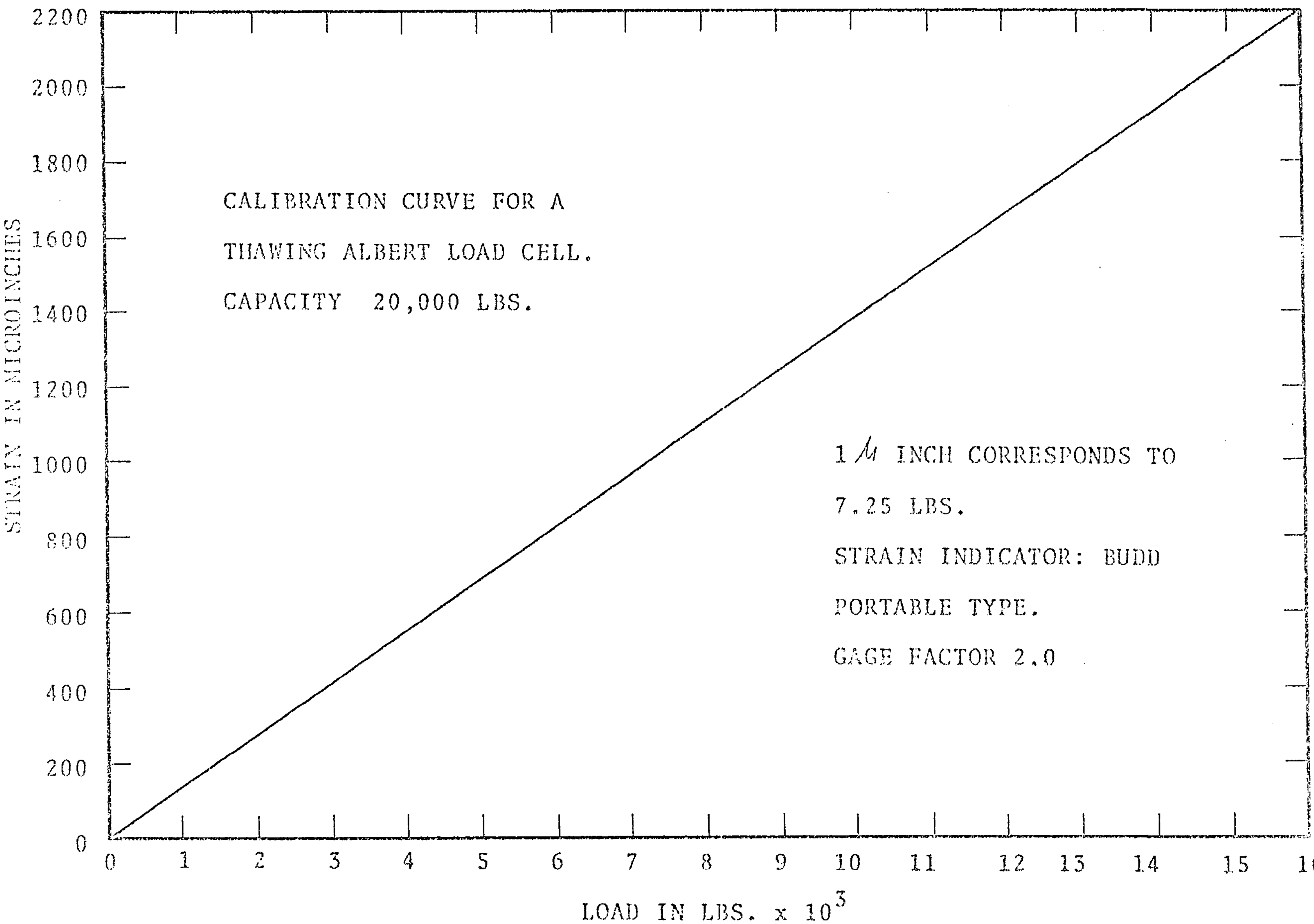
2200
2000
1800
1600
1400
1200
1000
800
600
400
200
0
STRAIN IN MICROINCHES
CALIBRATION CURVE FOR A
THAWING ALBERT LOAD CELL.
CAPACITY 20,000 LBS.
1 μ INCH CORRESPONDS TO
7.25 LBS.
STRAIN INDICATOR: BUDD
PORTABLE TYPE.
GAGE FACTOR 2.0
0 1 2 3 4 5 6 7 8 9 10 11 12 13 14 15 16
LOAD IN LBS. x 10^3

Fig. 2.24

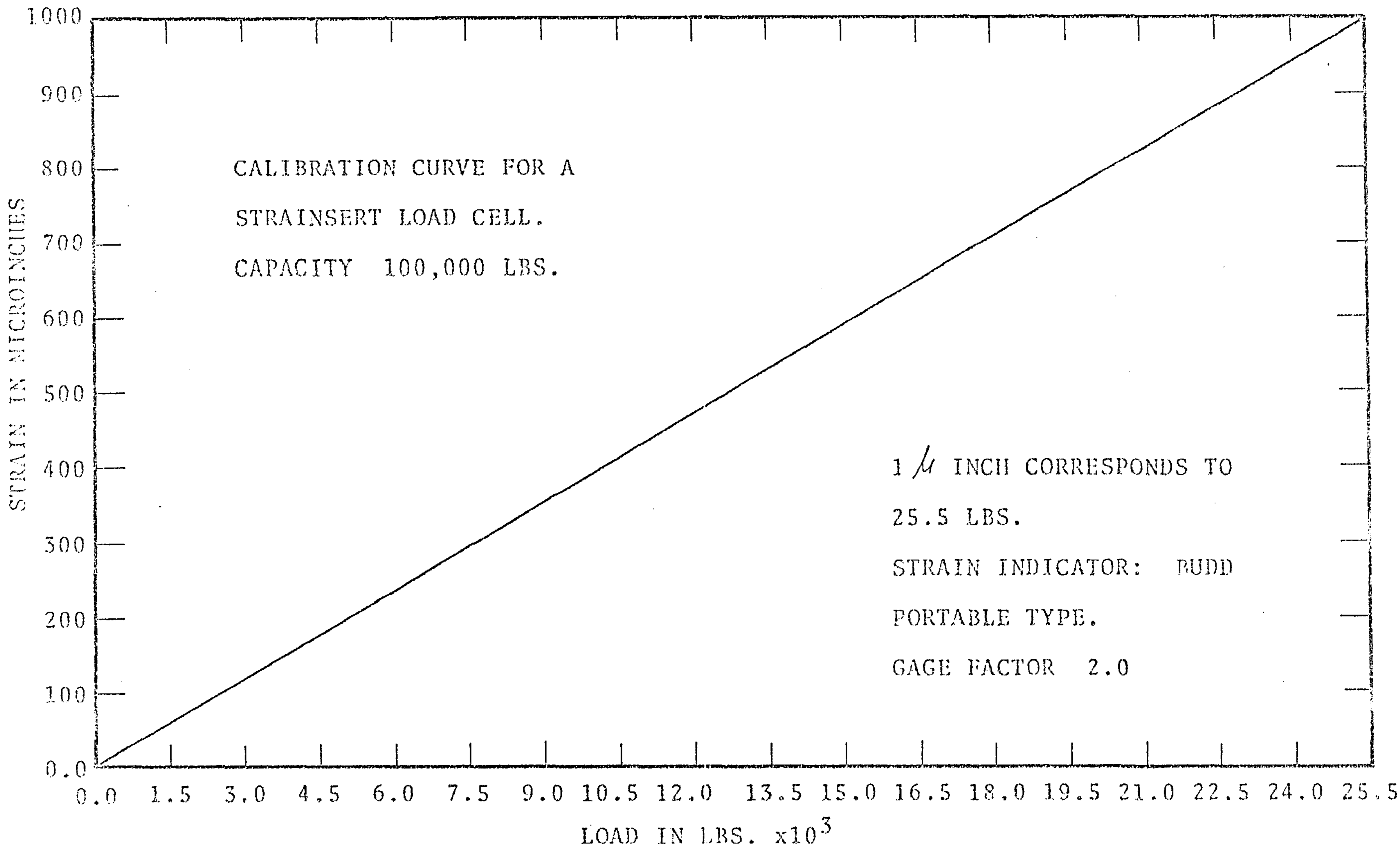
1000
900
800
700
600
500
400
300
200
100
0.0
STRAIN IN MICROINCHES
CALIBRATION CURVE FOR A
STRAINSERT LOAD CELL.
CAPACITY 100,000 LBS.
1 μ INCH CORRESPONDS TO
25.5 LBS.
STRAIN INDICATOR: BUDD
PORTABLE TYPE.
GAGE FACTOR 2.0
0.0 1.5 3.0 4.5 6.0 7.5 9.0 10.5 12.0 13.5 15.0 16.5 18.0 19.5 21.0 22.5 24.0 25.5
LOAD IN LBS. x10^3

Fig. 2.25

FIGURES

THEORETICAL RESULTS

No. of Girders	Spacing L_o	Spacing b_o	B_x/B_y	A_T/A_P	Ω
3	$L_x/2$	$L_y/2$	2.021	0.758	0.221
5	$L_x/4$	$L_y/4$	1.612	0.715	0.246
6	$L_x/5$	$L_y/5$	1.875	0.785	0.235
7	$L_x/6$	$L_y/6$	1.880	0.740	0.232
9	$L_x/8$	$L_y/8$	1.641	0.556	0.246

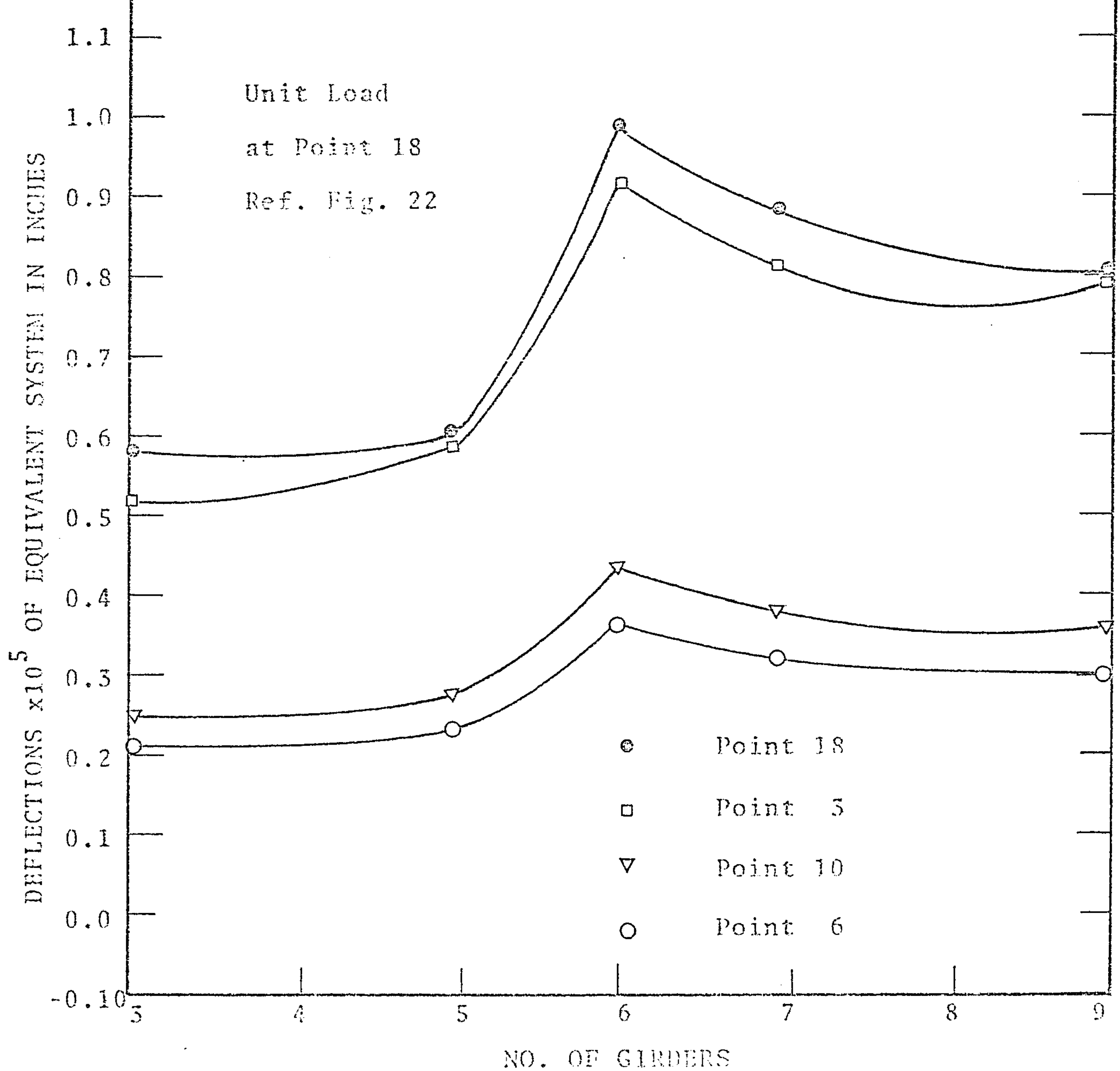

FIG. 3.1

VARIATIONS OF DEFLECTIONS WITH NO. OF GIRDERS

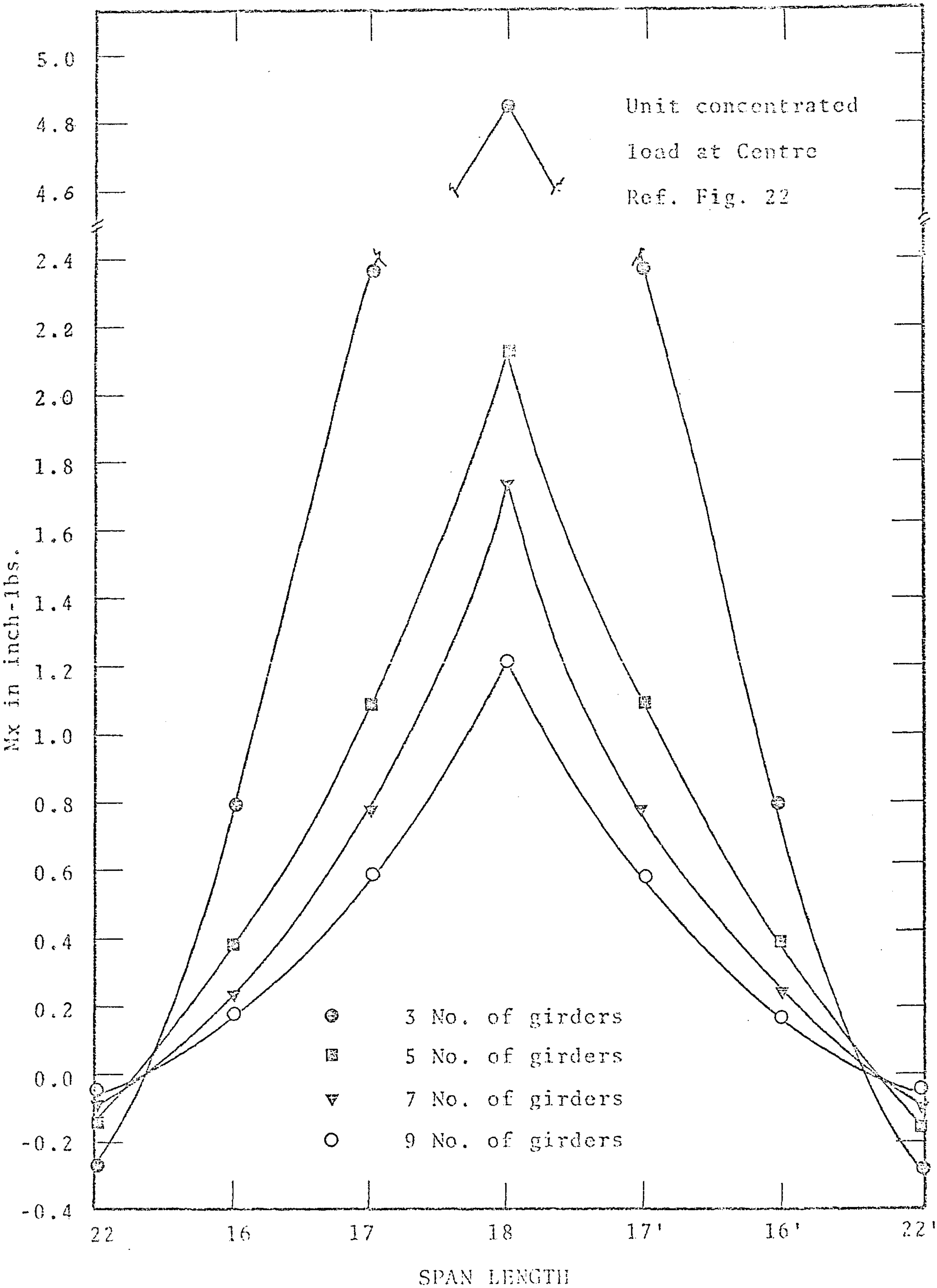

FIG. 3.2 VARIATIONS OF LONGITUDINAL CENTRAL GIRDER MOMENT Mx WITH SPAN LENGTH

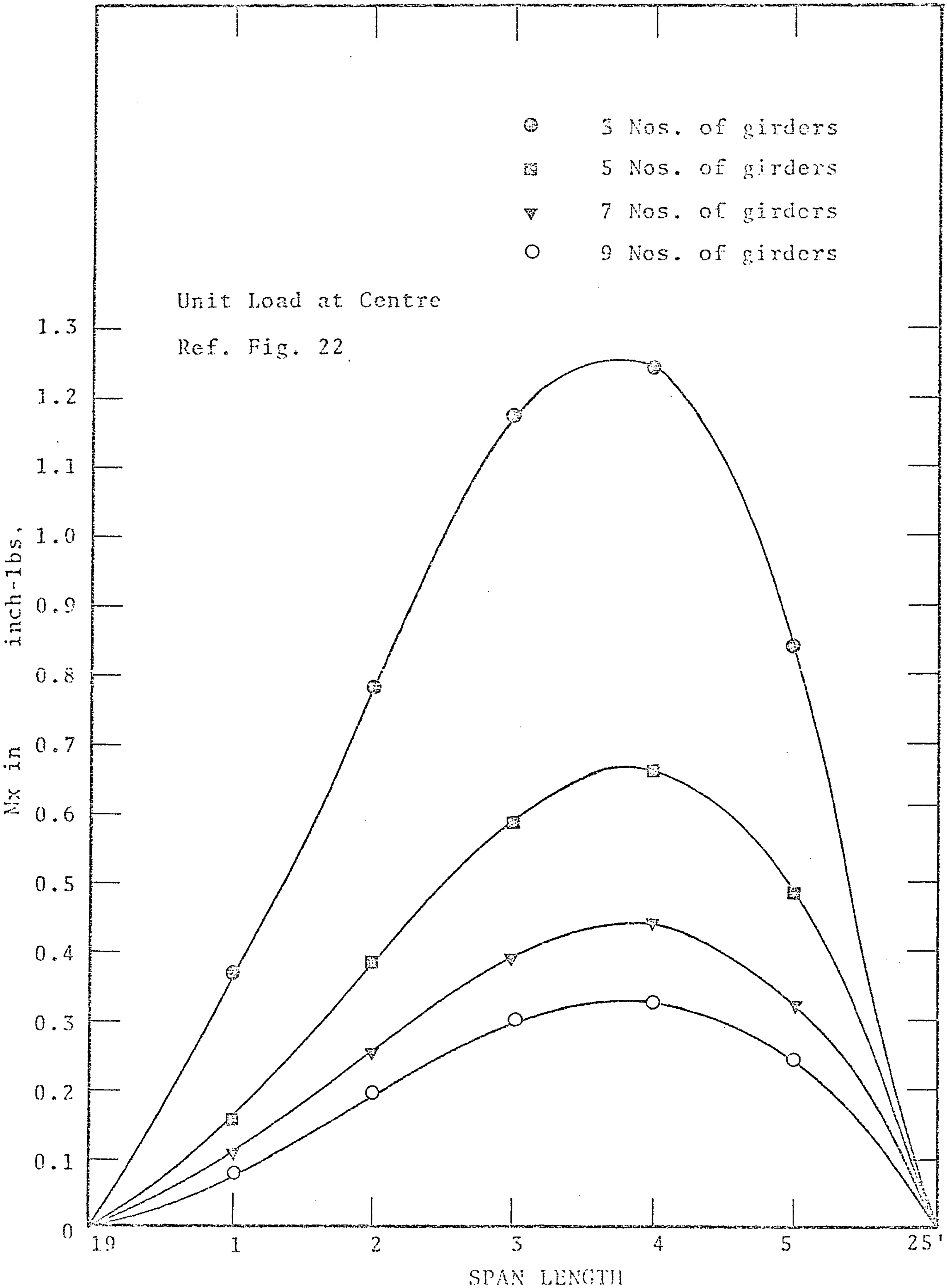

FIG. 3.3 EDGE GIRDER MOMENT Mx VS. SPAN LENGTH

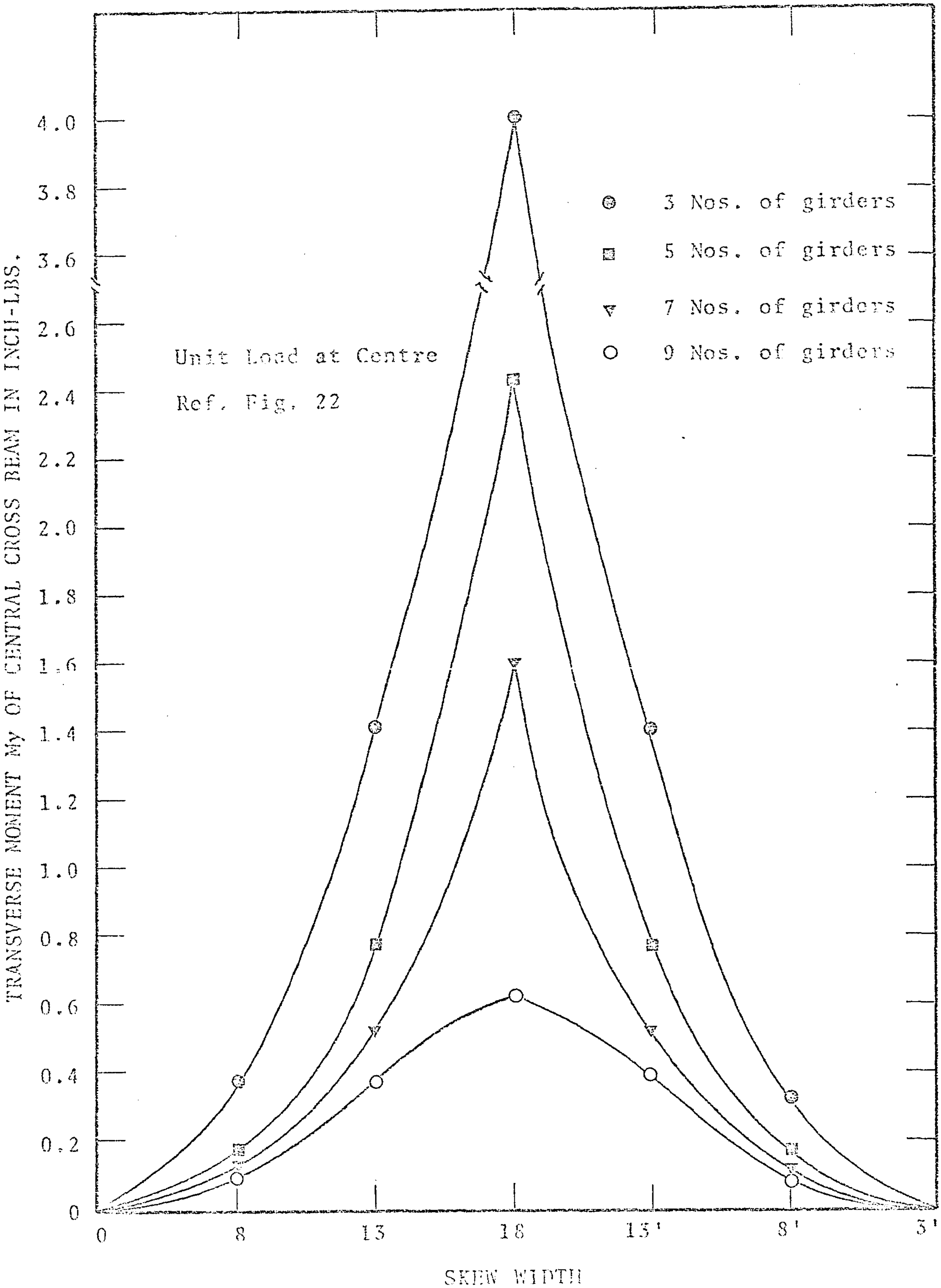

FIG. 3.4 VARIATIONS OF My WITH SKEW WIDTH

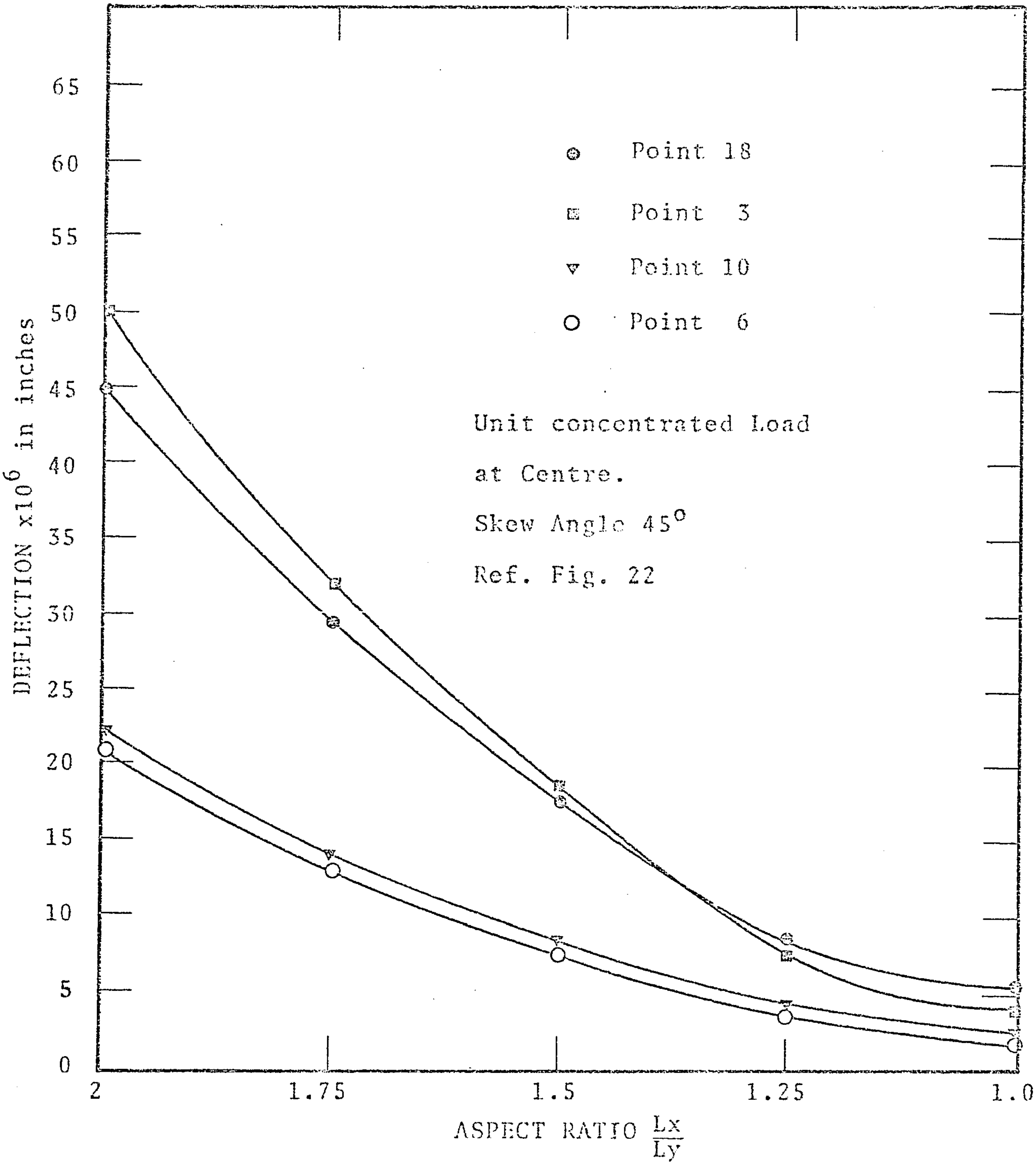

FIG. 3.5 DEFLECTION VS. ASPECT RATIO

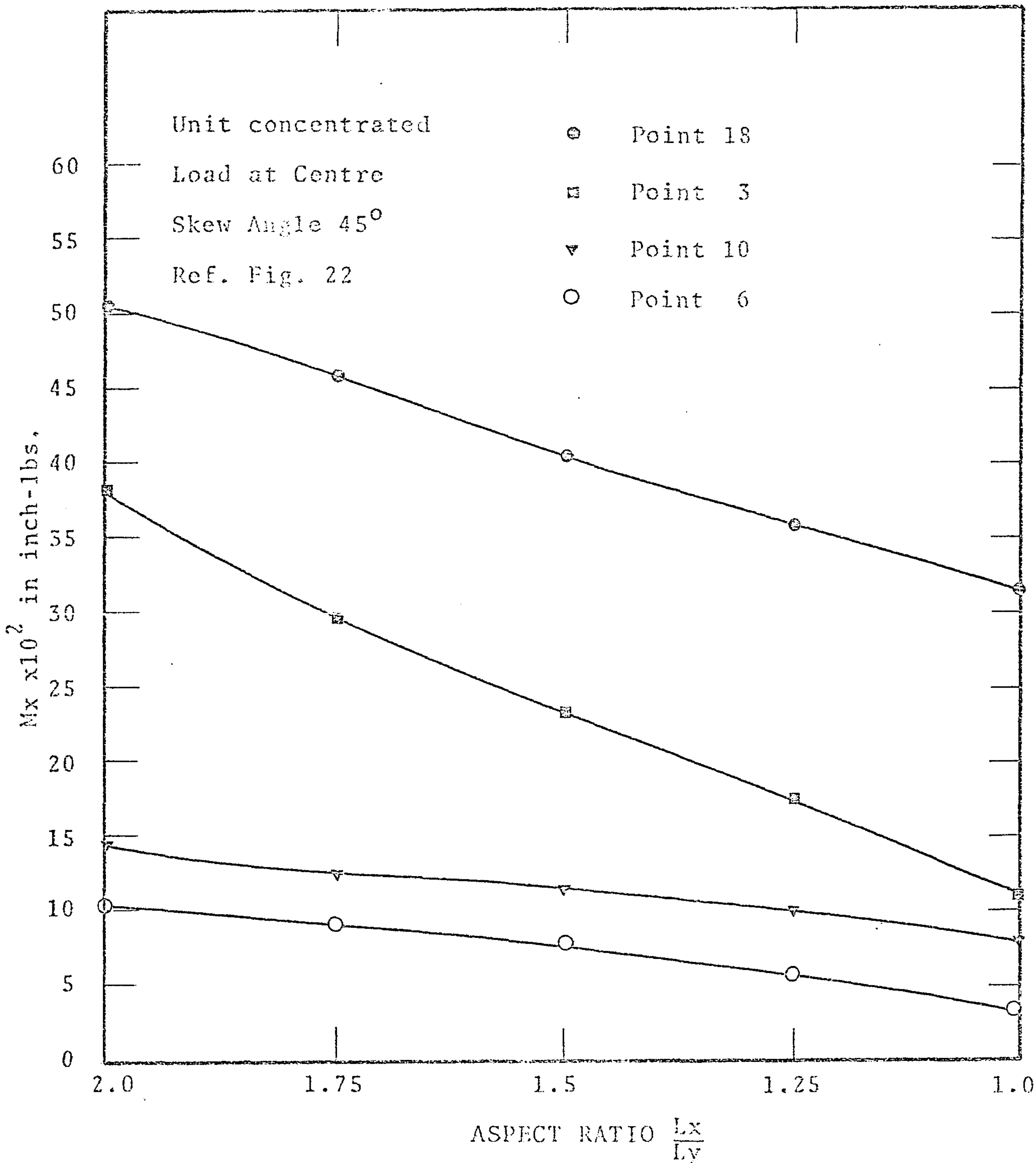

FIG. 3.6 Mx VS. ASPECT RATIO

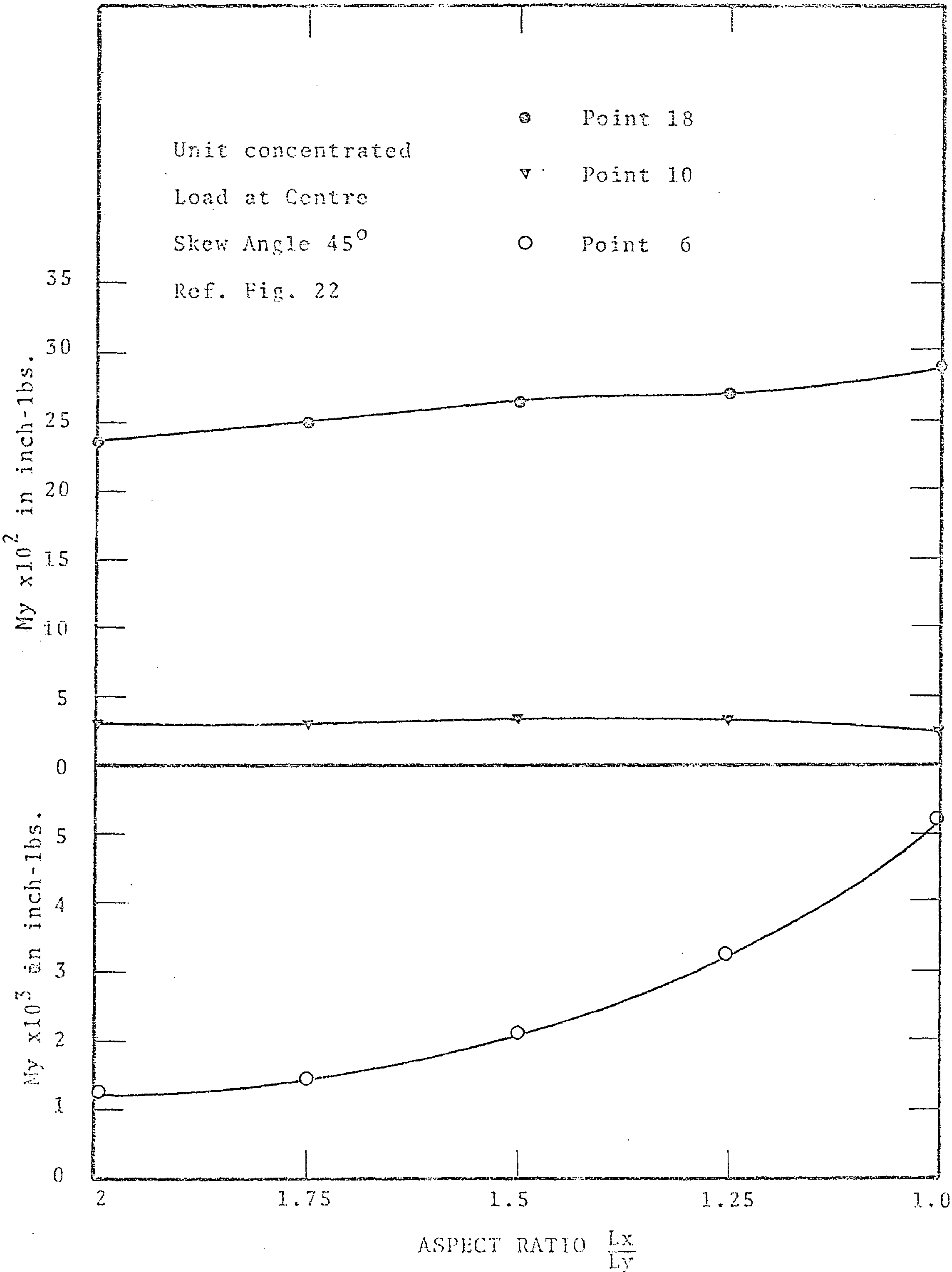

FIG. 3.7 My VS. ASPECT RATIO

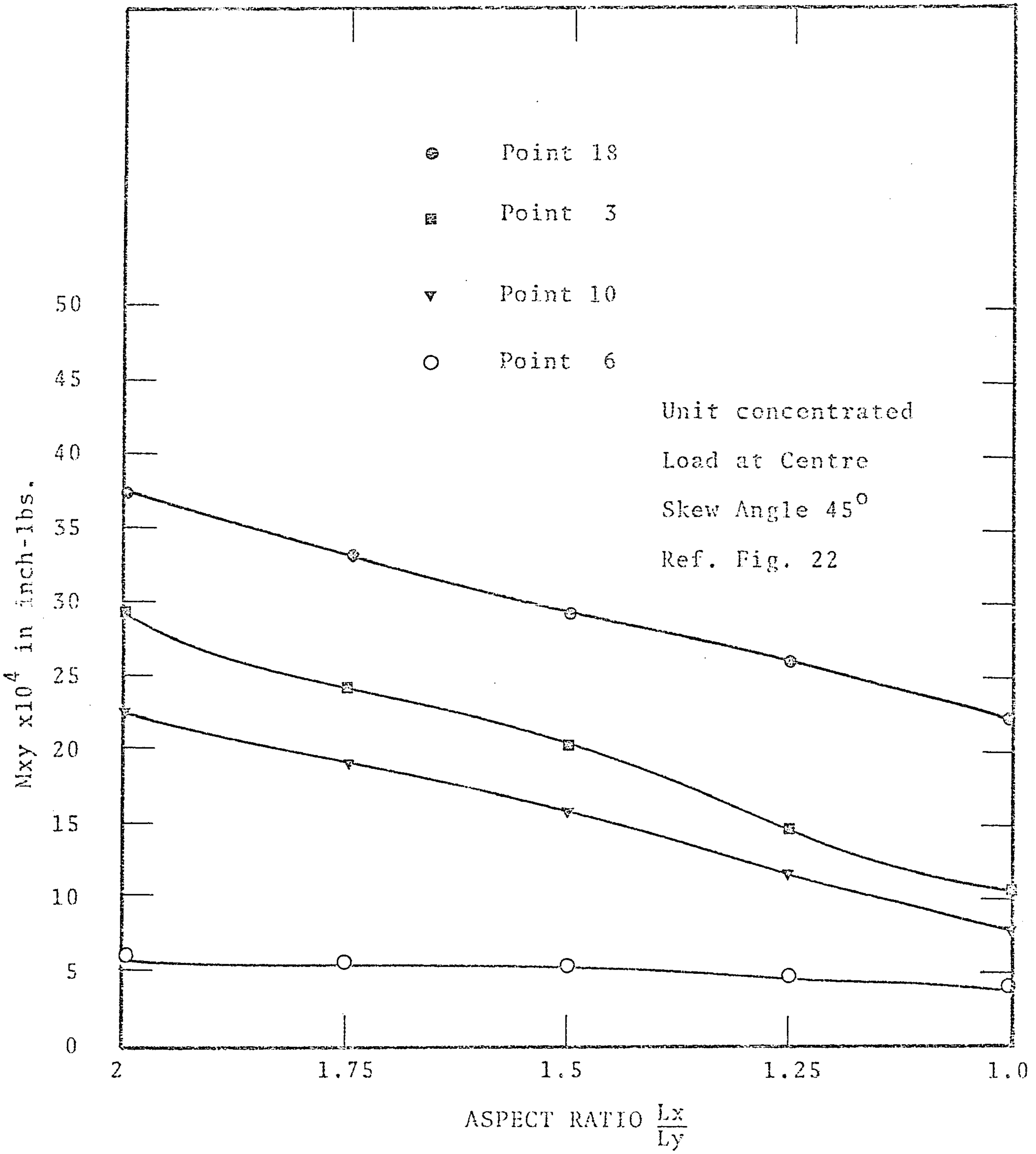

FIG. 3.8 Mxy VS. ASPECT RATIO

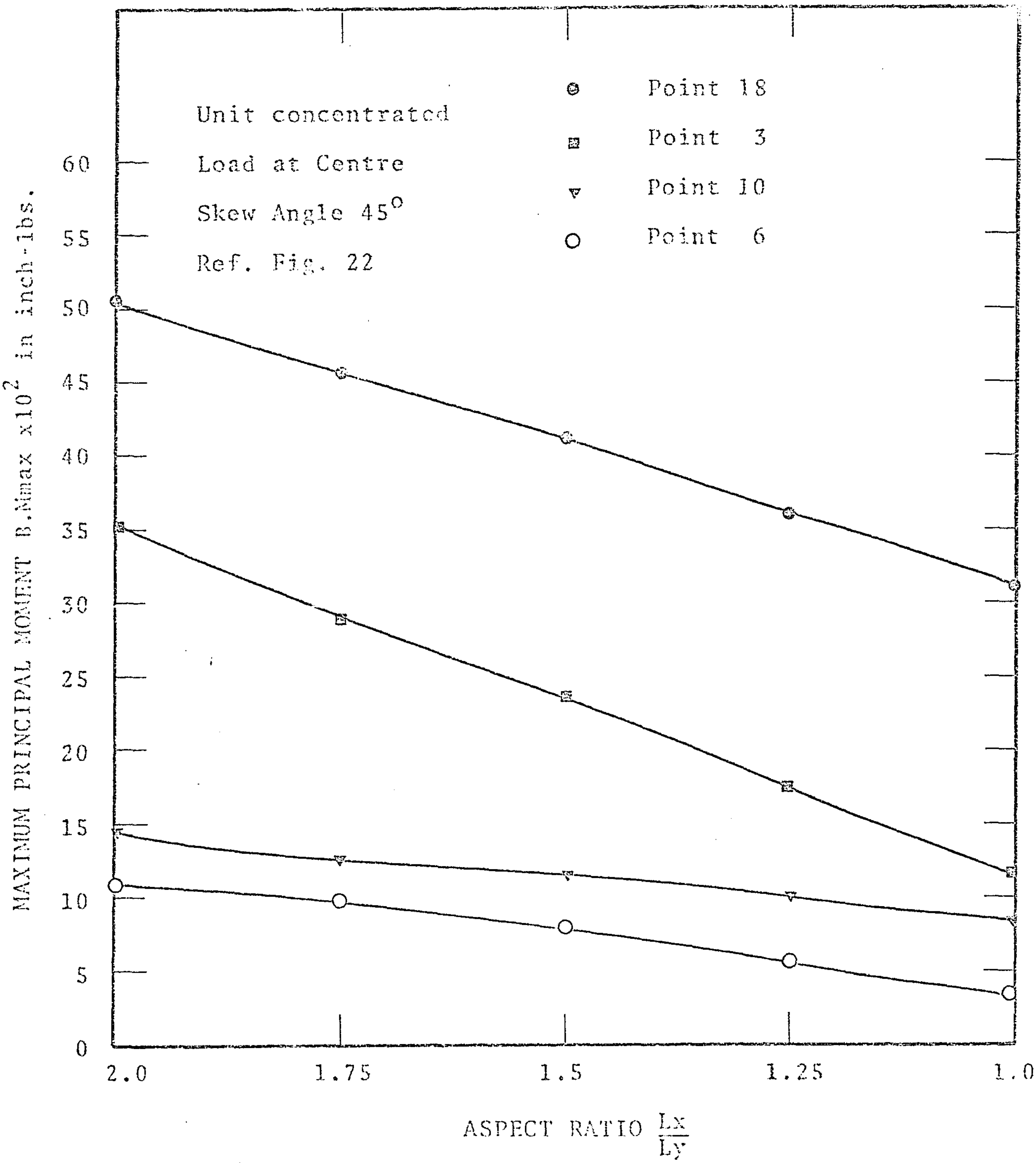

FIG. 3.9 MAXIMUM PRINCIPAL MOMENT B.M. max
VS. ASPECT RATIO

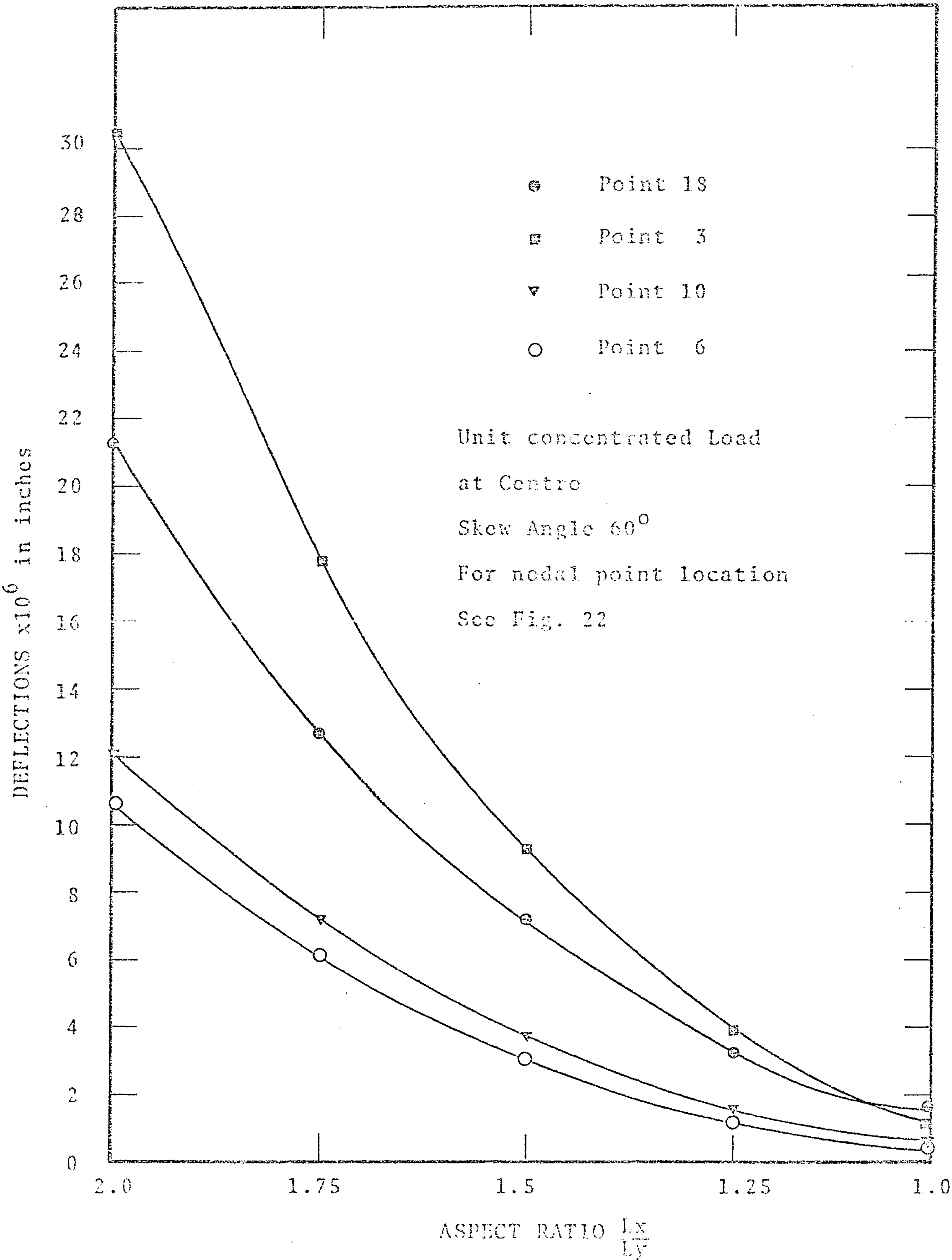

FIG. 3.10 DEFLECTIONS VS. ASPECT RATIO

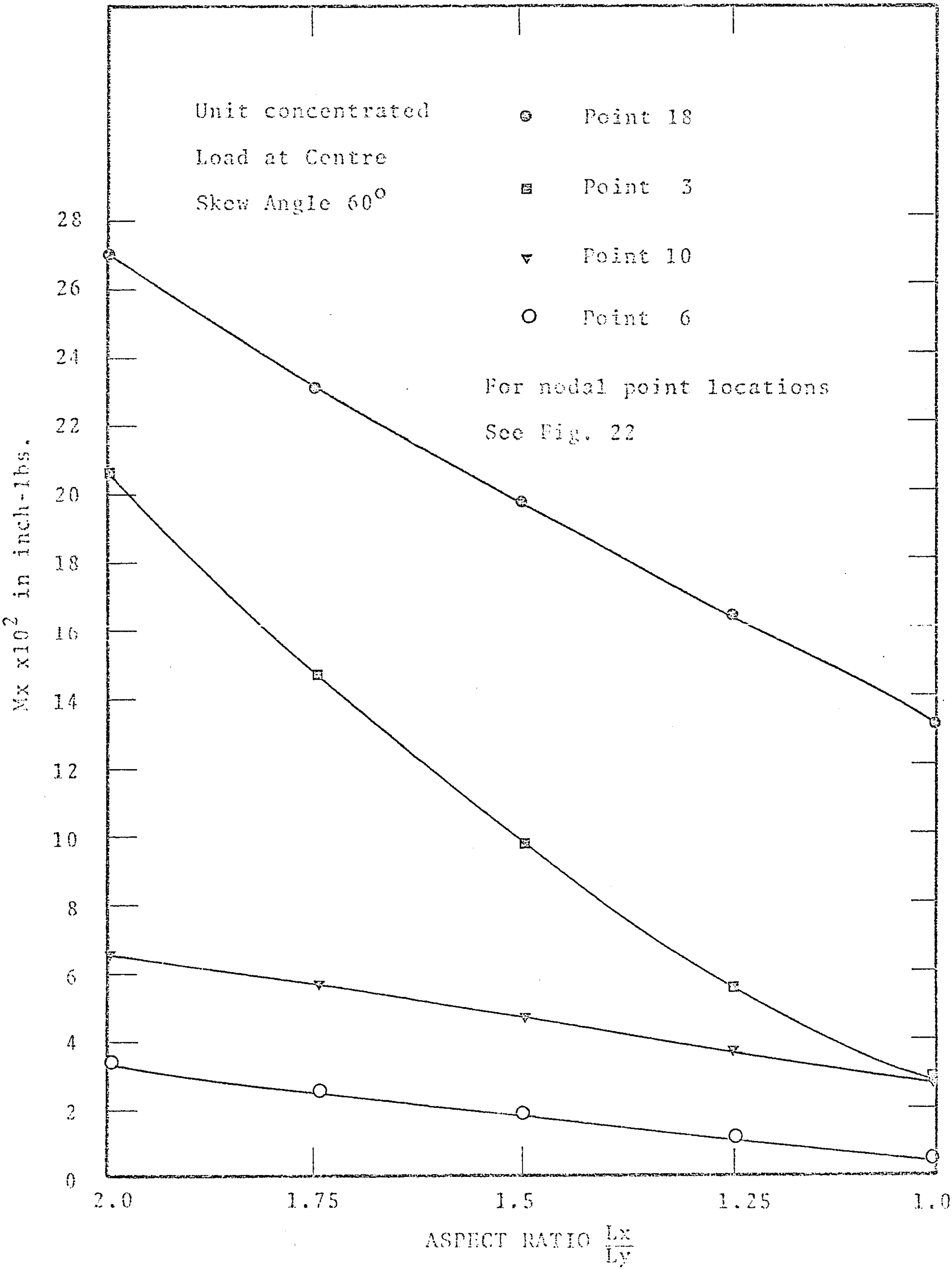

FIG. 3.11 Mx VS. ASPECT RATIO

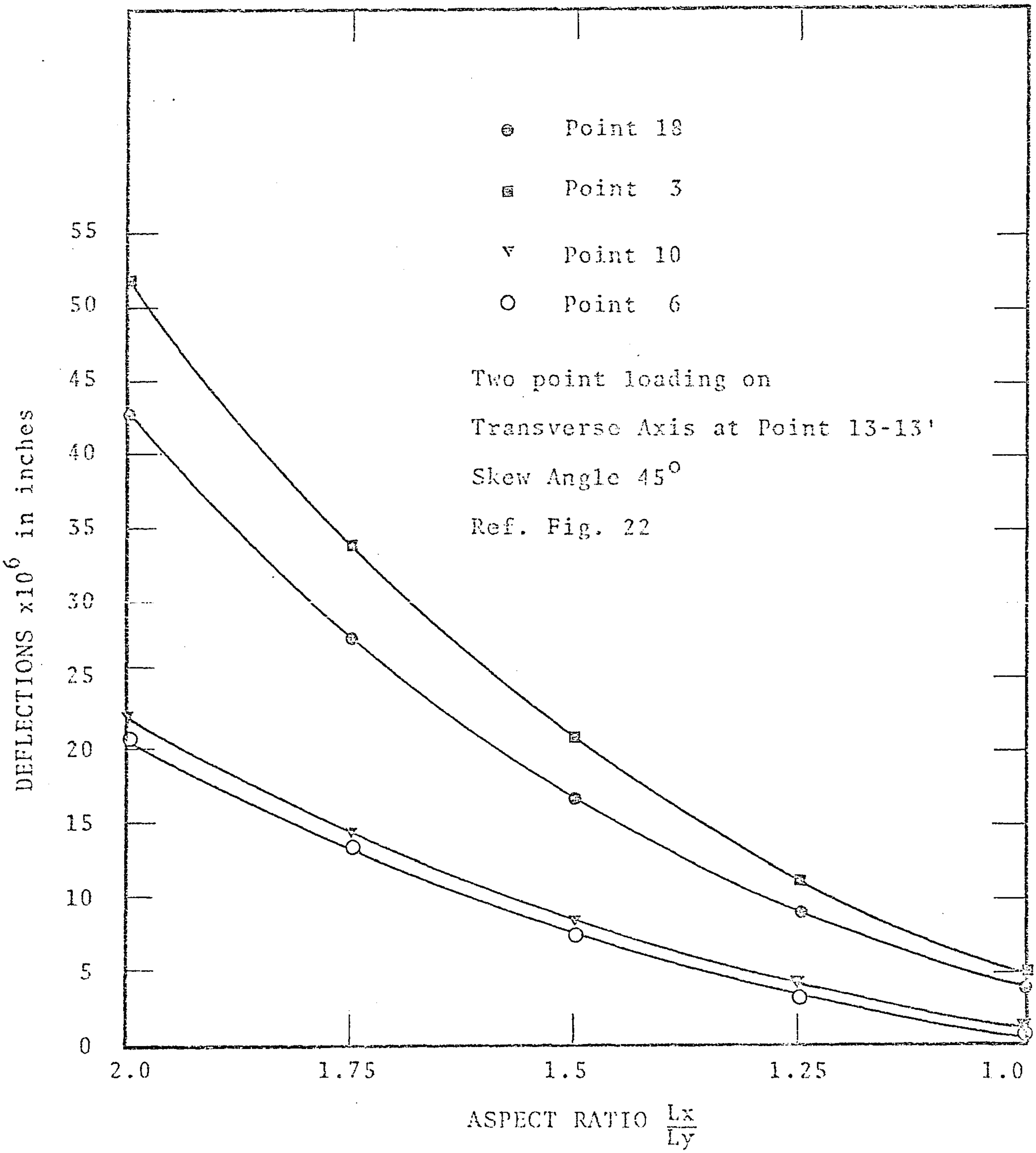

FIG. 3.12 DEFLECTION VS. ASPECT RATIO

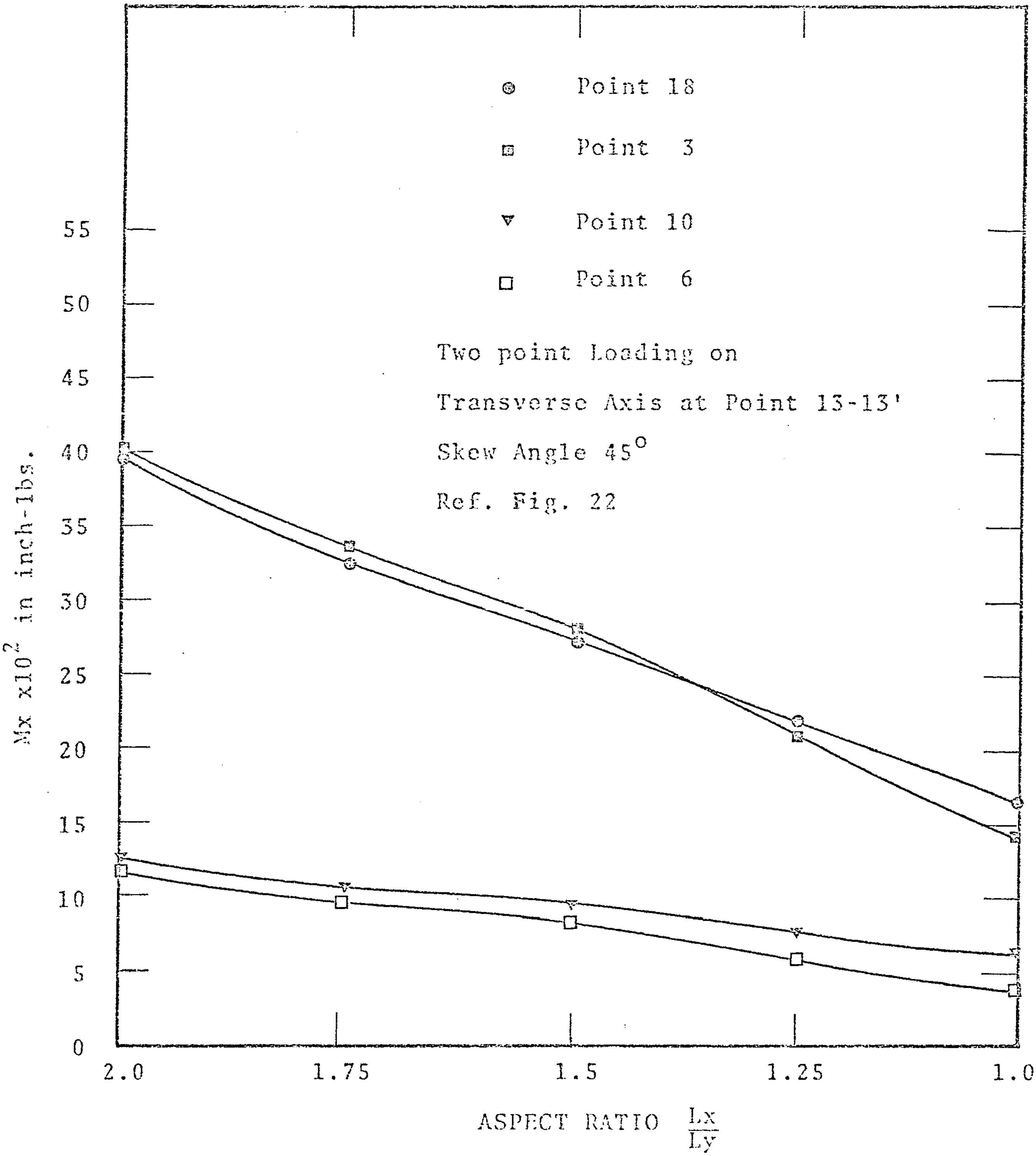

FIG. 3.13 Mx VS. ASPECT RATIO

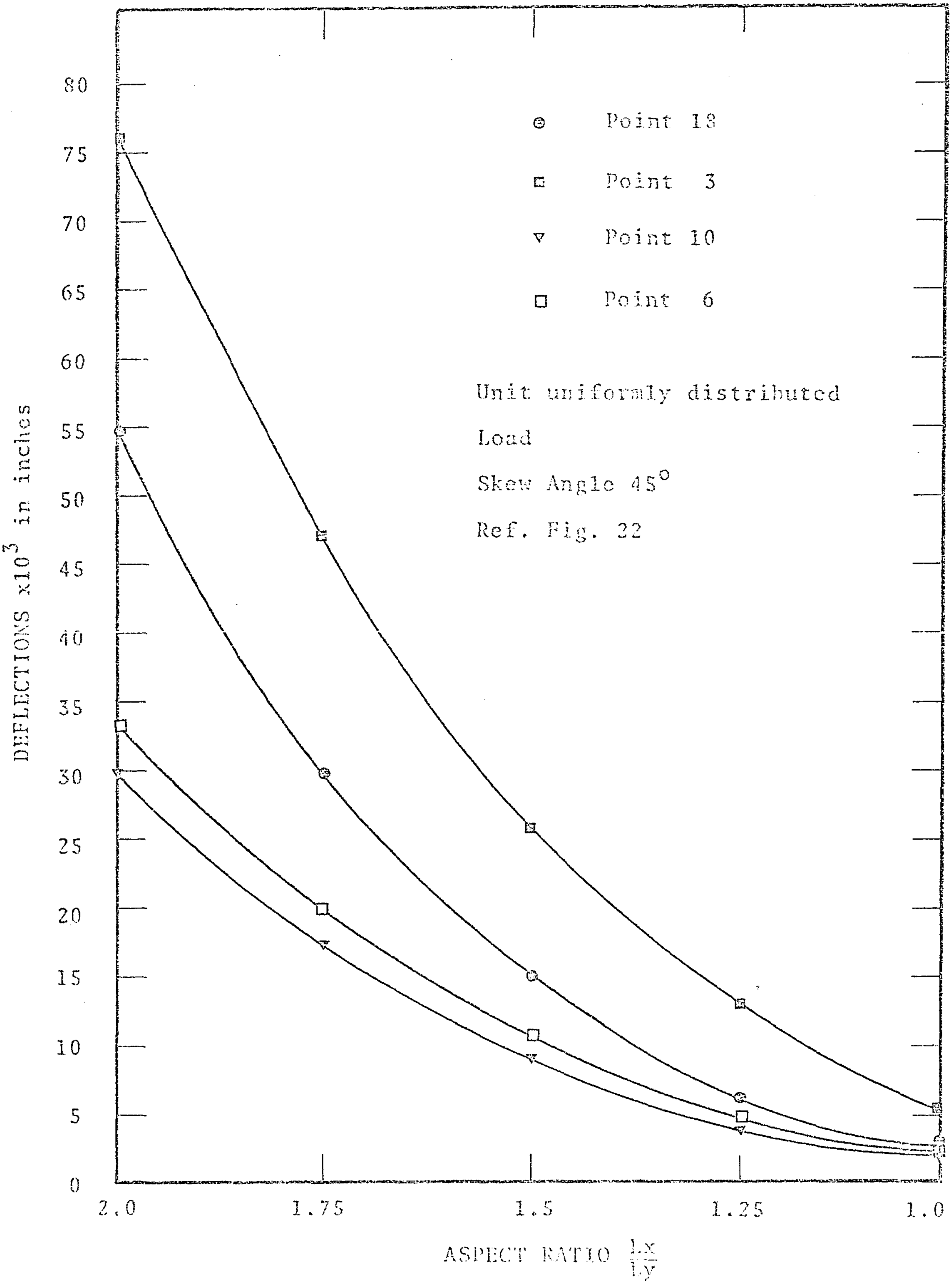

FIG. 3.14 DEFLECTION VS. ASPECT RATIO

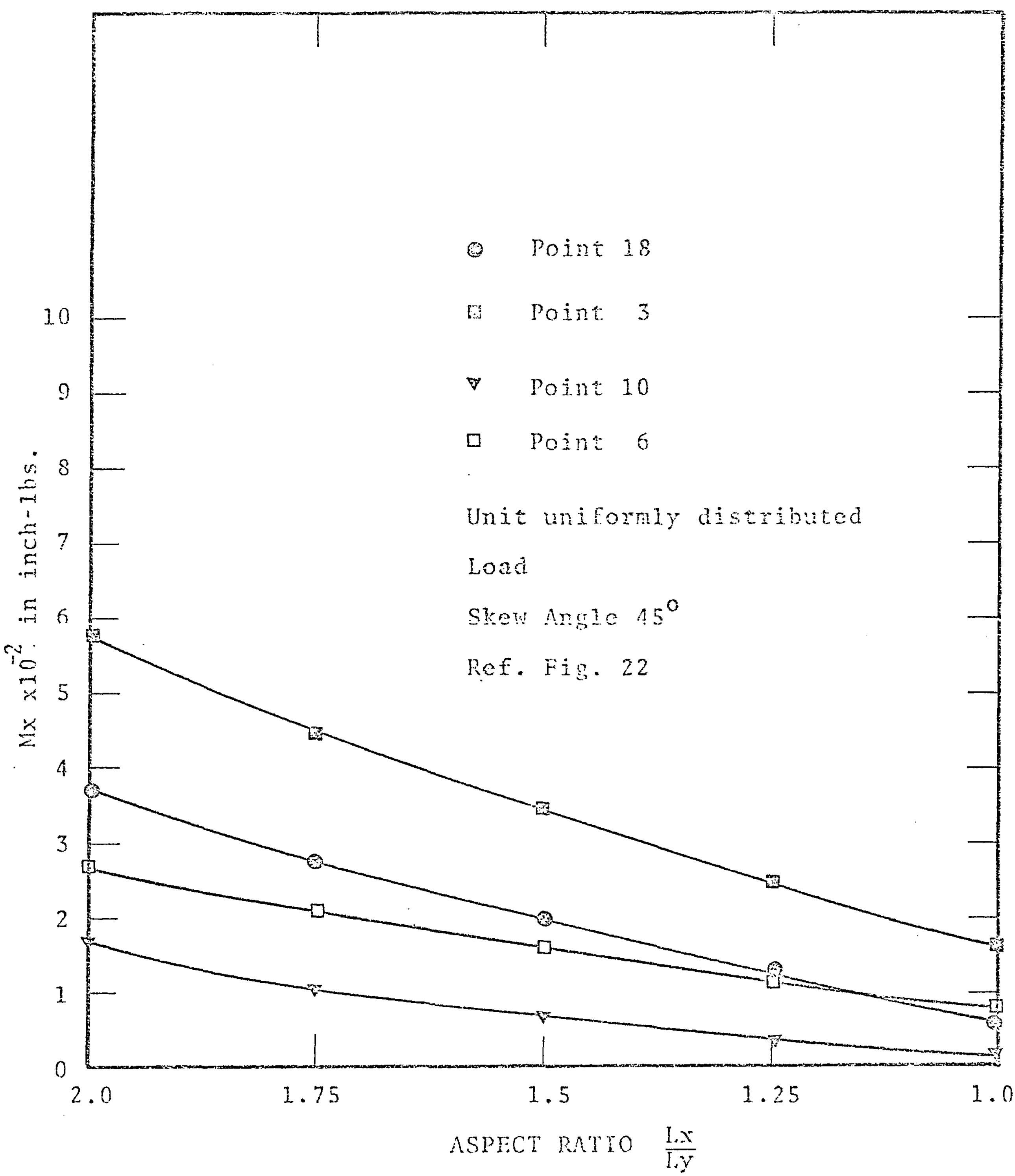

FIG. 3.15 Mx VS. ASPECT RATIO

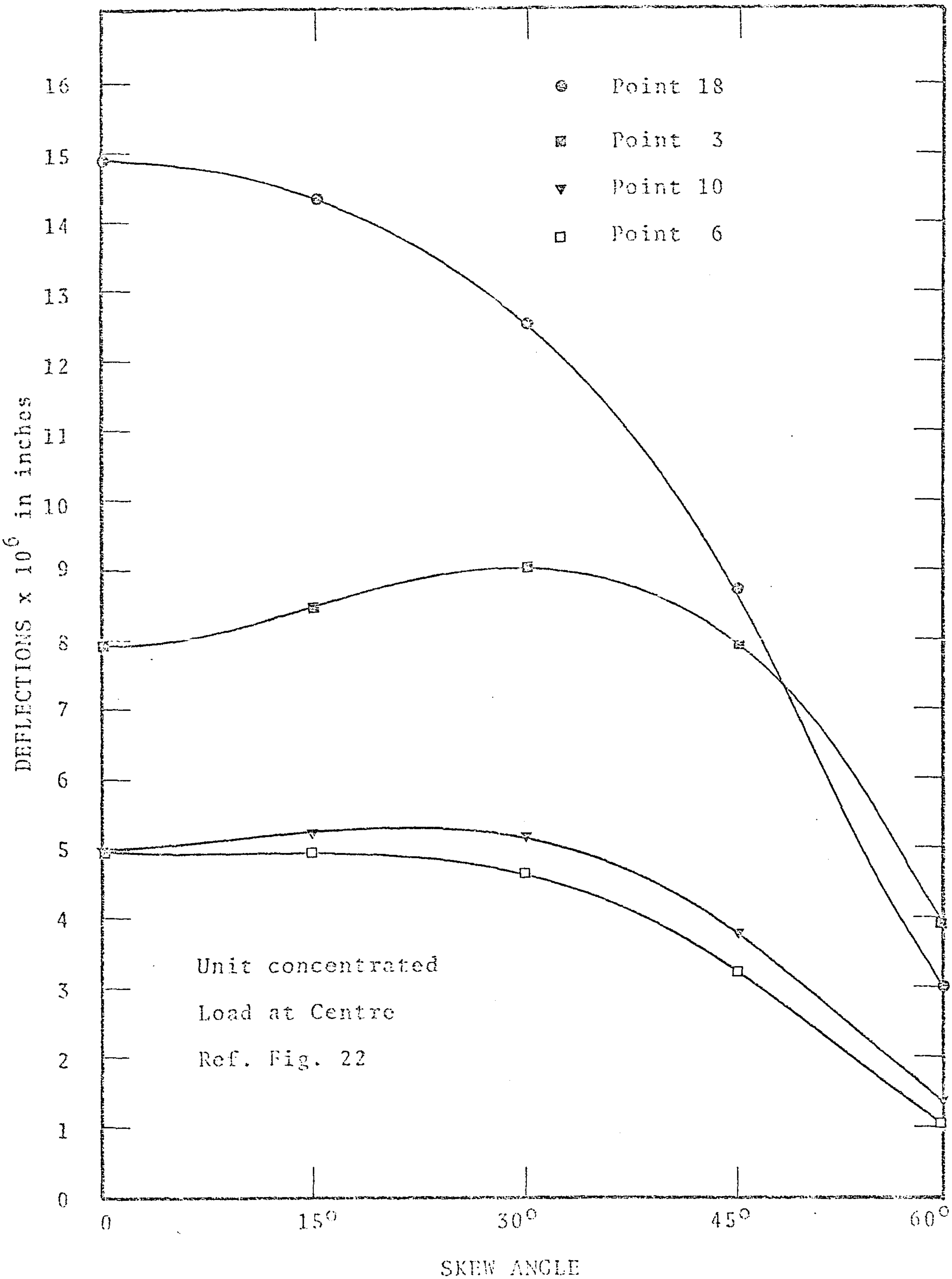

FIG. 3.16 DEFLECTIONS VS. ANGLE OF SKEW

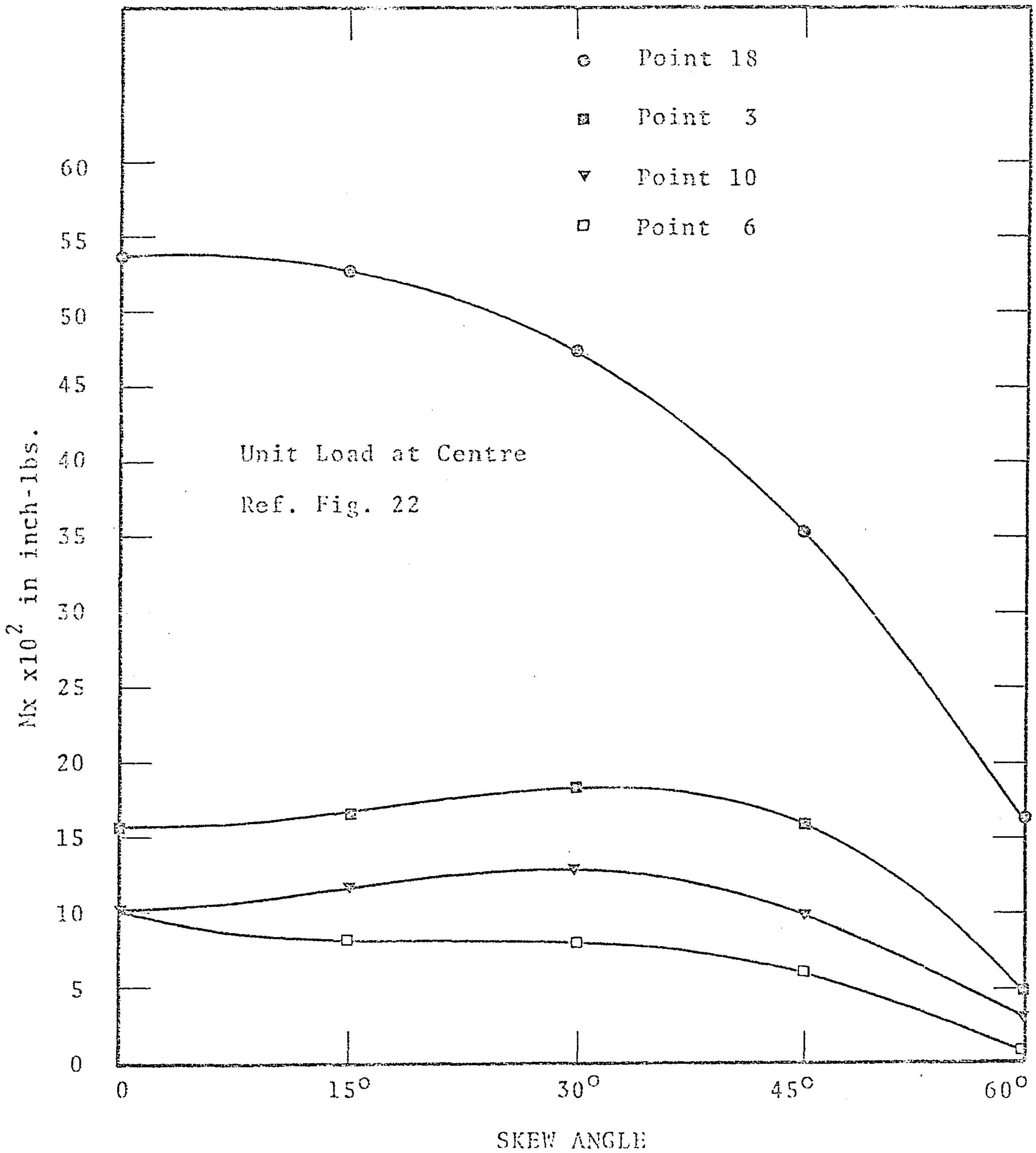

FIG. 3.17 Mx VS. ANGLE OF SKEW

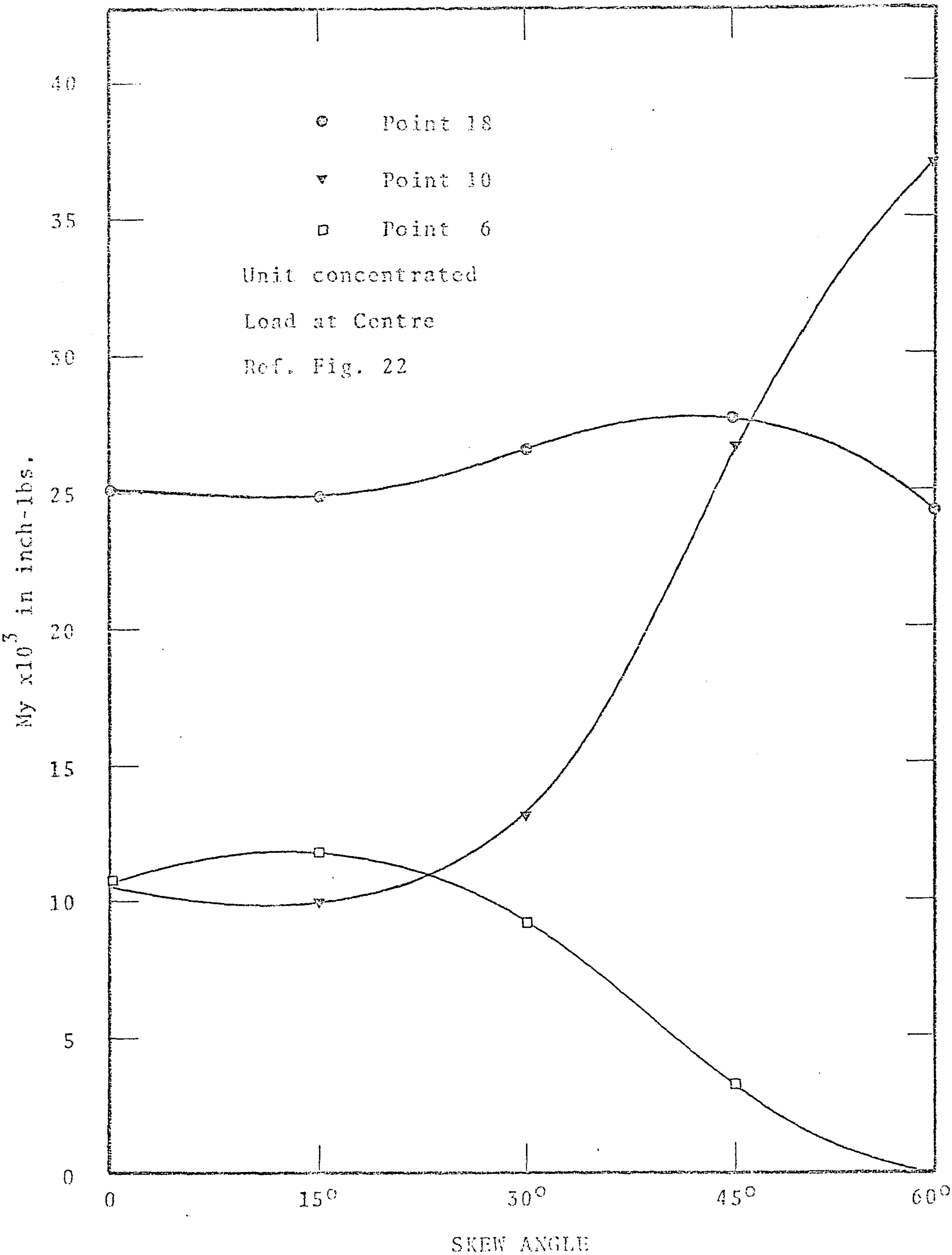

FIG. 3.18 My VS. ANGLE OF SKEW

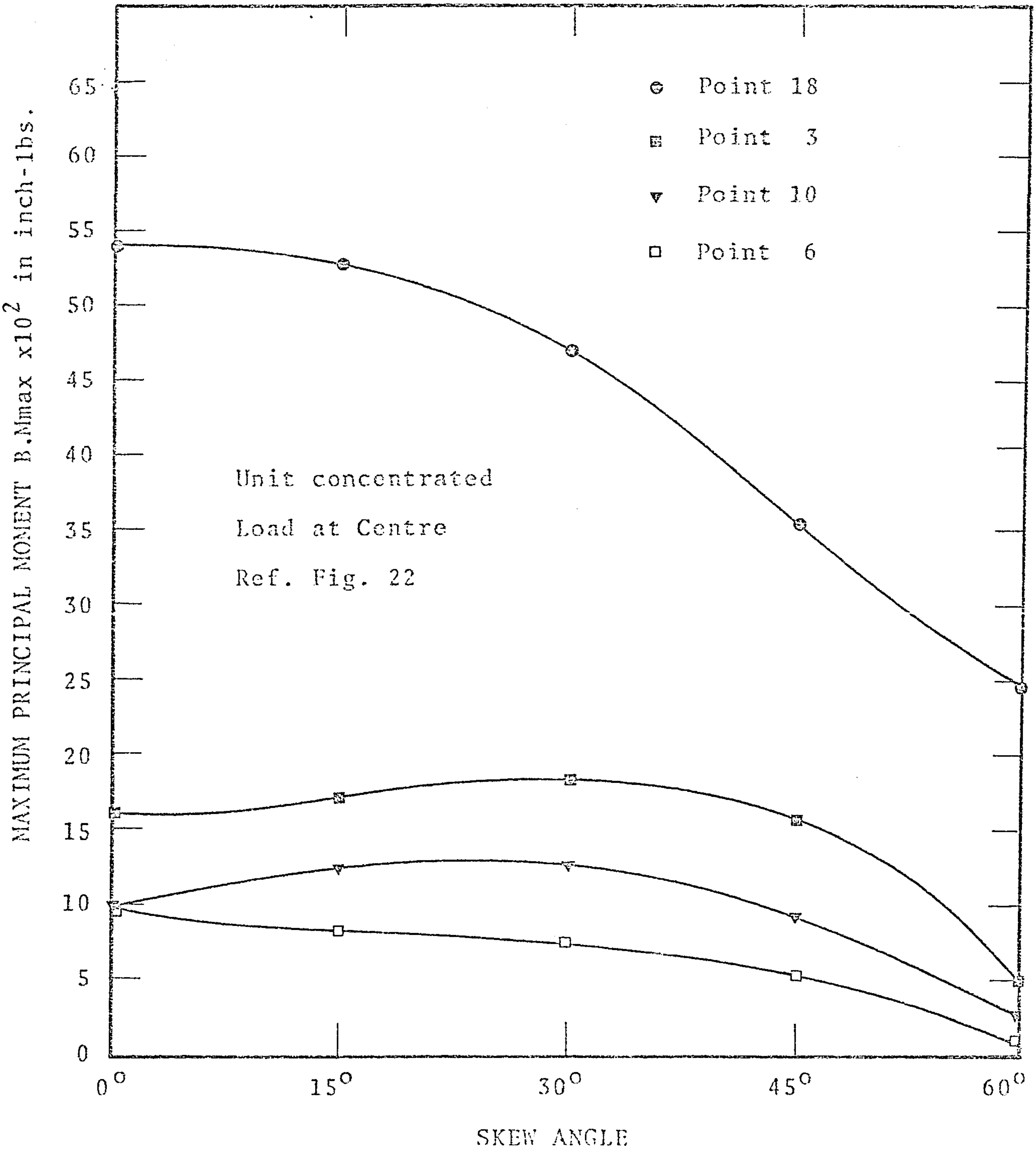

FIG. 3.19 B.Mmax VS. ANGLE OF SKEW

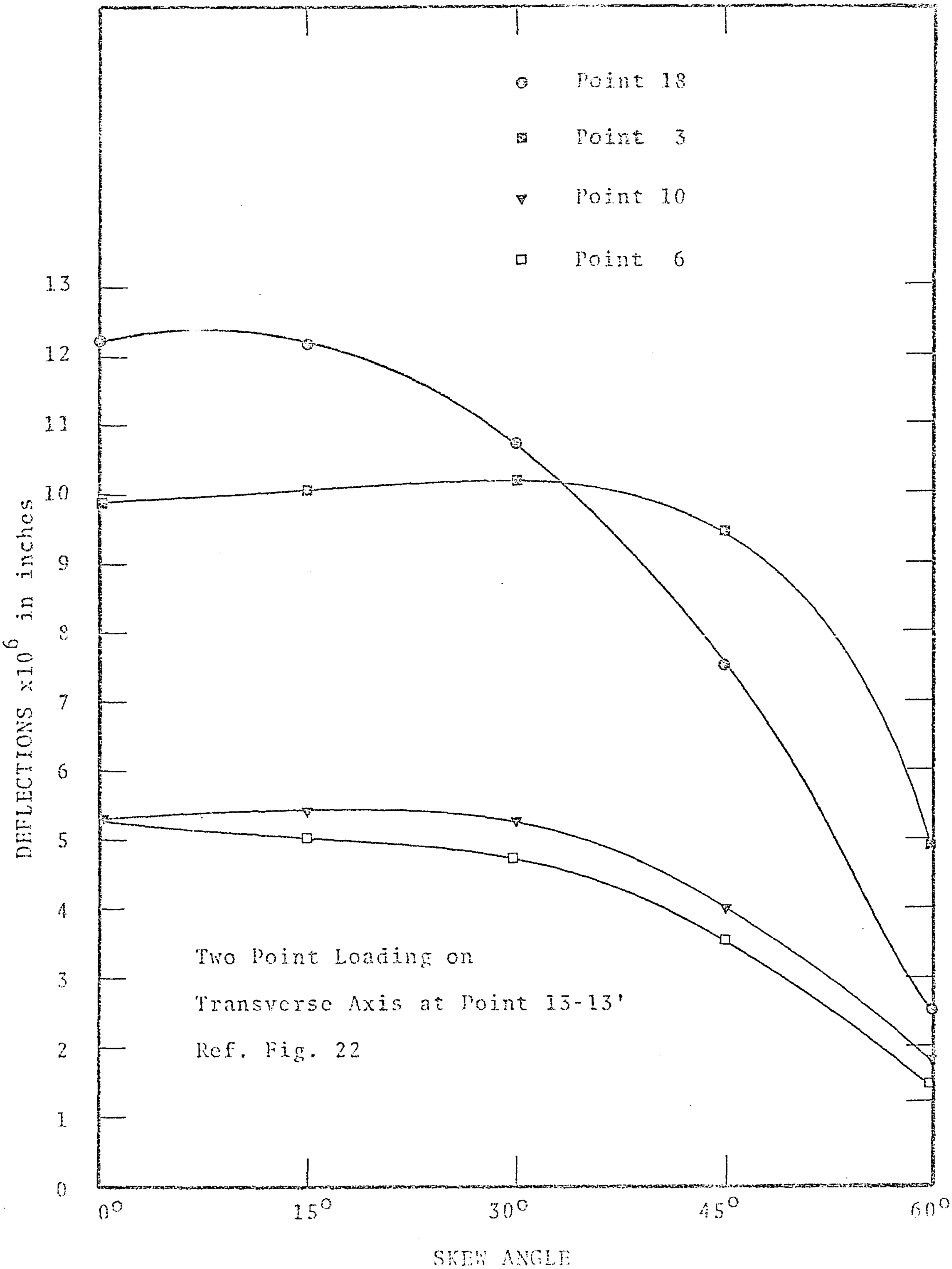

FIG. 3.20 DEFLECTIONS VS. ANGLE OF SKEW

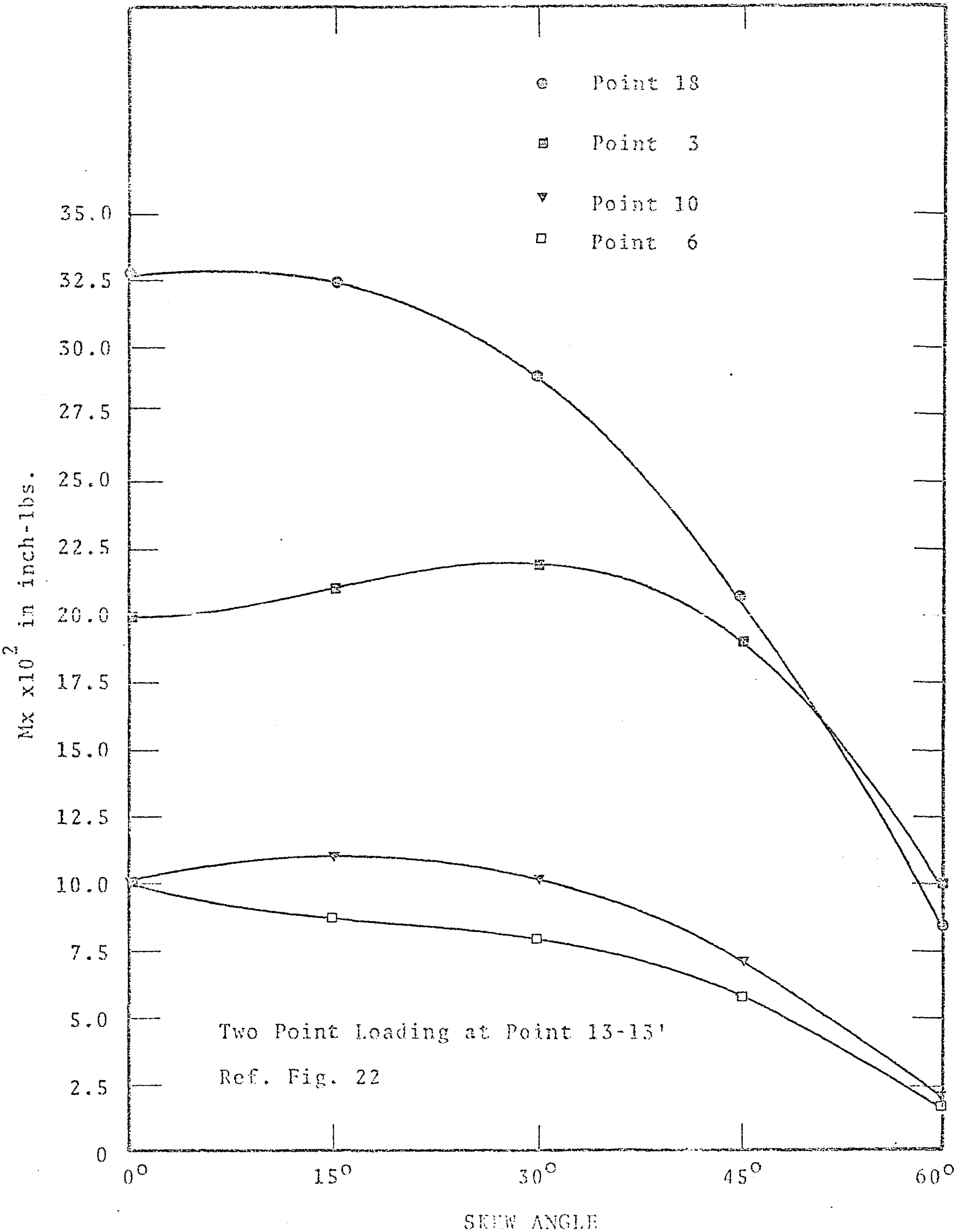

FIG. 3.21 Mx VS. ANGLE OF SKEW

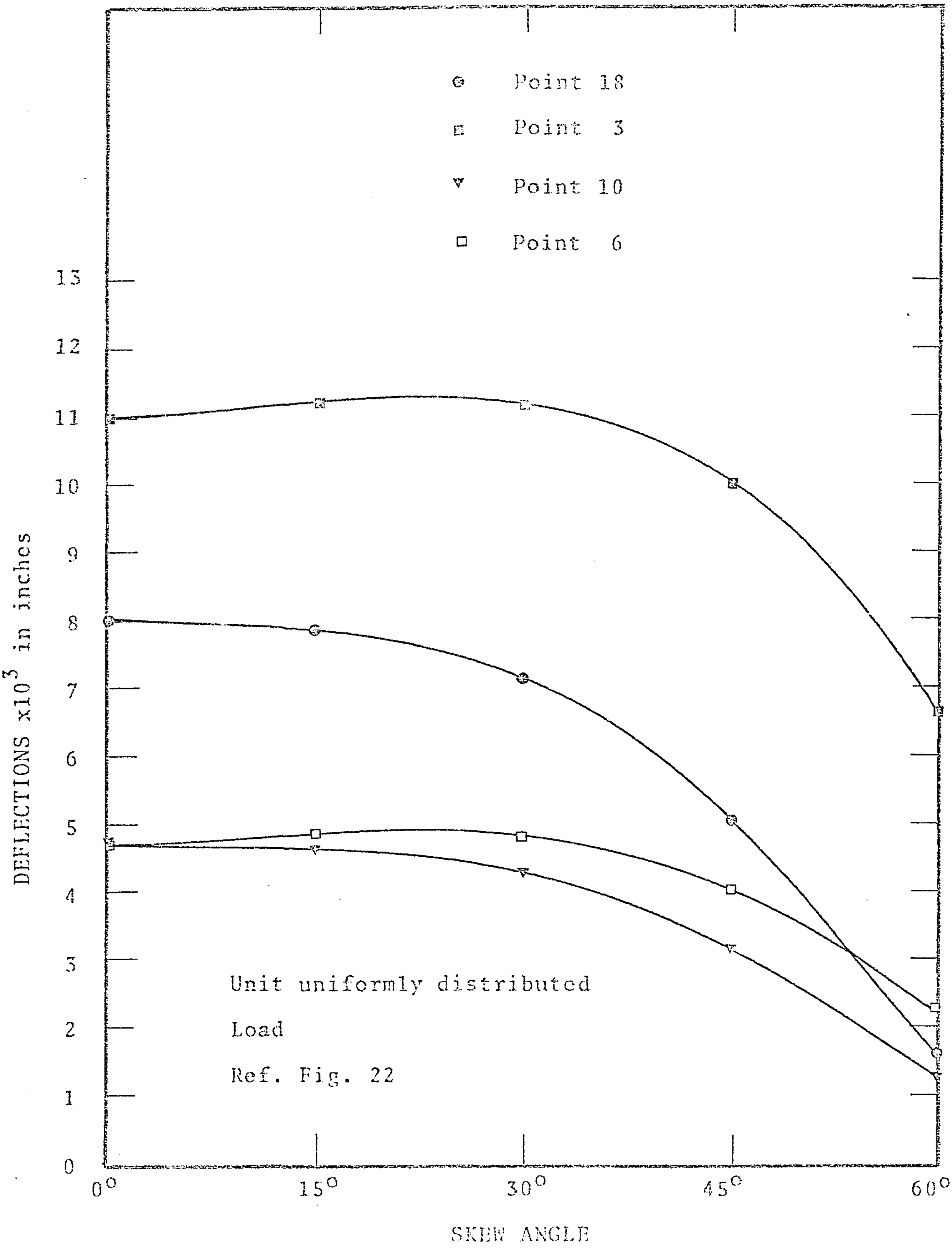

FIG. 3.22 DEFLECTIONS VS. ANGLE OF SKEW

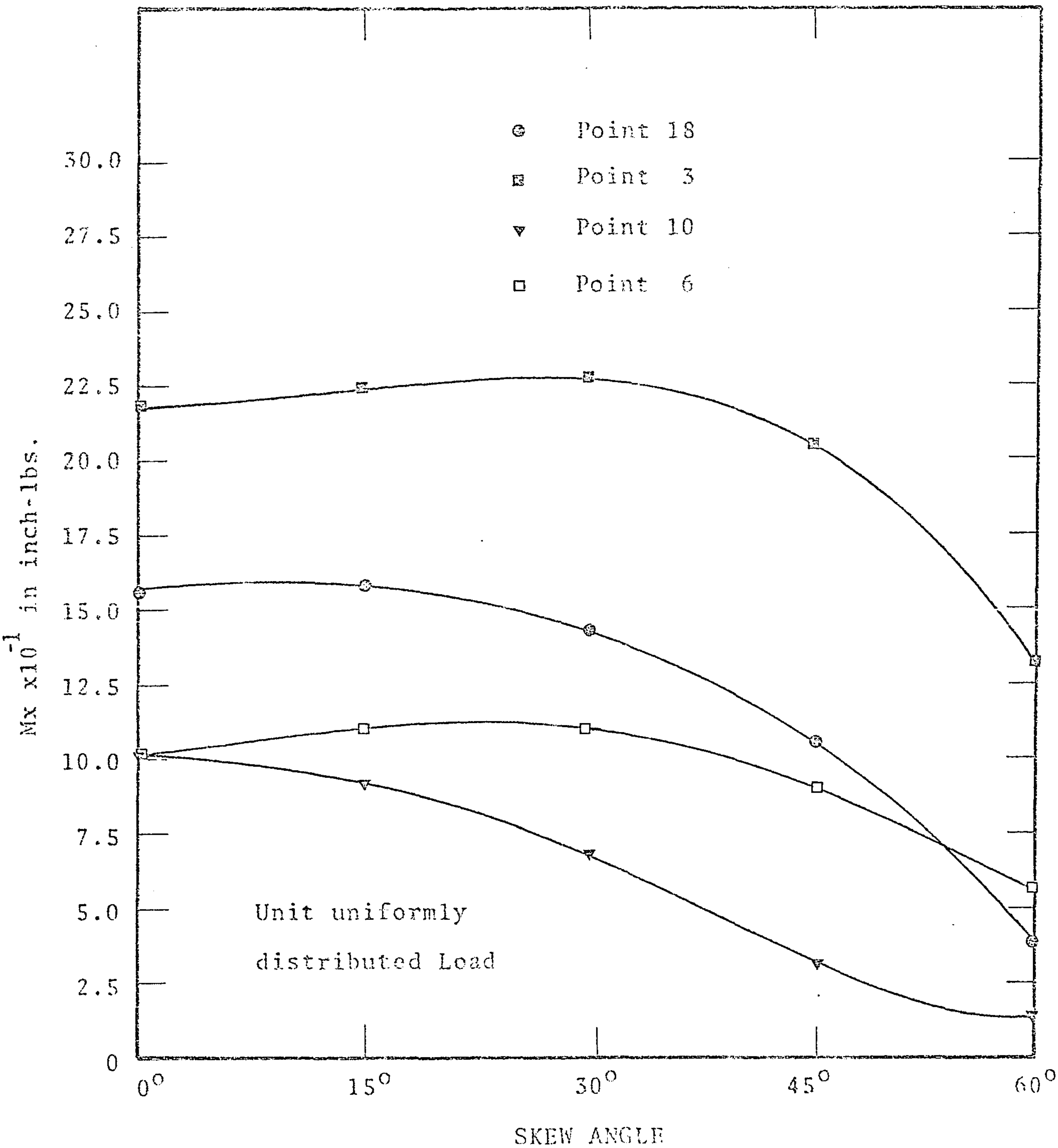

FIG. 3.23 Mx VS. ANGLE OF SKEW

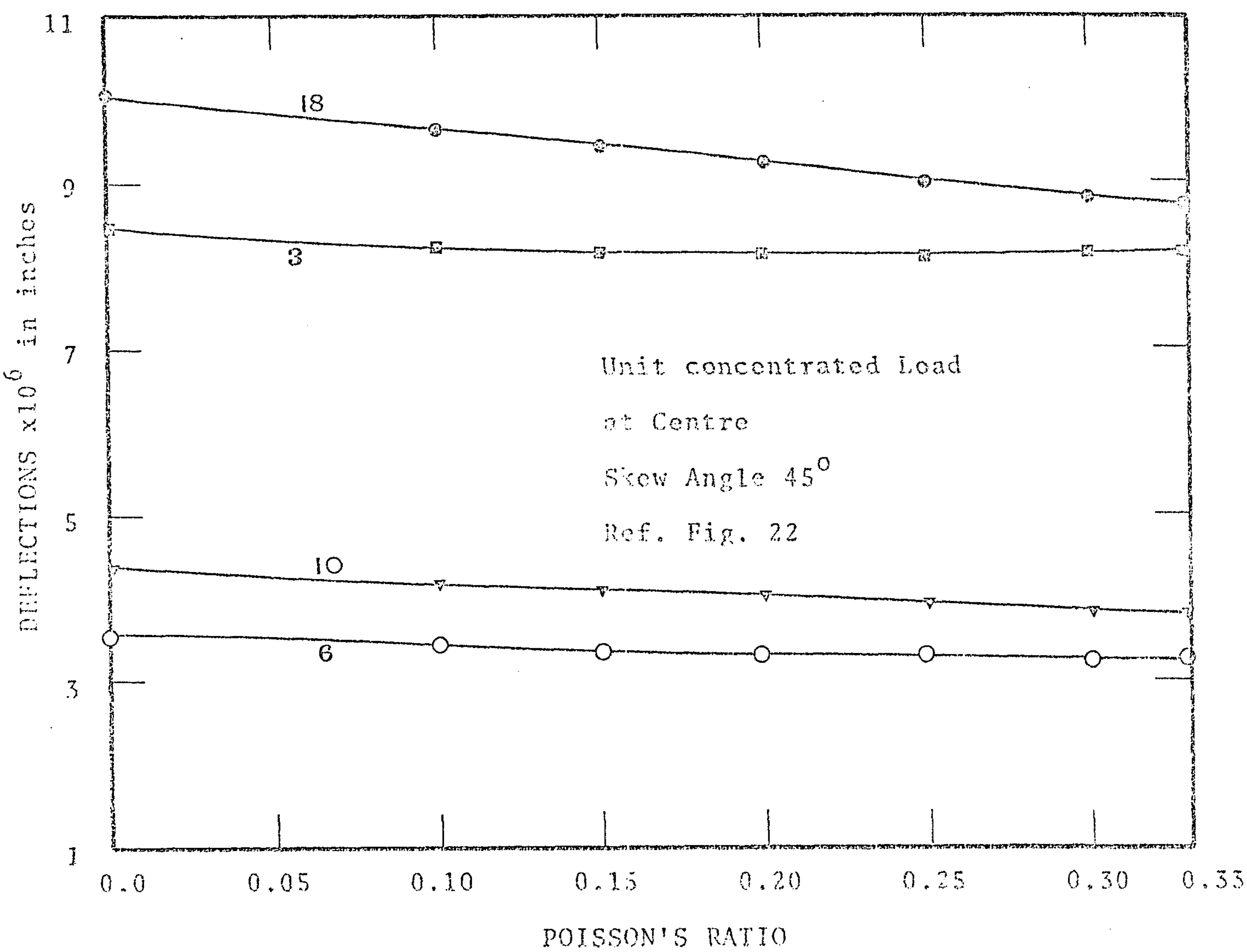

FIG. 3.24 DEFLECTIONS VS. POISSON'S RATIO

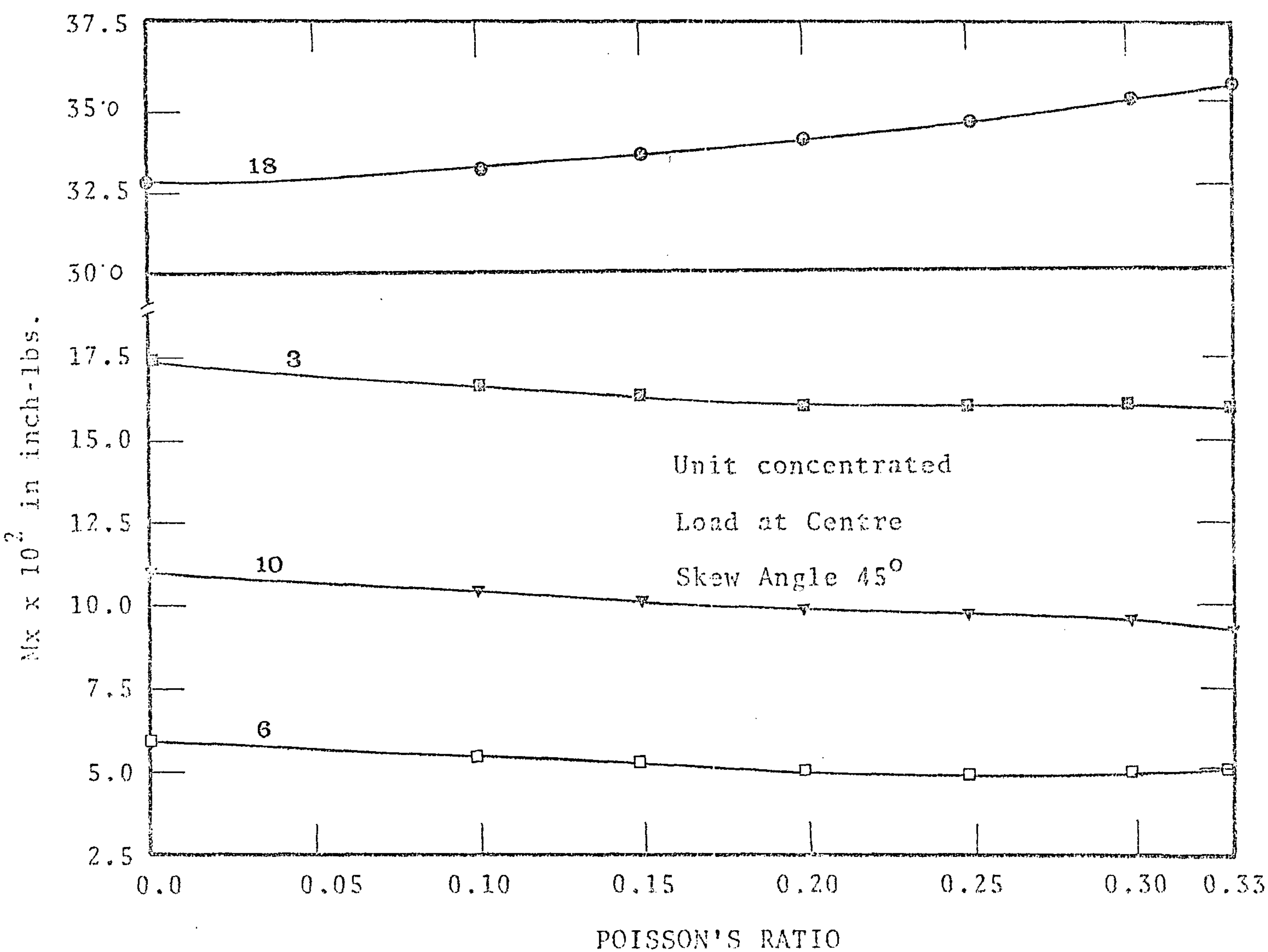

FIG. 3.25 Mx VS. POISSON'S RATIO

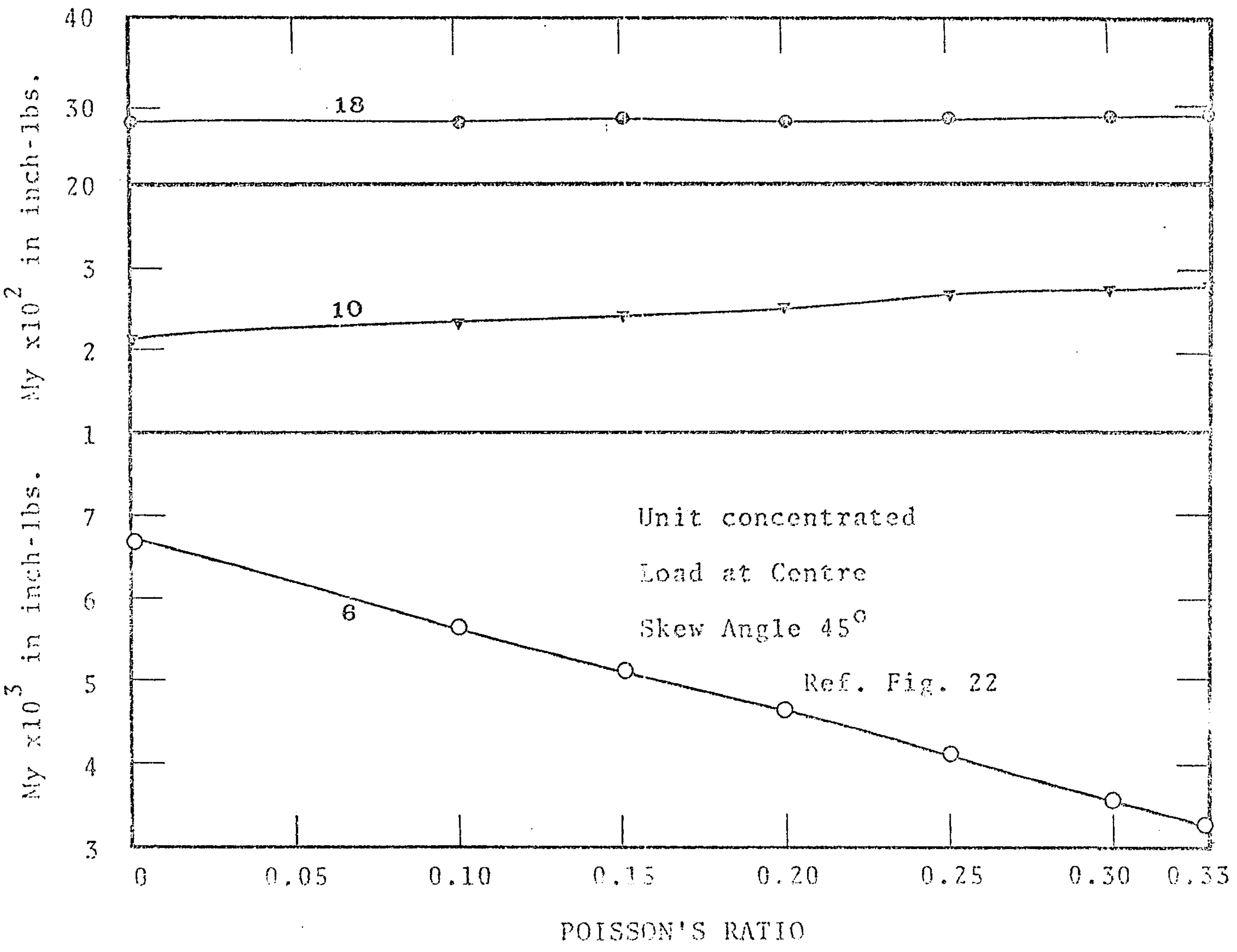

FIG. 3.26 My VS. POISSON'S RATIO

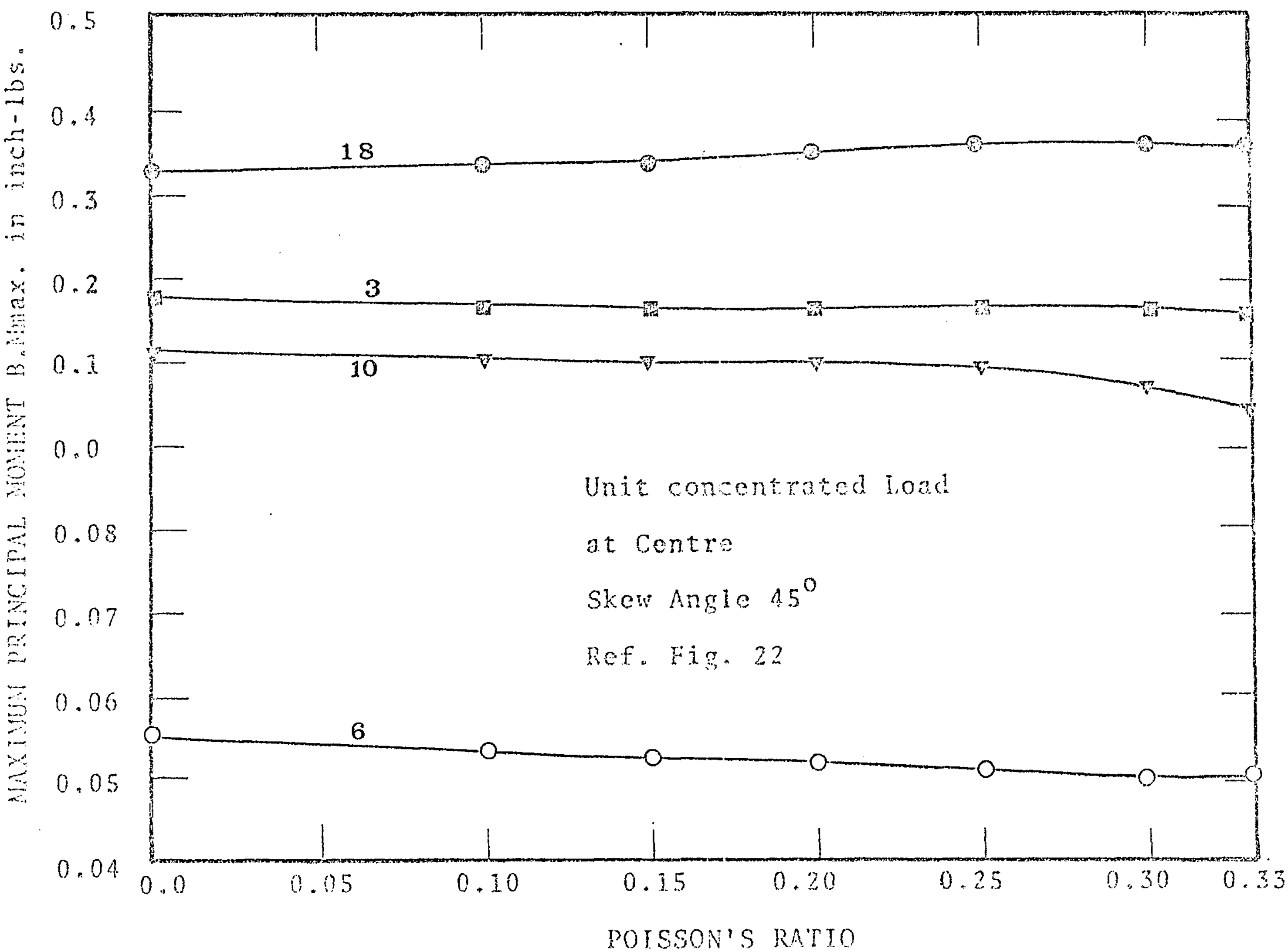

FIG. 3.27 B.Mmax VS. POISSON'S RATIO

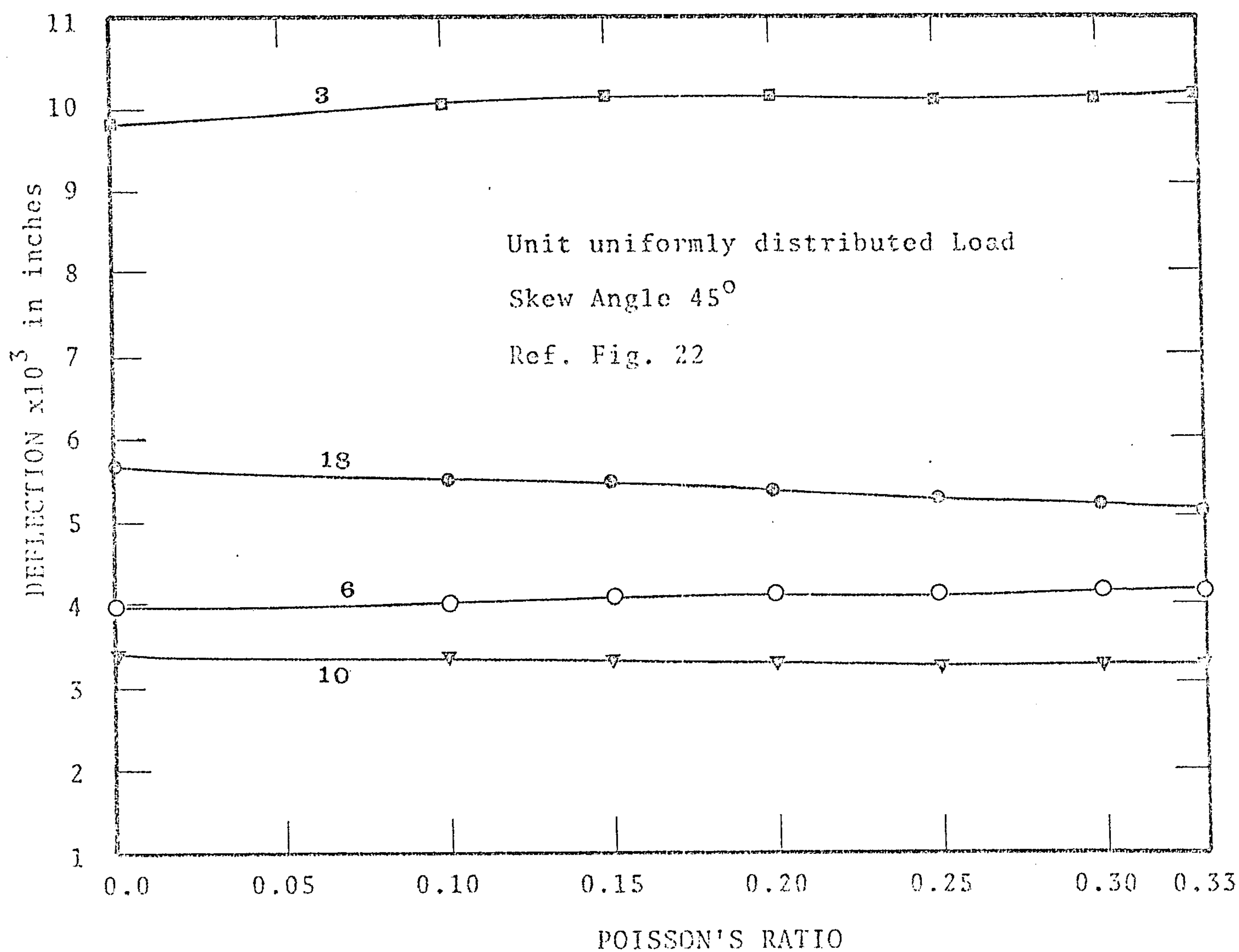

FIG. 3.28 DEFLECTION VS. POISSON'S RATIO

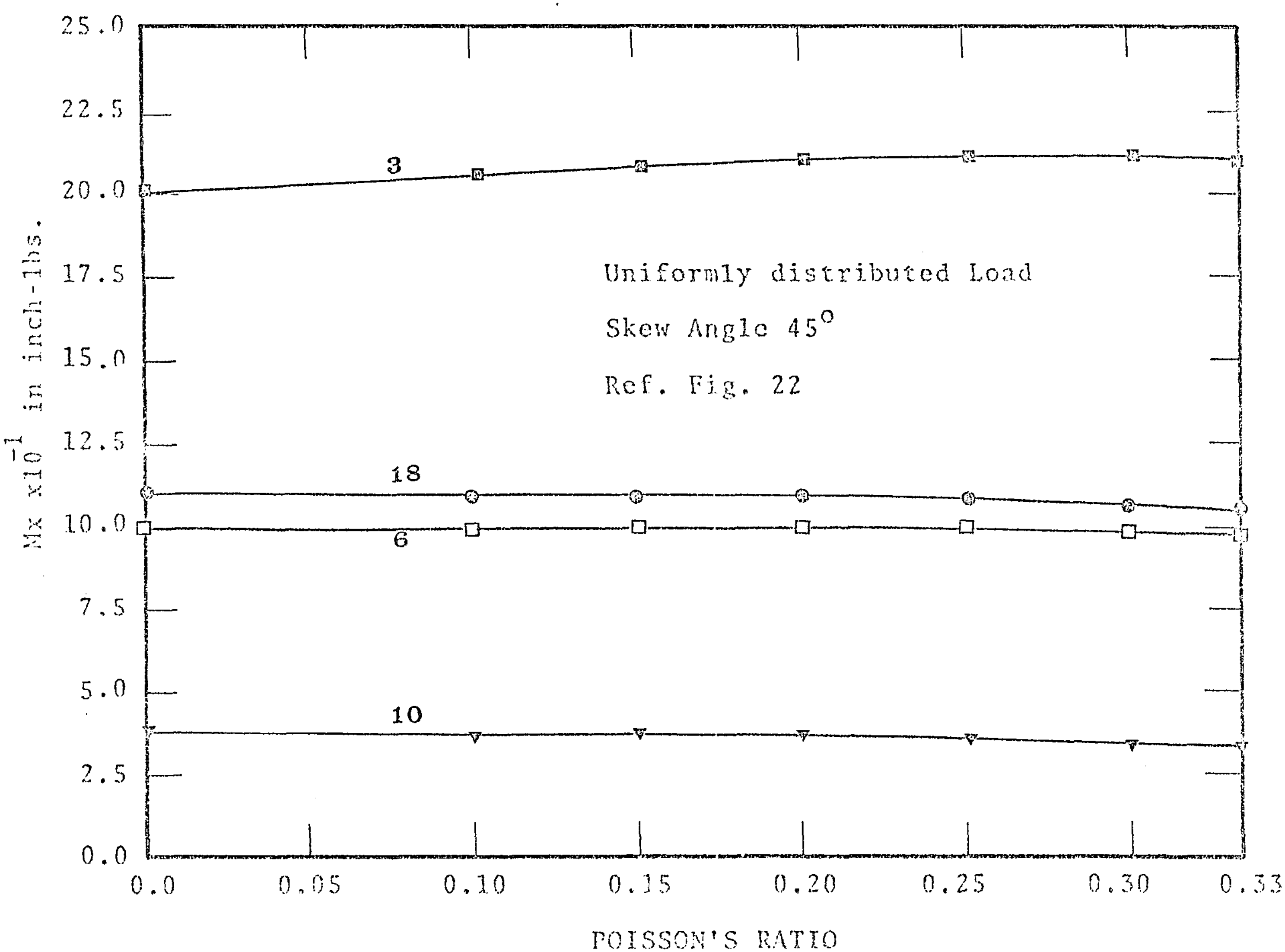

FIG. 3.29 Mx VS. POISSON'S RATIO

APPENDIX

A. APPLICATION OF FINITE DIFFERENCE EQUATIONS AT DIFFERENT MESH POINTS

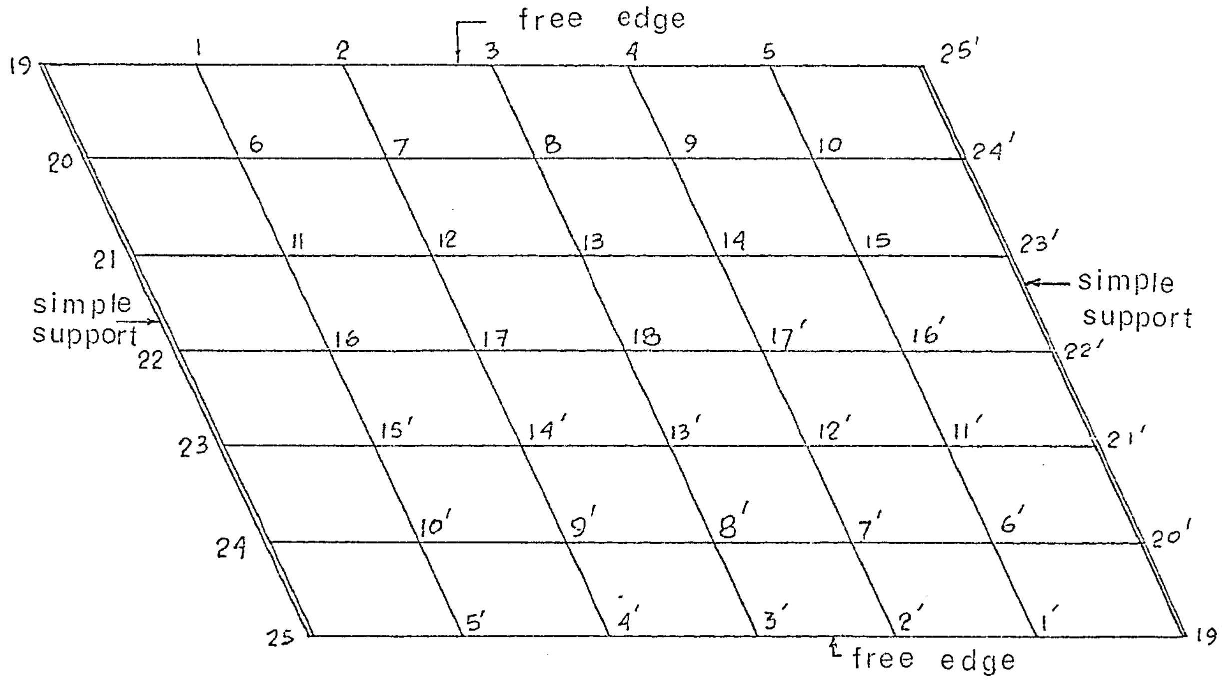

Model Bridge
ref. fig. 22

1. At point 18, Eq. (5.1) represented by Fig. 8(b) can be applied as follows:

$$\{2A(3\alpha+2) + By(\beta^2+4\alpha+6) + Dx^2(6\beta^2+4)\}w_{18} + \{-2By(\alpha+2) - 2(A + Dx^2)\}w_{13} + \{By(1-\beta^2/2)\}w_8 + \{-\beta . By\}w_7 + \{\beta^2 . \tfrac{By}{4}\}w_6$$

$$+ \{(1+\beta)(\alpha By + A + Dx^2) + 2\beta . By\}w_{12} + \{-2\alpha(2A+By) - 2Dx^2(2\beta^2+1) - 2A\}w_{17} + \{(1-\beta)(\alpha By + A + Dx^2) - 2\beta . By\}w_{14'} + \{\beta . By\}w_{9'}$$

$$+ \{-\beta/2\,(\alpha By + A + Dx^2)\}w_{11} + \{\alpha A + \beta^2(Dx^2 - By/2)\}w_{16}$$

$$+ \{\tfrac{\beta}{2}(\alpha By + A + Dx^2)\}w_{15'} + \{\beta^2 . \tfrac{By}{4}\}w_{10'}$$

$$+ \{\beta \cdot B_y\} w_9 + \{(1-\beta)(\alpha B_y + A + D\chi^2) - 2\beta \cdot B_y\} w_{14}$$
$$+ \{-2\alpha(2A + B_y) - 2D\chi^2(2\beta^2+1) - 2A\} w_{17}'$$
$$+ \{(1+\beta)(\alpha B_y + A + D\chi^2) + 2\beta \cdot B_y\} w_{12}' + \{-\beta \cdot B_y\} w_7' + \{\beta^2 \cdot \tfrac{B_y}{4}\} w_{10}$$
$$+ \{\tfrac{\beta}{2}(\alpha B_y + A + D\chi^2)\} w_{15} + \{\alpha A + \beta^2 (D\chi^2 - \tfrac{B_y}{2})\} w_{16}$$
$$+ \{-\tfrac{\beta}{2}(\alpha B_y + A + D\chi^2)\} w_{11}' + \{\beta^2 \cdot \tfrac{B_y}{4}\} w_6' + \{-2B_y(\alpha+2) - 2(A$$
$$+ D\chi^2)\} w_{13}' + \{B_y(1 - \beta^2/2)\} w_8' = \{\frac{P}{\lambda_x \lambda_y}\} \lambda_y^4 \quad \text{--- EQ. 1.}$$

2. At Point 3, Eq. (5.27) represented by Fig. 15(d) can be applied to obtain the following deflection equation:

$$\{\frac{\alpha\gamma}{2} + \frac{\psi}{2B_y}(A-\gamma) - \beta^2 \frac{B_y}{4} - \frac{D\chi^4/\mu_x}{2}\} w_1$$
$$+ \{-2\alpha\gamma - \gamma - \psi - \frac{2\psi}{B_y}(A-\gamma) + 2D\chi^4/\mu_x\} w_2$$
$$+ \{3\alpha\gamma + \frac{3\psi}{B_y}(A-\gamma) + 2(\psi+\gamma) + B_y(1+\beta^2/2) - 3D\chi^4/\mu_x\} w_3$$
$$+ \{-2\alpha\gamma - \gamma - \psi - \frac{2\psi}{B_y}(A-\gamma) + 2D\chi^4/\mu_x\} w_4 + \{\alpha\gamma/2 + \frac{\psi}{2B_y}(A-\gamma)$$
$$- \beta^2\frac{B_y}{4} - \frac{D\chi^4/\mu_x}{2}\} w_5 + \{\frac{\beta}{2}(A+\psi)\} w_6 + \{A - \beta \cdot B_y + \psi - \beta(A+\psi)\} w_7$$
$$+ \{+(A + \beta \cdot B_y) + \psi + \beta(A+\psi)\} w_9 + \{-\frac{\beta}{2}(A+\psi)\} w_{10}$$
$$+ \{-2(A + B_y + \psi)\} w_8 + \{\beta^2 \cdot \frac{B_y}{4}\} w_{11} + \{\beta \cdot B_y\} w_{12} + \{\beta\gamma(1-\beta^2/2)\} w_{13}$$
$$+ \{-\beta \cdot B_y\} w_{14} + \{\beta^2 \frac{B_y}{4}\} w_{15} = \left(\frac{P}{.5\lambda_x \lambda_y}\right) \frac{\lambda_y^4}{2} \quad \text{-- EQ. 14}$$

The formulation of the stiffness matrix [A] can now be easily performed when the appropriate finite difference equations are applied to each of the mesh points in a similar manner.

B COMPUTER LANGUAGE

NOMENCLATURE	COMPUTER LANGUAGE (In Order of Program)
Lx	TL
Ly	TB
m - No. of cross beams	AM
n - No. of longitudinal beams	AN
lo - Spacing of the cross beams	AL
bo - Spacing of the longitudinal beams	AB
$\emptyset$	FI
Ex	EX
Ey	EY
h - thickness of slab	T
b_1 - width of longitudinal beams	FY
(h_1-h) - clear depth of longitudinal beams	ZX
Hy - repeating width of slab in y-direction	HY
Z_1	Z1
b_2 - width of cross beam	FV
Fx - skewed width	FX = FV/COS(FI)
Hx - repeating width of slab in x-direction	HX
Z_2	Z2
(h_2-h) - clear depth of cross beam	ZY
Ix	XI
Iy	YI
μx	XMU
μy	YMU

NOMENCLATURE		COMPUTER LANGUAGE
B_x		BX
B_y		BY.
λ_y		AH
λ_x		BY
χ	$= \lambda_y/\lambda_x$	AS
β	$= \chi \tan\phi$	BET
F_T		FT
F_P		FP
G_x		GX
G_y		GY
A	$= B_y\beta^2 + B_x\chi^2$	AX
H	$= (B_x\mu_y + B_y\mu_x + 4C)/2$	H
α	$= \beta^2 + \chi^2$	ALP
γ	$= (B_x - B_y\mu_x)\chi^2$	GAM
D	$= 2H - B_x - B_y$	D
K_x	$= B_x + \mu_x B_y$	XK
K_y	$= B_y + \mu_y B_x$	YK
δ	$= \chi^2 K_x + \beta^2 K_y$	DEL
ψ	$= (2H - B_x\mu_y - B_x)\chi^2$	SI
Ω		OMEGA
M_x		RMX
M_y		RMY
M_{xy}		RMXY
B.M. max.	Principal moment of the equivalent plate	BMMAX
B.M. min.		BMMIN
θ	- Angle, the maxm. Principal moment make with x-axis	THETA

C. FLOW DIAGRAM OF GENERAL COMPUTER PROGRAM

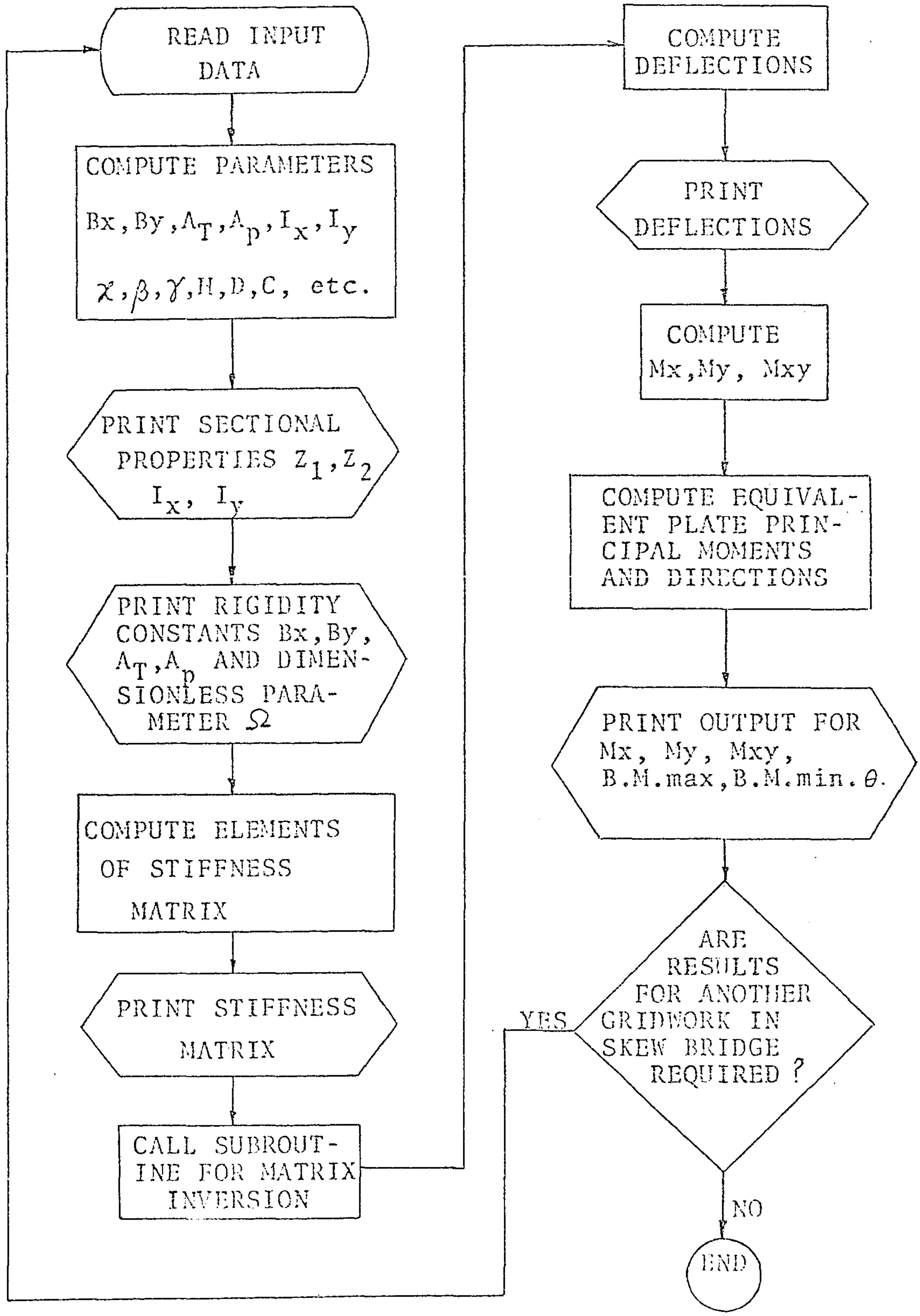

```
C      ELASTIC ANALYSIS OF GRIDWORK IN SKEW BRIDGES
       DIMENSION A(18,18),K(18),C(18),L(18),M(18),RMX(25),
      1RMY(25),RMXY(25),RMMAX(25),RMMIN(25),ZETA(25),THETA(25)
  700 READ 100,TL,TB,AM,AN
  100 FORMAT(4E15.6)
       AL=TL/(AM-1.)
       AB=TB/(AN-1.)
       READ 102,FI,EX
       IF (FI.LT.-.200000  E+01) GO TO 500
  102 FORMAT(2E15.6)
       EY=EX
       READ 103,T,FY,ZX
  103 FORMAT(3E15.6)
       HY=AB
       Z1=FY*ZX*(ZX+T)/(2.*HY*T+2.*FY*ZX)
       READ 104,FV,ZY,XMU
  104 FORMAT(3E15.6)
       FX=FV/COS(FI)
       HX=AL
       Z2=FX*ZY*(ZY+T)/(2.*HX*T+2.*FX*ZY)
       XI=T**3*HY/12.+Z1**2*HY*T+ZX**3*FY/12.+(ZX+T-2.*Z1)**2*FY*ZX/4.
       YI=T**3*HX/12.+Z2**2*HX*T+ZY**3*FX/12.+(ZY+T-2.*Z2)**2*FX*ZY/4.
       SIX=ZX**3*FY/12.+(ZX+T-2.*Z1)**2*FY*ZX/4.
       SIY=ZY**3*FX/12.+(ZY+T-2.*Z2)**2*FX*ZY/4.
       A30=-SIX*XMU/AB
       B30=T**3/12.+SIX/AB+Z1**2*T+XMU**2*SIY/AL
       C30=-T**3*XMU/12.-Z2**2*T*XMU-XMU*SIY/AL
       YMU=(-B30+SQRT(B30**2-4.*A30*C30))/(2.*A30)
       BX=T**3*EX/(12.-12.*XMU*YMU)+EX*SIX/AB+Z1**2*EX*T/(1.-XMU*YMU)
       BY=T**3*EY/(12.-12.*XMU*YMU)+EY*SIY/AL+Z2**2*EY*T/(1.-YMU*YMU)
       AH=TB/6.
       BH=TL/6.
       AS=AH/BH
       BET=AS*SIN(FI)/COS(FI)
       FT=T**3*HY*.333/2.+FY**3*ZX*.333
       FP=T**3*HX*.333/2.+FX**3*ZY*.333
       GX=EX*.5/(1.+SQRT(XMU*YMU))
       GY=EY*.5/(1.+SQRT(XMU*YMU))
       AT=FT*GX/AB
       AP=FP*GY/AL
       C=(AT+AP)/4.
       OMEGA=SQRT(XMU*YMU)+EX*.25*SQRT(YMU)*(FT/AB+FP/AL)/((1.+
      1SQRT(XMU*YMU))*(BY*SQRT(XMU)))
       H=(BX*YMU+BY*XMU+4.*C)/2.
       ALP=BET**2+AS**2
       AX=BET**2*BY+AS**2*BX
       D=2.*H-BX-BY
       GAY=AS**2*(BX-BY*XMU)
       XK=BX+XMU*BY
       YK=BY+YMU*BX
       BEI=AS**2*XK+BET**2*YK
       SI=AS**2*(2.*H-BY*YMU-BX)
       PI=3.1415926
       PRINT 121
  121 FORMAT (1H0,20HSECTIONAL PROPERTIES)
       PRINT 122,Z1,Z2,XI,YI
  122 FORMAT (1H ,6E13.6)
       PRINT 123
```

```
  123 FORMAT (1H0,40HDIMENSIONLESS PARAMETER OMEGA AND RIGIDITY CONSTS)
      PRINT 124,OMEGA,BX,BY,AT,AP,YMU
  124 FORMAT (1H ,6E13.6)
      DO 201 I=1,18
      DO 201 J=1,18
  201 A(I,J)=0.
      A(1,6)=BET**2*BY/2.
      A(1,7)=-2.*BET*BY
      A(1,8)=2.*BY*(1.-BET**2/2.)
      A(1,9)=2.*BET*BY
      A(1,10)=A(1,6)
      A(1,11)=-BET*(ALP*BY+AX+AS**2*D)
      A(1,12)=(2.+2.*BET)*(ALP*BY+AX+AS**2*D)+4.*BET*BY
      A(1,13)=-4.*BY*(ALP+2.)-4.*(AX+AS**2*D)
      A(1,14)=(2.-2.*BET)*(ALP*BY+AX+AS**2*D)-4.*BET*BY
      A(1,15)=BET*(ALP*BY+AX+AS**2*D)
      A(1,16)=2.*ALP*AX+BET**2*2.*(AS**2*D-BY/2.)
      A(1,17)=-4.*ALP*(2.*AX+BY)-AS**2*4.*D*(BET**2*2.+1.)-4.*AX
      A(1,18)=2.*AX*(3.*ALP+2.)+BY*(BET**2+4.*ALP+6.)
     1+AS**2*D*(BET**2*6.+4.)
      A(2,1)=BET**2*BY/4.
      A(2,2)=-BET*BY
      A(2,3)=BY*(1.-BET**2/2.)
      A(2,4)=BET*BY
      A(2,5)=BET**2*BY/4.
      A(2,6)=-BET*(ALP*BY+AX+AS**2*D)/2.
      A(2,7)=(1.+BET)*(ALP*BY+AX+AS**2*D)+2.*BET*BY
      A(2,8)=-2.*BY*(ALP+2.)-2.*(AX+AS**2*D)
      A(2,9)=(1.-BET)*(ALP*BY+AX+AS**2*D)-2.*BET*BY
      A(2,10)=BET*(ALP*BY+AX+AS**2*D)/2.
      A(2,11)=ALP*AX+BET**2*(AS**2*D-BY/4.)
      A(2,12)=-2.*ALP*(2.*AX+BY)-AS**2*2.*D*(BET**2*2.+1.)-2.*AX-BET*BY
      A(2,13)=2.*AX*(3.*ALP+2.)+BY*(7.+4.*ALP+BET**2/2.)
     1+AS**2*D*(BET**2*6.+4.)
      A(2,14)=-2.*ALP*(2.*AX+BY)-AS**2*2.*D*(BET**2*2.+1.)-2.*AX+BET*BY
      A(2,15)=ALP*AX+BET**2*(AS**2*D-BY/4.)
      A(2,17)=2.*(ALP*BY+AX+AS**2*D)
      A(2,18)=-2.*BY*(ALP+2.)-2.*(AX+AS**2*D)
      A(3,6)=-BET*BY
      A(3,7)=BY*(1.-BET**2/4.)
      A(3,9)=A(3,7)
      A(3,10)=BET*BY
      A(3,11)=(1.+BET)*(ALP*BY+AX+AS**2*D)+2.*BET*BY
      A(3,12)=-2.*BY*(ALP+2.)-2.*(AX+AS**2*D)-BET*(ALP*BY+AX+AS**2*D)/2.
      A(3,13)=2.*(ALP*BY+AX+AS**2*D)
      A(3,14)=BET*(ALP*BY+AX+AS**2*D)/2.-2.*BY*(ALP+2.)-2.*(AX+AS**2*D)
      A(3,15)=(1.-BET)*(ALP*BY+AX+AS**2*D)-2.*BET*BY
      A(3,16)=-2.*ALP*(2.*AX+BY)-AS**2*D*2.*(BET**2*2.+1.)-2.*AX
      A(3,17)=AX*(7.*ALP+4.)+BY*(BET**2/2.+4.*ALP+6.)
     1+AS**2*D*(BET**2*7.+4.)
      A(3,18)=A(3,16)
      A(4,1)=-BET*BY
      A(4,2)=BY*(1.-BET**2/2.)
      A(4,3)=BET*BY
      A(4,4)=BET**2*BY/4.
      A(4,6)=(1.+BET)*(ALP*BY+AX+AS**2*D)+2.*BET*BY
      A(4,7)=-2.*BY*(ALP+2.)-2.*(AX+AS**2*D)
      A(4,8)=(1.-BET)*(ALP*BY+AX+AS**2*D)-2.*BET*BY
```

```
      A(4,9)=BET*(ALP*BY+AX+AS**2*D)/2.
      A(4,11)=A(3,16)
      A1=AS**2*D*(BET**2*6.+4.)
      A(4,12)=2.*AX*(3.*ALP+2.)+BY*(BET**2*1.25+4.*ALP+6.)+A1
      A(4,13)=A(3,16)-BET*BY
      A(4,14)=ALP*AY+BET**2*(AS**2*D-BY/2.)+BY*(1.-BET**2/2.)
      A(4,15)=BET*BY
      A(4,16)=A(3,15)
      A(4,17)=-2.*BY*(ALP+2.)-2.*(AY+AS**2*D)-BET*(ALP*BY+AX+AS**2*D)/2.
      A(4,18)=A(3,11)
      A(5,6)=BET**2*AX*YK/(2.*DEL)+BY*(1.-BET**2*.75)
      A(5,7)=BET*BY
      A(5,8)=BET**2*BY/2.
      A(5,9)=-BET*BY
      A(5,10)=A(5,6)
      A2=AS**2*D*(BET/2.-2.-BET**3*YK/DEL)
      A(5,11)=-BY*(4.+2.*ALP-BET*ALP/2.)
     1+AY*(BET/2.-2.-ALP*BET*YK/DEL)+A2
      A(5,12)=A(4,8)
      A(5,14)=A(3,11)
      A3=AS**2*D*(-BET/2.-2.+BET**3*YK/DEL)
      A(5,15)=-BY*(4.+2.*ALP+BET*ALP/2.)
     1+AX*(-BET/2.-2.+ALP*BET*YK/DEL)+A3
      A4=BY*(6.+4.*ALP+BET**2*3./2.)
      A(5,16)=AX*(5.*ALP+4.)-BET**2*YK*AX/DEL
     1+AS**2*D*(4.+BET**2*5.)+A4
      A(5,17)=-2.*ALP*(2.*AX+BY)-2.*AY-AS**2*2.*D*(BET**2*2.+1.)
      A(5,18)=ALP*AX+BET**2*(AS**2*D-BY/2.)
      A(6,1)=A(5,6)
      A(6,2)=A(5,7)
      A(6,3)=BET**2*BY/4.
      A(6,6)=A(5,11)
      A(6,7)=A(4,8)
      A(6,8)=A(4,9)
      A(6,11)=A(5,16)
      A(6,12)=A(3,18)
      A(6,13)=ALP*AX+BET**2*(AS**2*D-BY/4.)
      A(6,14)=A(5,9)
      A(6,15)=A(5,6)
      A(6,16)=A(5,15)
      A(6,17)=A(4,6)
      A(6,18)=-A(2,10)
      A(7,2)=A(2,1)
      A(7,3)=A(2,2)
      A(7,4)=A(2,3)
      A(7,5)=A(2,4)
      A(7,7)=A(6,18)
      A(7,8)=A(4,6)
      A(7,9)=A(2,8)
      A(7,10)=A(2,9)
      A(7,11)=A(2,2)
      A(7,12)=A(4,14)
      A(7,13)=A(3,16)+BET*BY
      A(7,14)=A(4,12)
      A(7,15)=A(3,16)
      A(7,16)=A(2,11)
      A(7,17)=A(2,10)-2.*BY*(ALP+2.)-2.*(AX+AS**2*D)
      A(7,18)=A(2,9)
```

```
      A(8,3)=A(2,1)
      A(8,4)=A(2,2)
      A(8,5)=A(5,6)
      A(8,8)=A(6,18)
      A(8,9)=A(2,7)
      A(8,10)=A(5,15)
      A(8,11)=A(5,6)
      A(8,12)=A(5,7)
      A(8,13)=A(6,13)
      A(8,14)=A(3,18)
      A(8,15)=A(5,16)
      A(8,16)=A(5,11)
      A(8,17)=A(2,9)
      A(8,18)=A(2,10)
      A(9,1)=BY*(ALP+BET)+BET*(ALP*BY+GAM)+GAM+AS**2*D*(1.+BET)
      A(9,2)=-2.*BY*(1.+ALP)-2.*(GAM+AS**2*D)
      A(9,3)=BY*(ALP-BET)-BET*(ALP*BY+GAM)+GAM+AS**2*D*(1.-BET)
      A(9,4)=BET*(ALP*BY+GAM+AS**2*D)/2.
      A(9,6)=A(3,16)
      A5=AS**2*2.*D*(BET**2*3.+2.)
      A(9,7)=2.*AX*(3.*ALP+2.)+BY*(5.+4.*ALP+BET**2/2.)+A5
      A(9,8)=A(3,16)
      A(9,9)=A(6,13)
      A(9,11)=A(2,9)
      A(9,12)=-2.*BY*(ALP+2.)-2.*(AS**2*D+AX)
      A(9,13)=A(3,11)
      A(9,14)=A(6,18)
      A(9,16)=BET*BY
      A(9,17)=BY*(1.-BET**2/4.)
      A(9,18)=-BET*BY
      A(10,1)=-BET*(ALP*BY+GAM+AS**2*D)/2.
      A(10,2)=A(9,1)
      A(10,3)=A(9,2)
      A(10,4)=A(9,3)
      A(10,5)=-A(10,1)
      A(10,6)=A(6,13)
      A(10,7)=A(3,16)
      A(10,8)=A(9,7)
      A(10,9)=A(3,16)
      A(10,10)=A(6,13)
      A(10,11)=A(2,10)
      A(10,12)=A(2,9)
      A(10,13)=A(9,12)
      A(10,14)=A(3,11)
      A(10,15)=-A(2,10)
      A(10,16)=BET**2*BY/2.
      A(10,18)=BY*(1.-BET**2/2.)
      A(11,2)=A(10,1)
      A(11,3)=A(9,1)
      A(11,4)=A(9,2)
      A(11,5)=A(9,3)
      A(11,7)=A(6,13)
      A(11,8)=A(3,16)
      A(11,9)=A(9,7)
      A(11,10)=A(3,16)
      A(11,12)=A(2,10)
      A(11,13)=A(2,9)
      A(11,14)=A(9,12)
```

```
       A(11,15)=A(3,11)
       A(11,16)=A(9,18)
       A(11,17)=A(9,17)
       A(11,18)=A(9,16)
       A6=AS**2*D*(-2.+BET/2.-BET**3*YK/DEL)
       A(12,1)=-AX*ALP*BET*YK/DEL-2.*GAM-2.*BY*(ALP+1.)
      1+BET*(ALP*BY+GAM)/2.+A6
       A(12,2)=A(9,3)
       A(12,3)=A(9,4)
       A7=BY*(5.+4.*ALP+BET**2*.75)+AS**2*D*(4.+BET**2*5.)
       A(12,6)=AX*(5.*ALP+4.)+BET**2*YK*(GAM-AX)/(2.*DEL)+A7
       A(12,7)=A(3,16)
       A(12,8)=A(6,13)
       A(12,11)=AX*ALP*BET*YK/DEL-2.*AX-BY*ALP*BET/2.
      1-AX*BET/2.-2.*BY*(ALP+2.)+A3
       A(12,12)=A(3,11)
       A(12,13)=-A(2,10)
       A(12,16)=BY*(1.-BET**2*.75)+BET**2*YK*(AX-GAM)/(2.*DEL)
       A(12,17)=-BET*BY
       A(12,18)=BET**2*BY/4.
       A(13,3)=A(10,1)
       A(13,4)=A(9,1)
       A(13,5)=AX*ALP*BET*YK/DEL-2.*GAM-BET*(ALP*BY+GAM)/2.
      1-2.*BY*(ALP+1.)+A3
       A(13,8)=A(6,13)
       A(13,9)=A(3,16)
       A(13,10)=BET**2*YK*(GAM-AX)/(2.*DEL)+AX*(4.+5.*ALP)+A7
       A(13,13)=A(2,10)
       A(13,14)-A(2,9)
       A(13,15)=-AX*ALP*BET*YK/DEL-2.*AX-BY*(4.+2.*ALP)
      1+BET*(AX+ALP*BY)/2.+A6
       A(13,16)=A(12,16)
       A(13,17)=BET*BY
       A(13,18)=BET**2*BY/4.
       A8=AS**4*D*XMU
       A(14,1)=-2.*ALP*GAM-GAM-SI-2.*SI*(AX-GAM)/BY+2.*A8
       A9=BY*(1.+BET**2/2.)
       A(14,2)=3.*ALP*GAM+3.*SI*(AX-GAM)/BY+2.*(SI+GAM)+A9-3.*A8
       A(14,3)=A(14,1)
       A(14,4)=ALP*GAM/2.+SI*(AX-GAM)/(2.*BY)-BET**2*BY/4.-A8/2.
       A(14,6)=AX-BET*BY+SI-BET*(AX+SI)
       A(14,7)=-2.*(AX+BY+SI)
       A(14,8)=AX+BET*BY+SI+BET*(AX+SI)
       A(14,9)=-BET*(AX+SI)/2.
       A(14,11)=BET*BY
       A(14,12)=BY*(1.-BET**2/2.)
       A(14,13)=-BET*BY
       A(14,14)=BET**2*BY/4.
       A(15,1)=ALP*GAM/2.+SI*(AX-GAM)/(2.*BY)-BET**2*BY/4.-A8/2.
       A(15,2)=A(14,1)
       A(15,3)=A(14,2)
       A(15,4)=A(14,1)
       A(15,5)=A(14,4)
       A(15,6)=BET*(AX+SI)/2.
       A(15,7)=A(14,6)
       A(15,8)=A(14,7)
       A(15,9)=A(14,8)
       A(15,10)=A(14,9)
```

```
      A(15,11)=BET**2*BY/4.
      A(15,12)=A(14,11)
      A(15,13)=A(14,12)
      A(15,14)=A(14,13)
      A(15,15)=A(14,14)
      A(16,2)=A(15,1)
      A(16,3)=A(15,2)
      A(16,4)=A(15,3)
      A(16,5)=A(15,4)
      A(16,7)=A(15,6)
      A(16,8)=A(15,7)
      A(16,9)=A(15,8)
      A(16,10)=A(15,9)
      A(16,12)=A(15,11)
      A(16,13)=A(15,12)
      A(16,14)=A(15,13)
      A(16,15)=A(15,14)
      A10=BY*(1.+BET**2/4.)+2.*(GAM+SI)-BET**2*SI*YK/(2.*DEL)
      A(17,1)=-AX*BET**2*YK/(2.*DEL)+BET**2*BY/2.+2.5*ALP*GAM
     1+5.*SI*(AX-GAM)/(2.*BY)+A10-2.5*A8
      A(17,2)=A(14,1)
      A(17,3)=-BET**2*BY/4.+ALP*GAM/2.-SI*(GAM-AX)/(2.*BY)-A8/2.
      A(17,6)=-2.*(AX+BY+SI)-BET*SI/2.-AX*BET/2.
      A(17,7)=(AX+SI)*(1.+BET)+BET*BY
      A(17,8)=A(14,9)
      A(17,11)=BY*(1.-BET**2/4.)+BET**2*YK*(AX+SI)/(2.*DEL)-BET**2*BY/2.
      A(17,12)=-BET*BY
      A(17,13)=BET**2*BY/4.
      A(18,3)=A(15,1)
      A(18,4)=A(14,1)
      A(18,5)=A(17,1)
      A(18,8)=A(15,6)
      A(18,9)=AX-BET*BY+SI-BET*(AX+SI)
      A(18,10)=-2.*(AX+BY+SI)+AX*BET/2.+BET*SI/2.
      A(18,13)=BET**2*BY/4.
      A(18,14)=BET*BY
      A(18,15)=A(17,11)
      DO 999 IA=1,18
      DO 999 JA=1,18
  999 A(IA,JA)=A(IA,JA)*1.E-10
      PRINT 111
  111 FORMAT(1H0,11HMATRIX A IS)
      PRINT1000,((A(I,J),J=1,18),I=1,18)
 1000 FORMAT(1H ,6E13.6)
      CALLMINV(A,18,D,L,M)
      PRINT 444
  444 FORMAT (1H0,10HINVERSE IS)
      PRINT 1001,((A(I,J),J=1,18),I=1,18)
 1001 FORMAT(1H ,6E13.6)
      Q=1.
      DO 41 I=1,18
   41 B(I)=0.
      B(1)=AH**3*Q/BH
      DO 42 I=1,18
      W(I)=0.
      DO 43 J=1,18
      W(I)=W(I)+A(I,J)*B(J)*1.E-10
   43 CONTINUE
```

```
   42 CONTINUE
      PRINT 222
  222 FORMAT(1H0,15HDEFLECTIONS ARE)
      DO 21 I=1,18
   21 PRINT 71,I,W(I)
   71 FORMAT (1H0,30X,2HW%,I2,2H<#E13.6)
      PRINT 16,DETRM
   16 FORMAT (1H0,14HDETERMINANT IS/E13.6)
      B1=-BX/(AH**2)
      A20=(BET*YMU-BET*YK*(AS**2+BET**2*YMU)/DEL)*B1
      A21=(-BET*YMU+BET*YK*(AS**2+BET**2*YMU)/DEL)*B1
      RMX(25)=0.
      RMX(24)=A20*W(15)+A21*W(5)
      RMX(23)=A20*W(16)+A21*W(10)
      RMX(22)=A20*W(11)+A21*W(15)
      RMX(21)=A20*W(6)+A21*W(16)
      RMX(20)=A20*W(1)+A21*W(11)
      RMX(19)=0.
      RMX(18)=(-YMU*BET*W(12)+2.*YMU*W(13)+YMU*BET*W(14)
     1+2.*(AS**2+BET**2*YMU)*W(17)-2.*(AS**2+YMU+BET**2*YMU)*W(18))*B1
      RMX(17)=(-YMU*BET*W(11)/2.+YMU*W(12)+(AS**2+BET**2*YMU)*W(16)
     1-2.*(AS**2+YMU+BET**2*YMU)*W(17)+(AS**2+BET**2*YMU)*W(18)
     2+YMU*BET*W(15)/2.+YMU*W(14))*B1
      RMX(16)=(YMU*W(11)+YMU*BET*W(12)/2.-2.*(AS**2+YMU+BET**2*YMU)
     1*W(16)+(AS**2+BET**2*YMU)*W(17)+YMU*W(15)-YMU*BET*W(14)/2.)*B1
      RMX(15)=(-BET*YMU*W(9)/2.+YMU*W(10)+(AS**2+BET**2*YMU)*W(14)
     1-2.*(AS**2+YMU+BET**2*YMU)*W(15)+YMU*BET*W(17)/2.+YMU*W(16))*B1
      RMX(14)=(-BET*YMU*W(8)/2.+YMU*W(9)+YMU*BET*W(10)/2.
     1+(AS**2+BET**2*YMU)*W(13)-2.*(AS**2+YMU+BET**2*YMU)*W(14)
     2+(AS**2+BET**2*YMU)*W(15)+YMU*BET*W(18)/2.
     3+YMU*W(17)-YMU*BET*W(16)/2.)*B1
      RMX(13)=(-BET*YMU*W(7)/2.+YMU*W(8)+YMU*BET*W(9)/2.
     1+(AS**2+BET**2*YMU)*W(12)-2.*(AS**2+YMU+BET**2*YMU)*W(13)
     2+(AS**2+BET**2*YMU)*W(14)+YMU*BET*W(17)/2.+YMU*W(18)
     3-YMU*BET*W(17)/2.)*B1
      RMX(12)=(-BET*YMU*W(6)/2.+YMU*W(7)+YMU*BET*W(8)/2.
     1+(AS**2+BET**2*YMU)*W(11)-2.*(AS**2+YMU+BET**2*YMU)*W(12)
     2+(AS**2+BET**2*YMU)*W(13)+YMU*BET*W(16)/2.+YMU*W(17)
     3-YMU*BET*W(18)/2.)*B1
      RMX(11)=(YMU*W(6)+YMU*BET*W(7)/2.-2.*(AS**2+YMU+BET**2*YMU)*W(11)
     1+(AS**2+BET**2*YMU)*W(12)+YMU*W(16)-YMU*BET*W(17)/2.)*B1
      RMX(10)=(-BET*YMU*W(4)/2.+YMU*W(5)+(AS**2+BET**2*YMU)*W(9)
     1-2.*(AS**2+YMU+BET**2*YMU)*W(10)+YMU*BET*W(14)/2.+YMU*W(15))*B1
      RMX(9)=(-BET*YMU*W(3)/2.+YMU*W(4)+YMU*BET*W(5)/2.
     1+(AS**2+BET**2*YMU)*W(8)-2.*(AS**2+YMU+BET**2*YMU)*W(9)
     2+(AS**2+BET**2*YMU)*W(10)+YMU*BET*W(13)/2.+YMU*W(14)-YMU*BET*W(15)
     3/2.)*B1
      RMX(8)=(-BET*YMU*W(2)/2.+YMU*W(3)+YMU*BET*W(4)/2.
     1+(AS**2+BET**2*YMU)*W(7)-2.*(AS**2+YMU+BET**2*YMU)*W(8)
     2+(AS**2+BET**2*YMU)*W(9)+YMU*BET*W(12)/2.+YMU*W(13)
     3-YMU*BET*W(14)/2.)*B1
      RMX(7)=(-BET*YMU*W(1)/2.+YMU*W(2)+YMU*BET*W(3)/2.
     1+(AS**2+BET**2*YMU)*W(6)-2.*(AS**2+YMU+BET**2*YMU)*W(7)
     2+(AS**2+BET**2*YMU)*W(8)+YMU*BET*W(11)/2.+YMU*W(12)
     3-YMU*BET*W(13)/2.)*B1
      RMX(6)=(YMU*W(1)+YMU*BET*W(2)/2.-2.*(AS**2+YMU+BET**2*YMU)*W(6)
     1+(AS**2+BET**2*YMU)*W(7)+YMU*W(11)-YMU*BET*W(12)/2.)*B1
      A11=-BX*(1.-XMU*YMU)*AS**2/(AH**2)
```

```
      RMX(5)=A11*(W(4)-2.*W(5))
      RMX(4)=A11*(W(3)-2.*W(4)+W(5))
      RMX(3)=A11*(W(2)-2.*W(3)+W(4))
      RMX(2)=A11*(W(1)-2.*W(2)+W(3))
      RMX(1)=A11*(-2.*W(1)+W(2))
      DO 22 I=1,25
   22 PRINT 202,I,RMX(I)
  202 FORMAT (1H0,30X,4HRMX%,I2,2H<#E13.6)
      B2=-BY/(AH**2)
      RMY(25)=0.
      RMY(24)=-RMX(24)
      RMY(23)=-RMX(23)
      RMY(22)=-RMX(22)
      RMY(21)=-RMX(21)
      RMY(20)=-RMX(20)
      RMY(19)=0.
      RMY(18)=(-BET*W(12)+2.*W(13)+BET*W(14)+2.*(BET**2+AS**2*XMU)*W(17)
     1-2.*(1.+BET**2+AS**2*XMU)*W(18))*B2
      RMY(17)=(-BET*W(11)/2.+W(12)+(BET**2+AS**2*XMU)*W(16)
     1-2.*(1.+BET**2+AS**2*XMU)*W(17)+(BET**2+AS**2*XMU)*W(18)
     2+BET*W(15)/2.+W(14))*B2
      RMY(16)=(W(11)+BET*W(12)/2.-2.*(1.+BET**2+AS**2*XMU)*W(16)
     1+(BET**2+AS**2*XMU)*W(17)+W(15)-BET*W(14)/2.)*B2
      RMY(15)=(-BET*W(9)/2.+W(10)+(BET**2+AS**2*XMU)*W(14)
     1-2.*(1.+BET**2+AS**2*XMU)*W(15)+BET*W(17)/2.+W(16))*B2
      RMY(14)=(-BET*W(8)/2.+W(9)+BET*W(10)/2.+(BET**2+AS**2*XMU)*W(13)
     1-2.*(1.+BET**2+AS**2*XMU)*W(14)+(BET**2+AS**2*XMU)*W(15)
     2+BET*W(18)/2.+W(17)-BET*W(16)/2.)*B2
      RMY(13)=(-BET*W(7)/2.+W(8)+BET*W(9)/2.+(BET**2+AS**2*XMU)*W(12)
     1-2.*(1.+BET**2+AS**2*XMU)*W(13)+(BET**2+AS**2*XMU)*W(14)
     2+BET*W(17)/2.+W(18)-BET*W(17)/2.)*B2
      RMY(12)=(-BET*W(6)/2.+W(7)+BET*W(8)/2.+(BET**2+AS**2*XMU)*W(11)
     1-2.*(1.+BET**2+AS**2*XMU)*W(12)+(BET**2+AS**2*XMU)*W(13)
     2+BET*W(16)/2.+W(17)-BET*W(18)/2.)*B2
      RMY(11)=(W(6)+BET*W(7)/2.-2.*(1.+BET**2+AS**2*XMU)*W(11)
     1+(BET**2+AS**2*XMU)*W(12)+W(16)-BET*W(17)/2.)*B2
      RMY(10)=(-BET*W(4)/2.+W(5)+(BET**2+AS**2*XMU)*W(9)
     1-2.*(1.+BET**2+AS**2*XMU)*W(10)+BET*W(14)/2.+W(15))*B2
      RMY(9)=(-BET*W(3)/2.+W(4)+BET*W(5)/2.+(BET**2+AS**2*XMU)*W(8)
     1-2.*(1.+BET**2+AS**2*XMU)*W(9)+(BET**2+AS**2*XMU)*W(10)
     2+BET*W(13)/2.+W(14)-BET*W(15)/2.)*B2
      RMY(8)=(-BET*W(2)/2.+W(3)+BET*W(4)/2.+(BET**2+AS**2*XMU)*W(7)
     1-2.*(1.+BET**2+AS**2*XMU)*W(8)+(BET**2+AS**2*XMU)*W(9)
     2+BET*W(12)/2.+W(13)-BET*W(14)/2.)*B2
      RMY(7)=(-BET*W(1)/2.+W(2)+BET*W(3)/2.+(BET**2+AS**2*XMU)*W(6)
     1-2.*(1.+BET**2+AS**2*XMU)*W(7)+(BET**2+AS**2*XMU)*W(8)
     2+BET*W(11)/2.+W(12)-BET*W(13)/2.)*B2
      RMY(6)=(W(1)+BET*W(2)/2.-2.*(1.+BET**2+AS**2*XMU)*W(6)
     1+(BET**2+AS**2*XMU)*W(7)+W(11)-BET*W(12)/2.)*B2
      RMY(5)=0.
      RMY(4)=0.
      RMY(3)=0.
      RMY(2)=0.
      RMY(1)=0.
      DO 23 I=1,25
   23 PRINT 203,I,RMY(I)
  203 FORMAT(1H0,30X,4HRMY%,I2,2H<#E13.6)
      A12=-2.*C*AS/(AH**2)
```

```
      A23=(-BET**2*YK/DEL+1./2.)*A12
      A24=(BET**2*YK/DEL-1./2.)*A12
      RMXY(25)=A23*W(10)
      RMXY(24)=A23*W(15)+A24*W(5)
      RMXY(23)=A23*W(16)+A24*W(10)
      RMXY(22)=A23*W(11)+A24*W(15)
      RMXY(21)=A23*W(6)+A24*W(16)
      RMXY(20)=A23*W(1)+A24*W(11)
      RMXY(19)=A24*W(6)
      RMXY(18)=(-W(12)/2.+W(14)/2.+2.*BET*W(17)-2.*BET*W(18))*A12
      RMXY(17)=(-W(11)/4.+BET*W(16)-2.*BET*W(17)+BET*W(18)+W(15)/4.)*A12
      RMXY(16)=(W(12)/4.-2.*BET*W(16)+BET*W(17)-W(14)/4.)*A12
      RMXY(15)=(-W(9)/4.+BET*W(14)-2.*BET*W(15)+W(17)/4.)*A12
      RMXY(14)=(-W(8)/4.+W(10)/4.+BET*W(13)-2.*BET*W(14)
     1+BET*W(15)+W(18)/4.-W(16)/4.)*A12
      RMXY(13)=(-W(7)/4.+W(9)/4.+BET*W(12)-2.*BET*W(13)+BET*W(14))*A12
      RMXY(12)=(-W(6)/4.+W(8)/4.+BET*W(11)-2.*BET*W(12)
     1+BET*W(13)+W(16)/4.-W(18)/4.)*A12
      RMXY(11)=(W(7)/4.-2.*BET*W(11)+BET*W(12)-W(17)/4.)*A12
      RMXY(10)=(-W(4)/4.+BET*W(9)-2.*BET*W(10)+W(14)/4.)*A12
      RMXY(9)=(-W(3)/4.+W(5)/4.+BET*W(8)-2.*BET*W(9)+BET*W(10)
     1+W(13)/4.-W(15)/4.)*A12
      RMXY(8)=(-W(2)/4.+W(4)/4.+BET*W(7)-2.*BET*W(8)+BET*W(9)+W(12)/4.
     1-W(14)/4.)*A12
      RMXY(7)=(-W(1)/4.+W(3)/4.+BET*W(6)-2.*BET*W(7)
     1+BET*W(8)+W(11)/4.-W(13)/4.)*A12
      RMXY(6)=(W(2)/4.-2.*BET*W(6)+BET*W(7)-W(12)/4.)*A12
      RMXY(5)=((BET-.5)*W(4)-2.*BET*W(5)+W(9)*.5)*A12
      RMXY(4)=((BET-.5)*W(3)-2.*BET*W(4)+(BET+.5)*W(5)+W(8)*.5-W(10)
     1*.5)*A12
      RMXY(3)=((BET-.5)*W(2)-2.*BET*W(3)+(BET+.5)*W(4)+W(7)*.5-W(9)
     1*.5)*A12
      RMXY(2)=((BET-.5)*W(1)-2.*BET*W(2)+(BET+.5)*W(3)
     1+W(6)*.5-W(8)*.5)*A12
      RMXY(1)=(-2.*BET*W(1)+(BET+.5)*W(2)-W(7)*.5)*A12
      DO 24 I=1,25
   24 PRINT 204,I,RMXY(I)
  204 FORMAT (1H0,30X,5HRMXY%,I2,2H<=E13.6)
      DO 51 I=1,25
      RMMAX(I)=(RMX(I)+RMY(I))/2.+SQRT((RMX(I)-RMY(I))**2/4.
     1+(RMXY(I))**2)
   51 CONTINUE
      DO 52 I=1,25
      RMMIN(I)=(RMX(I)+RMY(I))/2.-SQRT((RMX(I)-RMY(I))**2/4.
     1+(RMXY(I))**2)
   52 CONTINUE
      DO 53 I=1,25
   53 PRINT 501,I,RMMAX(I)
  501 FORMAT (1H0,30X,6HRMMAX%,I2,2H<=E13.6)
      DO 54 I=1,25
   54 PRINT 502,I,RMMIN(I)
  502 FORMAT (1H0,30X,6HRMMIN%,I2,2H<=E13.6)
      DO 55 I=1,25
      ZETA(I)=.5*(ATAN(2.*RMXY(I)/(RMX(I)-RMY(I))))
   55 CONTINUE
      DO 56 I=1,25
      THETA(I)=ZETA(I)*180./(PI)
   56 CONTINUE
```

```
      DO 57 I=1,25
   57 PRINT 503,I,THETA(I)
  503 FORMAT (1H0,30X,6HTHETA*,I2,2H<=F12.6)
      GO TO 700
  500 STOP
      END
```

VITA AUCTORIS

1940	Born at Rangamati, Chittagong Hill Tracts, East Pakistan on January 12.
1957	Completed Secondary School from Rangamati Gov't. H.E. School and received first grade Scholarship.
1959	Stood first class second in order of merit in Intermediate Science Examination from Sir A.T. College, Kanungopara, under Dacca University.
1963	Stood First class Second in B.Sc. Engg. (Civil) final examination from East Pakistan University of Engg. and Technology, Dacca.
1964	Joined the Associated British Consultant Ltd., Chittagong, E.P. as an Assistant Engineer.
1965	Appointed as a Resident Engineer in 'The Engineers Ltd.' Dacca, E. Pakistan.
1967	Promoted to the Post of Senior Engineer (Design) and held this position until left for Canada for higher studies.
1968-70	Enrolled as a Graduate (Teaching and Research) Assistant in the University of Windsor, while pursuing a Master's Program in the Department of Civil Engineering.